

# **Investigating the role of host TTR-RBPs during SFV4 and MHV-68 infection**



UNIVERSITY OF  
LIVERPOOL

**Thesis submitted in accordance with the requirements of the University of  
Liverpool for the degree of Doctor in Philosophy by**

**Jamie Casswell**

October 2019

## Contents

<b>Figure Contents Page.....</b>	<b>7</b>
<b>Table Contents Page.....</b>	<b>9</b>
<b>Acknowledgements.....</b>	<b>10</b>
<b>Abbreviations.....</b>	<b>11</b>
<b>Abstract.....</b>	<b>17</b>
<b>1. Chapter 1 Introduction.....</b>	<b>19</b>
<b>1.1 DNA and RNA viruses.....</b>	<b>20</b>
<b>1.2 Taxonomy of eukaryotic viruses .....</b>	<b>21</b>
<b>1.3 Arboviruses .....</b>	<b>22</b>
<b>1.4 <i>Togaviridae</i> .....</b>	<b>22</b>
1.4.1 Alphaviruses.....	23
1.4.1.1 Semliki Forest Virus.....	25
1.4.1.2 Alphavirus virion structure and structural proteins .....	26
1.4.1.3 Alphavirus non-structural proteins.....	29
1.4.1.4 Alphavirus genome organisation .....	31
1.4.1.5 <i>Cis</i> -acting RNA elements in Alphavirus RNA .....	32
1.4.1.6 Alphavirus replication in mammalian cells .....	34
<b>1.5 <i>Herpesviridae</i> .....</b>	<b>39</b>
1.5.1 <i>Alphaherpesvirinae</i> and <i>Betaherpesvirinae</i> .....	39
1.5.2 <i>Gammapherpesvirinae</i> .....	39
1.5.2.1 MHV-68.....	40
1.5.2.3 Genome and virion structure of gammaherpesviruses .....	40
1.5.2.4 Replication of gammaherpesviruses.....	41

<b>1.6 Mammalian mRNA .....</b>	<b>42</b>
1.6.1 Mammalian mRNA maturation.....	42
1.6.2 mRNA export in mammalian cells.....	43
1.6.3 mRNA decay.....	44
1.6.4 Turnover and Translation RNA-binding proteins (TTR-RBPs) .....	45
1.6.4.1 HuR.....	45
1.6.4.2 PABPC.....	46
<b>1.7 Virus inhibition and manipulation of RNA decay pathways .....</b>	<b>47</b>
1.7.1 Host shut-off .....	47
1.7.1.1 muSOX.....	48
1.7.2 Virus utilisation of host TTR-RBPs.....	48
1.7.2.1 HuR in alphavirus infection .....	49
1.7.2.2 PABPC in viral infection.....	50
<b>1.8 General Aims.....</b>	<b>50</b>
<b>2.1 Cell culture .....</b>	<b>52</b>
2.1.1 Mammalian cell culture maintenance .....	52
Baby hamster kidney fibroblasts (BHK-21 cell line).....	52
2.1.2 Subculture of mammalian cells.....	53
2.1.3 Cryopreservation and resuscitation of cell stocks .....	53
<b>2.2 Generation of recombinant SFV4 infectious complementary DNA plasmids.....</b>	<b>54</b>
<b>2.3. Generation of virus stocks .....</b>	<b>56</b>
2.3.1. Generation of rSFV4 stocks.....	58
2.3.1.1. In vitro transcription of SFV4(3F)-ZsGreen .....	58
2.3.1.2 Transfection of rSFV4 encoding nucleic acid for virus propagation .....	58
2.3.1.3. Purification of rSFV4 viruses .....	59
2.3.2 Murine gammaherpesvirus-68 stocks .....	59

<b>2.4 General Virus Techniques .....</b>	<b>60</b>
2.4.1 Infections .....	60
2.4.2 Virus titration by Plaque Assay .....	61
<b>2.5 General bacterial techniques .....</b>	<b>62</b>
2.5.1 Bacterial Culture .....	62
2.5.2 Preparation and use of glycerol stocks .....	62
2.5.3 Transformation of competent <i>E.coli</i> .....	62
2.5.4 Plasmid DNA extraction from bacterial cultures .....	63
<b>2.6 General nucleic acid and molecular techniques .....</b>	<b>65</b>
2.6.1 Extraction of RNA from mammalian cells .....	65
2.6.2 Nuclear and Cytoplasmic Fractionation followed by RNA extraction.....	65
2.6.3 DNase Treatment of RNA samples.....	66
2.6.4 RNA clean-up of DNase Treated RNA samples .....	66
2.6.5 Reverse Transcription of RNA samples .....	66
2.6.6 Nucleic acid quantification .....	67
2.6.7 Restriction Digest and FastAP treatment .....	67
2.6.8 DNA Ligations.....	67
2.6.9 Gel Electrophoresis .....	68
2.6.10 Extraction of DNA from gels .....	68
2.6.11 Blunt-end TOPO cloning.....	68
2.6.12 Standard PCR .....	69
2.6.13 Colony PCR.....	70
2.6.14 Sequencing.....	70
<b>2.7 Genetic reversion analysis of viral mutants .....</b>	<b>70</b>
2.7.1 Genetic reversion analysis of rSFV4-URE/CSE viruses .....	70
2.7.2 Analysis of genetic reversion of MHV-68 ORF37stop virus .....	71
<b>2.8 Immunostaining and Confocal Microscopy .....</b>	<b>71</b>

<b>2.9 <i>In vitro</i> characterisation of rSFV4 URE/CSE mutants .....</b>	<b>74</b>
2.9.1 rSFV4-2SG- <i>Gluc</i> one-step and multi-step growth curves .....	74
2.9.2 rSFV4-infected cell viability and caspase 3/7 assays .....	74
<b>2.10 Quantitative real-time polymerase chain reaction.....</b>	<b>76</b>
2.10.1 RT-qPCR of host transcripts using Pfaffl method.....	76
<b>2.11 Statistical Analysis.....</b>	<b>79</b>
<b>3.1 Overview.....</b>	<b>81</b>
<b>3.2 HuR relocalisation in mammalian cells during alphaviral infection .....</b>	<b>81</b>
<b>3.3 SFV4 nsP2 nuclear localisation.....</b>	<b>81</b>
<b>3.4 SFV4 icDNAs .....</b>	<b>82</b>
<b>3.5 PABPC, gammaherpesviruses and muSOX .....</b>	<b>82</b>
<b>3.6 Objectives .....</b>	<b>83</b>
<b>3.7 Results .....</b>	<b>83</b>
<b>3.8 Discussion .....</b>	<b>88</b>
<b>4.1 Overview.....</b>	<b>93</b>
<b>4.2 SFV4 icDNAs .....</b>	<b>93</b>
<b>4.3 Objectives .....</b>	<b>94</b>
<b>4.4 Results .....</b>	<b>95</b>
4.4.1 rSFV4 viruses containing URE/CSE deletions or additions.....	95
4.4.2 Production of infectious virus from rSFV4 icDNAs .....	96
4.4.3 Viral reversion and mutagenic pressures .....	97
4.4.4 SFV4 infection causes HuR subcellular relocalisation.....	100
4.4.5 Viral replication of rSFV4 URE+CSE mutants .....	112
4.4.6 Analysis of caspase-mediated apoptosis following infection of rSFV4 URE+CSE mutants....	121
4.4.7 Effect on host-cell mRNA transcripts following sequestration of HuR.....	125

<b>4.5 Discussion .....</b>	<b>138</b>
<b>5.1 Overview.....</b>	<b>148</b>
<b>5.2 Objectives .....</b>	<b>149</b>
<b>5.3 Results .....</b>	<b>149</b>
<b>5.4 Discussion .....</b>	<b>160</b>
<b>6.1 Successful manufacture of recombinant viruses used in this study .....</b>	<b>166</b>
<b>6.2 Sub-cellular localisation of TTR-RBPs during SFV4 infection.....</b>	<b>166</b>
<b>6.3 Sub-cellular localisation of TTR-RBPs during MHV-68 infection.....</b>	<b>168</b>
<b>6.4 Interplay of HuR, TTP and RNase-L in SFV4 infection .....</b>	<b>168</b>
<b>6.5 Interplay of muSOX generated RNA loss and PABPC during MHV-68 infection .....</b>	<b>169</b>
<b>6.6 The effect of the manipulation of SFV4 URE on host and viral transcripts 170</b>	
<b>6.7 The effect of the manipulation of MHV-68 muSOX on host and viral transcripts.....</b>	<b>171</b>
<b>6.8 Evaluation of qRT-PCR data and subcellular fractionation method .....</b>	<b>172</b>
<b>6.9 Medical intervention for alphaviruses and gammaherpesviruses .....</b>	<b>172</b>
<b>7. References.....</b>	<b>170</b>

## Figure Contents

Figure	Page
Figure 1.1 The genetic material of viromes	20
Figure 1.2 Taxonomy of eukaryotic viruses	21
Figure 1.3 The schematics of the alphavirus genome.	32
Figure 1.4 The 3'UTR of SFV4 genome	34
Figure 1.5 Alphavirus infection of a murine fibroblast cell.	38
Figure 1.6 Schematic of the mammalian HuR protein domains.	46
Figure 3.1 HuR relocates to the cytoplasm during SFV4 and SFV4-RDR infection.	84
Figure 3.2 HuR partially relocates to the cytoplasm in NIH/3T3 cells where SFV4(3F)-ZsGreen is actively replicating and the relocated HuR does not colocalise with viral nsP3.	85
Figure 3.3 MHV-68 with functional muSOX gene causes PABPC to relocate to the nucleus.	86
Figure 3.4 MHV-68 ORF37stop fails to cause PABPC nuclear retention despite active replication in NIH/3T3 cells.	87
Figure 3.5 PABPC sub-cellular relocation to nucleus during MHV-68 infection is a gradual process beginning 4-8 h.p.i. and steadily increasing over the course of cellular infection.	88
Figure 4.1. Schematic representation of rSFV4 viral genomes	96
Figure 4.2 Time taken in days for evidence of virion production and CPE following transfection in to BHK-21 cells of rSFV4 icDNAs containing alterations to the SFV4 3'UTR	97
Figure 4.3. Sequencing of the 3'UTR of the rSFV4.	98
Figure 4.4 Plaque morphology from rSFV4.	100
Figure 4.5 During infection with SFV4(3F)-eGFP-WT HuR relocates predominantly to the cytoplasm by 9 h.p.i.	102
Figure 4.6 HuR relocates partially to the cytoplasm by 6 h.p.i. during SFV4(3F)-eGFP-ΔURE infection but remains predominantly nuclear	104
Figure 4.7 HuR relocates predominantly to the cytoplasm by 6 h.p.i. following infection with an SFV4 mutant containing four additional URE's in the 3'NTR	106

Figure 4.8 HuR relocalises predominantly to the cytoplasm by 6 h.p.i. with SFV4(3F)-eGFP-ΔCSE but remains partially nuclear during infection	<b>108</b>
Figure 4.9 HuR relocalises partially to the cytoplasm by 6 h.p.i. following infection with SFV4(3F)-eGFP-ΔURE/CSE	<b>110</b>
Figure 4.10 The percentage of total HuR immunostaining present in the cytoplasm in relation to the whole cell during infection with rSFV4 mutants containing URE and/or CSE deletions and/or additions to the viral 3'UTR	<b>111</b>
Figure 4.11 Growth kinetics of rSFV4-2SG-Gluc viruses in NIH/3T3 cells containing URE deletion or additions in the 3'NTR of the SFV4 genome as measured by plaque assay	<b>113</b>
Figure 4.12 Growth kinetics of rSFV4-2SG-Gluc viruses in NIH/3T3 cells containing deletions of the CSE and URE as measured by plaque assay	<b>115</b>
Figure 4.13 Growth kinetics of rSFV4-2SG-Gluc viruses in NIH/3T3 cells containing URE deletion or additions in the 3'NTR of the SFV4 genome as measured by Gaussia luciferase activity	<b>118</b>
Figure 4.14 Growth kinetics of rSFV4-2SG-Gluc viruses in NIH/3T3 cells containing partial deletion of the CSE as measured by Gaussia luciferase activity	<b>120</b>
Figure 4.15 Caspase 3/7 induction and drop in cell viability following infection of NIH/3T3 cells with SFV4-2SG-Gluc viruses containing deletion or additions of the URE from/to the 3'UTR of the SFV4 genome	<b>123</b>
Figure 4.16 Caspase 3/7 induction and drop in cell viability following infection of NIH/3T3 cells with SFV4-2SG-Gluc viruses containing varying CSE deletions	<b>124</b>
Figure 4.17 β-actin mRNA reduction during SFV infection is relative to abundance of uracil rich elements (to which HuR binds) in the viral 3'NTR.	<b>126</b>
Figure 4.18 IFN-β mRNA abundance during SFV infection following infection with rSFV4 with URE deletions or additions.	<b>128</b>
Figure 4.19 Caspase-9 mRNA abundance during SFV4 infection following infection with rSFV4 with URE deletions or additions	<b>130</b>
Figure 4.20 RNase-L mRNA abundance during SFV infection following infection with rSFV4 with URE deletions or additions	<b>132</b>
Figure 4.21 TTP mRNA abundance during SFV infection following infection with rSFV4 with URE deletions or additions	<b>133</b>



Figure 4.22 Viral nsP3 RNA abundance during SFV infection following infection with rSFV4 with URE deletions or additions.	<b>135</b>
Figure 4.23 During infection with SFV4 HuR relocalises to the cytoplasm, the majority of which does not colocalise with TTP	<b>137</b>
Figure 5.1 RAE1 builds-up around nuclear envelope following MHV-68 infection but not MHV-68 ORF37stop infection or NIC	<b>151</b>
Figure 5.2 MHV-68 and MHV-68 ORF37stop viruses produce comparable levels of MHV-68 gpB mRNA in the cytoplasmic and nuclear fraction following infection of NIH/3T3 cells	<b>153</b>
Figure 5.3 Cyclophilin A mRNA abundance is decreased in the cytoplasmic and nuclear fraction during MHV-68 infection compared to NIC or MHV-68 ORF37stop infection	<b>154</b>
Figure 5.4 Cytoplasmic PARN mRNA abundance is decreased in the cytoplasm and nucleus during MHV-68 infection compared to NIC or MHV-68 ORF37stop infection	<b>156</b>
Figure 5.5 Cytoplasmic XRN1 mRNA abundance is decreased in the cytoplasm and nucleus during MHV-68 infection compared to NIC or MHV-68 ORF37stop infection	<b>158</b>
Figure 5.6 Cytoplasmic Hsp70 mRNA abundance is decreased in the cytoplasm and nucleus during MHV-68 infection compared to NIC or MHV-68 ORF37stop infection	<b>159</b>

## Table Contents

<b>Table</b>	<b>Page</b>
Table 1.1 Clinically relevant New World and Old World alphaviruses	<b>24</b>
Table 1.2 The functions of structural components of the alphavirus virion	<b>28</b>
Table 1.3 The summarised functions of the alphavirus non-structural proteins and non-structural polyproteins.	<b>31</b>
Table 2.1 List of viruses used in this study	<b>57</b>
Table 2.2 Primers used in this study for standard PCR	<b>69</b>
Table 2.3 Antibodies used for immunostaining in this study	<b>73</b>
Table 2.4 List of qPCR primers used in this study	<b>78</b>

## Acknowledgements

Most of all I would like to thank my primary supervisors Dr. Bahram Ebrahimi and Dr. Rennos Fragkoudis for their unwavering patience, knowledge and encouragement. Dr. Ebrahimi always encouraged me to read as many scientific papers as I could and discussed them with me at length which I have no doubt helped me build my knowledge base. He also taught me many of my initial laboratory skills. Dr Fragkoudis drove my research forward at The Pirbright Institute ensuring I made some interesting viral mutants and obtained some quality results. Both supervisors were always willing to provide advice or assistance when I asked.

Aside from my primary supervisors, other scientists who have helped advise me on my project include Prof. Mark Caddick (secondary supervisor) who always gave encouraging advice, Prof. John Fazakerley (secondary supervisor) who provided valued insights in to SFV pathogenesis and Dr. Sue Jacobs who provided advice on viral mutagenesis and propagation. Support from other researchers include Dr. Heather Allison and Dr. Marco Marcello from The University of Liverpool and Dr. Lesley Bell-Sakyi and Dr. David Ulaeto from The Pirbright Institute.

I would like to thank the BBSRC, The University of Liverpool and The Pirbright Institute for making the research possible and driving forward our understanding of virus-host interactions.

A huge thank you and profound admiration to my patient and supportive partner Simon who managed to hear the word 'Thesis' about a zillion times and never jumped out of a window! Financial and emotional support from Simon, Barbara Fletcher, Aryan Ramkhalawon, Joe Barton and Liam Bunster deserves a special mention as do my lab buddies Sian Owen, Ewan Young, Anjeet Jhutti and Tom Nicholson. Finally, to all my friends who listened to me moan and whine and shielded me from failure all the way to the shamefully extended and sacred finish line:



## Abbreviations

<b>aeHUR</b>	aedes aegypti human antigen R (mosquito HuR homolog)
<b>AIDS</b>	acquired immune deficiency syndrome
<b>AIHV-1</b>	alcelaphine gammaherpesvirus 1
<b>ARE</b>	AU-rich elements
<b>AUF1</b>	AU-rich element RNA binding protein 1
<b>AU-rich</b>	adenine and uracil rich
<b>CBC</b>	cap-binding complex
<b>CBF2</b>	C promoter binding factor 2
<b>CCHFV</b>	Crimean-Congo haemorrhagic fever orthonairovirus
<b>CCR4</b>	carbon catabolite repressor 4
<b>cDNA</b>	complementary DNA
<b>CHIKV</b>	chikungunya virus
<b>CMV</b>	Cytomegalovirus
<b>CP</b>	capsid protein
<b>CPV-1</b>	type 1 cytopathic vacuole
<b>CRM1</b>	chromosome region maintenance 1
<b>CSE</b>	conserved sequence element
<b>CTD</b>	C-terminal domain
<b>CUGBP1</b>	CUG triplet repeat RNA-binding protein 1
<b>DCP</b>	decapping enzyme
<b>DENV</b>	denge virus
<b>DMEM</b>	Dulbecco's modified eagle's medium
<b>DNA</b>	deoxyribonucleic acid
<b>dsDNA</b>	double-stranded DNA
<b>dsRNA</b>	double-stranded RNA

<b>EBV</b>	Epstein-Barr virus
<b>EEEV</b>	eastern equine encephalitis virus
<b>eGFP</b>	enhanced green fluorescent protein
<b>eIF</b>	eukaryotic translation initiation factor
<b>ELAV</b>	embryonic lethal abnormal vision
<b>ePABP</b>	embryonic poly(A) binding protein
<b>EphA2R</b>	ephrin A2 receptor tyrosine kinase
<b>ER</b>	endoplasmic reticulum
<b>FCS</b>	foetal calf serum
<b>GDP</b>	guanosine diphosphate
<b>GFP</b>	green fluorescent protein
<b>GLEBS</b>	GLE2p-binding sequence
<b><i>Gluc</i></b>	<i>gaussia</i> luciferase
<b>GMEM</b>	Glasgow's minimum essential medium
<b>gp</b>	glycoprotein
<b>GTase</b>	guanylyltransferase
<b>GTP</b>	guanosine triphosphate
<b>GTPase</b>	guanosine triphosphatase
<b>G3BP</b>	Ras GTPase-activating protein-binding protein
<b>HCV</b>	hepatitis C virus
<b>HHV</b>	human herpesvirus
<b>HJV</b>	Highlands J virus
<b>hnRNP</b>	heterogeneous nuclear ribonucleoprotein
<b>HNS</b>	HuR nucleocytoplasmic shuttling
<b>h.p.i.</b>	hours post-infection
<b>HS</b>	heparan sulfate
<b>HSP70</b>	heat-shock protein 70

<b>HSV</b>	herpes simplex virus
<b>HuR</b>	human antigen R
<b>HVD</b>	hyper-variable domain
<b>icDNA</b>	infectious complementary DNA
<b>ICTV</b>	International Committee on Taxonomy of Viruses
<b>IFN</b>	interferon
<b>IL</b>	interleukin
<b>i.p.</b>	intraperitoneal
<b>ISG</b>	interferon stimulated genes
<b>KO</b>	knock-out
<b>KSHV</b>	Kaposi's sarcoma associated herpesvirus
<b>LANA</b>	latency-associated nuclear antigen (KSHV)
<b>LB</b>	Luria-Bertani
<b>MAYV</b>	Mayaro virus
<b>MCF</b>	malignant catarrhal fever
<b>MCS</b>	multiple cloning site
<b>MDA5</b>	melanoma differentiation-associated protein 5
<b>MHV-68</b>	murine gammaherpesvirus 68
<b>MIDV</b>	Middelburg virus
<b>miRNA</b>	microRNA
<b>MOI</b>	multiplicity of infection
<b>mRNA</b>	messenger RNA
<b>MTase</b>	methyltransferase
<b>NBCS</b>	newborn calf serum
<b>NBF</b>	neutral buffered formaldehyde
<b>NC</b>	nucleocapsid
<b>NLS</b>	nuclear localisation signal

<b>NOT</b>	negative on TATA
<b>NPC</b>	nuclear pore complex
<b>nsP</b>	non-structural protein (of alphaviruses)
<b>nt</b>	nucleotide
<b>NTPase</b>	nucleoside triphosphatase
<b>NUP98</b>	nucleoporin 98
<b>NXF1</b>	nuclear export factor 1
<b>ORF</b>	open reading frame
<b>OvHV-2</b>	ovine gammaherpesvirus 2
<b>PABP</b>	poly(A)-binding protein
<b>PABPC</b>	poly(A)-binding protein cytoplasmic
<b>PABPN</b>	poly(A)-binding protein nuclear
<b>PAMP</b>	pathogen associated molecular pattern
<b>PAN</b>	poly(A) nuclease
<b>PARN</b>	poly(A) specific ribonuclease
<b>PBS</b>	phosphate buffered saline
<b>PBSA</b>	phosphate buffered saline albumin
<b>PCBP1</b>	poly(rC)-binding protein 1
<b>PCR</b>	polymerase chain reaction
<b>PFA</b>	paraformaldehyde
<b>PKR</b>	protein kinase R
<b>POWV</b>	Powassan virus
<b>Poly(A)</b>	poly adenylate
<b>PRR</b>	pattern recognition receptors
<b>qPCR</b>	quantitative PCR
<b>RAE1</b>	ribonucleic acid export 1
<b>RAN</b>	Ras-related nuclear protein

<b>RBP</b>	RNA-binding protein
<b>RIG-I</b>	retinoic acid-inducible gene I
<b>RNA</b>	ribonucleic acid
<b>RNAi</b>	RNA interference
<b>RNAPII</b>	RNA polymerase II
<b>RRM</b>	RNA recognition motif
<b>RRV</b>	Ross River virus
<b>RSE</b>	repeated sequence element
<b>rSFV</b>	recombinant Semliki Forest virus
<b>RTA</b>	replication transactivation activator (KSHV)
<b>RT-qPCR</b>	quantitative reverse transcription PCR
<b>RVFV</b>	Rift Valley fever phlebovirus
<b>SAV</b>	salmon pancreas disease virus
<b>SDV</b>	sleeping disease virus
<b>SFNV</b>	sandfly fever Naples phlebovirus
<b>SFV</b>	Semliki Forest virus
<b>SINV</b>	Sindbis virus
<b>snRNP</b>	small nuclear ribonucleoprotein
<b>sPBS</b>	sterile phosphate buffered saline
<b>ssRNA</b>	single-stranded RNA
<b>TATase</b>	terminal adenylyltransferase
<b>TBEV</b>	tick-borne encephalitis virus
<b>TF</b>	transframe
<b>TNF-<math>\alpha</math></b>	tumour necrosis factor alpha
<b>tPAPB</b>	testis-specific poly(A)-binding protein
<b>TREX</b>	transcription export complex
<b>TTP</b>	tristeraprolin

<b>TTR-RBP</b>	turnover and translation regulatory RNA-binding proteins
<b>URE</b>	uracil rich element
<b>UTR</b>	untranslated region
<b>VEEV</b>	Venezuelan equine encephalitis virus
<b>VSV</b>	varicella-zoster virus
<b>WEEV</b>	western equine encephalitis virus
<b>WNV</b>	West Nile virus
<b>WT</b>	wild-type
<b>XRN1</b>	5'-3' exoribonuclease 1
<b>ZIKV</b>	Zika virus



## Abstract

The stability and translation of messenger RNA (mRNA) in a cell is partially controlled by an array of turnover and translation regulatory RNA-binding proteins (TTR-RBPs). These proteins bind to the untranslated regions (UTRs) and poly(A) tail of mRNA and facilitate its processing, nuclear export, turnover and translation. Interestingly, a diverse range of viruses utilise different host TTR-RBPs to facilitate infection of host cells.

Human antigen R (HuR) is a TTR-RBP which binds uracil rich sequences in mRNA, leading to increased mRNA stability and translation. Mammalian HuR has been shown to bind RNA sequences rich in uracil in the 3'UTR of a range of alphavirus genomes. Disruption of this interaction via deletion of the HuR binding sequences in the viral genome or knock-down of HuR by RNAi has been shown to significantly decrease virus titre during Sindbis virus (SINV) infection of mammalian cells. Semliki Forest virus (SFV) genomic RNA also binds HuR via a uracil rich element (URE) and a conserved sequence element (CSE) at the 3' of its 3'UTR.

The main aim of this study was to investigate the significance of the URE and CSE of the SFV4 3'UTR during SFV4 infection of mammalian cells. This was achieved by engineering rSFV4 mutants with deletions of the URE and CSE from the SFV4 3'UTR and a rSFV4 with an additional four UREs in its 3'UTR. These rSFV4 mutants also expressed a reporter protein, either eGFP or *Guassia* luciferase for detection by confocal imaging and analysis of replication by luciferase assay, respectively.

Akin to infection with SINV, this study identified that during infection of mammalian cells with SFV4, host HuR translocates from the nucleus to the cytoplasm. Infection of NIH/3T3 cells with rSFV4 lacking the URE in its 3'UTR resulted in significantly less HuR relocating to the cytoplasm. A concurrent reduction in infectious virions, a reduction in viral RNA abundance, and a reduction in viral gene expression was also observed. In comparison, an addition of four UREs to the SFV4 3'UTR, increased the rate and amount of HuR relocating to the cytoplasm post-infection, increased the concentration of infectious virions, increased viral RNA abundance and increased viral gene expression. These results suggest a significant role for the URE of the SFV4 3'UTR during infection in mammalian cells and suggest that the interaction between the URE of SFV4 and host HuR may, at least in part, be responsible for this effect.

Mammalian cytoplasmic poly(A) binding protein (PABPC) protects mRNA transcripts from deadenylation and 3' end degradation, facilitates mRNA nuclear export and mRNA translation. Infection of mammalian cells with the gammaherpesviruses of the *Herpesviridae* family results in the striking nuclear influx of PABPC from the cytoplasm. During lytic infection of mammalian cells with murine gammaherpesvirus 68 (MHV-68) the viral protein muSOX elicits shut-off of host gene expression. This is achieved by the degradation of bulk host mRNA via an incompletely understood mechanism. The expression of muSOX on a transfected expression plasmid also results in the nuclear influx of PABPC suggesting a possible link between host shut-off and the nuclear influx of host PABPC.

The secondary aim of this study was to investigate the role that PABPC may play during the host shut-off of gene expression elicited by the viral muSOX protein during MHV-68 infection. To investigate this, an MHV-68 mutant encoding muSOX with a premature stop codon (MHV-68 ORF37stop) was utilised. This study found that the nuclear influx of PABPC during infection of mammalian cells with MHV-68 occurred gradually over the course of lytic infection and did not occur during infection with MHV-68 ORF37stop virus. Since gradual nuclear influx of PABPC occurs in mammalian cells following a block in mRNA nuclear export, the possibility of MHV-68 causing a block in mRNA nuclear export was investigated. By separation of the nuclear and cytoplasmic fractions post-infection and analysis of host mRNA abundance by RT-qPCR, no block in mRNA nuclear export was detected during MHV-68 infection despite PABPC relocating to the nucleus.

The roles which TTR-RBPs play during infection of host cells with a range of viruses are still being fully elucidated. These results suggest that HuR plays a significant role during Semliki Forest virus infection of mammalian cells and proposes HuR and other TTR-RBPs as novel targets for antiviral drugs.

# Chapter 1

## Introduction

## 1.1 DNA and RNA viruses

Despite being the most abundant entities in the biosphere, viruses can not replicate by themselves and require host cells to propagate. Different viruses may consist of different genetic material, either DNA or RNA, which can either be single-stranded (ss) or double-stranded (ds), as represented by the Baltimore classification of viruses. Interestingly, viruses which infect prokaryotes typically have a dsDNA or ssDNA genome, whereas viruses which infect eukaryotes most commonly have a positive-sense ssRNA (+ssRNA) genome closely followed by ssDNA and dsDNA genomes (Figure 1, Koonin *et al.*, 2015).

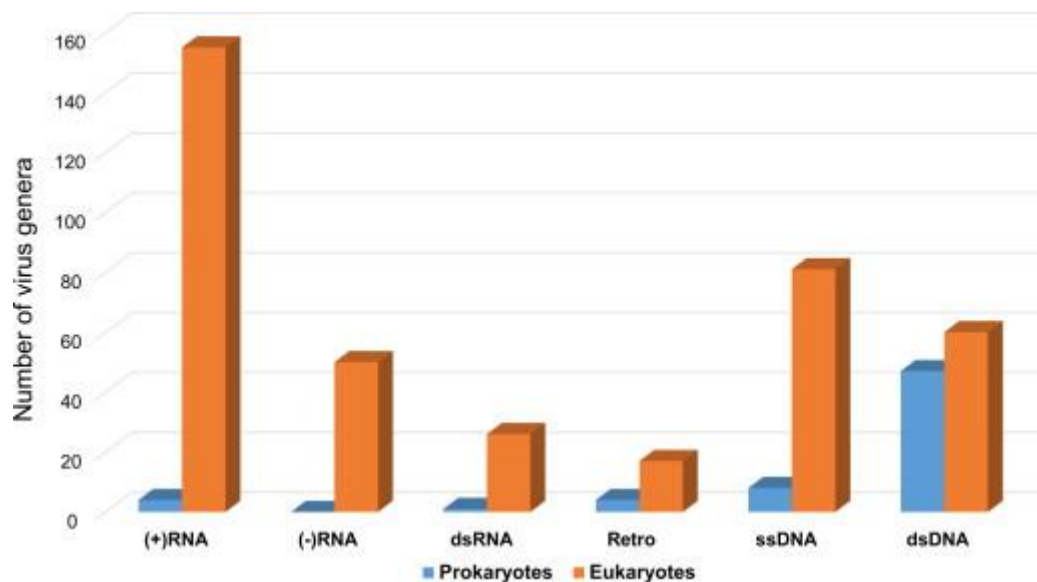


**Figure 1.1 The genetic material of viromes.** The number of virus genera which infect prokaryotes and eukaryotes separated in to the different Baltimore classes of viruses which represent the genetic material of the virus. Figure taken from (Koonin *et al.*, 2015).

Both DNA and RNA viruses subvert the normal metabolic processes of the cells they infect to promote the efficient replication of their viral genomes and the manufacture of new replicate virions. A diverse range of RNA binding proteins that help regulate mRNA decay and mRNA translation, termed ‘turnover and translation regulatory RNA-binding proteins (TTR-RBPs)’, are targeted by a range of viruses to help establish infection (Pullmann *et al.*, 2007; Pullmann and Rabb, 2014). For DNA viruses, such as the those of the *Herpesviridae* family, these proteins do not bind to the viral genome but to the viral mRNA after transcription of the viral genome in the nucleus. For RNA viruses, particularly

+ssRNA viruses such as those of the *Togaviridae* family, the TTR-RBPs can bind directly to the viral genome.

## 1.2 Taxonomy of eukaryotic viruses

The taxonomy of eukaryotic viruses is based on a number of factors including the nucleic acid of their genomes. The virion structure, virion size, mode of replication, range of host organisms and presence of a lipid envelope are also considered. Viruses of the *Togaviridae* and *Herpesviridae* both contain an icosahedral nucleocapsid, and a host-derived lipid envelope.

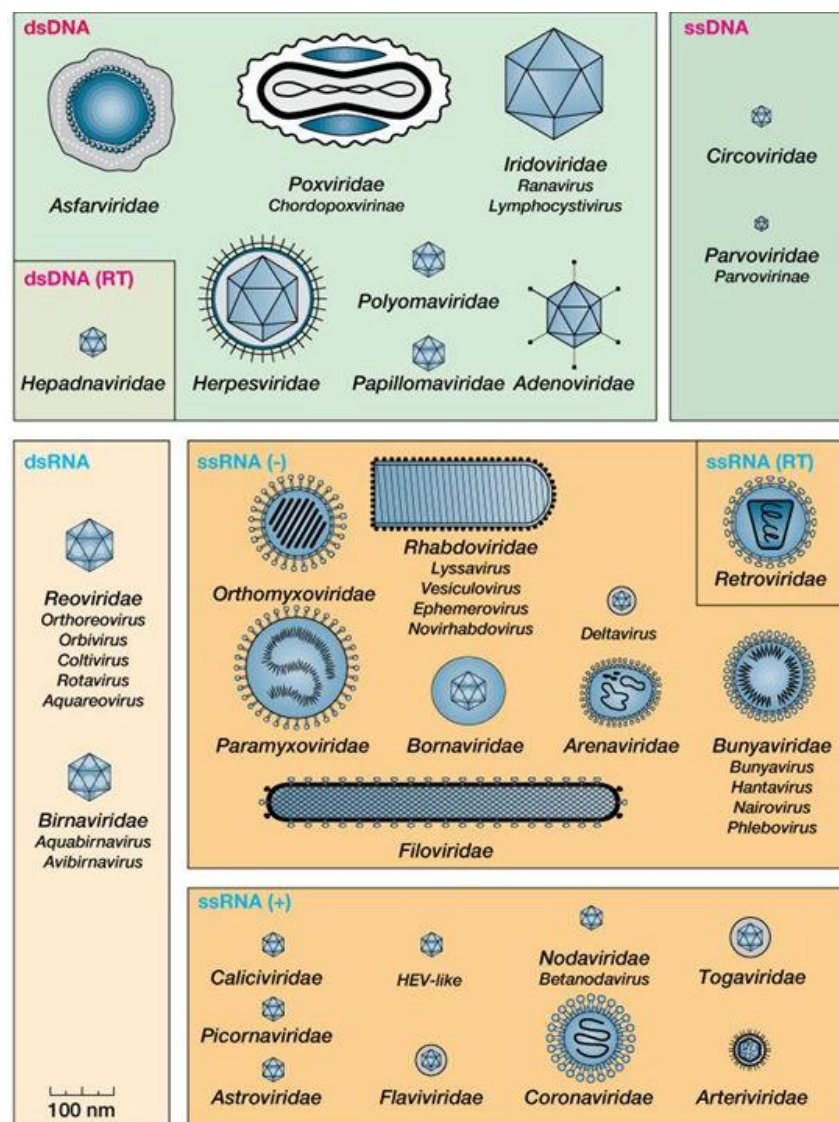


**Figure 1.2 Taxonomy of eukaryotic viruses.** Eukaryotic viruses are predominantly classified depending on their genetic material, virion structure and mode of replication. Image taken from (Slideplayer, 2015).

### 1.3 Arboviruses

Arboviruses are transmitted via arthropod vectors to either vertebrates or plants. The three families of viruses that contain the majority of arboviruses which infect mammals are *Flaviviridae*, *Reoviridae* and *Togaviridae* (Beckham and Tyler, 2015). Many arboviruses are also classified under the new *Bunyavirales* order (originally the *Bunyaviridae* family). The more clinically relevant arboviruses are spread by mosquito, tick and sandfly species (Beckham and Tyler, 2015; Kuno and Chang, 2005). The transmission cycle of arboviruses is not always limited to transmission via an arthropod host and can less commonly be transmitted through other routes such as ingestion of tissues from infected vertebrates (Kuno, 2001). Furthermore, humans are incidental hosts for some alphaviruses because significant viremia is not achieved during infection for transmission back to the arthropod vector (Kuno and Chang, 2005).

The Powassan virus (POWV) and the tick-borne encephalitis virus (TBEV) of the *Flaviviridae* family are transmitted by ticks, predominantly by species of the *Ixodes* and *Dermacentor* genera (Kemenesi and Banyai, 2019; Chitimia-Dobler *et al.*, 2019; Ostfeld and Brunner, 2015). Other viruses of the *Flaviviridae* family are transmitted by mosquitoes. The *Aedes aegypti* and *Aedes albopictus* species are the most common vectors that spread dengue virus (DENV) and Zika virus (ZIKV) whereas *Culex pipiens* is the principal vector for West Nile virus (WNV) (Higuera and Ramirez, 2019; Ferreira-de-Lima and Lima-Camara, 2018; Magalhaes *et al.*, 2018; Vogels *et al.*, 2017).

Rift Valley fever phlebovirus (RVFV), Crimean-Congo hemorrhagic fever orthonairovirus (CCHFV) and sandfly fever Naples phlebovirus (SFNV) of the *Bunyavirales* order are transmitted via mosquitoes, ticks or phlebotomine sandflies respectively (Schoffel *et al.*, 2018; Papa *et al.*, 2017; Tavana, 2015). Akin to many viruses of the *Bunyavirales* order and *Flaviviridae* family, most alphaviruses of the *Togaviridae* family are spread by arthropod vectors.

### 1.4 Togaviridae

*Alphavirus* is the sole genus of the *Togaviridae* family of viruses. As of 2019 the International Committee on Taxonomy of Viruses (ICTV) recognize that there are 31 species in the *Alphavirus* genus. In 2018 the *Rubivirus* genus, in which the rubella virus is classified under, was moved from the *Togaviridae* family to the new *Matonaviridae* family. Alphaviruses infect a range of vertebrate hosts, namely mammals and birds; and their transmission route is predominantly via an arthropod host.

### **1.4.1 Alphaviruses**

Alphaviruses have been traditionally divided in to the Old World and New World alphaviruses depending on the geographical location in which they were initially prevalent (Powers *et al.*, 2001). They are predominantly transmitted via an arthropod host, most commonly the mosquito. A small number of alphaviruses are unlikely to be spread by an arthropod host, including sleeping disease virus (SDV) and salmon pancreas disease virus (SAV), both of which infect fish (Villoing *et al.*, 2000; Weston *et al.*, 1999). The classification and general symptoms of the more clinically relevant alphaviruses are summarised in table 1.1.

Alphavirus	New or Old World	Geographical location	Primary Vector	Host	Symptoms in humans
<b>Semliki Forest Virus (SFV)</b>	Old World	Africa, Asia	<i>Aedes</i> mosquitoes	Humans, birds, rodents	Mild fever, rash, malaise and arthralgia
<b>Chikungunya virus (CHIKV)</b>	Old World	Africa, Asia, Americas and Europe	<i>Aedes</i> mosquitoes	Humans, primates, rodents, birds	Fever, rash, malaise and arthralgia
<b>Sindbis virus (SINV)</b>	Old World	Africa, Asia, Europe, Australia	<i>Aedes, Culiseta and Culex</i> mosquitoes	Humans, horses, birds, rodents	Fever, rash, malaise and arthralgia
<b>O'nyong'nyong virus (ONNV)</b>	Old World	Africa	<i>Anopheline</i> mosquitoes	Humans	Fever, rash, malaise and arthralgia
<b>Ross River virus (RRV)</b>	Old World	Australia	<i>Aedes, Culex, and Anopheline</i> mosquitoes	Humans, kangaroos, wallabies, horses, possums, flying fox	Fever, rash, malaise and arthralgia
<b>eastern equine encephalitis virus (EEEV)</b>	New World	North and South America	<i>Culiseta</i> mosquitoes	Humans, horses, birds	Encephalitis, fever, headache, mortality (40-85%), neurological sequelae (~75% of survivors).
<b>western equine encephalitis virus (WEEV)</b>	New World	North and South America. Last human case was in Uruguay in 2009.	<i>Culex and Culiseta</i> mosquitoes	Humans, horses, birds	Encephalitis, fever, headache, mortality (3-7%), neurological sequelae (~90% of survivors).
<b>Venezuelan equine encephalitis virus (VEEV)</b>	New World	North and South America	<i>Aedes, Psorophora, and Culex</i> mosquitoes	Humans, horses, rodents	Encephalitis, fever, headache, mortality (~1%), neurological sequelae (~14% of survivors).
<b>Mayaro virus (MAYV)</b>	New World epidemiology, Old World clinical symptoms	South America	<i>Haemagogus and Aedes</i> mosquitoes	Humans, primates	Fever, rash, malaise and arthralgia

**Table 1.1 Clinically relevant New World and Old World alphaviruses.** Despite some genera of mosquitos being the primary vector in transmission cycles of specific alphaviruses in the wild, most alphaviruses are capable of being transmitted by a range of mosquito species (Fragkoudis *et al.*, 2008; Wesula Olivia *et al.*, 2015; Wiggins, Eastmond and Alto, 2018; Weaver and Forrester, 2015; Armstrong and Andreadis, 2010; Lim *et al.*, 2018; Kenney, Adams and Weaver, 2010; Torres *et al.*, 2017; Carey *et al.*, 2019).



There is currently no clinically used antiviral or vaccine for new world alphaviruses but research is focused on targeting both the viral proteins themselves as well as virus-host interactions (Carey *et al.*, 2019). Incidence in humans is currently low, with only several reported cases of eastern equine encephalitis virus (EEEV) infections each year (Lindsey, Staples and Fischer, 2018). Despite this, there is concern of possible future outbreaks and given the morbidity and mortality following infection with some of the new world alphaviruses there is an urgent requirement for successful, regulatory body approved vaccines or antivirals. Infection in humans with EEEV, western equine encephalitis virus (WEEV) and Venezuelan equine encephalitis virus (VEEV) can also be achieved through aerosol dissemination. These features give rise to considerations of the new world alphaviruses as serious bioterrorism threats (Sidwell and Smee, 2003; Steele and Twenhafel, 2010).

The mortality rates for the old world alphaviruses are relatively lower than those of the new world alphaviruses but can still elicit severe and persistent symptoms in humans (Herrero *et al.*, 2016). Chikungunya virus (CHIKV) is of increasing concern due to recent outbreaks affecting millions of individuals worldwide across Africa, Asia (including India and Thailand), several European countries and the Americas (Feng *et al.*, 2019). Specific mutations in CHIKV envelope proteins, namely E1-A226V and E2-L210Q, and the widespread distribution of *Aedes* mosquitoes have facilitated CHIKV outbreaks (Tsetsarkin *et al.*, 2007; Sahu *et al.*, 2013; Tsetsarkin and Weaver, 2011; Fortuna *et al.*, 2018). The arthralgia occurring in many patients following CHIKV infection can persist for many years and cause significant decrements to quality of life. Because of its relatively small risk of serious clinical illness in humans compared to CHIKV, SFV is often used in the laboratory as a model for old world alphaviruses.

#### **1.4.1.1 Semliki Forest Virus**

Semliki Forest virus (SFV) infection in humans can cause a mild febrile illness characterised by fever, headache myalgia and arthralgia. SFV was originally isolated in 1942 from *Aedes abnormalis* mosquitoes resident in the Semliki Forest in Uganda (Smithburn and Haddow, 1944).

SFV infection has been well studied *in vivo* in laboratory mice. Following intraperitoneal (ip) inoculation of mice, SFV replicates in smooth muscles, endothelial cells and the pancreas resulting in high titre plasma viraemia that facilitates its access across the blood-brain barrier (Fazakerley *et al.*, 2006; Soiluunninen *et al.*, 1994). SFV is neuroinvasive in mice, replicating in neurones and oligodendrocytes and promoting the immune system facilitated demyelination of neurons and viral encephalitis (Fazakerley *et al.*, 2006). *In vitro*, SFV replicates in a broad range of commonly used

laboratory cells including NIH/3T3, HEK293, chicken embryo fibroblasts (CEF), Vero and BHK-21 cells (Reigel and Koblet, 1979; Barry *et al.*, 2009; Kiiver *et al.*, 2008).

Several strains of WT SFV exist in laboratory circulation and are categorised by their virulence in adult mice. All strains currently analysed in the laboratory are virulent in neonatal or suckling mice (Bradish, Allner and Maber, 1971). Virulent strains in adult mice include Prototype, L10, Osterrieth and V13 whereas avirulent strains include A7, A7(74), V42 and A8 (Bradish, Allner and Maber, 1971; Deuber and Pavlovic, 2007; Glasgow *et al.*, 1991).

The A7(74) strain was derived through selection for avirulence in adult mice from the AR2066 strain isolated from Mozambique in 1959 (McIntosh, Brooke Worth and Kokernot, 1961). A7(74) causes limited central nervous system infection in adult mice and is usually cleared by 10 days post infection despite remaining virulent in neonatal mice (Fazakerley *et al.*, 1993). The difference for the age-related difference in disease progression are thought to be a result of the inability of SFV A7(74) to complete the replication cycle in mature murine neurons resulting in aggregation of virus particles in the cytoplasm (Fazakerley *et al.*, 1993).

The L10 and Prototype strains were derived from passages in adult mice of the original SFV strain isolated from a pool of *Aedes abnormalis* mosquitoes from the Semliki Forest in Uganda (Smithburn and Haddow, 1944; Bradish, Allner and Maber, 1971). SFV4 is a molecular cDNA clone of the Prototype strain (Liljestrom and Garoff, 1991). SFV4 and L10 strains therefore have the same origin as each other and show similar replication kinetics in cell culture but varying virulence in adult mice.

SFV L10 is highly virulent in mice irrespective of age or route of inoculation. Despite this, SFV4 is only neurovirulent in mice *in vivo* when inoculated intracerebrally or at high doses (Fragkoudis *et al.*, 2007). Differences in virulence in mice between the SFV strains have been attributed to nucleotide sequence differences in the E1 and E2 glycoprotein genes, the 5' and 3' untranslated regions and the non-structural genes, especially nsP3 (Saul *et al.*, 2015; Tuittila and Hinkkanen, 2003; Tarbatt *et al.*, 1997).

#### **1.4.1.2 Alphavirus virion structure and structural proteins**

High resolution images of alphavirus virions have been achieved by cryo-EM and X-ray crystallography (Vaney, Duquerroy and Rey, 2013). Resolution as high as 3.5 Å has been achieved for Sindbis virus particles (Chen *et al.*, 2018). The mature virion is 65-70nm in diameter with a molecular mass of around  $5.2 \times 10^6$  Da (Jose, Snyder and Kuhn, 2009; Mukhopadhyay *et al.*, 2006).

Viruses have evolved to utilise ribosomal frameshifting to translate additional viral proteins without increasing genome size (Chirico, Vianelli and Belshaw, 2010). During translation of 6K in the alphavirus structural polyprotein the host ribosome can frameshift resulting in a C-terminal extension of the 6K protein (Firth *et al.*, 2008). This novel protein, named transframe (TF), is encoded in the -1 open reading frame and terminates the translation of the polyprotein in the C-terminus of E1. SINV TF mutants result in reduced mortality rates in infected mammals, and reduced levels of virion release following infection in both insect and mammalian cells (Snyder *et al.*, 2013). The SINV  $\Delta$ TF mutant replicates the viral genome at comparable levels to WT suggesting the reduction in virion levels may be related to virion assembly and/or virion budding (Snyder *et al.*, 2013). The arrangement and functions of the structural proteins and molecules of the mature virion are summarised in table 1.2.

The virions are composed of ~11.5 kb positive-strand genomic RNA encapsulated in an icosahedral nucleocapsid (NC) made of 240 capsid protein (CP) monomers. The NC is enveloped in a host derived lipid bilayer with 240 E1 and 240 E2 protruding viral glycoproteins arranged in 80 spikes making an icosahedral lattice anchored in to the NC (Jose, Snyder and Kuhn, 2009). Each glycoprotein spike is composed of three E1-E2 heterodimers and contain transmembrane helixes which span the lipid bilayer. The glycosylation pattern of E1 and E2 differs between viruses of the genus and can affect the level of infectivity in different mammalian and arthropod species (Mukhopadhyay *et al.*, 2006; Vaney, Duquerroy and Rey, 2013). E1 and E2 are also palmitoylated at or near to their transmembrane domains (Schmidt, Bracha and Schlesinger, 1979).

A viral 6kDa membrane-associated protein, 6K, associates with E1-E2 spikes at the endoplasmic reticulum and is partially retained in low numbers in the mature virion (Lusa, Garoff and Liljestrom, 1991). An SFV  $\Delta$ 6k mutant forms unstable infectious virions with altered E1-E2 spike structure and significantly reduced fusion levels (McInerney *et al.*, 2004).

Viral Structural Protein	Structural Features	Function
<b>E1</b>	Glycoprotein forming viral surface spikes. Ectodomain contains class II fold and three domains in a linear arrangement and transmembrane helix embedded in lipid bilayer. Fusion loop.	E1 ectodomain forms a protein lattice covering most of lipid bilayer. Fusion of the virion envelope with host endosomal membrane via fusion loop. Fusion loop hidden at the E1-E2 interface at normal pH but exposed at low pH (i.e. in endosomes after cell entry).
<b>E2</b>	Glycoprotein forming viral surface spikes. Ectodomain contains three domains (A, B and C) in linear arrangement with Ig superfamily-type folds. Transmembrane helix embedded in lipid bilayer.	Receptor binding and subsequent receptor-mediated endocytosis for cell entry. Most neutralising antibodies are targeted against E2 Residues interact with CP for structural scaffolding and to drive budding. Varying amino acid sequence and glycosylation of E2 among alphaviruses can confer varying tissue and species specificity.
<b>E3</b>	Polyprotein with E2 until trans-Golgi network.	Prevents p62/P1 from priming for fusion in the acidity of the golgi network by bracing domain B of E2 on to E1 fusion loop. Cleaved from p62 at trans-Golgi network through the action of furin but has some affinity for E2 post cleavage. Identified in mature virions including SFV and VEEV, suggesting some E3 may be retained.
<b>p62 (in SFV, pE2 in other alphaviruses)</b>	Precursor to E2 and E3.	p62 interacts with folded E1 in the ER to form p62-E1 heterodimer. E3 cleaved by furin in the Golgi, followed by E1-E2 priming for fusion at low pH and translocation of E1-E2 heterodimers to the plasma membrane.
<b>Capsid protein (CP)</b>	Forms the case of the nucleocapsid. Chymotrypsin-like C-terminal domain with a hydrophobic pocket. Highly basic N-terminal tail.	Chymotrypsin-like domain functions as a serine protease which autocleaves the CP from its polyprotein. Disordered N-terminal tail interacts with viral genomic RNA. Residues interact with E2 for virion formation and to drive budding. C-terminal domain has hydrophobic pocket that binds the C-terminal domain of E2 in mature virion.
<b>6K peptide</b>	Two transmembrane domains, one luminal domain, and one palmitoylated cytoplasmic domain. Translated to comparable concentrations to E1 and E2 yet mostly omitted from mature virion.	Reduced infectivity and stability of virion following deletion of 6K peptide in SFV. Forms cation-selection ion channels in lipid bilayers that and thus may be involved in virion formation and budding. May facilitate ability to infect multiple species, i.e. a range of mammalian and arthropod species.
<b>TF</b>	Protein translated by frameshifting to extend the C-terminus of 6K.	Proposed roles in virion assembly and/or release. SINV ΔTF confers reduced mortality rates in mammals compared to WT.

**Table 1.2 The functions of structural components of the alphavirus virion.** The alphaviruses are enveloped, small, spherical virions composed of multiple structural proteins that convey a multitude of interconnected functions in virion assembly and infection (Mukhopadhyay *et al.*, 2006; Vaney, Duquerroy and Rey, 2013; Ziemiecki, Garoff and Simons, 1980; Kielian and Rey, 2006; Voss *et al.*, 2010; Li *et al.*, 2010; Sjöberg, Lindqvist and Garoff, 2011; Zhang *et al.*, 2011; Tang *et al.*, 2011; Myles, Pierro and Olson, 2003; Loewy *et al.*, 1995; McInerney *et al.*, 2004; Wilkinson *et al.*, 2005; Snyder *et al.*, 2013).

#### 1.4.1.3 Alphavirus non-structural proteins

All four viral non-structural proteins (nsPs) are required for viral RNA replication as first determined using SINV temperature sensitive mutants (Hahn, Strauss and Strauss, 1989; Rupp *et al.*, 2015). Despite working cooperatively to form the viral RNA replication complexes, the nsPs also have their own individual functions and subcellular locations during infection.

nsP4 elicits the RNA-dependent RNA polymerase activity required for viral RNA replication. Despite this the nsP4 alone is not capable of replicating the viral RNA during infection and functions as part of replicase complexes with the other viral nsPs (Rupp *et al.*, 2015). The P123+nsP4 replicase complex synthesises negative strand RNA from the full viral RNA genome. Following further cleavage of P123, complexes of nsP1+P23+nsP4 and nsP1+nsP2+nsP3+nsP4 both synthesise positive strand genomic and subgenomic viral RNA (Shirako and Strauss, 1994). The synthesis of the subgenomic positive sense RNA is in part selected for by nsP2 which acts as a transcription factor recruiting the nsP1+nsP2+nsP3+nsP4 replicase complex to the negative sense subgenomic promoter sequence (Suopanki *et al.*, 1998). The core catalytic domain of nsP4 also possesses terminal adenylyltransferase (TATase) activity suggesting roles in the maintenance of poly(A) tails on viral RNAs (Tomar *et al.*, 2006).

The viral nsP1 contains Rossman-like methyltransferase (MTase) and guanylyltransferase (GTase) domains that catalyse the addition of a methylated guanine cap to the 5' of viral genomic and subgenomic RNAs (Rozanov, Koonin and Gorbalenya, 1992; Rupp *et al.*, 2015). nsP1 also contains an amphipathic helix and palmitoylation site which allow for nsP1 and the replicase complexes to be anchored in to host cell membranes (Ahola *et al.*, 1999; Spuul *et al.*, 2007; Kiiver *et al.*, 2008). Nascent viral RNAs are prepared for nsP1 mediated capping by removal of a 5' phosphate group through the nucleoside triphosphatase (NTPase) activity of nsP2. The NTPase domain is located at the N-terminus of nsP2 along with a helicase domain whereas the C-terminus contains a protease domain (Russo, White and Watowich, 2006; Saisawang *et al.*, 2015; de Cedron *et al.*, 1999). Other putative domains exist within the protein with unconfirmed functions (Rupp *et al.*, 2015). The helicase and NTPase domains unwind viral RNA secondary structures during viral RNA replication. The protease activity of nsP2 is required for the proteolytic processing of the non-structural polyprotein (Saisawang *et al.*, 2015; Vasiljeva *et al.*, 2003). The cleavage of the non-structural polyprotein by nsP2 can occur in both *trans* and *cis* depending on the cleavage site and the virus species. The site of the nsP3-nsP4 junction is preferentially cleaved early in infection whereas the nsP2-nsP3 junction is preferentially cleaved later in infection (Vasiljeva *et al.*, 2003).

Multiple domains of nsP2 are utilised to elicit inhibition of host transcription (Tamm, Merits and Sarand, 2008). During infection nsP2 resides in the cytoplasm and on host lipid membranes within replication complexes but also partially translocates to the nucleus during infection (Peranen *et al.*, 1990). Nsp2 of Sindbis virus (including SFV nsP2 on a VEEV icDNA) has been shown to interact with Rbpb1, the catalytic subunit of RNAPII. This interaction results in the ubiquitination and subsequent degradation of Rbpb1 and global transcription inhibition (Akhrymuk, Kulemzin and Frolova, 2012).

Akin to the other nsP's, mutations in nsP3 result in defects in viral RNA synthesis. The functions of nsP3 during infection are less well defined than for the other nsP's. The C-terminus of nsP3 comprises a hyper-variable domain (HVD), the centre contains a zinc-binding domain and the N-terminus contains a macrodomain. The HVD has been attributed to multiple interactions with host cell proteins early in infection (Gotte, Liu and McInerney, 2018). The degradation and thus controlled expression of nsP3 in some alphaviruses, including SFV4, is partially controlled through a degradation signal at the C-terminus of the protein (Varjak, Zusinaite and Merits, 2010). The subcellular location of nsP3 during infection is either at the active sites of viral RNA replication as part of the replicase complexes on internal host cell membranes or in nsP3 cytoplasmic aggregates (Gotte, Liu and McInerney, 2018). In SFV, the majority of nsP3 is found at replication complexes and colocalises with dsRNA (Salonen *et al.*, 2003; Gotte, Liu and McInerney, 2018). This feature allows for the identification of the subcellular location of replicase complexes during SFV infection through identification of the subcellular location of nsP3.

nsP3 elicits RNAi suppressor activity in mosquito cell lines and mutations in nsP3 nucleotide sequence can affect vector specificity indicating important roles of nsP3 during infection of mosquito cells (Lastarza, Grakoui and Rice, 1994; Mathur *et al.*, 2016). The nucleotide sequence of nsP3 has also been shown to be a key regulator of neurovirulence in mice between different SFV strains. The replacement of nsP3 from neurovirulent strains of SFV like SFV4 to the avirulent A7(74) strain result in a neurovirulent A7(74) mutant (Tuittila *et al.*, 2000; Saul *et al.*, 2015).

In mammalian cells, there are multiple nsP3-host interactions that facilitate infection and inhibit the host cell antiviral response (Gotte, Liu and McInerney, 2018). One well defined nsP3 interaction is with the isoforms of Ras GTPase-activating protein-binding protein (G3BP). This interaction inhibits G3BP's roles in stress granule formation leading to the disassembly of stress granules during alphavirus infection (Scholte *et al.*, 2015; Panas *et al.*, 2012).

Non-structural protein	Function
<b>nsP1</b>	Methyltransferase and Guanylttransferase. Anchoring of replicase complexes to host membranes Component of viral RNA replicase
<b>nsP2</b>	Transcription Factor for subgenomic viral RNA replication NTPase and Helicase Protease (used for proteolytic processing of non-structural polyproteins) Inhibition of host transcription/gene expression Component of viral RNA replicase
<b>nsP3</b>	Component of viral RNA replicase Interaction with a range of host proteins including G3BP leading to disassembly of stress granules Key virulence determinant
<b>nsP4</b>	RNA dependent RNA polymerase Component on viral RNA replicase TATase activity
<b>P123+nsP4</b>	Short lived, negative viral RNA synthesis
<b>nsP1+P23+nsP4</b>	Very short lived, transient complex
<b>nsP1+nsP2+nsP3+nsP4</b>	Genomic and subgenomic positive sense viral RNA

**Table 1.3 The summarised functions of the alphavirus non-structural proteins and non-structural polyproteins.** Each viral nsP has individual functions during infection as well as functioning as part of RNA replicase complexes. Most function in the cytoplasm or on host membranes apart from nsP2 which partially translocates to the nucleus to inhibit host transcription.

#### 1.4.1.4 Alphavirus genome organisation

The alphavirus genome is encoded on single stranded positive sense RNA. The genomic RNA contains a 7-methyl-GpppA cap and a poly(A) tail that mimics host mRNA. There are two open reading frames encoding the polyproteins for the non-structural proteins required for RNA synthesis and the structural proteins encoding new virus particles (Pietla, Hellstrom and Ahola, 2017). The structural polyprotein is under the control of a subgenomic promoter present in the negative strand RNA replication intermediate.

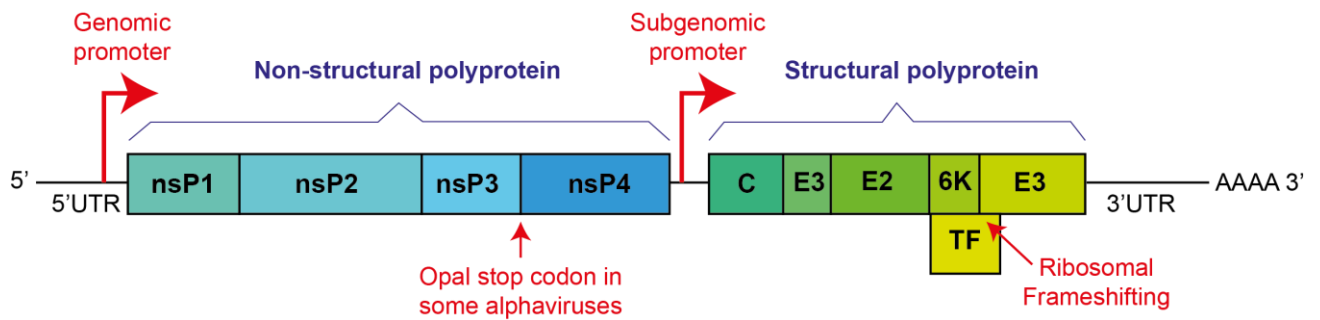


**Figure 1.3 The schematics of the alphavirus genome.** The ss(+)RNA genome encodes two polyproteins under the control of a genomic and subgenomic promoter and mimics host mRNA.

Many alphaviruses including most strains of CHIKV have an opal stop codon at the 3' of the nsP3 genome sequence (Jones *et al.*, 2017). The opal stop codon causes translation to terminate after nsP3 yielding P123 polyprotein. There is a read through efficiency of 15% which yields the full P1234 polyprotein (Kim *et al.*, 2004). SFV4 encodes an arginine codon at this position so does not translate a P123 polyprotein and instead constitutently translates the full P1234 polyprotein. The avirulent SFV A7(74) strain encodes an opal stop codon at this position and substitution with an arginine codon increases pathogenicity suggesting a role in SFV pathogenesis in mice (Gotte, Liu and McInerney, 2018; Tuittila and Hinkkanen, 2003).

#### 1.4.1.5 *Cis*-acting RNA elements in Alphavirus RNA

Multiple *cis*-acting RNA sequences and RNA secondary structures present in the alphaviral genomic RNA, subgenomic RNA and negative sense RNA replication intermediate elicit roles in alphavirus replication. The RNA sequences and secondary structures mostly function via interaction with viral or host *trans*-acting proteins. Some of these sequences exist in the coding regions of the viral RNA but many are also located in the untranslated regions (UTR's). Four of these RNA sequences and/or RNA secondary structures are conserved amongst virus species in the *alphavirus* genus and termed conserved sequence elements (CSE's). There are three untranslated regions in the alphavirus genome; the 5'UTR, the 3'UTR and a junction region in between the non-structural and structural polyprotein sequences.

#### Conserved RNA sequence elements (CSEs) in the alphavirus genome

At the 5' of the alphavirus RNA genome a CSE (CSE1) consisting of approximately the first 44 nt in the 5'UTR shows conserved secondary structure (Ou, Strauss and Strauss, 1983). CSE1 forms a stem-loop



structure and has proposed roles as a promoter for positive strand synthesis on the negative strand template (Jose, Snyder and Kuhn, 2009). A 51nt CSE (CSE2) exists within the coding region of nsP1 near the 5' end of the genome. This CSE (CSE2) functions as an enhancer element for RNA synthesis (Frolov, Hardy and Rice, 2001; Michel *et al.*, 2007). Mutations in the alphavirus CSEs have been shown to have different degrees of inhibition on viral replication depending on the species of the host cell. For instance, mutations to the 51 nt CSE of SINV result in a greater inhibition on viral replication in mosquito cell lines than mammalian cell lines (Fayzuln and Frolov, 2004). These differences suggest that the CSE elements interact in *trans* with host cell proteins.

There is also a 24 nt CSE (CSE3) located in the junction region between the non-structural and structural polyprotein ORFs. This conserved sequence acts as a highly efficient subgenomic promoter sequence in the negative strand for the subgenomic structural polyprotein (Levis, Schlesinger and Huang, 1990; Raju and Huang, 1991; Wielgosz, Raju and Huang, 2001).

Finally, a conserved 19 nt (CSE4) resides at the 3' end of the 3'UTR adjacent to the poly(A) tail. This sequence is heavily conserved among all alphavirus species and has been proposed to act as an RNA promoter for negative strand synthesis (Hill *et al.*, 1997; Lemm *et al.*, 1998). This CSE also contains uracil (U)-rich regions known to interact with host cell RNA binding proteins including the host protein Human antigen R (HuR) (Dickson *et al.*, 2012). The 19nt CSE of Sindbis virus has been shown to be required for negative strand synthesis through experiments utilising full or partial CSE deletion SINV mutants (Hardy and Rice, 2005). These findings support a role for the CSE as a copromoter for negative strand RNA synthesis.

Other groups have shown that SINV lacking part (Kuhn, Hong and Strauss, 1990) or all (Raju *et al.*, 1999) of the 19nt CSE in its 3'NTR is still able to produce viable virus and propagate an infection of BHK-21 cells. Following a number of passages some but not all of these SINV CSE deletion mutants gained AU-rich additions to their 3'NTR (Raju *et al.*, 1999; George and Raju, 2000). These data suggest that although not absolutely required for infection in BHK-21 cells the CSE is important for viral RNA replication and the AU-richness of the CSE plays an important role in its function.

### **Other RNA elements in the alphavirus RNA genome**

An RNA packaging signal interacts with capsid protein during nucleocapsid formation. This RNA element varies in position amongst alphavirus species but usually resides in the 5' of the genome so that only full genomic RNA is encapsulated in to virion particles (Weiss *et al.*, 1989; Linger *et al.*, 2004). Many alphaviruses have 40-60 nt repeated sequence elements (RSEs) in their 3'UTR (Ou, Trent and

Strauss, 1982). The function of the RSEs are mostly unconfirmed but show RNA secondary structure and are thought to interact with host cell proteins (Ou, Trent and Strauss, 1982; Rupp *et al.*, 2015).

To the immediate 5' of the 3' CSE (CSE4) is an adjacent uracil rich region that is conserved amongst most of the old world and new world alphaviruses. This uracil rich element (URE) is evident in this position in WEEV, EEEV, VEEV, Highlands J virus (HJV), Middelburg virus (MIDV) SINV and SFV (both SFV4 and A7 strains) amongst others (Santagati *et al.*, 1994; Ou, Trent and Strauss, 1982). Alphavirus URE and CSE (CSE4) RNA sequence fragments from WEEV, VEEV, EEEV, SINV and SFV have been shown to bind the host protein HuR (Sokoloski *et al.*, 2010). Furthermore, during mammalian cellular infection with WEEV or SINV the bulk of cellular HuR relocates to the cytoplasm from the nucleus. The cytoplasmic build-up of host HuR is also evident during CHIKV and RRV infection despite the absence of a URE in this position in the 3'UTR in these viruses. However, CHIKV and RRV contain other uracil rich regions elsewhere in their 3'UTRs. These alternative uracil rich regions and the CSE4 have been shown to bind HuR despite lacking the conserved URE seen in other alphaviruses (Dickson *et al.*, 2012). The sequence and position of the URE, CSE4 and the RSEs in the SFV4 3'UTR are illustrated in figure 1.4. The role of HuR binding the SINV 3'UTR during infection is discussed later in this chapter.

```
guuaggguaaggcaauuggauuagcaagaaaauugaaaacagaaaaaguuaggguaagcaauuggaauuaacca
uaacuguaaacuuguaacaaagcgcaacaagaccugcgcaauuggccccgugguccgccucacggaaacucggggcaac
ucauauugacacauuaauuggcauaauuggaagcuuacauaagcuuaauucgacgaauaauuggaauuuuuuuuuu
auuuugcaauugguuuuuuauauuuucc(poly(A))
```

GREY = RSE    Green = URE    Blue = CSE (CSE4)

**Figure 1.4 The 3'UTR of SFV4 genome.** The Uracil rich element (URE) and conserved sequence element (CSE) are uracil and adenine rich and are known to bind host HuR. The repeated sequence elements have no confirmed function. Sequence taken from NCBI Accession Number: NC\_003215.1.

#### 1.4.1.6 Alphavirus replication in mammalian cells

In mammalian cells alphaviruses have a life cycle consisting of attachment, entry, replication, assembly of virions and budding off the plasma membrane. The alphavirus virion binds to host cell receptors via E2. Interaction with host-cell receptors induces conformational changes of the E1-E2 spikes (Li *et al.*, 2010). Following clathrin-dependent receptor-mediated endocytosis (De Tulleo and Kirchhausen, 1998), the virion enters the cell encapsulated in an endosome. Alphaviral surface proteins embedded in endosome membrane form cation permeable pores leading to a net loss of

cations to the cytoplasm and lowering the pH of the endosome (Wengler, Koschinski and Dreyer, 2003). The low pH of the endosome induces further conformational change in the E1-E2 glycoprotein heterodimer spikes resulting in their dissociation and the exposure of the fusion loop of E1 (Li *et al.*, 2010; Gibbons *et al.*, 2004). The fusion loop inserts in the endosomal membrane and initiates fusion of the viral lipid membrane with the endosomal membrane (Vaney, Duquerroy and Rey, 2013; Kielian and Rey, 2006). Of note, the low pH may not be required for fusion in mosquito cells (Hernandez, Luo and Brown, 2001). Post fusion the NC is released in to the cytoplasm where it disassembles, possibly through interaction with ribosomes (Wengler and Wurfner, 1992) or through priming for disassembly from the acidic environment of the endosome during cell entry (Melton *et al.*, 2002; Wengler and Gros, 1996).

Depending on the alphavirus species and strain, the full genomic RNA is translated to produce either one non-structural polyprotein; P1234, or two non-structural polyproteins; P1234 and P123. The latter is a result of an opal termination codon that exists to the immediate 3' of the nsP3 ORF sequence with a readthrough efficiency of around ~15%. Termination of translation at this sequence yields a truncated form of the full non-structural polyprotein. SFV4 contains an arginine codon instead of the opal stop codon which is present in other strains of SFV such as SFV A7(74). Insertion or deletion of the opal stop codon in various strains of alphaviruses have been shown to affect replication, pathology and tissue specificity (Jones *et al.*, 2017).

Alphavirus replication occurs in the cytoplasm. Replication complexes form on smooth membranes (spherules) within type 1 cytopathic vacuoles (CPV-1) (Kujala *et al.*, 2001). In sindbis virus (SINV) and SFV infection these are thought to initially develop at the plasma membrane and then move more internally in to the cytoplasm via endosomal-lysosomal compartments (Frolova *et al.*, 2010). These structures help prevent recognition of viral dsRNA (a replication intermediate) from the cell innate immune defences which recognise dsRNA as pathogen associated molecular pattern (PAMP) (Akira and Hemmi, 2003).

The non-structural polyprotein is cleaved in cis by the papain-like cysteine protease at the C-terminal domain of nsP2. The full polyprotein, the partially cleaved polyprotein intermediates and the individual nsPs are all involved viral replication (Pietla, Hellstrom and Ahola, 2017). A replication complex consisting of P123 polyprotein and nsP4 synthesise minus-strand RNA early in infection. As P123 is cleaved in to individual viral proteins a replication complex of the individual nsPs forms the replicase responsible for plus-strand viral RNA synthesis (Pietla, Hellstrom and Ahola, 2017). This ensures plus-strand genomic RNA and plus-strand subgenomic RNA are produced later in cellular infection, with subgenomic RNA in roughly a three-fold excess to full genomic RNA (Pietla, Hellstrom

and Ahola, 2017). A role for RNase-L in the switch from negative to positive sense viral RNA synthesis has also been postulated (Sawicki *et al.*, 2003). Cleavage of the polyproteins to yield individual nsPs is required for some of the individual viral nsP functions (other than replicase formation) during infection (Gorchakov *et al.*, 2008).

Association of the replication complexes with membranes in the CPV1 spherules is required for their activity and hence visualisation of nsP3 during infection identifies the location of the replication complexes (Pietla, Hellstrom and Ahola, 2017). The compact nature of the spherules prevents most host proteins interacting with the active viral RNA replication however a small number of host factors can be identified within replication spherules. Host G3BP1 and G3BP2 are present in replication spherules and interact with the C-terminal domain of nsP3 (Pietla, Hellstrom and Ahola, 2017). This interaction also inhibits stress granule formation during infection (Fros *et al.*, 2012). Other host proteins known to interact with the viral RNA and viral RNA replicase complexes include PCBP1, hnRNP M, hnRNP A1, hnRNP K and hnRNP C (Varjak *et al.*, 2013). Furthermore, hnRNP A1 has been shown to play significant roles in SINV RNA synthesis and bind to the viral genomic and subgenomic promoters (Lin *et al.*, 2009; Gui *et al.*, 2010).

The N-terminal domain of nsP2 utilises its RNA triphosphatase activity to prepare viral RNAs for 5'capping by removing the 5' gamma-phosphate of nascent viral RNAs (Vasiljeva *et al.*, 2000). Nsp1 anchors in the membranes of replication complexes and facilitates the 5'capping and cap methylation of genomic and subgenomic viral RNAs using its innate guanine-7-methyltransferase and guanyltransferase enzymatic activities (Cross, 1983; Ahola *et al.*, 1999; Jose, Snyder and Kuhn, 2009).

Host HuR protein binds to uracil rich elements in the 3'UTR of full genomic and subgenomic positive strand viral RNA. This stabilises the viral RNA and may facilitate translation of the viral polyproteins. HuR is then bound to the viral RNA and so builds-up in the cytoplasm.

Following the replication of the subgenomic RNA the structural polyproteins, CP-p62-6K-E1 and CP-p62-TF, are produced in large quantities. The capsid protein is released from these polyproteins by autoproteolysis and the new N-terminus signals the sequence for insertion in to the ER membrane. The translated p62 interacts with folded E1 in the ER to form p62-E1 heterodimers (Ziemiecki, Garoff and Simons, 1980; Li *et al.*, 2010). Three p62-E1 heterodimers interact and develop in to trimeric p62-E1 spikes which translocate to the Golgi apparatus. In the trans-Golgi network p62 is cleaved by furin to release E3, forming (E1-E2-E3)<sub>3</sub> spikes and subsequent (E1-E2)<sub>3</sub> spikes at neutral pH, priming the E1-E2 trimeric spike for fusion at low pH (Mulvey and Brown, 1996; Vaney, Duquerroy and Rey, 2013; Voss *et al.*, 2010; Sjoberg, Lindqvist and Garoff, 2011). The E1-E2 trimeric spikes are transported in vesicles to the plasma membrane.

In the cytoplasm newly synthesised full genomic RNA interacts with capsid protein via a packaging RNA signal sequence in the viral RNA to form the nucleocapsid. Residues of C in the nucleocapsid interact with E2 at the plasma membrane during the formation of virions and help drive budding (Tang *et al.*, 2011). Newly infectious alphavirus particles are released in to the extracellular space.

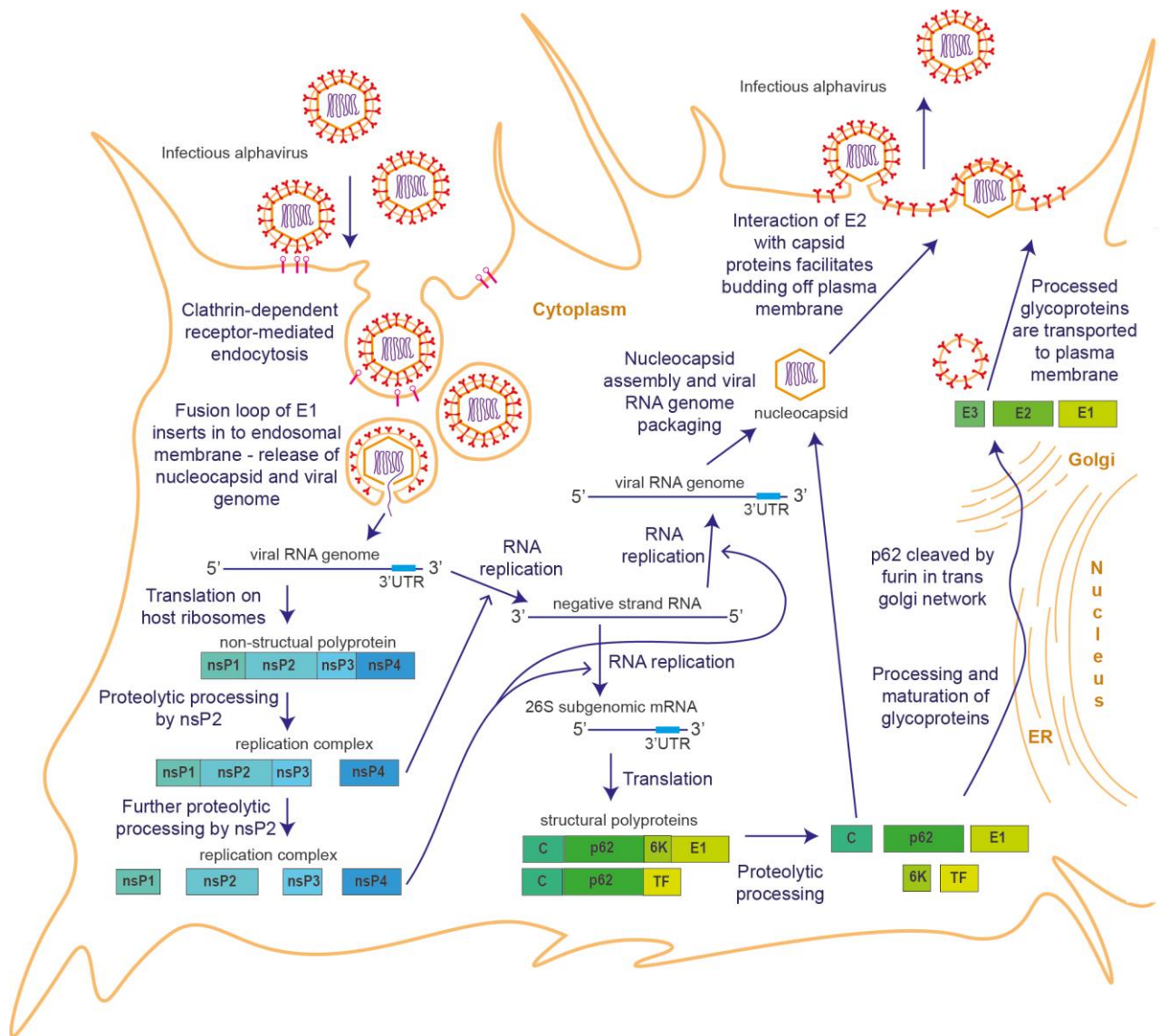


**Figure 1.5 Alphavirus infection of a murine fibroblast cell.** Following endocytosis, the viral genome is released in to the cytoplasm where host ribosomes translate the non-structural polyprotein. Replicase complexes formed from the nsPs replicate negative strand RNA and subsequently full genomic and subgenomic positive strand RNA. The structural proteins translated from the subgenomic RNA are processed and matured in the ER and golgi apparatus and exported to the host cell membrane. Newly formed full genomic RNA interacts with capsid protein forming the nucleocapsid. The nucleocapsid interacts with the processed glycoproteins at the cell membrane to drive budding and virion release.

## **1.5 Herpesviridae**

The *Alpha*-, *Beta*- and *Gamma-herpesvirinae* are the three subfamilies of viruses that exist in the *Herpesviridae* family, part of the *Herpesvirales* order. A key feature of herpesviruses is their ability to elicit lytic replication while also establishing latency in a subset of host cells (Ackermann, 2006).

### **1.5.1 *Alphaherpesvirinae* and *Betaherpesvirinae***

Herpes simplex virus type 1 (HSV-1), herpes simplex virus type 2 (HSV-2) and varicella-zoster virus (VSV) are the clinically relevant human herpesviruses in the *Alphaherpesvirinae* subfamily (Enquist *et al.*, 1999). These viruses establish latent infection in the peripheral nervous system of the host remaining there until death of the host and reactivating lytic replication intermittently.

Human herpesviruses 6 and 7 (HHV-6 and HHV-7) and cytomegalovirus (CMV) are the clinically relevant human herpesviruses in the *Betaherpesvirinae* subfamily (Santos, 2016). CMV infection can result in several end-organ diseases such as hepatitis, gastrointestinal ulceration and pneumonitis (Clement and Humphreys, 2019).

### **1.5.2 *Gammaherpesvirinae***

There are four genera in the *gammaherpesvirinae* subfamily; *Lymphocryptovirus*, *Macavirus*, *Percavirus* and *Rhadinovirus*. The two clinically relevant human viruses in this subfamily are human gammaherpesvirus 8 (HHV-8, also known and referred to in this report as Kaposi's sarcoma associated herpesvirus (KSHV)) of the *Rhadinovirus* genus and human gammaherpesvirus 4 (HHV-4, also known and referred to in this report as Epstein-Barr virus (EBV)) of the *Lymphocryptovirus* genus. The host range for gammaherpesviruses is diverse including mammals, birds and amphibians.

Many gammaherpesviruses are of importance in veterinary medicine. For instance, the alcelaphine gammaherpesvirus 1 (AIHV-2) and ovine gammaherpesvirus 2 (OvHV-2) of the *Macavirus* genus are both agents of malignant catarrhal fever (MCF), a fatal lymphoproliferative disease, in wildebeest and sheep respectively (Mushi and Rurangirwa, 1981; Ackermann, 2005; Bildfell *et al.*, 2017). Most information regarding host interactions during infection with gammaherpesviruses comes from research using HHV-4, HHV-8 and murine gammaherpesvirus 68 (MHV-68).

KSHV is causative agent of four human diseases; Kaposi's sarcoma, multicentric Castleman's disease, KSHV inflammatory cytokine syndrome and primary effusion lymphoma (Taylor and Blackbourn, 2011). Kaposi's sarcoma was first identified in AIDS patients and generally only presents in immunocompromised patients. Multicentric Castleman's disease is a lymphoproliferative disorder and primary effusion lymphoma is an aggressive B-cell lymphoma (Ali and Rayes-Danan, 2016).

Epstein–Barr virus (EBV) is one of the most common viruses found in humans, infecting B cells and epithelial cells (Ackermann, 2006). EBV is a causative agent for several lymphoproliferative diseases such as Hodgkin’s lymphoma, hemophagocytic lymphohistiocytosis and Burkitt’s lymphoma. EBV can also cause hairy leukoplakia and central nervous system lymphomas in immunocompromised patients (Taylor and Blackbourn, 2011).

#### **1.5.2.1 MHV-68**

Murid gammaherpesvirus 68 is in the *Rhadinovirus* genus and considered a model virus for studying the pathogenesis of gammaherpesviruses in mammalian host cells. Despite this MHV-68 was first isolated from bank voles (*Myodes glareolus*) in Slovakia and then passaged through a mouse brain (Terry *et al.*, 2000; Blaskovic *et al.*, 1981). While both *Myodes glareolus* of the *Cricetidae* family and *Mus musculus* of the *Muridae* family are both from the *Rodentia* Order, these species are from different families. Four other murine gammaherpesvirus strains were isolated at the same time in Slovakia as MHV-68 (Blaskovic *et al.*, 1981). These murine herpesviruses were shown to be closely antigenically related by complement fixation and viral neutralization experiments (Svobodova *et al.*, 1982). After initially being classed as an alphaherpesviruses (Svobodova, Blaskovic and Mistrikova, 1982) they, along with MHV-68, were later sequenced and identified as gammaherpesviruses (Virgin *et al.*, 1997). MHV-68 was then selected for use in future research.

#### **1.5.2.3 Genome and virion structure of gammaherpesviruses**

The gammaherpesviruses have a linear, monopartite, double-stranded DNA (dsDNA) genome of ~180 kbp. The genome is encapsulated by capsid proteins to form the nucleocapsid. This is surrounded by an amorphous protein layer called the tegument (Liu and Zhou, 2007). Herpesviruses also have an outer lipid envelope derived from the host cell membrane. The genome contains internal and terminal reiterated DNA sequences that act as origins of replication (White, Calderwood and Whitehouse, 2003). The large size of the dsDNA genome allows gammaherpesviruses to encode most of their viral proteins from individual DNA promoters with individual transcription start sites (Ueda, 2018). These genes are transcribed in to separate mRNA transcripts encoding 5’ and 3’ UTRs and a poly(A) tail.

Some of the open reading frames (ORFs) overlap and some of the coding regions of genes overlap within the same ORF. Furthermore, some ORFs can be encoded from more than one promoter and many of the ORFs are antisense to each other (Arias *et al.*, 2014). These features maximize the coding



capacity of the genome size allowing for a relatively large number of viral proteins with high capacity for gene regulation compared to the 10 individual viral proteins encoded by alphaviruses. Most genes are not spliced but some splicing and splice variants do occur (Majerciak and Zheng, 2016).

During the evolution of gammaherpesviruses many host genes have been taken and incorporated in to the viral genomes. For instance, KSHV encodes a complement binding protein, cyclin-D, BCL-2, a G protein coupled receptor, Flice inhibitory protein and interferon regulatory factor, all of which are believed to have originated from the host genome (Cannon, 2007; Ueda, 2018). MHV-68 encodes over 80 genes, ORF 4-69 have homologs in KSHV and M1-M14 are believed to be MHV-68 specific genes although similar proteins exist in other gammaherpesviruses (Virgin *et al.*, 1997).

#### **1.5.2.4 Replication of gammaherpesviruses**

Infection of laboratory mice with MHV-68 via intranasal inoculation initiates with virus replication in the lung that yields high titres of infectious virus. Concomitant with lytic infection, the virus establishes latent infection within epithelial and B cells in the lungs. From the lungs, the virus spreads to the spleen where latency is established within B cells (Hughes *et al.*, 2010).

Different glycoproteins mediate attachment and entry of gammaherpesvirus virions to different cell types. Some of these glycoproteins are indispensable for viral entry to certain cell types whereas others are not. For instance the homologs gp150, K8.1 and gp350 from MHV-68, KSHV and EBV respectively, mediate efficiency of attachment and entry of virion particles to specific cell types such as B cells but are not indispensable for replication (Carel *et al.*, 1990; Stewart *et al.*, 2004; Luna *et al.*, 2004). Host cell factors utilised by KSHV for cell entry include heparan sulfate (HS), integrins ( $\alpha 3\beta 1$ ,  $\alpha V\beta 3$  and  $\alpha V\beta 5$ ), and EphA2 receptor tyrosine kinase (EphA2R) (Kumar and Chandran, 2016).

Following cell entry, the virus capsid protein is uncoated, and the DNA enters the host cell nucleus. Viral DNA is synthesised in the nucleus and viral mRNAs are exported out the nucleus to be translated on host ribosomes (Flemington, 2001). The viral genes have been appointed to three groups depending on the time of expression during lytic infections. These are immediate-early, early and late genes but most of the viral genes are still expressed at lower concentrations at other times points (de Mello, Bloom and Paixao, 2016). Capsid proteins enter the nucleus and combine with viral genomes to form new nucleocapsids (Peng *et al.*, 2010). The nucleocapsid buds through the nuclear membrane and then also through cellular membranes of the golgi apparatus before leaving the cell.

Gammaherpesviruses also establish latent infection in a subset of host cells. After KSHV lytic infection the virus enters lymphocytes and via expression of the viral latency-associated nuclear antigen (LANA) establishes latency (Wei *et al.*, 2016). Gammaherpesvirus genomes exist as circular pieces of DNA called episomes which are tethered to cellular chromosomes via LANA (or the LANA homolog in MHV-68) (Ponnusamy *et al.*, 2015). External stimuli such as inflammation are believed to stimulate the virus to re-enter lytic replication. ORF50 replication transactivation activator (RTA) is known to be the primary viral protein responsible for lytic reactivation (Wu *et al.*, 2000). Following expression of RTA, it activates synthesis of a cascade of viral proteins that drive viral replication.

## **1.6 Mammalian mRNA**

### **1.6.1 Mammalian mRNA maturation**

The process of mammalian mRNA maturation includes capping, splicing and polyadenylation to yield mature mRNA. Within the cell these processes do not occur independently but rather begin co-transcriptionally the moment the new nascent immature pre-mRNA emerges from the RNA polymerase (Carmody and Wente, 2009).

Mammalian mRNA is synthesised during host gene transcription by RNA polymerase II. This polymerase recognizes a core promoter region just upstream of transcription start sites. The polymerase assembles on the promoter with the assistance of host transcription factors that bind this region. Transcription factors also bind proximal and distal promoter sequences that lie further upstream of the transcription start site (Martinez, 2002). Transcription initiation precedes phosphorylation of the C-terminal domain (CTD) of RNA polymerase II (Lee and Young, 2000) leading transcription elongation and the synthesis of a nascent pre-mRNA transcript (Casamassimi and Napoli, 2007).

The mammalian capping enzyme complex is recruited to the pre-mRNA via the phosphorylated CTD of RNA polymerase II and adds a guanine nucleotide via a 5' to 5' triphosphate linkage which is then methylated by methyl transferase. The cap not only inhibits RNA degradation from 5' to 3' exonucleases but it is also bound by the cap-binding complex (CBC) (Coller and Parker, 2004). The CBC is recognized by splicing proteins, mRNA export proteins and the translation initiation factor eIF4E (Pabis *et al.*, 2013). The pre-mRNA undergoes splicing to remove a selection or all of the introns in the pre-mRNA. This is most commonly catalysed by the spliceosome (a complex of small nuclear ribonucleoproteins (snRNP's) (Zheng, 2004).

A ~250 nt or longer poly(A) tail is synthesised on the 3' end of the mRNA by polyadenylate polymerase and poly(A) binding protein nuclear 1 (PABPN1) (Eckmann, Rammelt and Wahle, 2011). Poly(A) binding protein cytoplasmic 1 (PABPC1) and poly(A) binding protein cytoplasmic 4 (PABPC4) bind the poly(A) tail in the nucleus and facilitates nuclear mRNA export and subsequent mRNA stability and translation (Goss and Kleiman, 2013).

Pre-mRNA is also bound by heterogeneous ribonucleoprotein particles (hnRNPs) which facilitate the proper processing and folding of pre-mRNAs. Some hnRNPs release host mRNA at the nuclear pore complex (NPC) while others are exported along with the mature mRNA and then shuttle back to the nucleus from the cytoplasm (Zheng, 2004).

The nuclear export of mRNA is achieved through two main pathways utilising complexes of nuclear export proteins, some of which initially bind the nascent pre-mRNA as it undergoes maturation in the nucleus (Amaral *et al.*, 2008).

### **1.6.2 mRNA export in mammalian cells**

Bulk mRNA nuclear export is achieved through the nuclear export factor 1 (NXF1) pathway. NXF1 and its binding partner NXT1 co-transcriptionally bind to ribonucleoprotein complexes on mRNA via recruitment by REF of the Transcription Export Complex (TREX) (Carmody and Wentz, 2009). The NXF1-NXT1-mRNA-ribonucleoprotein complex is brought to the nuclear pore complexes by ribonucleic acid export 1 (RAE1) which shuttles between the nucleus and cytoplasm while predominantly localising in the nucleus. RAE1 brings NXF1-NXT1-mRNP to the nuclear envelope by interacting with a Gle2p-binding sequence (GLEBS motif) in the N-terminus of NUP98 in the nuclear pore complexes (Pritchard *et al.*, 1999). NXF1 directly interacts with NUP98 through two binding domains, one located on the C terminus and the other formed across the binding site of NXF1-NXT1 (Blevins *et al.*, 2003). Once on the cytoplasmic side of the nuclear envelope NXF1 is actively transported back to the nucleus leaving the mature mRNA in the cytoplasm ready to interact with ribosomes.

A second pathway utilizes chromosome region maintenance 1 (CRM1) but requires an adaptor protein such as HuR to bind to the mRNA and interact with CRM1 (Watanabe *et al.*, 1999; Brennan, Gallouzi and Steitz, 2000). This pathway exports a subset of mRNAs across the nuclear envelope. CRM1 is an active pathway, driven by the interaction of CRM1 with RanGTP which is hydrolysed to RanGDP on the cytoplasmic side of the nuclear pore (Askjaer *et al.*, 1998).

### 1.6.3 mRNA decay

Mammalian mRNA is subject to degradation immediately following transcription. Different transcripts will have varying half-lives due to a range of *cis* acting RNA sequences and RNA secondary structures. These sequences are often located in the 5'UTR and 3'UTR but can occur in the coding regions as well (Xu, Chen and Shyu, 1997; Yamashita *et al.*, 2005). A range of *trans* acting factors interact with these sequences. RNA secondary structures inhibiting degradation include stem loop structures at the 5' and 3' which prevent access to host cell RNA decapping and deadenylation machinery and exonucleases (Conrad *et al.*, 2007). Furthermore, identical transcripts may have different half-lives at different times depending on the physiological state of the cell and a range of *trans* acting RNA turnover proteins.

In mammalian cells deadenylation is usually the rate-limiting step unless the mRNA is cleaved by an endonuclease such as RNase-L (Chen and Shyu, 2011). Deadenylation can be orchestrated by two main pathways in humans. A super complex of the PAN2-PAN3 complex and CCR4-NOT complex containing CAF1 binds PABPC1 and shortens poly(A) tail length in deadenylation reactions. More commonly however poly(A) specific ribonuclease (PARN) is responsible for deadenylation in mammalian cells (Wu *et al.*, 2005). Access for PARN to the 3' end of mRNA is inhibited by the interaction of eukaryotic initiation factors 4E and 4G (eIF4E and eIF4G) with PABPC. However CUGBP1 (amongst other RNA binding proteins) can bind to sequences in the 3'UTR of transcripts and recruit PARN to the poly(A) tail (Moraes, Wilusz and Wilusz, 2007). Sequences in the 3'UTR can also bind microRNAs (miRNAs) that have complementary sequences and recruit the RNA-induced silencing complex which in turn stimulates the PAN2-PAN3 and CCR4-NOT complexes to begin deadenylation of the poly(A) tail (Piao *et al.*, 2010; Fabian *et al.*, 2012).

Once the tail is removed deadenylation-dependent decapping can occur utilising the decapping complex (Chen and Shyu, 2011). The decapping enzymes 1 and 2 (DCP1 and DCP2) catalyse the m<sup>7</sup>G cap removal (Coller and Parker, 2004; Ingelfinger *et al.*, 2002). The transcript is then degraded by the exosome (from 3' end) or XRN1 (from 5' end) (Parker and Song, 2004).

Degradation of mRNA is also actively initiated if an mRNA transcript is deemed as aberrant i.e. contains a premature stop codon, has been spliced incorrectly, or become hyper-polyadenylated to name a few. In these cases the RNA surveillance machinery detects the fault and actively promotes the transcripts degradation by endo- and exo-nucleases (Chang, Imam and Wilkinson, 2007; Houseley, LaCava and Tollervey, 2006; Houseley and Tollervey, 2009; Wang and Pestov, 2011).

#### 1.6.4 Turnover and Translation RNA-binding proteins (TTR-RBPs)

The rate of mRNA decay is also heavily influenced by RNA binding proteins which directly bind mRNA and inhibit or stimulate their degradation. These *trans*-acting proteins often bind to AU-rich elements (AREs) in the 3' untranslated (3'UTR) region of mRNA (Xu, Chen and Shyu, 1997). Many of the mRNA transcripts with AREs are involved in immune responses, inflammation, the cell cycle or other response pathways that require rapid and transient control (Barrett, Fletcher and Wilton, 2012; Xu, Chen and Shyu, 1997).

Different RNA-binding proteins will bind different mRNA transcripts dependent on the RNA sequence and RNA secondary structure. The RNA-binding proteins which effect host mRNA translation and turnover were originally termed 'AU-rich element RNA binding proteins (ARE-RBPs)'. This was because RNA binding proteins which affect turnover and translation were initially shown to exclusively bind Uracil and Adenine rich elements, such as the binding of tristetraprolin (TTP) to the pentamer 'AUUUA' (Kedar *et al.*, 2012; Wilusz, Wormington and Peltz, 2001). However, more recent analysis indicates some RNA binding proteins affecting turnover and translation can bind a broader set of sequences and thus the term 'Turnover and translation regulatory RNA-binding proteins (TTR-RBPs)' has been proposed (Pullmann *et al.*, 2007; Pullmann and Rabb, 2014). Mammalian TTR-RBP's elicit their effect on mammalian RNA in a heavily co-ordinated and integrated manner. Many of the TTR-RBPs bind to their own cognate mRNA or the mRNA of other TTR-RBPs and regulate their expression (Pullmann *et al.*, 2007).

The TTR-RBP AUF1 transcribes in to four splice variants with two quasi-RNA recognition motif (RRM) domains which bind AU-rich elements on mammalian mRNA transcripts. Two isoforms, p37 AUF1 and p40 AUF1, bind to AU-rich elements in mRNAs and promote their degradation (Gratacos and Brewer, 2010). TTP also binds AU-rich elements in mRNAs and initiates deadenylation of the RNA transcripts to which it binds by recruitment of the CCR4-NOT deadenylation complex (Fabian *et al.*, 2013). For instance TTP binds to TNF-alpha mRNA and promotes its deadenylation and subsequent degradation (Lai *et al.*, 1999).

##### 1.6.4.1 HuR

In contrast to TTR-RBPs which facilitate mRNA decay, Human Antigen R (HuR, related to Drosophila ELAV (Ma *et al.*, 1996)) binds to AU-rich elements on a subset of mRNAs and inhibits their degradation (Fan and Steitz, 1998; Peng *et al.*, 1998). This process can help regulate core cellular processes e.g. cell

proliferation or the innate immune response (Wang *et al.*, 2000). Predominantly located in the nucleus, HuR utilises a novel HNS sequence in its hinge domain to aid shuttling between the nucleus and the cytoplasm, co-transporting and protecting mRNA transcripts from the nucleus (Fan and Steitz, 1998). Moreover, HuR can bind the same mRNA transcripts as TTR-RBPs that promote degradation such as AUF1 or TTP, developing a dynamic system that changes depending on the given mRNA transcript, physiological conditions and external stimuli (Khalaj *et al.*, 2017; Lal *et al.*, 2004). The protein domains in the mammalian HuR protein can be seen in *figure 1.6*.

Aside from inhibiting mRNA degradation HuR can facilitate mRNA nuclear export via interaction with CRM1, affect mRNA splicing and polyadenylation, and facilitate translation of mRNA via interaction with PABPC (Brennan and Steitz, 2001; Kimura *et al.*, 2004; Izquierdo, 2008). The mRNA of HuR can be regulated by HuR itself and other TTR-RBPs such as TTP. Furthermore, polyadenylation variants of the HuR transcript have been identified which help regulate its half-life (Al-Ahmadi *et al.*, 2009a; Pullmann *et al.*, 2007). The function of HuR has been proposed to be affected by its phosphorylation state and sub-cellular location but these features have not been clearly or conclusively defined (Kim and Gorospe, 2008).

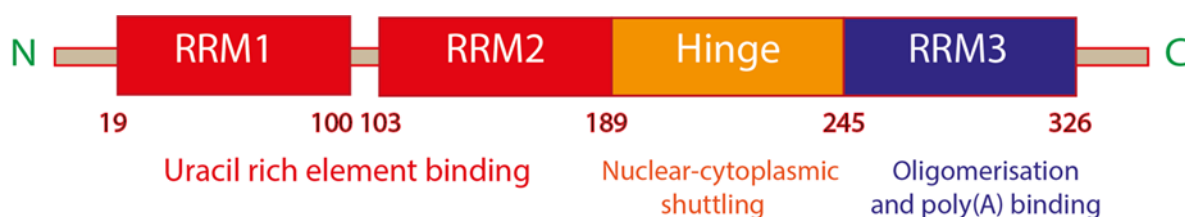


**Figure 1.6 Schematic of the mammalian HuR protein domains.** RRM1 and RRM2 bind uracil and adenine rich regions in mRNAs. The hinge region contains the nuclear localisation and nuclear shuttling signals. The RRM3 is responsible for oligomerisation and interaction with PABPC. The interaction with PABPC facilitates the translation of mRNA to which HuR has bound (Venigalla and Turner, 2012).

#### 1.6.4.2 PABPC

PABPC is technically a TTR-RBP since it binds mRNA and helps regulate mRNA turnover and translation. There are multiple poly(A) binding proteins (PABPs) in mammalian cells, some are tissue specific (tPABP and ePABP) while others are universally expressed (PABPN1, PABPC1, PABPC4) (Goss and Kleiman, 2013). The nuclear PABP, PABPN1, with significant sequence variation to other forms, binds poly(A) tails in the nucleus and stimulates polyadenylate polymerase to extend poly(A) tail length to

~250 nucleotides (Eckmann, Rammelt and Wahle, 2011). The cytoplasmic versions, PABPC1 and PABPC4, are predominantly located in the cytoplasm despite being a nucleocytoplasmic shuttling protein. PABPC is translocated to the nucleus by importin- $\alpha$  which binds to PABPC's RNA recognition motifs when not bound to mRNA (Kumar, Shum and Glaunsinger, 2011). PABPC nuclear build-up has been shown to occur when mRNA export via NXF1 is inhibited and thus it is suggested that PABPC nuclear export is dependent upon mRNA nuclear export (Burgess *et al.*, 2011).

PABPC1 and PABPC4 bind poly(A) tails on mRNA and protect the 3' end of the transcript from exonucleases and deadenylation complexes (Houseley and Tollervey, 2009). The C-terminal domain of PABPC1 also binds the eukaryotic initiation factor 4G (eIF4G) in the translation initiation complex forming a stem-loop structure. This further protects the mRNA ends from degradation and also promotes translation initiation (Goss and Kleiman, 2013; Mangus, Evans and Jacobson, 2003).

## **1.7 Virus inhibition and manipulation of RNA decay pathways**

Viruses of all eukaryotic cells manipulate RNA maturation, mRNA nuclear export and RNA decay pathways. For instance, hepatitis C virus (HCV) utilises host rck/p54, LSm1 and PatL1 for the translation of HCV RNA's and this interaction is mediated via the HCV 5' and 3' UTRs (Scheller *et al.*, 2009). Poliovirus avoids degradation from Xrn1 by forming a RNA cloverleaf secondary structure at the 5' of its genome. This structure binds poly(rC) binding proteins in infected cells which protects the genome from degradation at the 5' end (Kempf and Barton, 2008). Aside from evading or manipulating the host RNA degradation pathways, viruses also seek to inhibit host gene expression by inhibiting transcription, initiating RNA degradation, inhibiting RNA translation or blocking mRNA nuclear export.

### **1.7.1 Host shut-off**

Mammalian detection of viral infection at the cellular level is achieved through pattern recognition receptors (PRRs) including Toll-like receptors and the cytoplasmic receptors MDA5 and RIG-I which recognise pathogen associated molecular patterns (PAMPs) such as viral glycoproteins or viral dsRNA (Akira and Hemmi, 2003; Takeuchi and Akira, 2008). When a mammalian cell detects a virus one of its primary responses is the production of Interferons, including type I (IFN- $\alpha$  X 12 subtypes, IFN- $\beta$ , IFN- $\omega$ , IFN- $\kappa$ , and IFN- $\epsilon$ ), type II (IFN- $\gamma$ ), and type III (IFN- $\lambda$  X 3 subtypes) and the subsequent activation of the IFN stimulated genes (ISGs) (Gonzalez-Navajas *et al.*, 2012).

Following detection of viral infection by PRRs, host protein kinase R (PKR) is activated which phosphorylates eukaryotic initiation Factor-2 (eIF-2) which then forms an inactive complex with eukaryotic initiation factor 2B (eIF-2B), thereby inhibiting viral and host AUG translation initiation. Furthermore, gene expression of IFNs leads to activation of 2'-5'-oligoadenylate synthetase 1, an enzyme which is further activated by dsRNA to synthesize 2',5'-oligoadenylates which in turn activates RNase L. RNase L forms a dimer and partially degrades global RNA (Ryman *et al.*, 2002). The RNA degradation products stimulate IFN- $\beta$  in a positive feedback loop. IFNs also stimulate a wide range of interferon stimulated genes (ISGs) through signalling cascades such as the JAK-STAT pathway (Joshi *et al.*, 2010). Many of the genes which are upregulated in this way are involved in modulating anti-viral proteins such as RNase L.

In a contrast to host cells inhibiting gene expression as part of an anti-viral response, many viruses themselves attempt to shut-off host gene expression. This process has likely evolved to inhibit the anti-viral response of host cells such as expression of IFNs and ISGs.

#### **1.7.1.1 muSOX**

The gammaherpesviruses have been shown to achieve significant loss of host cell mRNA transcripts during lytic infection and this is attributed to the viral mu-SOX protein (homologs SOX in KSHV and BGLF5 in EBV) (Rowe *et al.*, 2007). muSOX (and homologs) have two distinct domains that are genetically separable; one with DNase activity is used to help package the viral genome and the second is associated with host-shut off activity (Glaunsinger, Chavez and Ganem, 2005). muSOX distribution is predominantly nuclear during infection however its cytoplasmic localisation is required for it to elicit host mRNA turnover. muSOX also causes the relocalisation of PABPC to the nucleus. How SOX orchestrates host mRNA degradation is discussed in further detail in *chapters 3 and 5*.

#### **1.7.2 Virus utilisation of host TTR-RBPs**

Viruses utilise and manipulate the roles of host TTR-RBPs. For instance, Epstein-Barr virus (EBV) utilises AUF1 in a complex; C promoter binding factor 2 (CBF2), which binds to the EBV genome to enhance transcription of genes required for EBV-induced immortalization of B lymphocytes (Fuentes-Panana *et al.*, 2000). During infection with alphaviruses the host HuR protein is utilised to enhance infection.



### 1.7.2.1 HuR in alphavirus infection

HuR binds to alphavirus RNA via a conserved sequence element (CSE) and a uracil rich element (URE) just upstream of the poly(A) tail in both mosquito C6/36 and mammalian cells (Sokoloski *et al.*, 2010; Dickson *et al.*, 2012). The absence of a URE in the 3'NTR of chikungunya virus (CHIKV) and ross river virus (RRV) is compensated by the presence of novel repeated sequence elements in the 3'NTR which HuR has been shown to bind to (Dickson *et al.*, 2012). During alphavirus infection the distribution of HuR changes from predominantly nuclear to predominantly cytoplasmic. Although the mosquito HuR homolog (aeHUR) binds to the 3'NTR of alphaviruses, no significant change in its sub-cellular location is observed, probably because it is already co-localised to the nucleus and cytoplasm in non-infected cells (Sokoloski *et al.*, 2010). The relocalisation in mammalian cells is achieved in part by a change in the phosphorylation state of HuR. The binding of HuR to viral transcripts is likely to protect viral transcripts from degradation. In addition the depletion of HuR from the nucleus may aid in degradation of host mRNA and thus host shutoff of protein production (Barnhart *et al.*, 2013).

The importance of HuR binding the 3'NTR of alphaviruses has been studied extensively in the context of SINV. Using a C6/36 mosquito cell lysate deadenylation assay it was shown that the presence of the URE/CSE from SINV, VEEV, Eastern equine encephalitis virus (EEEV), Western equine encephalitis virus (WEEV) and SFV inhibit deadenylation for up at least 9 minutes of mock mRNA's compared to controls (Sokoloski *et al.*, 2010; Dickson *et al.*, 2012). The mechanism by which alphaviruses protect their transcripts by binding HuR has not been fully elucidated in mammalian cells. The inhibition of deadenylation has been shown in mosquito cell extracts in respect to SINV but this was not conclusively shown in mammalian cells.

In HuR RNAi depleted mammalian (293T) and aeHUR RNAi depleted mosquito cells (Aag2) SINV viral RNA was shown to have significantly shorter half-lives compared to controls (Sokoloski *et al.*, 2010). Furthermore, a 10-fold and 5-fold decrease in SINV viral growth was observed in mammalian and mosquito cells which were depleted (via RNAi) of HuR and aeHUR respectively. This suppression was observed to the same extent when infection with SINV with a deleted URE was analysed. Importantly infection of SINV-ΔURE in HuR reduced 293T or aeHUR reduced Aag2 cells did not have an accumulative repressive effect on viral growth, suggesting these elements are acting synergistically rather than individually (Sokoloski *et al.*, 2010).

Since HuR is a host cell protein it functions to protect the transcripts of a subset of host cell transcripts. Therefore, one would hypothesise that depleting the host cell nucleus and the nuclear mRNA transcripts of HuR, would reduce the stability of those host cell transcripts that bind HuR. This is seen

in the context of SINV infection whereby the sequestration of HuR in the cytoplasm has resulted in the significant increase in decay of a sub-set of host mRNA's in mammalian cells (Barnhart *et al.*, 2013).

#### **1.7.2.2 PABPC in viral infection**

Due to its roles in host mRNA stability and initiation of translation, poly(A) binding protein C (PABPC) is targeted by a range of viruses in order to inhibit host cell protein production. One way this is achieved is by direct cleavage of the protein by protease 3C of the Norovirus (Kuyumcu-Martinez *et al.*, 2004) amongst others from the *caliciviridae* family, and by proteases 2A and 3C of the poliovirus (Rivera and Lloyd, 2008) amongst others of the *picornaviridae*. Another strategy adopted by Rubella virus utilises its capsid protein to bind to the C-terminal half of PABPC so that it cannot interact with translation initiation factors (Ilkow *et al.*, 2008). The diverse set of viruses that target PABPC in this way strongly suggests that partially/fully inhibiting PABPC function is beneficial to virus replication in general. This suggests the nuclear build-up of PABPC observed during infection with a range of *herpesviridae*, *bunyaviridae* and *reoviridae*, namely; herpes-simplex virus 1 & 2 (Dobrikova *et al.*, 2010; Salaun *et al.*, 2010), epstein-barr virus (Park *et al.*, 2014), kaposi's sarcoma herpes virus (Covarrubias *et al.*, 2009), bunyamweravirus and rotavirus (Harb *et al.*, 2008) is a direct effect of viral proteins in an attempt to promote host shut-off. PABPC also builds up in the nucleus following a block in mRNA nuclear export (Burgess *et al.*, 2011).

### **1.8 General Aims**

The general aim of this study was to investigate the significance of the URE of the SFV4 3'UTR during infection of mammalian cells. A secondary general aim was to assess the role of PABPC in the host shut-off seen during in MHV-68 infection of mammalian cells.

# Chapter 2

## Materials and Methods

## **2.1 Cell culture**

### **2.1.1 Mammalian cell culture maintenance**

All tissue culture was performed in a Class II Biological Safety cabinet under aseptic conditions. BHK-21 and NIH/3T3 cells were obtained from long-term stocks of Dr.E Ebrahimi, University of Liverpool for MHV-68 experiments or from long term-term stocks of Dr. R Fragkoudis, The Pirbright Institute for SFV4 experiments.  $\alpha\beta$ RKO cells were from long-term stocks of Dr.E Ebrahimi, University of Liverpool.

#### **Baby hamster kidney fibroblasts (BHK-21 cell line)**

BHK-21 cells [C-13] (ATCC CCL-10™) were purchased from American Type Culture Collection (ATCC) and used for titration of MHV-68 and rSFV4 virus stocks and for rSFV4 propagation from icDNA plasmids. BHK-21 cells were maintained in Glasgow's minimal essential medium with high-glucose and L-glutamine (GMEM, Gibco) supplemented with 10% (w/w) new born calf serum (NBCS, Gibco), 10% (w/w) tryptose phosphate broth (TPB, Gibco), penicillin (100 U/ml) and streptomycin (100 µg/ml). This medium will be referred to as complete GMEM-10 (cGMEM-10).

#### **Murine Fibroblasts (NIH/3T3 cell line)**

Murine NIH/3T3 cells (ATCC CRL-1685) were used for cell culture experiments as a model mammalian host-cell with a functional IFN system. For experiments involving SFV4, NIH/3T3 cells were maintained in Dulbecco's Modified Eagle's Medium (DMEM, Gibco) with glucose (4500 mg/L) and L-Glutamine (584 mg/L) supplemented with 10% newborn calf serum (NBCS, Gibco), penicillin (100 U/ml) and streptomycin (100 µg/ml). This will be referred to as complete DMEM-10 (cDMEM-10). Prior to use, NBCS was decomplexed by heating to 56 °C for 30 minutes. For experiments involving MHV-68, NIH/3T3 cells were maintained in the same conditions, but 10% heat-inactivated foetal calf serum (FCS, Gibco) was used instead of NBCS.

#### **Interferon alpha/beta receptor null murine fibroblasts (IFN $\alpha\beta$ RKO cell line)**

Interferon alpha/beta receptor null (IFN  $\alpha\beta$ RKO) cells lack interferon alpha beta receptors so have a defective Type 1 IFN system (Muller *et al.*, 1994). These cells were obtained from IFN $\alpha/\beta$  KO 129/Sv mice embryo fibroblasts (Dr. Ebrahimi, Personal Communications). The IFN $\alpha\beta$ RKO cells were maintained in the same medium as the NIH/3T3 cells. Virus working stocks for MHV-68 and MHV-68 ORF37stop viruses were obtained by infecting  $\alpha\beta$ RKO cells with corresponding sub-master virus stocks.

### **2.1.2 Subculture of mammalian cells**

Mammalian cells were maintained in sterile T175 cm<sup>2</sup> tissue culture flasks at 37 °C in a humidified atmosphere of 5% CO<sub>2</sub>. Cells were sub-cultured when they reached 80-90% confluence. At this point, the culture medium was removed, and cells were washed with either 10 ml of sterile phosphate buffered saline (sPBS) for SFV4-related work or versene for MHV-68-related work. After removal of the sPBS or versene, 5 ml of trypsin-EDTA (0.25%, Gibco) was added to the cells and they were incubated at 37 °C for 1-3 minutes until the cells detached from the plastic surface. The trypsin-EDTA was neutralised by the addition of 10 ml of complete medium and centrifuged at 400 x g at room-temperature for 5 minutes to pellet the cells. The supernatant was then discarded, and the cell pellet dislodged and resuspended in 10 ml of complete medium. The cells were diluted 1 in 10 in sPBS, evenly mixed and 10 µl with trypan blue exclusion assay was used to calculate the concentration of cells per millilitre using a Neubauer haemocytometer. The cells were then seeded into 175 cm<sup>2</sup> tissue culture flasks to maintain a stock of cells, or into 6-well, 24-well or 96-well plates for experiments. Cells were passaged up to 30 times before fresh lower passage aliquots were resuscitated from frozen stocks.

### **2.1.3 Cryopreservation and resuscitation of cell stocks**

#### **Freezing cells for generation of stocks**

Frozen stocks for all cell lines were prepared and stored in liquid nitrogen. Briefly, cells were trypsinised during their exponential growth phase at 75-80% confluency and counted using a Neubauer haemocytometer. Cells were then centrifuged at 400 x g for 5 minutes at room temperature and the supernatant discarded. The cells pellet was then re-suspended in freezing medium (92.5% (w/w) c-DMEM-10 for NIH/3T3 and αβRKO cells or cGMEM-10 for BHK-21 cells and 7.5% (w/w) dimethyl sulfoxide (DMSO, Sigma Aldrich)) to give a concentration of 5 x 10<sup>6</sup> cells/ml. Aliquots of 1ml were then placed in cryovials (Nunc) and transferred to a Cool-Cell alcohol-free chamber (Corning) and placed at -80 °C. The Cool-Cell chamber controls temperature reduction at a rate of -1 °C per minute. After 24 hours the cells were transferred to a vapour-phase of a liquid nitrogen tank for long-term storage.

#### **Thawing cells from frozen stocks**

Cells were taken from liquid nitrogen and placed on dry ice until they were thawed by placing the vial in a 37 °C water bath. The cells were then added to 10 ml medium and centrifuged at 400 x g for 5 minutes to remove freezing medium. The cell pellet was then resuspended in 4 ml of pre-warmed

complete medium, transferred to a 25 cm<sup>2</sup> (Nunc) flask and incubated at 37 °C with 5% CO<sub>2</sub> until 80-90% confluent. Cells were then passaged as described above (Section 2.1.2).

## **2.2 Generation of recombinant SFV4 infectious complementary DNA plasmids**

Infectious SFV4 virus was produced from transfecting BHK-21 cells with infectious complementary DNA (icDNA) plasmids encoding the full SFV4 genome under control of a human cytomegalovirus (CMV) immediate-early promoter. An exception was for SFV4(3F)-ZsGreen virus which was propagated from transfected *in-vitro* transcribed mRNA from a pSP6-SFV4(3F)-ZsGreen construct in BHK-21 cells. pCMV-SFV4 virus was previously generated from a full-length icDNA clone of SFV4 virus kindly provided by Professor Andres Merits (University of Tartu, Estonia). All pCMV-rSFV4 virus constructs were generated through molecular cloning to insert mutant or reporter DNA sequences with a pCMV-SFV4 backbone. Two reporter pCMV-SFV4 backbones were utilised in this study: the first with a *Gaussia* luciferase reporter gene engineered under the control of a second sub-genomic promoter (pSFV4-2SG-Gluc); the second was constructed with an enhanced green fluorescent protein (eGFP) gene fused to viral nsP3 (pCMV-SFV4(3F)-eGFP).

### **Design of SFV4 constructs**

The genome organisation of SFV4 constructs used in this study are shown in Chapter 4. Recombinant SFV4 icDNA plasmids containing CSE/URE deletions or additions were designed using ApE plasmid editor (M. Wayne Davis) using the published/known sequences of existing SFV4 plasmid constructs pCMV-SFV4, pSFV4-2SG-Gluc and pCMV-SFV4(3F)-eGFP.

### **Generation and cloning of pCMV-SFV4-2SG-Gluc**

Due to the need for a suitable 5' restriction site before the URE in the 3'NTR of the SFV4 reporter icDNA plasmids, a single *BamH I* site was retained at this position. This modified the sequence of CMV-SFV4-2SG-Gluc. This was achieved by insertion of a synthesised DNA sequence containing a single *BamH I* site and encoding a second sub-genomic promoter and *Gaussia* luciferase gene (2SG-Gluc) inserted in a pCMV-SFV4 backbone immediately after the structural genes. The sequence spanned the 3'NTR and poly(A) tail of the SFV4 icDNA plasmid. The synthesised DNA sequence was supplied in the pUC57 backbone by Genscript. It was excised with *Apa I* and *Bpu 10I* restriction enzymes (Section 2.6.7), run on an agarose gel (Section 2.6.9) and gel purified (Section 2.6.10). The gel purified product was ligated (Section 2.6.8) into pCMV-SFV4 previously digested with restriction enzymes *Apa I* and *Bpu 10I* with FastAP treatment (Section 2.6.7). Five microliters of ligation reaction was transformed into JM109 competent cells (Section 2.5.3), and subjected to mini-prep (Section 2.5.4), restriction digest analysis (Section 2.6.7) and sequencing (Section 2.6.14).

### **Generation and cloning of pCMV-SFV4-2SG-*Gluc* URE/CSE mutants**

The URE/CSE mutant rSFV4 luciferase reporter constructs were generated through recombination of synthesised DNA sequences with the pCMV-SFV4-2SG-*Gluc* backbone. Briefly, the synthesised mutant dsDNA sequences were supplied in pUC57 by Genscript. The sequences corresponded to a modified 3'NTR and poly(A) tail of the SFV4 genome. Sequences were cloned in-to pCMV-SFV4-2SG-*Gluc* and confirmed as described above for the 2SG-*Gluc* insert in pCMV-SFV4 except that a 5' *BamH I* site (located downstream of *Gaussia* luciferase) was utilised instead of a 5' *Apal* site.

### **Generation and cloning of pCMV-SFV4(3F)-eGFP URE/CSE mutants**

Several attempts were unsuccessful to produce the desired construct while attempting to clone URE/CSE mutant sequences into a pCMV-SFV4(3F)-eGFP backbone. Therefore, an alternative approach was taken for the GFP reporter constructs. Briefly, the second sub-genomic promoter and luciferase gene were removed from a selection of pCMV-SFV4-2SG-*Gluc* URE/CSE mutants by digesting with *Apal* and *BamH I* (Section 2.6.7) with FastAP treatment (Section 2.6.7). A pair of oligonucleotides which encode a multiple cloning site (MCS) were subjected to *in-situ* hybridisation to anneal. The annealed oligonucleotide pair was then used to ligate the plasmid ends. Oligos 5'-CACTAGTCCCGGGGCGCGCCG-3' and 5'-GATCCGCGCGCCCCGGGACT-AGTGGGCC-3' were purchased from Eurofins. Briefly, oligos were annealed in a thermocycler by heating to 98 °C for 10 minutes and by gradual cooling to 25 °C over a 45 minute period. Annealed oligos were then digested with *Apal* and *BamH I* followed by enzyme inactivation (Section 2.6.7). Digested oligos were ligated into the digested and FastAP treated pCMV-SFV4 URE/CSE mutant backbones (Section 2.6.8), transformed into JM109 competent cells (Section 2.5.3), and subjected to mini-prep (Section 2.5.4), restriction digest analysis (Section 2.6.7) and sequencing (Section 2.6.14). The addition of a DNA sequence encoding nsP3(3F)-eGFP was achieved by excising the nsP3(3F)-eGFP section of the icDNA SFV4 plasmid from pCMV-SFV4(3F)-eGFP provided by Dr. R Fragkoudis (The Pirbright Institute). Briefly, a selection of the pCMV-SFV4 URE/CSE mutants was digested with *SacI* and *NotI* and FastAP (Section 2.6.7). The nsP3(3F)-eGFP was excised by digesting pCMV-SFV4(3F)-eGFP with *SacI* and *NotI* (Section 2.6.7), resolved through a 1% (w/v) agarose gel electrophoresis (Section 2.6.9), gel purified (Section 2.6.10) and ligated (Section 2.6.8) to each pCMV-SFV4 URE/CSE mutant backbone. Ligation products were then transformed into JM109 competent cells (Section 2.5.3), and subjected to mini-prep (Section 2.5.4), restriction digest analysis (Section 2.6.7) and sequencing (Section 2.6.14).

### **2.3. Generation of virus stocks**

Wild-type and mutant strains of MHV-68 and SFV4 were used in this study (Table 2.1).



**Table 2.1 List of viruses used in this study**

Virus Strain	Virus Name	Source	Modification
<b>SFV4</b>	SFV4-2SG- <i>Gluc</i>	Andres Merits	<i>Gluc</i> reporter gene under the control of a duplicated sub-genomic promoter
<b>SFV4</b>	SFV4-2SG- <i>Gluc</i> -ΔURE	This study	Identical to SFV4-2SG- <i>Gluc</i> with the URE (5'-auuuuuuuuuuuuuuugc-3') deleted from the 3'NTR of the SFV4 genome
<b>SFV4</b>	SFV4-2SG- <i>Gluc</i> -ΔUREΔCSE	This study	Identical to SFV4-2SG- <i>Gluc</i> with the URE (5'-auuuuuuuuuuuuuuugc-3') and 18 bases from the CSE (5'-aauggguuuuuuuuuuu-3') deleted from the 3'NTR of the SFV4 genome
<b>SFV4</b>	SFV4-2SG- <i>Gluc</i> -ΔUREΔ11CSE	This study	Identical to SFV4-2SG- <i>Gluc</i> with URE (5'-auuuuuuuuuuuuuuugc-3') and 11 bases from the CSE (5'-aauggguuuuu-3') deleted from the 3'NTR of the SFV4 genome
<b>SFV4</b>	SFV4-2SG- <i>Gluc</i> -5xURE	This study	Identical to SFV4-2SG- <i>Gluc</i> with 4 additional duplicated URE (5'-auuuuuuuuuuuuuuugc-3') added immediately upstream to the original URE in the 3'NTR of the SFV4 genome
<b>SFV4</b>	SFV4(3F)-eGFP	Andres Merits	Enhanced green fluorescent protein ( <i>eGFP</i> ) was fused to viral nsP3
<b>SFV4</b>	SFV4(3F)-eGFP-ΔURE	This study	Identical to SFV4(3F)-eGFP with the URE (5'-auuuuuuuuuuuuuuugc-3') deleted from the 3'NTR of the SFV4 genome
<b>SFV4</b>	SFV4(3F)-eGFP-ΔCSE	This study	Identical to SFV4(3F)-eGFP with 18 bases from the CSE (5'-aauggguuuuuuuuuuu-3') deleted from the 3'NTR of the SFV4 genome
<b>SFV4</b>	SFV4(3F)-eGFP-ΔUREΔCSE	This study	Identical to SFV4(3F)-eGFP with the URE (5'-auuuuuuuuuuuuuuugc-3') and 18 bases from the CSE (5'-aauggguuuuuuuuuuuc-3') deleted from the 3'NTR of the SFV4 genome
<b>SFV4</b>	SFV4(3F)-eGFP-5xURE	This study	Identical to SFV4(3F)-eGFP with 4 additional duplicated URE (5'-auuuuuuuuuuuuuuugc-3') added immediately upstream to the original URE in the 3'NTR of the SFV4 genome
<b>MHV-68</b>	MHV-68	X	No modifications
<b>MHV-68</b>	MHV-68 ORF37stop	Bahram Ebrahimi	A premature stop codon within the ORF37 of the MHV-68 genome thus encoding a non-functional muSOX gene.

### 2.3.1. Generation of rSFV4 stocks

The icDNA rSFV4 plasmids with a CMV promoter were transfected directly into BHK-21 cells to propagate infectious virus. The rSFV4(3F)-ZsGreen virus was encoded by a cDNA plasmid with an SP6 promoter. It was first *in-vitro* transcribed and then the RNA was transfected into BHK-21 cells. Infectious cDNA rSFV4 plasmids, once cloned and sequenced as described (Section 2.2), were produced on a larger scale using an endo-free plasmid maxi kit (Qiagen) (Section 2.5.4).

#### 2.3.1.1. In vitro transcription of SFV4(3F)-ZsGreen

RNA from a pSP6-SFV4(3F)-ZsGreen construct was extracted prior to transfection due to the lack of a eukaryotic supported promoter which would enable expression of the plasmid-derived mRNA in eukaryotic cell lines. The construct was linearised using *Spe I* (Section 2.6.7), run on an 0.8% agarose gel (Section 2.6.9) and gel purified (Section 2.6.10). The gel-purified linearised plasmid was transcribed into mRNA using a MegaScript SP6 kit (Ambion). Briefly, each *in vitro* transcription reaction contained nuclease-free water up to 20  $\mu$ l, 2  $\mu$ l each of ATP solution, CTP solution and UTP solution (50 mM, Promega), 2  $\mu$ l of a diluted GTP solution (10 mM, Promega), 2  $\mu$ l of m<sup>7</sup>G(5')ppp(5')G cap analog (40 mM, Promega), 2  $\mu$ l of 10X reaction buffer, 1  $\mu$ g of *Spe I* linearised pSP6-SFV4(3F)-ZsGreen, and 2  $\mu$ l of enzyme mix. The reaction mixture was incubated at 37°C for 5 hours. The reaction was then kept on ice and 10  $\mu$ l of the reaction was immediately electroporated into BHK-21 cells (section 2.3.1.2).

#### 2.3.1.2 Transfection of rSFV4 encoding nucleic acid for virus propagation

The rSF4 strains were propagated by electroporating rSFV4 CMV plasmids into BHK-21 cells with the exception of SFV4(3F)-ZsGreen for which *in-vitro* transcribed mRNA (Section 2.3.1.1) was used. Briefly, less than 90% confluent BHK-21 cells grown in 175 cm<sup>2</sup> flasks (Nunc) were trypsinised, counted and resuspended in sPBS at cell density of  $2.5 \times 10^7$  per ml. Thirty micrograms of each rSFV4 plasmid (or 10  $\mu$ l of *in vitro* transcribed mRNA) was mixed with 400  $\mu$ l of  $2.5 \times 10^7$  per ml of BHK-21 cells in ice-cold sPBS in a 0.4 cm electroporation cuvette (Bio-Rad). Cells were then electroporated in a Gene Pulser X-cell Electroporator (Bio-Rad) using the following protocol: square wave protocol at 850V, for 2 pulses of 4 milliseconds each with a 5 second interval between pulses. Each aliquot of  $1 \times 10^7$  cells was added to a 175 cm<sup>2</sup> flask with pre-warmed cGMEM-10 and incubated at 37 °C and 5% CO<sub>2</sub>. The supernatant containing rSFV4 viruses was collected at 24 and 48 hours post-transfection by which point luciferase signal (luciferase-expressing viruses) or GFP fluorescence (GFP-expressing viruses) and CPE were detected. Supernatant from cells infected with rSFV4 viruses with deletion of part or all of the CSE from the 3'NTR was taken when CPE was observed and luciferase signal (luciferase-expressing

viruses) or GFP fluorescence (GFP-expressing viruses) was present. Typically, this occurred on day 5 post-transfection for rSFV4 containing  $\Delta$ CSE, day 7 for  $-\Delta$ URE $\Delta$ 11CSE and day 8 for  $-\Delta$ URE $\Delta$ CSE.

### **2.3.1.3. Purification of rSFV4 viruses**

Supernatant from transfected BHK-21 cells containing SFV4 virus particles was centrifuged at 4000 x g for 20 minutes at 4 °C to pellet cell debris and the supernatant containing virus particles was stored at -80 °C. For purification, all virus supernatants from a given virus preparation were thawed at 37 °C in a water bath. Viral particles were then precipitated from the supernatant by overnight incubation in a solution of 0.7% polyethylene glycol 8000 (PEG, Sigma-Aldrich) in 2.3% NaCl (Sigma-Aldrich) at 4 °C with continuous gentle stirring. PEG-bound viral particles were precipitated by centrifugation at 10,000 x g for 20 minutes at 4 °C and the PEG-virus pellet was resuspended in 10 ml of sterile low salt buffer (LSB, 0.15 M NaCl, 10 mM Tris, pH 7.4). The re-suspended virus was then purified by ultracentrifugation through a 20% sucrose cushion as follows. The virus suspension was added to an ultra-clear ultracentrifugation tube (Beckman) and a sucrose cushion (20% (w/v) sucrose in TNE buffer pH 7.4 (50 mM Tris-HCl pH 7.4, 100 mM NaCl and 0.1 mM EDTA pH 8.0), filter sterilised) was carefully added below virus suspension until the tube was full. The viral particles were then pelleted using a SW32 Ti rotor in an Optima XPN-100 ultracentrifuge (Beckman Instruments) at 82,700 x g for 1.5 hours at 4 °C. The supernatant was carefully decanted and the virus pellet re-suspended in 1 ml of LSB and left for 1 hour at 4 °C to fully re-suspend. The re-suspended viral particles were then aliquotted (20  $\mu$ l) into cryovials (Nunc) and stored at -80 °C.

### **2.3.2 Murine gammaherpesvirus-68 stocks**

MHV-68 and MHV-68 ORF37stop viral stocks were generated by infecting BHK-21 cells at a very low MOI with existing sub-master stocks (provided by Dr. Bahram Ebrahimi, The University Of Liverpool) and crude viral particles harvested by homogenisation of infected cells. Briefly, 3 X 10<sup>7</sup> BHK-21 cells suspended in cDMEM-10 were infected with either MHV-68 or MHV-68 ORF37stop virus at an MOI of 0.001. Virus and cells were incubated for 1 hour with vigorous shaking (220 rpm) at 37 °C. Cells were then plated at 3 X 10<sup>6</sup> cells per 175 cm<sup>2</sup> tissue culture flask (Nunc) and incubated at 37 °C with 5% CO<sub>2</sub>. Virus was harvested upon visualisation of CPE approximately 5-6 days post infection. Cells were gently scraped off into suspension and centrifuged at 500 x g at 4 °C for 20 minutes. The supernatant was discarded, and the cell pellet was resuspended in 4 ml of sPBS. Resuspended pellets were transferred to a pre-chilled (4 °C) sterile dounce homogeniser (VWR International Ltd) and homogenised 20-30 times with intermittent incubation on ice to prevent the homogeniser from over-heating. The homogenised pellet suspension was then transferred to a sterile glass universal container and

sonicated in an ice bath for 15 minutes and then centrifuged again as described above. The supernatant was kept on ice and resultant pellet was resuspended in 1 ml of sPBS and re-homogenised and centrifuged as described above. The two supernatant fractions were aliquoted in to cryovials and stored at -80 °C as virus stock.

## **2.4 General Virus Techniques**

### **2.4.1 Infections**

To calculate the necessary amount of virus required to infect a given number of cells at the desired MOI the following formula was used:

$$\text{Volume of virus stock required} = \frac{\text{MOI} \times \text{Number of cells to be infected}}{\text{Titre of virus stock}}$$

#### **SFV4 infection**

Cells were infected with SFV4 by incubation in 0.75% bovine serum albumin (Sigma-Aldrich) in PBS (PBSA). Briefly, cells were infected when they reached 70-90% confluency as described. Medium was removed and the SFV4 virus suspension was added directly onto the adherent cells and incubated at room temperature for 1 hour with gentle rocking. The virus suspension was then removed and replaced with medium or agar overlay before returning the cells to 37 °C with 5% CO<sub>2</sub> incubation.

#### **MHV-68 Infection**

MHV-68 infections were conducted by the addition of the necessary amount of virus to the total number of cells to be infected in a small volume of cDMEM. Briefly, 80-90% confluent cells were trypsinised and pelleted as described (Section 2.1.2), resuspended in 4 ml of complete medium and counted using a Neubauer haemocytometer. The cell suspension was then diluted if required to give 0.25X the number of cells required per ml that are to be infected. From this cell suspension 4 ml were placed into a bijou tube and the necessary amount of virus stock added. The 5-ml bijou tube with cells and virus was placed in a 50 ml centrifuge tube and incubated at 37 °C with vigorous agitation at 220 rpm. Cells were then seeded at 80-90% density (1 X 10<sup>6</sup> cells per well) into 6-well plates (plaque assay Section 2.4.2, qPCR Section 2.10) or at 75,000 cells per well in a 24-well plate (Immunostaining, Section 2.8). Cells were then returned to 37 °C and 5% CO<sub>2</sub> incubation.

## 2.4.2 Virus titration by Plaque Assay

SFV4 and MHV-68 were titrated by plaque assay using BHK-21 cells in six-well and 24-well plates for stocks and samples respectively. To calculate the PFU/ml of each sample the following formula was used:

$$PFU/ml = \frac{\text{Average number of plaques for given dilution}}{\text{Volume of inoculum (ml) } \times \text{ dilution factor}}$$

### SFV4 virus titration assay

Six-well plates were seeded with  $3 \times 10^5$  BHK-21 cells in 3 ml of cDMEM-10 and incubated at 37 °C and 5% CO<sub>2</sub> until cells were 80% confluent. Ten-fold serial dilutions of virus stocks were generated as follows. Briefly, 12 µl of virus stock was added to 1188 µl of PBSA to create a 10<sup>-2</sup> dilution, followed by mixing by pipetting, taking 120 µl of the 10<sup>-2</sup> dilution and adding to 1080 µl of PBSA to create a 10<sup>-3</sup> dilution. This was repeated until 10<sup>-12</sup> dilution was prepared. Medium was removed from the BHK-21 cells and 2 X 500 µl of each virus dilution were added to duplicate wells. Virus was incubated on cells for one hour at room temperature with gentle rocking. Following incubation, the virus suspension was removed, and 3 ml of 40-42 °C 4% Bacto agar and c-DMEM-2 in a 10:3 ratio was added to cells. Agar was allowed to set at room temperature for 5 minutes and then the cells were incubated at 37°C and 5% CO<sub>2</sub> for 3 days. Cells were fixed by addition of 10% neutral buffered formaldehyde (NBF; Leica Biosystems) directly on top of the agar in the wells and allowed to incubate at room temperature in a fume-cabinet for 1 hour. The agar and NBF discarded and the fixed cells were stained with 0.1% toluidine blue (Sigma-Aldrich) for one hour at room temperature with gentle rocking. Cells were then washed gently with tap water, allowed to air dry overnight and the plaques counted under a light microscope. The method was scaled down for 24-well plates.

### MHV-68 virus titration assay

A  $6.7 \times 10^5$  BHK-21 cells/ml suspension was prepared in cGMEM-10 from 80-90% confluent cells in T175 cm<sup>2</sup> flasks as described (Section 2.1.2). Three millilitres of the cell suspension were added to each of 10 bijoux tubes. The serial dilutions were created identically as described for SFV4 with the exception that sPBS was used instead of PBSA. Each bijoux was labelled with a serial dilution and one millilitre of the corresponding virus dilution was added to the cells. Bijoux were placed in 50 ml Falcon tubes and incubated for 1 hour at 37 °C and vigorous agitation at 220 rpm. Following incubation, 2 ml of each cell dilution were added to 6-well plates to give 100,000 cells per well. Cells were allowed to

adhere for 8 hours, then an agar overlay was applied as described for SFV4. Cells were also fixed, stained and counted 4 days post-infection as described for SFV4.

## **2.5 General bacterial techniques**

### **2.5.1 Bacterial Culture**

Transformed bacteria were grown in Luria-Bertani (LB) medium or LB agar plates containing suitable antibiotic and grown overnight at 37 °C. Individual colonies were picked at random or selected via colony PCR (Section 2.6.13) and used to inoculate 10 ml of LB media. All LB medium was pre-sterilised by autoclaving before addition of appropriate antibiotic. Inoculated media were incubated overnight at 37 °C and 220 rpm. For large scale plasmid preparation, 150 ml of sterile LB medium with appropriate antibiotic was inoculated with 150 µl of bacterial culture containing the desired plasmid. Kanamycin was the antibiotic used for selection for all icDNA SFV4 plasmids and pCR-Blunt II-TOPO (Thermo Fisher) used in this study while ampicillin was the selective antibiotic for pUC18 (used as a positive control for bacterial transformations). The working concentration used for Kanamycin was 50 µg/ml while Ampicillin was used at 100 µg/ml.

### **2.5.2 Preparation and use of glycerol stocks**

Once the identity of a plasmid has been confirmed by sequencing, the colony or culture from which it was derived was used to inoculate 5 ml of LB Broth containing the appropriate antibiotic. The culture was incubated overnight at 37 °C and 220 rpm. The bacteria were then pelleted by centrifugation at 500 x g for 10 minutes. The pellet was re-suspended in 50% glycerol in sterile water, mixed well and stored at -80°C. When required, the stocks were removed from -80 °C and placed immediately in dry ice to prevent the culture from thawing. A pipette tip was used to scrape a small amount of frozen bacteria culture from the tube and this was used to inoculate 5ml of LB media containing appropriate antibiotic and incubated overnight at 37 °C.

### **2.5.3 Transformation of competent *E.coli***

Competent *E. coli* bacteria were transformed with SFV4 icDNA plasmids or ligation products (derived from plasmids) to expand the desired clone via bacterial growth in culture followed by DNA plasmid extraction. Two commercially available strains of chemically competent *Escherichia coli* were used.

#### **Single-use JM109 with greater than 10<sup>8</sup> colony forming unites/µg**

Competent JM109 bacteria were pre-aliquotted into 50 µl microtubes and kept at -80 °C. Prior to use, competent cells were thawed on ice. Either 10 ng of (plasmid) DNA in a maximum volume of 5 µl or

5 µl of ligation product was added to the bacteria, were mixed gently and returned to the ice. To act as a positive control, one microlitre of 100 pg/µl of pUC18 was added to one aliquot of competent bacteria cells; another aliquot of bacteria with no DNA acted as a negative control. Competent bacteria were incubated with plasmid DNA for 30 minutes on ice before being heat-shocked for 20 seconds at 42 °C in a water bath. Bacteria were then replaced on ice for 2 minutes followed by the addition of 450 µl of SOC medium (Sigma-Aldrich) without antibiotics before being incubated at 37 °C and 220 rpm for 1 hour. Following incubation, 10µl and 100 µl aliquots of transformed bacteria were plated on separate LB agar plates with appropriate antibiotic. For ligation reactions, transformed bacterial culture was centrifuged at 500 x g for 10 minutes. All but 50 µl of supernatant was removed, the pellet was re-suspended by vortexing and then spread on a pre-warmed LB agar plate with appropriate antibiotic. Plates were incubated overnight at 37 °C.

#### **XL10-Gold® ultra-competent cells**

Bacteria were thawed on ice and 100 µl aliquots transferred to pre-chilled microtubes. Then 4 µl of β-mercaptoethanol was added to each aliquot followed by very gentle mixing by pipetting and incubation on ice for 10 minutes. DNA or ligation product were added to competent cells. The subsequent steps were then the same as described for JM109 cells with the exception that the heat shock at 42 °C was conducted for 30 seconds.

### **2.5.4 Plasmid DNA extraction from bacterial cultures**

#### **Mini DNA Preparation**

Small-scale extraction of plasmid DNA from bacterial cultures were carried out using the Isolate II Plasmid Mini Kit (Bioline Cat. No. BIO-52056). All centrifugations were carried out using benchtop microfuges at 11,000 x g (~ 13,000 rpm) at room temperature. Briefly, 10 ml of sterile LB broth with appropriate antibiotic was inoculated with a bacterial colony and incubated for 12-16 hours at 37 °C at 220 rpm. After incubation, 5ml of bacterial culture was centrifuged at 11,000 x g for one minute, supernatant discarded; the remaining 5 ml were stored at 4 °C for future use. The pelleted cells were re-suspended in 250 µl of Resuspension Buffer P1 containing RNase A followed by lysis of bacteria with the addition of 250 µl of Lysis Buffer P2 and incubation at room temperature for 4-5 minutes. Lysis was then inhibited by addition of 300 µl of neutralisation buffer and several tube inversions followed by centrifugation at 11,000 x g for 10 minutes at room temperature. The supernatant was added to an Isolate II Plasmid Mini Spin Column placed in a collection tube, centrifuged for one minute and the supernatant discarded. The column was then washed twice, first with 500 µl of Wash Buffer PW1 pre-heated to 50 °C and then with 600 µl of room-temperature Wash Buffer PW2 (first

supplemented with ethanol according to manufacturer's instructions); the column was centrifuged for one minute after each wash with the flow-through discarded. Finally, columns were centrifuged for 2 minutes to remove any traces of alcohol. The column was then placed in a nuclease-free tube, 30  $\mu$ l of 70 °C water was added to the membrane and the column centrifuged for one minute. The concentration of plasmid DNA retained in the flow-through was measured using a Nanodrop spectrophotometer (Section 2.6.6) and the preparation was stored at -20 °C.

### **Endotoxin-free Maxi DNA Preparations**

Large-scale preparations of plasmid DNA for later transfection into mammalian cells were extracted from bacterial cultures using the Endo-Free Plasmid Maxi-Kit (QIAGEN). Briefly, 100 ml of LB broth with appropriate antibiotic was inoculated with 100  $\mu$ l of starter culture obtained from a culture used for mini-prep containing confirmed correct plasmid from DNA sequencing. Inoculated broth was incubated overnight at 37 °C and 220 rpm then centrifuged at 6000 x g for 15 minutes at 4 °C and the supernatant was discarded. The pellet was re-suspended in 10 ml of Buffer P1 containing RNase A followed by lysis of bacteria by addition of 10 ml of Buffer P2, gentle mixing and incubation for 5 minutes at room temperature. Lysis was then inhibited by addition of 10 ml of pre-chilled Buffer P3 and mixed by several tube inversions. The lysate was then added to a QIAfilter cartridge with the nozzle cap in place. After 10 minutes of stationary incubation the nozzle cap was removed, and the lysate forced through the membrane by insertion of a cartridge plunger. Then 2.5 ml of Buffer ER was added to the filtered lysate with mixing by inversion and incubation for 30 minutes on ice to remove endotoxins. During the incubation, a Qiagen-tip 500 was equilibrated by adding 10 ml of Buffer QBT to the column and allowing it to empty by gravity flow. The filtered lysate was then added and allowed to flow through the column followed by two additions of 30 ml of Buffer QC to wash the membrane, the flow-through liquid being discarded each time. The DNA was then eluted by the addition of 15 ml of Buffer QN to which 10.5 ml (0.7 volumes) of room-temperature isopropanol was added, mixed and then centrifuged at 15,000 x g for 30 minutes at 4 °C. The supernatant was then discarded, and the pellet washed in 10 ml of 70% ethanol and centrifuged again at 15,000 x g for 10 minutes. The supernatant was then discarded, the pellet air-dried for 3-5 minutes and re-suspended in 200  $\mu$ l of nuclease-free water. The DNA concentration was measured using a Nanodrop spectrophotometer (Section 2.6.6) and stored at -20 °C.



## **2.6 General nucleic acid and molecular techniques**

### **2.6.1 Extraction of RNA from mammalian cells**

RNA was extracted using an RNeasy Mini Kit (Qiagen). All centrifugations were performed using a benchtop microfuge and at room temperature unless stated otherwise. Briefly, 70% confluent NIH/3T3 cells were infected (section 2.4.1) with rSFV4 at an MOI of 10. At given timepoints post-infection, the supernatant was discarded, and the cells were washed, trypsinised and pelleted as described for seeding flasks/plates (Section 2.1.2). The cell pellet was re-suspended in 600  $\mu$ l of buffer RLT with 1% (v/v)  $\beta$ -mercaptoethanol and centrifuged in a QIAshredder spin column (Qiagen) for 2 minutes. Six hundred microliters of 70% ethanol was then added to the homogenised lysate, mixed well and then centrifuged in two sets of 600  $\mu$ l through a RNeasy spin column for 15 seconds at 8000 x g and the flow-through discarded. The column membrane was then subjected to three washes, firstly by addition of 700  $\mu$ l of Buffer RW1, followed by two separate additions of 500  $\mu$ l of Buffer RPE. The column was centrifuged at 12,000 x g for 15 seconds between each wash and for 2 minutes following the last wash; the flow-through was discarded after each wash step. The column was then centrifuged in a clean collection tube for 2 minutes at 12,000 x g to remove residual wash buffer and alcohol. RNA was eluted in two elution steps into an RNase-free tube by two separate additions of 30  $\mu$ l of RNase-free water directly to the membrane and centrifugation at 8000 x g for 1 minute after each addition. RNA samples were stored at -80 °C.

### **2.6.2 Nuclear and Cytoplasmic Fractionation followed by RNA extraction**

The nuclear and cytoplasmic fractions of NIH/3T3 cells were separated and RNA extracted using the PARIS kit (ThermoFisher Scientific). Briefly, cells in sPBS were pelleted at 500 x g at 4 °C for 5 minutes and re-suspended in 500  $\mu$ l ice-cold cell fractionation buffer with gentle pipetting followed by a 10-minute incubation on ice. The nuclear fraction was then pelleted at 500 x g at 4 °C for 5 minutes and the supernatant containing the cytoplasmic fraction was separated into a clean RNase-free microfuge tube and incubated on ice. To prevent contamination with any left-over cytoplasmic fraction, 500  $\mu$ l of ice-cold fractionation buffer was then added to the nuclear pellet, followed by very gentle pipetting and centrifugation as before, and the supernatant was discarded. The nuclear pellet was then lysed by addition of 500  $\mu$ l of ice-cold disruption buffer with sequential mixing by vortex and one minute incubations on ice until a homogenous lysate was achieved. 500  $\mu$ l of 2 X lysis/binding solution containing  $\beta$ -mercaptoethanol was then mixed well with each of the lysates at room temperature followed by mixing with 500  $\mu$ l of 100% ethanol (Sigma). The nuclear and cytoplasmic lysates were each then applied to individual PARIS RNA kit filter cartridges, placed in collection tubes in two sets of 700  $\mu$ l, and centrifuged at 14,000 x g at room temperature for one minute with the flow-through

discarded at the end of each spin step. The cartridges were then washed 3 times, first with 700 µl of wash solution 1, and then twice with 500 µl of wash solution 2/3. The cartridges were centrifuged at 14,000 x g at room temperature for one minute after addition of each wash solution. Cartridges were centrifuged again at 14,000 x g to remove residual traces of wash solution. RNA was eluted with two sets of 40 µl of elution solution heated to 97 °C, and centrifuged as before after each addition of elution solution. RNA was stored at -80 °C.

### **2.6.3 DNase Treatment of RNA samples**

To ensure complete removal of DNA, the RNA samples were subjected to treatment with Turbo DNase (Ambion). Briefly, 0.1 volume of Turbo DNase buffer was added to the RNA samples followed by 1 µl of Turbo DNase, the solution mixed and incubated for 37 °C for 30 minutes. Then 0.1 volume of DNase Inactivation Reagent was added and incubated for 5 minutes at 24 °C with intermittent mixing by flicking the tube. The samples were then centrifuged at 10,000 x g for 1.5 minutes and the supernatant (RNA) transferred to clean RNase-Free tubes.

### **2.6.4 RNA clean-up of DNase Treated RNA samples**

The RNeasy MinElute clean-up kit (Qiagen) was used to remove the enzyme solution post DNase-1 treatment and to concentrate the RNA. All centrifugations were carried out using benchtop microfuges at 11,000 x g (13,000 rpm) at room temperature. Briefly, RNA samples were adjusted to total volume of 100 µl where necessary by addition of nuclease-free water. Then 350 µl of buffer RLT and 250 µl of 100% ethanol were added to the samples with mixing by pipetting in between each addition. The samples were transferred to individual RNeasy mini elute spin columns and centrifuged at 8,000 x g for 15 seconds with the flow-through discarded. The columns were washed twice, first with 500 µl of buffer RPE and next with 500 µl of 80% ethanol. The columns were spun at 8,000 x g for 15 seconds for the first wash, 2 minutes for the second and at 12,000 x g for 5 minutes in a clean collection tube after both washes to remove any traces of solution. Columns were then placed in clean RNase-free tubes and RNA was eluted by addition of 14 µl of RNase-free water and centrifugation at 12,000 x g for 1 minute. RNA was then measured using a Nanodrop spectrophotometer (Section 2.6.6) and stored at -80 °C.

### **2.6.5 Reverse Transcription of RNA samples**

For RNA samples that were not used in a one-step qPCR reaction, the RNA was reverse transcribed to complementary DNA (cDNA). RNA samples were first treated with Turbo DNase followed by Turbo DNase inactivation reagent (Section 2.6.3) and then purified (Section 2.6.4). To obtain cDNA, the RNA

sample was reverse transcribed using SuperScript III reverse transcriptase (Invitrogen) and a poly(dT) primer (Sigma). Briefly, the necessary amount of RNase-free water was added to a PCR tube for a reaction volume of 13 µl for the given sample followed by 300 ng of oligo (dT)<sub>18</sub>, 1 µl of 10 mM dNTP mix and 1 µg of total RNA. The mixture was heated to 65 °C for 5 minutes followed by a 1-minute incubation on ice. Then 4 µl of 5X first-strand buffer, 1 µl 0.1 M DTT, 1 µl RNaseOUT Recombinant RNase Inhibitor and finally 1 µl of SuperScript III RT (200 units/µl) were added. The reaction was incubated for 60 minutes at 50 °C and then heat-inactivated at 70 °C for 15 minutes. RNA was then digested by the addition of 1 µl of RNase H and incubation at 37 °C for 20 minutes, followed by heat-inactivation at 65 °C for 20 minutes.

#### **2.6.6 Nucleic acid quantification**

The quantity and quality of nucleic acid samples (total RNA and dsDNA) was estimated using UV/VIS spectrophotometry using 1 µl of sample and a NanDrop 1000 Spectrophotometer (ThermoFisher).

#### **2.6.7 Restriction Digest and FastAP treatment**

Digestion of double-stranded DNA was required for generation and cloning of rSFV4 infectious plasmids and was achieved using FastDigest restriction enzymes (ThermoFisher). This enabled insertion of manufactured dsDNA sequences (GenScript) into icDNA SFV4 plasmid backbones for the development of new rSFV4 viruses. FastAP thermosensitive alkaline phosphatase (ThermoFisher) was used to catalyse the release of the 5' phosphate group from linearised icDNA SFV4 plasmids acting as a backbone prior to ligation. FastAP thermosensitive alkaline phosphatase and all FastDigest restriction enzymes used (*BamHI*, *ApaI*, *Bpu10I*, *SacI*, *NotI*, *SpeI*, *HpaI*) (ThermoFisher) have an optimal reaction temperature of 37 °C and are active in FastDigest Buffer (ThermoFisher). Reactions were set up in sequential order with nuclease-free water up to 20 µl, 2 µl of 10 X FastDigest Reaction Buffer, 1 µg of the given plasmid, 1 µl of each required restriction enzyme and 1 µl of FastAp thermosensitive alkaline phosphatase for digesting backbone (FastAp not added to insert). Reaction mixtures were incubated for 2 hours at 37 °C followed by heat-inactivation by heating at 80 °C for 10 minutes.

#### **2.6.8 DNA Ligations**

DNA ligations were performed using T4 DNA Ligase (Thermo Fisher). Briefly, insert and backbone DNAs were mixed together in a 3:1 molar ratio up to a total of 100 ng of DNA in x µl (where x is ≤ 7 µl) in a PCR tube. Then seven minus x µl of nuclease-free water was added, followed by 2 µl of 5 X ligation buffer and finally 1 µl of T4 ligase. The reaction was mixed well and centrifuged at 500 x g for 15 seconds, then left in water and ice to warm gradually to room temperature overnight. The following

morning ligation reactions were taken out of the water bath and left at room temperature for 5 hours followed by transformation into competent bacteria cells (Section 2.5.3).

### **2.6.9 Gel Electrophoresis**

Linearised DNA was analysed and separated by agarose gel electrophoresis. DNA was run on an agarose gel with the ideal agarose concentrations depending on the size of DNA 0.8% (for >10kb), 1% (for 2-10kb), 1.5% (1kb-4kb), 2% (50bp-1kb). Agarose was dissolved in 1 X TAE buffer with 0.5 µg/ml ethidium bromide (ThermoFisher). Samples that did not contain FastDigest Green Buffer (ThermoFisher) or GoTaq Green Buffer (Promega), used in the restriction digest or PCR reaction respectively, were mixed with 6X loading dye (ThermoFisher). DNA samples were loaded into individual lanes alongside appropriate DNA molecular size markers: GeneRuler 100 bp plus or GeneRuler 1 kb plus (ThermoFisher). DNA fragments were resolved by gel electrophoresis (between 40 and 100 volts depending on the size of DNA being separated and the percentage of agarose in gel) for 45-120 minutes. Nucleic acid bands were visualised using a BioRad Gel Doc XR+ UV transilluminator (BioRad).

### **2.6.10 Extraction of DNA from gels**

DNA was extracted from TAE agarose gels using the Isolate II PCR and Gel Kit (Bioline). Briefly, under UV illumination the given DNA band was excised from the gel using a sterile scalpel and placed in a nuclease-free microtube. The excised gel was weighed and 200 µl of Binding Buffer CB was added per 100 mg of gel, followed by incubation at 50 °C for 10 minutes with intermittent vortexing. Samples were loaded onto Isolate II PCR and Gel Kit columns placed in collection tubes and centrifuged for one minute at 11,000 x g (~13,000 rpm). The flow-through was discarded and the membrane was washed twice with 700 µl Wash Buffer CW added to the column with centrifugation for one minute at 11,000 x g after each wash; the flow-through was discarded after each spin. The membrane was then dried by centrifugation for 2 minutes at 11,000 x g and the DNA was then eluted into a nuclease-free microtube by addition of 15 µl of 70 °C Elution Buffer C. The concentration of the extracted DNA was measured by NanoDrop (Section 2.6.6) and the samples were stored at -20 °C.

### **2.6.11 Blunt-end TOPO cloning**

The PCR products were confirmed by gel electrophoresis (Section 2.6.9) to be of a suitable size to correspond to the distance between the two primers in the SFV4 genome. The Zero Blunt TOPO PCR Cloning Kit (Invitrogen) was used to clone the blunt PCR product into a suitable vector, pCR-Blunt II-TOPO, to enable amplification and DNA sequencing. Briefly, 4 µl of each PCR reaction (after DNA

polymerase had been deactivated) was mixed with 1 µl of salt solution and 1 µl pCR-Blunt II-TOPO reagent. The reaction was incubated for 30 minutes at room temperature, followed by incubation on ice and transformation into competent JM109 cells (Section 2.5.3).

### 2.6.12 Standard PCR

Standard PCR was performed using Q5 High-Fidelity DNA polymerase (New England Biolabs) when 3'-5' exonuclease activity was used to minimise possible errors during polymerisation. Other standard PCRs were conducted using GoTaq G2 DNA polymerase (Promega). The 50 µl reactions contained 1 µl of 10 mM dNTPs, 2.5 µl of 10 µM forward primer, 2.5 µl of 10 µM reverse primer, 10-100 ng of template DNA or 2 µl of cDNA from reverse transcription reaction (Section 2.6.5), 10 µl of 5 X Q5 or GoTaq reaction buffer, 0.5 µl Q5 or GoTaq G2 DNA polymerase and nuclease-free water to make up the total volume to 50 µl. Water was added first, followed by buffer, then all other reagents and finally enzyme. The PCR reactions were performed using a standard thermocycler. The initial denaturation stage was set at 98 °C for 30 seconds (Q5 reactions) or 95 °C for 2 minutes (GoTaq reactions). The cycling stage was set for 30-35 cycles and consisted of denaturation, annealing and elongation steps in succession. The denaturation was set to 98 °C for 10 seconds for Q5 reactions and 95 °C for 30 seconds for GoTaq reactions. The annealing temperature was set depending on the primer pair used (Table 2.2) for 30 seconds for both Q5 and GoTaq reactions. The elongation step was set to 72 °C for all reactions plus 30 seconds per kb for Q5 polymerase and one minute per kb for GoTaq polymerase. After the cycling stage, a final extension stage of 72 °C for 2 minutes (Q5 reactions) and 5 minutes (GoTaq reactions) was incorporated into the cycling parameters to ensure completion of DNA chain elongation before holding the reactions at 4 °C. PCR products were stored long-term at -20 °C.

### Standard PCR primers

PCR primers used in this study are shown in table 2.2:

Primer Name	Primer Sequence	Annealing temperature used (°C)
B4-ApaI-FWD	5'-GGTGCAGAAAATCTCGGGTG-3'	54
B4-BamHI-FWD	5'-GCCAGGTGGACAAGATCAAG-3'	54
ORF37StopFA	5'-GACATCGACGGAGGAAGCAG-3'	60
ORF37StopRB	5'-GTCTTTGATGTTGCCAGGAG-3'	60

**Table 2.2 Primers used in this study for standard PCR**

### **2.6.13 Colony PCR**

When it was necessary to detect correct cloning products from a ligation reaction and subsequent bacterial transformation, a colony PCR was utilised. Briefly, reactions with GoTaq G2 DNA polymerase were set up identical to those described above (Section 2.6.12) in a 96-well plate with the exception of no template added. Colonies were then picked with a sterile pipette tip, rinsed briefly into the PCR reaction mixture in the 96-well plate and then spread on a corresponding numbered grid on a kanamycin LB agar plate. The reaction followed the PCR protocol for GoTaq G2 DNA Polymerase (Section 2.6.12) in a standard thermocycler with an additional 8 minutes for the initial denaturation step. Colony PCR products were run through an agarose gel by gel electrophoresis (Section 2.6.9). Colonies corresponding to correct inserts (based on positive PCR reactions) were selected for and used to inoculate 5 ml of LB Broth with Kanamycin (50 µg/ml). The overnight cultures were then used in mini plasmid DNA preparation (Section 2.5.4) followed by sequencing (Section 2.6.14)

### **2.6.14 Sequencing**

All recombinant plasmids were sequence-verified by commercial sequencing (Source biosciences, Nottingham, UK). Results were aligned and edited using ApE plasmid Editor.

## **2.7 Genetic reversion analysis of viral mutants**

Viral mutants were assessed for genetic reversion to wild-type strain sequence or other genetic variation by PCR and/or sequencing analysis. For this assessment genetic material from SFV4 ((+)ssRNA virus) was reverse transcribed while that from MHV-68 (dsDNA virus) was used directly.

### **2.7.1 Genetic reversion analysis of rSFV4-URE/CSE viruses**

The URE/CSE deletions and additions to the 3'NTR of the SFV4 genome manufactured in this study were checked for genetic reversion in virus stocks. Genetic reversion could occur during propagation of the virus from icDNA plasmids through genetic mutation during viral replication.

#### **Screening of rSFV4-URE/CSE mutants for alterations in the 3'UTR**

NIH/3T3 monolayers were infected with each of the SFV4-2SG-*Glu*c and SFV4(3F)-eGFP viruses (Table 2.1) at MOI of 10 and cells were collected at 9 hours post infection (h.p.i.). Briefly, 6-well plates were seeded with  $3 \times 10^5$  NIH/3T3 cells and incubated at 37 °C with 5% CO<sub>2</sub>. When the monolayers reached 75-80% confluence, medium was removed, and 500 µl of test rSFV4 virus diluted in PBSA was added to the cell monolayer. The cells were incubated at room temperature for one hour with gentle rocking. This was followed by removal of virus in PBSA and replacement with 3 ml of pre-warmed cDMEM-10

and incubation at 37 °C with 5% CO<sub>2</sub>. At 9 h.p.i. medium was removed and cells were collected by trypsinisation and centrifugation as described (Section 2.1.2). RNA was then extracted (Section 2.6.1), treated with Turbo DNase (Section 2.6.3), purified and concentrated (Section 2.6.4). Purified viral RNA was then used for cDNA synthesis using oligo (dT)<sub>18</sub> (Section 2.6.5). The 3'NTR of region of viruses was amplified by PCR (2.6.12) using the primers '3'race' and either 'B4-ApaI-FWD' or 'B4-BamHI-FWD' for the rSFV4-2SG-*Gluc* viruses and the rSFV4(3F)-eGFP viruses respectively. PCR products were cloned into pCR-Blunt II-TOPO (Section 2.6.11) and grown on kanamycin LB agar plates (Section 2.5.1). Colonies were analysed by colony PCR (Section 2.6.13) for the presence of the 3'NTR in SFV4 genomes. Colonies with correctly cloned sequences were selected to inoculate 5ml of LB Broth with Kanamycin (Section 2.5.1) and grown overnight at 37 °C. Bacterial culture was used for mini-prep plasmid extraction (Section 2.5.4). Purified plasmids were verified by sequencing (Section 2.6.14) utilising the primers 'M13-For' and 'M13-Rev' which are complementary to 5' and 3' of the insert site of the pCR-Blunt II-TOPO vector.

### **2.7.2 Analysis of genetic reversion of MHV-68 ORF37stop virus**

The MHV-68 ORFstop mutant stock was checked for reversion by proteolytic lysis of virions and subsequent PCR using viral DNA as the template. The MHV-68 viral stock was used as a control. A 50 µl reaction as set up using GoTaq G2 polymerase as described (Section 2.6.12) with the exception of the addition of 1 µl of proteinase K recombinant PCR grade (ThermoFisher) instead of GoTaq DNA polymerase. The template used was 1µl of the test virus stock. The reaction mixture was then incubated for 20 minutes at 55 °C followed by enzyme deactivation by heating to 95 °C for 10 minutes. Following deactivation and cooling, 0.25 µl of GoTaq G2 DNA polymerase (5U/µl) was added to the reaction mixture followed by the PCR reaction (section 2.6.12) for 35 cycles with an annealing temperature of 60 °C. 15 µ each PCR reaction was used in a diagnostic restriction enzyme digest (Section 2.6.7) using *HpaI* for 2 hours. Results were analysed by gel electrophoresis on a 2% agarose gel (Section 2.6.9).

## **2.8 Immunostaining and Confocal Microscopy**

### **Sample preparation**

Immunostaining was performed in 24-well plates (Nunc). Prior to seeding cells, a sterile poly-D-lysine coated 12mm sterile coverslip was placed in each well. NIH/3T3 cells were seeded at 50,000 cells per well 12 hours prior to SFV infection (Section 2.4.1) and at 75,000 cells per well post MHV-68 infection (Section 2.4.1). Following infection, cells were incubated at 37 °C and 5% CO<sub>2</sub> until they were fixed at the desired time point post infection.

### **Fixing of adherent cells and immunostaining**

At the required time post infection, medium was removed and cells were washed twice for 1 minute in sPBS. Cells were then fixed for 10 minutes in 4% paraformaldehyde (PFA, Sigma-Aldrich). PFA was made fresh prior to fixing by dissolving 4g of paraformaldehyde in 100 ml of sPBS with 67 µl of 5M NaOH and heating at 55 °C until dissolved. The PFA was then cooled to room temperature and adjusted to pH 7.4 with HCl. Cells were then washed three more times in sPBS for 5 minutes each and then treated with 0.3% Triton-X-100 (Sigma-Aldrich) in sPBS for 10 minutes followed by a single 5 minute wash in sPBS. To block non-specific binding sites, the cells were then subjected to blocking by adding 5% normal goat serum (NGS, Sigma-Aldrich) in sPBS for 30 minutes. The NGS was then removed and immediately followed by incubation with primary antibody(s) for 1 hour. Primary antibodies were used simultaneously in concentrations as stated (table 2.3) diluted in sPBS with 1% NGS. Following incubation, primary antibodies were removed and cells were washed three times for 5 minutes each using sPBS. Secondary antibodies were then added and incubated at room temperature in the dark for 1 hour. Secondary antibodies (Table 2.3) were used at a dilution of 1 in 500 in sPBS with 1% NGS. Following antibody incubation, the cells were washed three more times in sPBS for 5 minutes each time. Nuclear staining was then achieved by addition of NucBlue® Reagent (2 drops per ml of sPBS, ThermoFisher) or TO-PRO®-3 Iodide (2 µl per 1ml of sPBS, ThermoFisher) and incubated for 15 minutes. Nuclear staining was followed by three washes in sPBS for 5 minutes each. Coverslips were then mounted on microscope slides (Superfrost) using 10 µl of Vectashield® Antifade Mounting Medium (VectorLabs) and stored in the dark at 4 °C until imaging. Immunostained cells were imaged on a Zeiss LSM 510 confocal microscope using AIM image software.

### **Image data analysis**

Image analysis was conducted using Image J software. To calculate the percentage of a protein (staining) found in the nucleus or cytoplasm compared to that found in the whole cell, the signal (corrected integrated density) from the area was divided by the signal (corrected integrated density) obtained from the whole cell. Integrated density was corrected for background fluorescence using the formula: corrected integrated density = integrated density – (selected area X mean fluorescence of background readings).



**Table 2.3 Antibodies used for immunostaining in this study**

Name	Host	Target	Primary / secondary	Antibody Type	Dilution used	Source
Anti-HuR (19F12AE12)	Mouse	HuR	Primary	Monoclonal, IgG1	1 in 200	Abcam, ab170193
Anti-PABPC	Rabbit	PABPC, C-terminus	Primary	Polyclonal, IgG	1 in 200	Abcam, ab21060
Anti-mrnp41 (D-18)	Rabbit	RAE1 (mrnp41), internal region	Primary	Polyclonal, IgG	1 in 400	Santa Cruz, sc-74891
Anti-TTP (H-20)	Rabbit	TTP, C-terminus	Primary	Polyclonal, IgG	1 in 200	Santa Cruz, sc-14030
Anti-MHV-68-ORF65 (12B8)	Mouse	MHV-68 viral capsid	Primary	Monoclonal, IgG2a	1 in 3	Dr Stevenson, Cambridge University
Anti-MHV-68-gB (MG4D11)	Mouse	MHV-68 gB, C-terminus	Primary	Monoclonal, IgG2a	1 in 3	Dr Stevenson, Cambridge University
Alexa Fluor 488 goat anti-mouse, high-cross adsorbed	Goat	Mouse IgG (H+L)	Secondary	Polyclonal, IgG	1 in 500	ThermoFisher, A-11029
Alexa Fluor 568 goat anti-rabbit, highly cross-adsorbed	Goat	Rabbit IgG (H+L)	Secondary	Polyclonal, IgG	1 in 500	ThermoFisher, A11036
Alexa Fluor 568 goat anti-mouse, preadsorbed	Goat	Mouse IgG (H+L)	Secondary	Polyclonal, IgG	1 in 500	Abcam, ab175701
Alexa Fluor 633, goat anti-rabbit	Goat	Rabbit IgG (H+L)	Secondary	Polyclonal, IgG	1 in 500	ThermoFisher, A21070

## **2.9 *In vitro* characterisation of rSFV4 URE/CSE mutants**

### **2.9.1 rSFV4-2SG-*Gluc* one-step and multi-step growth curves**

#### **Cell preparation, infection and sample acquisition**

NIH/3T3 monolayers were infected with rSFV4-2SG-*Gluc* viruses at an MOI of 0.01 or 10 and samples were taken at suitable time points for quantification of luciferase activity and infectious virus. Briefly, 6-well plates were seeded with  $3 \times 10^5$  NIH/3T3 cells and incubated at 37 °C with 5% CO<sub>2</sub>. Infections for each rSFV4-2SG-*Gluc* virus at each MOI were set up in triplicate wells. When the monolayers reached 75-80% confluence, medium was removed and 500 µl of the given rSFV4-2SG-*Gluc* virus at the required MOI diluted in PBSA was added onto the cells in the given well (time point 0). The cells were incubated at room temperature for 1 hour with gentle rocking. This was followed by removal of virus in PBSA and replacement with 3 ml of pre-warmed cDMEM-10 and incubation at 37 °C with 5% CO<sub>2</sub>. Samples (2 X 200 µl) were taken at 0, 3, 6, 9, 12, 18, 24 and 48 hours post-infection and frozen immediately at -20 °C or -80 °C for luciferase and plaque assays respectively. Medium removed for samples was replaced with 400 µl of sterile cDMEM-10 at each time point. Plaque assays for growth curves of rSFV4 were conducted in 24-well plates as described (Section 2.4.2).

#### **Luciferase assay**

To measure the activity of secreted *Guassia* luciferase, 5 µl of each medium sample was added to a 96 well plate for each time point and then assayed for luminescence using the Dual Luciferase Reporter Assay (Promega) and a GloMax-Multi detection luminometer (Promega). The luciferase assay substrate and buffer and the stop-n-glow substrate and buffer were diluted 1 in 10 with milliQ water compared to manufacturers recommended concentrations. Each well was analysed by initially adding 70 µl of luciferase assay substrate to initiate the *FFluc* reaction. This was followed by addition of 70 µl of diluted Stop&Glo substrate and buffer to quench the *FFluc* reaction and initiate the *Rluc* reaction. Both reactions were given a 10 second equilibration time and a 10 second integration time. The *Rluc* activity was measured by the luminometer in relative light units. The *Rluc* reading corresponded to the activity of the levels of *Gluc* in the given sample. *Gluc* readings were normalised against non-infected controls, firefly readings have not been reported in this report.

### **2.9.2 rSFV4-infected cell viability and caspase 3/7 assays**

#### **Cell preparation, infection and sample acquisition**

The effect of the URE/CSE alterations on SFV4-induced host cell caspase activity and cell death were analysed using the Caspase-Glo 3/7 Assay (Promega) and CellTiter-Glo 2.0 Assay (Promega). The two

assays were conducted simultaneously on separate plates. Cells were infected with rSFV4-2SG-*Gluc* URE/CSE mutant viruses at MOI of 10 and 0.01. Briefly, 96-well plates were seeded with 7,500 NIH/3T3 cells per well (Section 2.1.2). When cells were ~75% confluence, medium was removed and 20 µl of the given virus in PBSA was added to cells (this is time point 0) followed by incubation for one hour at room temperature with gentle rocking. The virus inoculum was then removed and 100 µl of cDMEM-10 was added to wells followed by incubation at 37 °C and 5% CO<sub>2</sub>. Cells were prepared for analysis at regular intervals post-infection from 0 to 72 hours. Cells without virus treatment acted as negative control. All infections were performed in triplicate.

### **CellTiter-Glo 2.0 Assay**

CellTiter-Glo® 2.0 measures the level of metabolically active cells by measuring ATP present in a sample through the emission of a luminescent signal from the ATP- dependent mono-oxygenation of luciferin molecules by a recombinant luciferase enzyme. When cells die they become metabolically inactive and the available ATP is diminished, thus a decrease in luminescence signal signifies cell death. CellTiter-Glo® 2.0 assay plates were first equilibrated to room temperature for 30 minutes, then 100 µl of CellTiter-Glo® 2.0 Reagent was added to each well and the side of the plate was vigorously tapped for 2 minutes to ensure complete cell lysis. Luminescence signal was stabilised by incubating the plate for 10 minutes at room temperature before reading the luminescence signal using the GloMax-Multi detection luminometer with a one second integration time.

### **The Caspase 3/7 Assay**

The Caspase-Glo® 3/7 assay system was used to assess cell death because of apoptosis by measuring the relative activities of caspase 3 and/or 7 in cells. In addition to virus-infected cells, a negative control (no virus infection), and a blank reaction control containing Caspase-Glo® 3/7 reagent and cDMEM-10 alone were also run in triplicate per plate for subsequent normalisation calculations. Briefly, at the correct time point, plates were removed from the incubator and held at room temperature for 20 minutes. Then 75 µl of cDMEM-10 was removed from each well and 25 µl of Caspase-Glo® 3/7 assay was added. Lysis was ensured by tapping the side of the plate vigorously for 2 minutes followed by one hour incubation at room temperature to reach peak, stable luminescence signal. Luminescence signal was measured using the GloMax-Multi Detection Luminometer with a one second integration time.

## **2.10 Quantitative real-time polymerase chain reaction**

### **2.10.1 RT-qPCR of host transcripts using Pfaffl method**

#### **Cell preparation and rSFV4 infection**

Six-well plates were seeded with  $3 \times 10^5$  NIH/3T3 cells per well (Section 2.1.2). When 75-80% confluent, cells were infected (Section 2.4.1) with SFV4-2SG-*Gluc*, SFV4-2SG-*Gluc*-dURE or SFV4-2SG-*Gluc*-5xURE at a MOI of 10 with 3 replicates per virus and 3 replicate NIC wells. Cells were then incubated in cDMEM-10 at 37 °C and 5% CO<sub>2</sub>. At 6 and 12 h.p.i. medium was removed and cells were trypsinised and pelleted as described (Section 2.1.2). Cells were then washed in 1 ml ice-cold sPBS and placed in a RNase-free microtube ready for nuclear and cytoplasm fractionation with RNA extraction (Section 2.6.2), Turbo DNase treatment (Section 2.6.3) and subject to qPCR.

#### **Cell preparation and MHV-68 infection**

NIH/3T3 cells were infected with MHV-68 or MHV-68 ORF37stop as described (Section 2.4.1) and then seeded in 6-well plates at  $1 \times 10^6$  cells/well. RNA samples were taken at 9 h.p.i. as described for SFV4 infection.

#### **One-step qRT-PCR of RNA samples**

Purified and DNase-treated nuclear and cytoplasmic RNA samples were reverse-transcribed and quantified using a 1-step SYBR Green qPCR reaction and results analysed using the  $2^{-\Delta\Delta CT}$  Livak method. 18S ribosomal RNA gene was used as reference for normalization of input total RNA between samples. All primers were used with 10 ng of purified total RNA sample apart from 18S RNA which was used with 100 pg of purified total RNA because of the high prevalence of 18S RNA present in eukaryotic cells. A Power SYBR® Green RNA-to-CT™ 1-Step Kit (ThermoFisher Scientific) was utilised for all qPCRs in this project. Briefly, 10 ng of the given purified RNA template sample was used for each reaction in a 96-well reaction plate. Reactions were repeated in triplicate wells for each replicate sample and primer set used (Table 2.4). Negative controls contained all PCR reaction components including primers but no RNA. For each independent variable (different viruses used and NIC) a master mix of 221 µl of dH<sub>2</sub>O, 250 µl of 2x RT-PCR mix (2x) and 4 µl of 125x RT enzyme mix was added to an RNase-Free tube and vortexed. Seventy-six microlitres of the master mix was added to a separate RNase-free tube to which 400 pg of the given template diluted in RNase-Free water was added and briefly vortexed. This less concentrated template mix was used for the 18S RNA qPCR reactions. 210 ng of the given template was added to the remaining master mix and briefly vortexed. 19 µl of the template reaction mix was then added to the corresponding well of a 96-well plate. For the negative controls,

79.56 µl of water, 90 µl of 2x RT-PCR mix and 1.44 µl of 125x RT enzyme mix were added to an RNase-free tube, vortexed and 19 µl of this was added to each negative control well. Then 1 µl of diluted primer pair was added to each designated well to give a final primer concentration of 100 nM. Samples were run in a StepOnePlus® RealTime PCR System (Applied Biosystems). The reaction underwent three stages. The first was a reverse transcription (RT) step of 48 °C for 30 minutes to reverse transcribe the RNA samples in to cDNA. The second stage activated the PCR enzyme by heating to 95 °C for 10 minutes. The final stage was 40 cycles of two steps in succession. The first of these was a denaturation step of 95 °C for 15 seconds and the second was an annealing and extension step of 60 °C for 1 minute.

#### **Calculation of amplification efficiency of primer pairs**

Each primer pair was subject to qPCR using the same kit at different concentrations of template to work out the primer efficiencies. For each primer pair, dilutions of RNA template of 100 ng, 10 ng, 1 ng, 100 pg and 10 pg were used. Amplification efficiency was calculated using the slope of the standard curve of  $C_T$  values from the concentration gradient in the following formula:  $E = 10^{-1/slope}$ . The amplification efficiency percentage was then worked out with the following formula:  $\%E = (E - 1) \times 100$ .

#### **Calculating relative abundance of RNA samples using the $2^{-\Delta\Delta C_T}$ Livak Method**

The relative RNA abundance in a virus infected sample compared to a non-infected control (NIC) was calculated using the Livak method. The formula used was:

Normalisation of the target gene to the reference gene for both control and test samples:

$$\Delta C_{T(\text{Test})} = C_{T(\text{Target, Test})} - C_{T(\text{Ref, Test})}$$

$$\Delta C_{T(\text{Control})} = C_{T(\text{Target, Control})} - C_{T(\text{Ref, Control})}$$

Normalisation of  $\Delta C_T$  of the test sample to the  $\Delta C_T$  of the control sample:

$$\Delta\Delta C_T = \Delta C_{T(\text{Test})} - \Delta C_{T(\text{Control})}$$

Calculation of the normalised expressed ratio:

$$2^{-\Delta\Delta C_T} = \text{Expression Ratio}$$

The reference gene was 18S RNA, the control was RNA from NIC and the test sample was RNA from the given virus-infected sample.

**Table 2.4 List of qPCR primers used in this study**

Target mRNA/cDNA	Forward Primer	Reverse Primer
18S RNA	5'-CGGACAGGATTGACAGA-3'	5'-CAATCGCTCCACCAACTAA-3'
β-Actin	5'-AGGTGACAGCATTGCTTC-3'	5'-GCTGCCTCAACACCTCAA-3'
IFN- β	5'-CCGAGCAGAGATCTTCAGGAA-3'	5'-CCTGCAACCACCACTCATTCT-3'
HuR	5'-CCACATGGCGGAAGACTGC-3'	5'-CACAAAACCGTAGCCCAAGC-3'
TTP	5'-CACCATGGATCTCTCTGCCA-3'	5'-GGTCATGGCTCATCGACTGG-3'
RNase L	5'- GCATTGAGGACCATGGAGAC-3'	5'- GGAGGAGAAGCTTTACAAGGT3 -3'
Caspase 9	5'-AGTCCCGGGTGGTGTCTAT -3'	5'-GCCATGGTCTTTCGCTCAC-3'
MHV-68 glycoproteinB	5'-TGTTGGATGTACCCTACAGT-3'	5'-AGAGTGGTTGGCTGACATAC-3'
Cyclophilin A	5'-GGATTTGGCTATAAGGGTTC-3'	5'-CTGCCGCCAGTGCCATTATG-3'
PARN	5'-CTCTTCAGCGCCTTCGGTAACAT-3'	5'-TATTAACGGCAATTTGTACTTGT-3'
Xrn1	5'-GGAGTCATTCTGATCGGGATGC-3'	5'-ATTCCAATGACGGTGCCTCGAAG-3'
Hsp70	5'-ACAAGAGCACCGGCAAGGCC-3'	5'-CTCGGCCTCCTGCACCATGC-3'

### **2.11 Statistical Analysis**

Graph pad Prism v7 was used for graph preparation, calculation of means, standard deviation (SD) and p-values. One-way or Two-way ANOVAs were used to assess significance of group data. Additionally, the Graph pad Prism multiple t-test was utilised to assess statistical significance at individual time points in group data. Data was considered statistically significant with p values < 0.05.

# Chapter 3

PABPC and HuR subcellular localisation

---

during SFV4 and MHV-68 infection

---



### 3.1 Overview

A broad range of host RNA-binding proteins are utilised by viruses to replicate their genomes and avoid host cell mediated RNA degradation. The TTR-RBPs discussed in chapter 1 play key roles in facilitating successful infection cycles for a broad range of virus families. Host TTR-RBPs, such as HuR, bind specific cis-acting sequences present in viral genomic RNA (RNA viruses) (Sokoloski *et al.*, 2010; Shwetha *et al.*, 2015) or in viral transcribed mRNA (DNA viruses) (Jehung *et al.*, 2018). The binding of these host TTR-RBPs can directly affect the stability, splicing, nuclear export, translation or sub-cellular location of the host and viral RNA (Pullmann *et al.*, 2007). TTR-RBPs can also act as adapter proteins to recruit other host cellular proteins to the bound RNA (Kim *et al.*, 2009). Furthermore, the quenching of host TTR-RBPs after binding to viral RNA can reduce the availability of TTR-RBPs to bind to host-cell RNA affecting host-cell processes which utilise the TTR-RBPs (Hyde *et al.*, 2015).

### 3.2 HuR relocation in mammalian cells during alphaviral infection

HuR, a TTR-RBP, binds mRNA in a cell affecting the mRNA stability (usually by increasing its half-life), mRNA translation and in some cases splicing, polyadenylation and/or nuclear export (Brennan and Steitz, 2001; Barnhart *et al.*, 2013). Alphavirus genomic RNA, such as that of SINV, bind HuR during the course of an infection of host cells which is evident in both mammalian and mosquito cell lines (Sokoloski *et al.*, 2010). During infection of mammalian cells with SINV, WEEV and CHIKV host HuR changes from a predominantly nuclear to a predominantly cytoplasmic distribution (Dickson *et al.*, 2012). In mosquito cells, where the sub-cellular distribution of HuR is more uniform there is no obvious change in distribution despite mosquito cellular HuR still binding to the alphaviral 3'UTR (Sokoloski *et al.*, 2010). There is no direct confirmation of a change in sub-cellular distribution of HuR during SFV infection despite evidence that HuR binds SFV4 3'UTR. It has been previously postulated that nsP2 of SINV and other alphaviruses could be targeting HuR or the nucleo-cytoplasmic shuttling of HuR. This suggestion is rooted in the fact that viral nsP2 translocates partially in to the nucleus during infection where most HuR resides under basal conditions in mammalian cells (Sokoloski *et al.*, 2010).

### 3.3 SFV4 nsP2 nuclear localisation

The nsP2 of SFV4 contains a nuclear localisation signal consisting of three arginines (RRR). An SFV4 nsP2 mutant (SFV4-RDR) where the second arginine in the nuclear localisation signal is substituted for aspartic acid (RDR) loses its ability for nsP2 to enter the nucleus (Breakwell *et al.*, 2007; Rikkinen, 1996). In contrast to this finding nsP2, during infection of BHK-21 cells with SFV4-RDR, has been shown to partially relocate in to the nucleus (both at 8 and 24 h.p.i.) (Tamm, Merits and Sarand, 2008). The SFV4-RDR virus elicits a significantly larger Type I IFN response during infection of MEFs compared to SFV4 wild type virus suggesting a failure to inhibit the IFN response in host-cells following infection

(Breakwell *et al.*, 2007). Interestingly in the same study, SFV4-RDR virus infection in mammalian cells inhibited host RNA production to comparable levels to SFV4 (Breakwell *et al.*, 2007), although DNA synthesis was significantly less inhibited in an earlier study (Rikonen, 1996).

The shut off of host-cell transcription seen during old world alphaviral infection has been partially attributed, at least in part, to nsP2 function in the nucleus where it promotes the ubiquitination and subsequent degradation of Rbp1, a catalytic subunit of RNAPII (Akhrymuk, Kulemzin and Frolova, 2012). This host shut off activity was demonstrated during infection of SINV and through expression of nsP2 from SINV, SFV and CHIKV in transient transfection assays (Akhrymuk, Kulemzin and Frolova, 2012). Interestingly, a SINV mutant, SINV/2V/GFP, incapable of the catalytic processing of nsP2-nsP3 and thus preventing nsP2 from entering the nucleus, inhibits host cell transcription significantly less than SINV (Akhrymuk, Kulemzin and Frolova, 2012). Taken together with the previous finding that SFV4-RDR inhibits host cell RNA transcription to comparable levels to SFV4 (Breakwell *et al.*, 2007) this suggests that SFV4-RDR either allows enough nsP2 in to the nucleus to inhibit host cell transcription through ubiquitination of Rbp1 or inhibits host cell RNA production through other mechanisms.

### **3.4 SFV4 icDNAs**

The full genome of many strains of most alphaviruses including SFV4 are encoded on expression plasmids as infectious cDNA (icDNA). The schematics of these are discussed more in Chapter 4. The icDNA can be transcribed *in vitro* to mRNA which can then be transfected in to host cells and produce infectious virus. Furthermore, if the expression vector contains a promoter capable of expression in the host cell then the icDNA can be transfected directly in to the cell to cultivate the virus. In this study SFV4s-Green was *in-vitro* transcribed from pSP6-SFV4(3F)-Zs-Green and the infectious mRNA was transfected in to BHK-21 cells. SFV4 and SFV4-RDR used were originally created from SP6 plasmids using an identical methodology.

### **3.5 PABPC, gammaherpesviruses and muSOX**

Given PABPC roles in host RNA stability and translation it is not surprising that a diverse set of viruses families (Alvarez *et al.*, 2006; Zhang *et al.*, 2007; Piron *et al.*, 1998; Blakqori, van Knippenberg and Elliott, 2009) inhibit PABPC's roles in host cell protein production and/or utilise PABPC's capabilities to increase viral RNA stability and translation. As discussed in Chapter 1 infection of mammalian cell lines with a range of viruses result in the build-up of host PABPC in the nucleus (Blakqori, van Knippenberg and Elliott, 2009; Harb *et al.*, 2008; Kumar and Glaunsinger, 2010). For gammaherpesviruses this has been attributed to a single viral protein, muSOX/SOX/BGLF5 (MHV-68 (Covarrubias *et al.*, 2009) / KSHV (Lee and Glaunsinger, 2009) / EBV (Park *et al.*, 2014)), capable of causing nuclear retention of PABPC when expressed independently on an expression plasmid or during

virus lytic infection. However, at the time of this study, subcellular location of PABPC has not been investigated during lytic infection of mammalian cells with a gammaherpesvirus lacking a functional muSOX (or its homolog) gene. A MHV-68 virus lacking a functional muSOX gene, MHV-68 ORF37stop, results in lytic infection and RNA loss in a Type 1 IFN-receptor KO cell line (Sheridan *et al.*, 2014). In this study MHV-68 ORF37stop was able to replicate in NIH/3T3 cells (a cell line with functional IFN-receptors) and was used to assess the subcellular location of PABPC during infection without a function muSOX gene.

### 3.6 Objectives

The aim of this study was to determine:

1. The subcellular location of HuR during SFV4, SFV4-RDR, MHV-68 and MHV-68 ORF37stop virus infection of NIH/3T3 cells.
2. The subcellular location of PABPC during SFV4, SFV4-RDR, MHV-68 and MHV-68 ORF37stop infection of NIH/3T3 cells.
3. The subcellular location of PABPC at multiple time points post infection with MHV-68 and MHV-68 ORF37stop infection in NIH/3T3 cells.

### 3.7 Results

The subcellular location of HuR during SFV4 and SFV4-RDR infection was assessed. HuR is predominantly found in the nucleus in basal conditions in mammalian cell lines. Following both SFV4 and SFV4-RDR infection of murine NIH/3T3 cells, cellular HuR accumulated in the cytoplasm with a concomitant reduced abundance in the nucleus (Figure 3.1). This suggested that the nuclear localisation of nsP2 is not required for SFV4 induced HuR relocalisation from the nucleus to the cytoplasm. There were also small correlated foci of PABPC and HuR staining that occurred in infected cells.

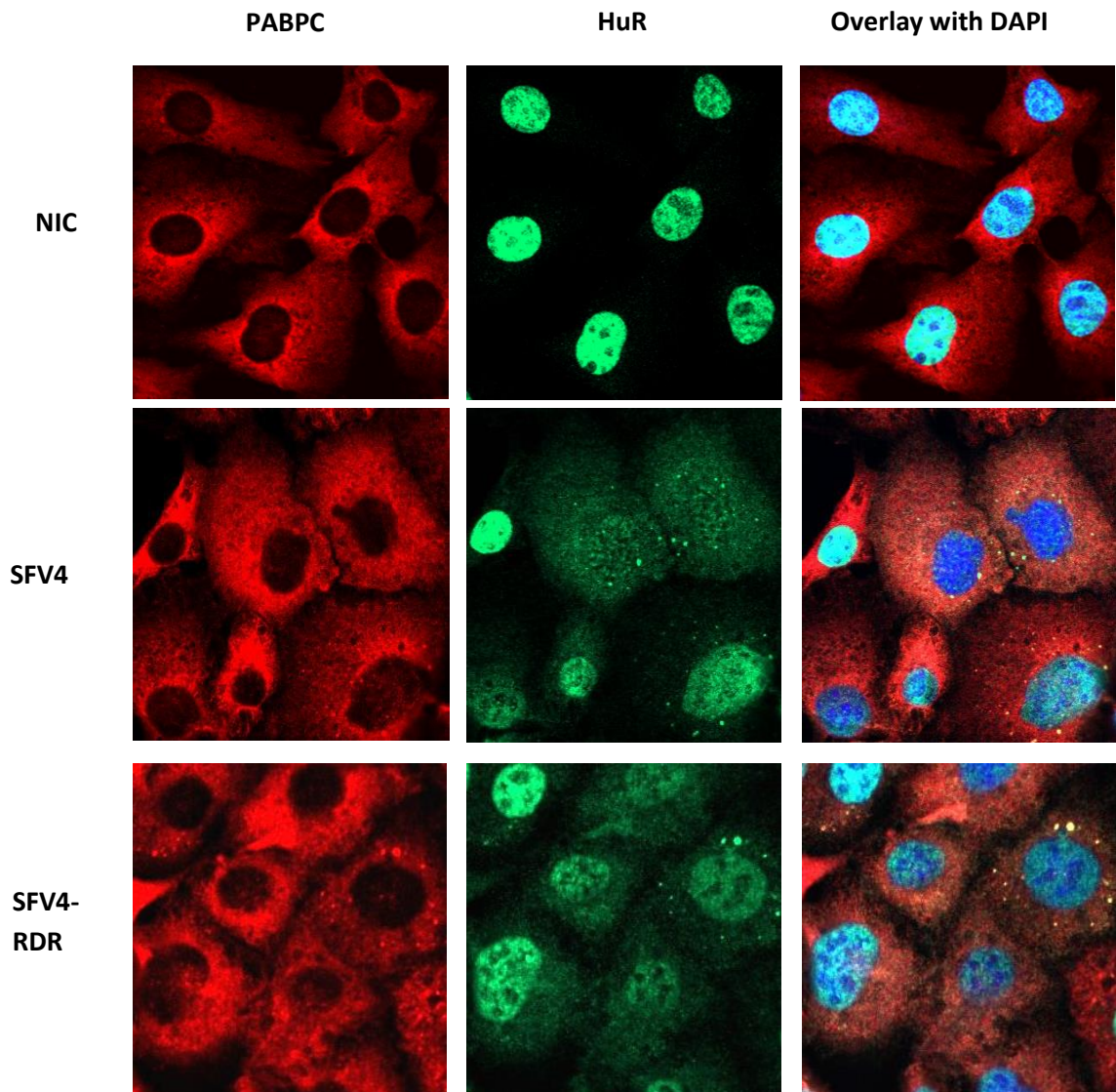


**Figure 3.1 HuR relocates to the cytoplasm during SFV4 and SFV4-RDR infection.** NIH/3T3 cells were infected with SFV4 or SFV4-RDR at 5 MOI and fixed at 6 h.p.i. Fixed cells were immunostained against PABPC (red) and HuR (green) with DAPI stain (blue).

To confirm SFV4 virus replication in NIH/3T3 where HuR had relocated to the cytoplasm, NIH/3T3 cells were infected with SFV4(3F)-ZsGreen (Figure 3.2). The Zs-Green is fused with nsP3 and therefore indicates the subcellular location of nsP3 and by extension the replication complexes within spherules/CPV-1 within the cell (discussed in Chapter 1).

The relocalised HuR did not exclusively co-localise with SFV4 nsP3 suggesting that the relocalised HuR in the cytoplasm may be omitted from the SFV4 replication complexes. There are some areas in the cytoplasm where HuR and PABPC did appear to co-localise but this may be due to the abundance of the proteins and the intensity of the immunostaining.

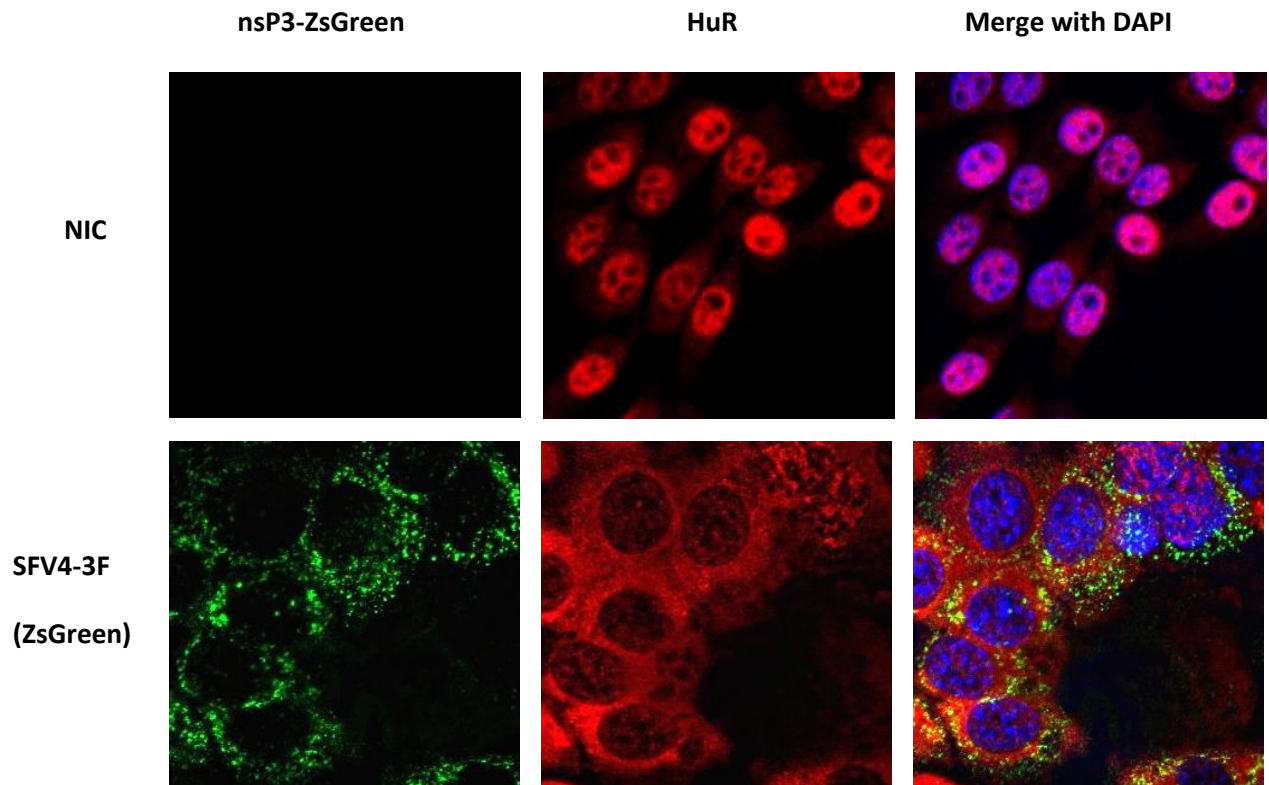


**Figure 3.2 HuR partially relocalises to the cytoplasm in NIH/3T3 cells where SFV4(3F)ZsGreen is actively replicating and the relocalised HuR does not colocalise with viral nsP3.** NIH/3T3 cells were infected with SFV4(3F)-ZsGreen at 10 MOI and fixed at 9 h.p.i. Fixed cells were stained against HuR (red) with DAPI (blue), nsP3-ZsGreen is shown in green.

PABPC and HuR sub-cellular location were also assessed in the context of MHV-68 and MHV-68 ORF37stop infection (Figure 3.3). During MHV-68 infection PABPC abundance increased in the nucleus. In the cells where PABPC relocated to the nucleus the HuR staining was less intense however unlike during SFV4 infection HuR remained nuclear. This suggests that MHV-68 infection of NIH/3T3 cells resulted in PABPC relocation to the nucleus. Furthermore, there may be a small reduction in HuR protein expression. This possible reduction appears to be evident during infection with MHV-68 ORF37stop virus suggesting the muSOX is not responsible for the possible reduction in intensity of HuR immunostaining.



During infection of NIH/3T3 cells with MHV-68 lacking a functional muSOX protein, host PABPC remains predominantly in the cytoplasm. The increased abundance of PABPC in the nucleus following MHV-68 infection and the absence of this during MHV-58 ORF37stop infection confirms that muSOX is responsible or at least required for the build-up of PABPC in the nucleus during MHV-68 infection in NIH/3T3 cell.

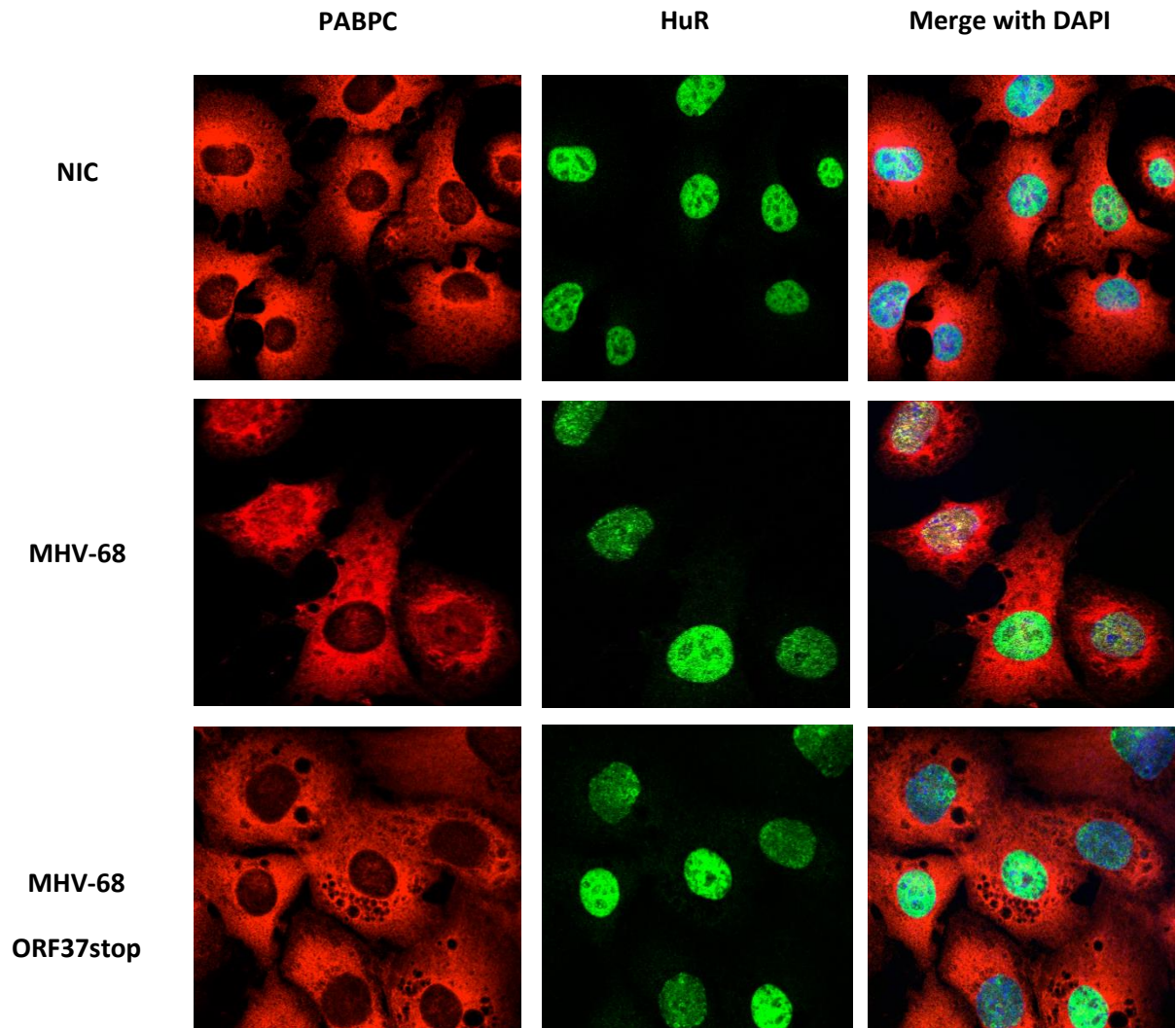


**Figure 3.3 MHV-68 with functional muSOX gene causes PABPC to relocate to the nucleus.** NIH/3T3 cells were infected with MHV-68 or MHV-68 ORF37stop at MOI of 1 and fixed at 12 h.p.i. Cells were stained against PABPC (red), HuR (green) and DAPI stain (blue). PABPC resides in the cytoplasm under basal conditions, relocated to the nucleus following MHV-68 infection and remained in cytoplasm following MHV-68 ORF37stop infection.

Utilisation of an antibody against MHV-68 glycoprotein confirmed MHV-68 was actively replicating in NIH/3T3 cells in which PABPC became retained in the nucleus. Furthermore, this confirmed that MHV-68 ORF37stop virus was capable of replicating in cells without apparent relocalisation of PABPC to the nucleus (Figure 3.4).

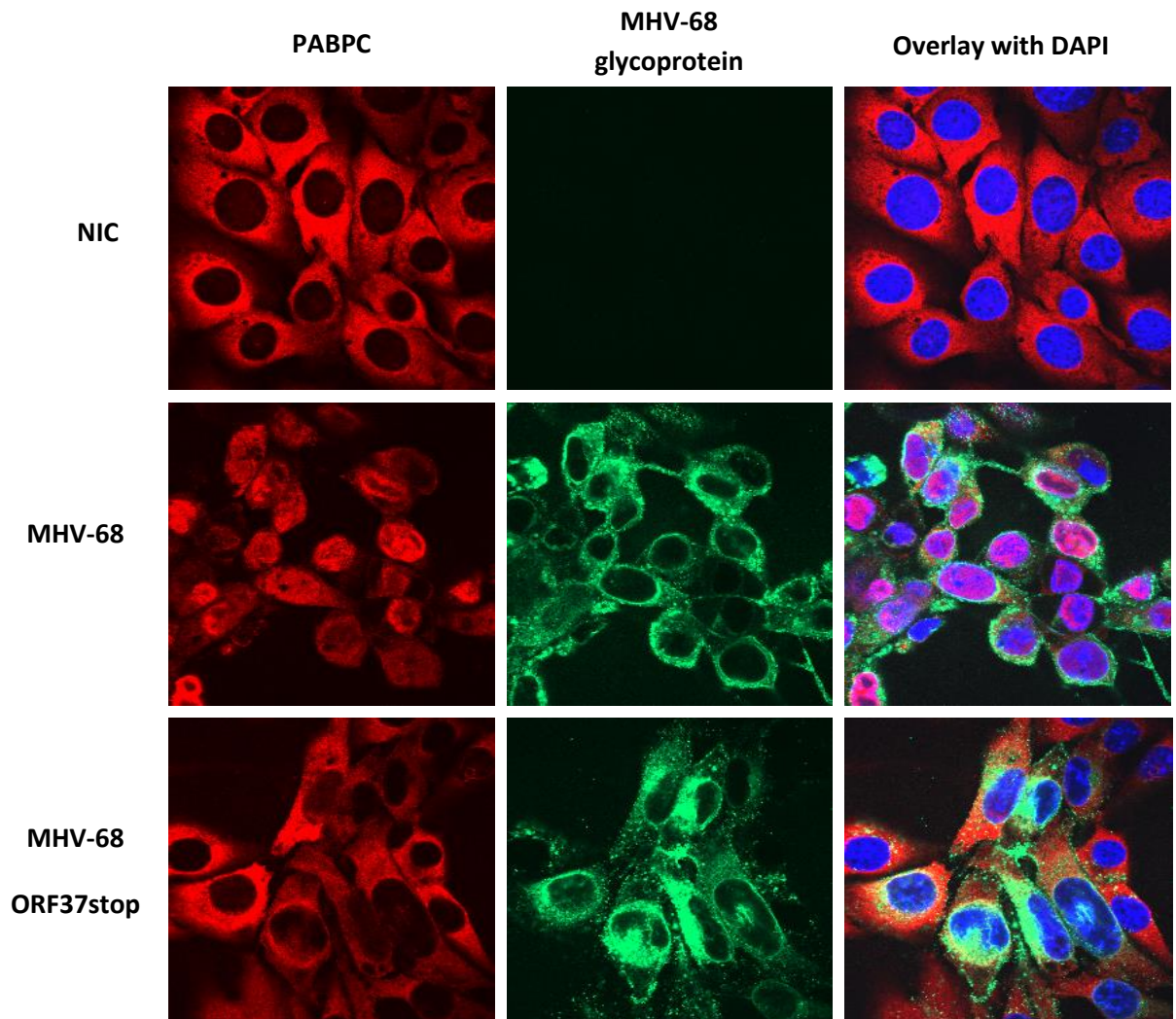


**Figure 3.4 MHV-68 ORF37stop fails to cause PABPC nuclear retention despite active replication in NIH/3T3 cells.** NIH/3T3 cells were infected with MHV-68 or MHV-68 ORF37stop at MOI of 5 and fixed at 24 h.p.i. Cells were stained against PABPC (red), MHV-68 glycoprotein (green) and DAPI stain (blue).

NIH/3T3 cells were infected with MHV-68 or MHV-68 ORF37stop virus and every two hours post infection the percentage of PABPC which was nuclear at each time point was calculated (Figure 3.5). There was a significantly higher percentage of PABPC in the nucleus compared to the cytoplasm in NIH/3T3 cells at every hour post infection assayed from 8 hours onwards compared to infection with

MHV-68 ORF37stop or NIC ( $p > 0.01$ ). The PABPC nuclear build-up was a gradual process accumulating over time post lytic infection with MHV-68.

There was no significant difference ( $p < 0.05$ ) in the percentage of PABPC that is nuclear at any time point post infection with MHV-68 ORF37stop virus compared to NIC (Figure 3.5). This confirmed that the absence of PABPC build-up during MHV-68 ORF37stop infection was not a delayed or intermittent phenotype but persisted throughout lytic infection.

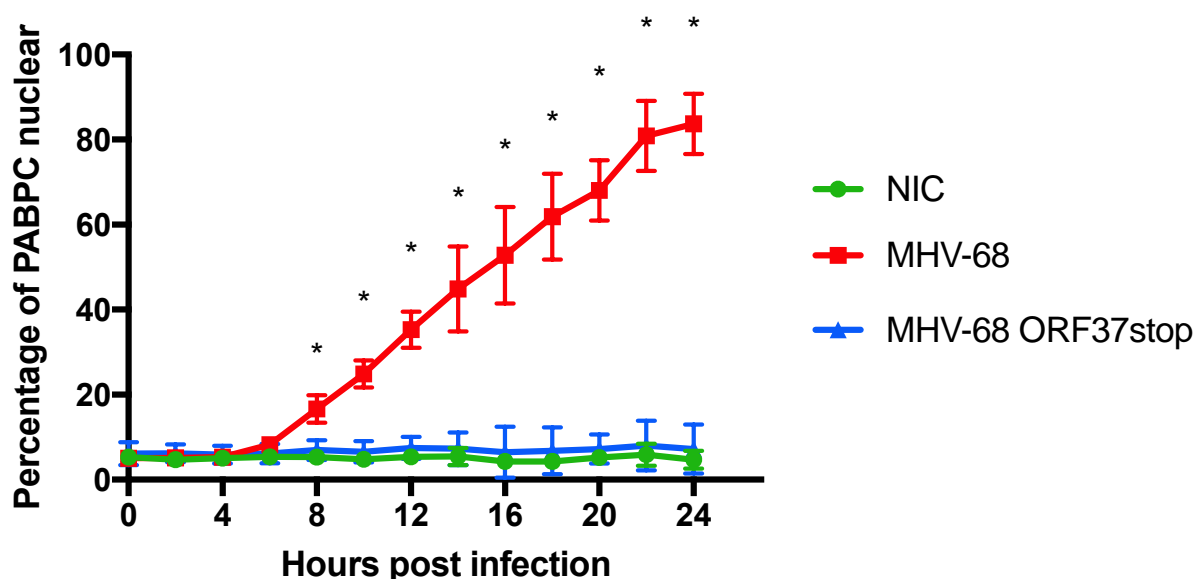


**Figure 3.5 PABPC sub-cellular relocation to nucleus during MHV-68 infection is a gradual process beginning 4-8 h.p.i. and steadily increasing over the course of cellular infection.** NIH/3T3 cells were fixed and immunostained against PABPC every two hours post infection with MHV-68 or MHV-68 ORF37stop virus. The influx and nuclear retention of PABPC during MHV-68 infection was statistically significant from 8 h.p.i. onwards compared to NIC and MHV-68 ORF37stop. The percentage of nuclear PABPC during MHV-68 ORF37stop infection was not statistically different to NIC at any time point post infection but a higher variation between cells was observed.

### 3.8 Discussion

HuR has been shown to bind to the URE/CSE element of the SINV 3'UTR in the context of a SINV infection in both mammalian and mosquito cells (Sokoloski *et al.*, 2010). Furthermore, it has also been demonstrated HuR binds to the 3'UTR of SFV expressed on capped and polyadenylated reporter RNAs in cell-free mosquito cell extracts (Sokoloski *et al.*, 2010). The relocalisation of HuR to the cytoplasm



has been documented in mammalian cells during SINV, WEEV, CHIKV and RRV infection (Dickson *et al.*, 2012) but at the time of this study, this observation was yet to be made during SFV infection. This study confirms that, akin to infection with other alphaviruses, HuR subcellular location changes from a predominantly nuclear distribution to a cytoplasmic one in NIH/3T3 cells following infection with SFV4.

The cytoplasmic HuR observed during SFV4 infection in NIH/3T3 cells co-localised with PABPC. This may be attributed to both HuR and PABPC binding the SFV4 genomic RNA (Sokoloski *et al.*, 2010). HuR has been shown to bind the SFV4 3'UTR and SFV4 genomic RNA contains a poly(A) tail, possibly maintained by nsP4 terminal adenylyltransferase activity (Rubach *et al.*, 2009; Tomar *et al.*, 2006), which will bind host PABPC. There are also small intensely stained foci of PABPC and HuR staining that occur in some infected cells. These foci may be attributed to stress-granules. PABPC and HuR are known to localise within stress-granules in mammalian cells (Buchan and Parker, 2009) however further study is required to confirm the identity of the PABPC and HuR foci observed in this study. SFV4 is known to stimulate stress-granule formation via eIF2 $\alpha$  phosphorylation and then locally disassemble the stress-granules in areas of the cytoplasm containing high viral RNA concentration (McInerney *et al.*, 2005).

It has been postulated that a viral protein may be responsible for the initial influx of HuR to the cytoplasm and that nsP2 which partially resides in the nucleus during alphaviral infection may be responsible for this observation (Sokoloski *et al.*, 2010). However, this study has shown the HuR relocalisation still occurs within six h.p.i. following infection with SFV4-RDR virus. This suggests that the nuclear localisation of nsP2 is not required for the initial relocalisation of HuR to the cytoplasm during SFV4 infection in NIH/3T3 cells. This does not exclude cytoplasmic nsP2 or another viral protein from being responsible for an initial influx of HuR to the cytoplasm. Furthermore, nsP2 following infection with SFV4-RDR partially resides in the nucleus during SFV4 infection of mammalian cells (Tamm, Merits and Sarand, 2008).

It is evident that HuR does relocate to the cytoplasm after 24 hours following transfection of URE/CSE SINV containing RNAs (Barnhart *et al.*, 2013). This suggests that a viral protein is not required for the ultimate sub-cellular location of HuR post-infection during SINV infection but may be responsible for the initial influx from the nucleus. It should be noted that HuR is a nucleo-cytoplasmic shuttling protein, which constantly shuttles between the nucleus and cytoplasm (Kim and Gorospe, 2008). In physiological conditions, the vast majority of HuR resides in the nucleus. Therefore, if URE/CSE SINV containing RNAs bind HuR and retain it in the cytoplasm then over time as HuR shuttles between the two cellular compartments its cytoplasmic distribution may increase. Whether or not the URE/CSE

element is responsible alone for the change in distribution of HuR seen during SFV4 infection or another initial trigger is involved is investigated in Chapter 4.

Akin to many TTR-RBPs, the phosphorylation state of HuR is thought to have varying degrees of control on its subcellular location (Kim and Gorospe, 2008; Pullmann *et al.*, 2007). There is evidence that during SINV infection host HuR is partially dephosphorylated compared to mock infected cells (Dickson *et al.*, 2012). This suggests that SINV infection causes an alteration in the phosphorylation state of HuR which may be at least in part responsible for its change in sub-cellular location, or possibly a consequence of the change in sub-cellular location.

HuR can also be induced to a predominantly cytoplasmic distribution following certain cellular stressors as discussed in chapter 1 (Bhattacharyya *et al.*, 2006). It is therefore possible that the stress of the viral infection of alphaviruses may be contributing to the change in HuR sub-cellular localisation. It should be noted that HuR remains nuclear in many other viral infections, including MHV-68 as assessed in this study as well as measles and dengue virus infections (Dickson *et al.*, 2012). The significance of the URE and CSE of the SFV4 3'UTR to induce the build-up of HuR in the cytoplasm during SFV4 infection and the subsequent consequences of this were investigated in Chapter 4.

The nuclear HuR which has relocated during SFV4 infection to the cytoplasm does not appear to co-localise with viral nsP3. SFV4 nsP3 (green, Figure 3.2) localises within replication complexes where the SFV4 RNA is actively replicating. These replication structures (as discussed in Chapter 1), built-up of membrane invaginations and SFV4 nsPs, form at the plasma membrane and later fuse with endosomes in the cytoplasm to create cytopathic vacuoles type 1 (CPV-1) (Kujala *et al.*, 2001; Frolova *et al.*, 2010). These replication spherules are thought to restrict access to many host cellular proteins by physical hindrance thus allowing viral replication to occur in the absence of many host cellular proteins (Kallio *et al.*, 2016; Kujala *et al.*, 2001).

The possible reduction of HuR staining intensity following MHV-68 and MHV-68 ORF37stop infection may indicate a reduction in HuR expression however further protein expression analysis, such as western blot, are required to confirm this reduction in HuR protein levels. The possible reduction in HuR protein levels appears to be evident during MHV-68 ORF37stop infection suggesting this possible reduction is not predominantly a consequence of muSOX mediated host mRNA degradation. Despite not being a direct consequence of muSOX, a reduction in HuR concentration may facilitate muSOX mediated degradation of host mRNA transcripts. For instance, binding of HuR to IL-6 mRNA provides a significant level of protection from KSHV SOX mediated degradation (Hutin, Lee and Glaunsinger, 2013).

The build-up of PABPC in the nucleus of mammalian cells infected with MHV-68, KSHV and EBV has been attributed to muSOX (Covarrubias *et al.*, 2009), SOX (Lee and Glaunsinger, 2009) and BGLF5 (Park *et al.*, 2014) viral proteins respectively. The absence of nuclear accumulation of PABPC in this study in NIH/3T3 cells following MHV-68 ORF37stop virus confirms the requirement of a functional muSOX gene for the build-up of PABPC in the nucleus during MHV-68 infection. During rotavirus infection of mammalian cells the nuclear build-up of PABPC is attributed to nsP3 (Piron *et al.*, 1998; Harb *et al.*, 2008). Rotavirus nsP3 has a higher affinity for eIF4G than PABPC and competitively inhibits the eIF4G-PABPC interaction (Piron *et al.*, 1998). The exact mechanism of PABPC nuclear localisation during rotavirus infection remains unclear but it is correlated with a reduction in interaction of PABPC with mRNA in the cytoplasm.

The relocalisation of PABPC to the nucleus during MHV-68 infection of NIH/3T3 cells was shown in this study to be a gradual process over the course of infection. This is akin to the time-dependent relocalisation of PABPC to the nucleus during HSV-1 infection (Salaun *et al.*, 2010). Like HuR, PABPC is a nucleo-cytoplasmic shuttling protein. PABPC is exported out of the nucleus bound to mRNA and is imported back in to the nucleus through the action of importin- $\alpha$ . It is thought the reduction of mRNA in the cytoplasm due to the mRNA degradation initiated by muSOX contributes to the build-up of PABPC in the nucleus (Kumar, Shum and Glaunsinger, 2011). When PABPC is unbound from mRNA in the cytoplasm its binding affinity for importin- $\alpha$  increases. In addition, since PABPC is exported out the nucleus bound to mRNA, mammalian PABPC has been shown to build-up in the nucleus when NXF1 mediated mRNA nuclear export is inhibited (Burgess *et al.*, 2011). This suggests that a block in mRNA nuclear export may be at least partially responsible for the nuclear retention of PABPC during MHV-68 infection. This possibility is investigated in Chapter 5.

# Chapter 4

## The SFV4 3'UTR and HuR

## 4.1 Overview

The binding of host trans-acting factors to viral RNA can significantly affect the rate of translation of viral genes, viral genome replication and elicit evasion from the host anti-viral response. The 3'UTR from both the Old and New world alphaviruses have been shown to bind the host protein HuR and cause its redistribution from the nucleus to the cytoplasm in mammalian cells (Sokoloski *et al.*, 2010). Alphaviral 3'UTRs also bind the *Aedes* mosquito HuR homolog, abbreviated to eaHuR, during infection of mosquito cell lines (Sokoloski *et al.*, 2010). In *Aedes* mosquito cell lines where there is already a comparable distribution of eaHuR between the nucleus and cytoplasm the subcellular redistribution of eaHUR is not observed following alphavirus infection (Dickson *et al.*, 2012).

The specific SFV4 genome sequences which bind HuR in the SFV4 genome have been determined to be a Uracil Rich Element (URE) and a Conserved Sequence Element (CSE) in the SFV4 3'UTR immediately 5' of the poly(A) tail (Sokoloski *et al.*, 2010). Alphaviruses which do not contain the conserved URE in their 3'UTR, namely Chikungunya virus (CHIKV) and Ross River virus (RRV), still bind HuR during infection of mammalian cells via their CSE and other U-rich sequences in their 3'UTR (Dickson *et al.*, 2012). When HuR binding sites in the SINV genome are removed or HuR mRNA is knocked-down (via siRNA interference) prior to SINV infection, a significant reduction in virus replication is observed (Sokoloski *et al.*, 2010). Taken together, these observations strongly suggest a key role played by cellular HuR in alphaviral genomic RNA processing and replication.

## 4.2 SFV4 icDNAs

SFV and SINV are amongst the most thoroughly studied alphaviruses due to their relatively lower safety classification (Containment Level 2, CL2) and the existence of easily manipulated expression vectors enabling efficient and intensive research in to their replication and interactions with host cells. SFV4 has a multitude of developed icDNA plasmids which encode the full viral genome including antibiotic resistance genes for replication of the plasmid in bacterial vectors and CMV promoters enabling expression of the virus in transfected cells. This negates the need of *in vitro* synthesis of the mRNA as required for more rudimental icDNAs which utilised an SP6 or similar promoter. Reporter genes such as GFP can also be relatively easily added to the icDNAs fused to viral genes such as nsP3 (Tamberg *et al.*, 2007) or expressed under a duplicated subgenomic promoter (Karlsson and Liljeström, 2004). This enables tracking of viral proteins within cells during infection and analysis of viral genome replication.

### 4.3 Objectives

The significance of the URE and CSE of the SFV4 3'UTR for SFV4 replication in mammalian cells was investigated in this study. The hypothesis predicted that a lack of HuR binding sites in the SFV4 3'UTR would inhibit virus replication in mammalian cells as well as examining if the sequestration of host HuR on SFV4 RNA had an indirect effect on the abundance of host-cell mRNA transcripts.

#### Specific objectives

1. Generate recombinant SFV4 (rSFV4) infectious complementary DNA (icDNAs) containing nucleotide sequence deletions or additions from/to the URE and CSE of the SFV4 3'UTR. Then grow infectious virus stocks from engineered icDNAs.
2. Determine if genetic reversion and/or other nucleotide changes occur in the generated virus stocks at the site of mutation generated in the corresponding icDNA.
3. Assess the subcellular localisation of host HuR during the course of infection of NIH/3T3 cells with the rSFV4 viruses.
4. Evaluate the growth characteristics of rSFV4 viruses in NIH/3T3 cells.
5. Determine impact on induction of caspase activity and cell death following infection with the rSFV4 viruses.
6. Assess if presence or absence of HuR binding sites in the SFV4 3'UTR affect the abundance and/or the nuclear export of mammalian host mRNA transcripts that contain putative HuR binding sites.

## 4.4 Results

### 4.4.1 rSFV4 viruses containing URE/CSE deletions or additions

Two sets of rSFV4 icDNAs, each with a different reporter protein, were utilised for the experiments in this chapter. Firstly a icDNA encoding *Guassia* luciferase (*Gluc*) expressed under a duplicated subgenomic promoter (Karlsson and Liljeström, 2004), and secondly, a rSFV4 encoding eGFP fused to viral nsP3 (Tamberg *et al.*, 2007) (*Figure 4.1.i*).

The URE and CSEs which bind HuR are present in the viral 3'UTR immediately upstream of the poly(A) tail. Five rSFV4 icDNAs containing deletions of all or parts of these elements were engineered including one icDNA with 4 additional duplicated UREs (*Figure 4.1.iii*).

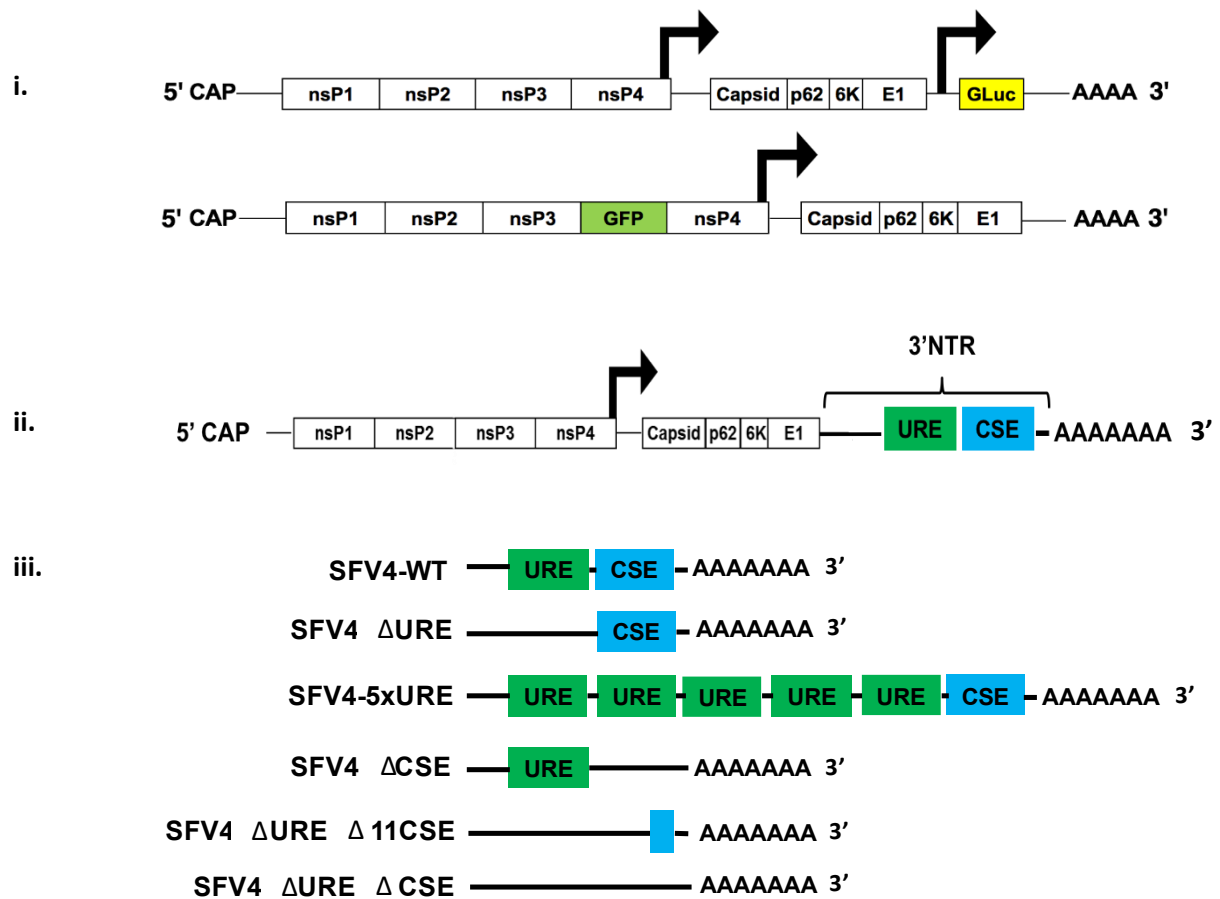


**Figure 4.1. Schematic representation of rSFV4 viral genomes** i. SFV4 genome encoding *Gaussia* luciferase under the control of a duplicated subgenomic promoter and the SFV4 genome encoding GFP fused to nsP3. ii. The URE element and conserved sequence element in the 3'UTR of SFV4 are located immediately 5' of the poly(A) tail. iii. Schematics of the rSFV4 viruses used in this study showing deletions and/or additions of the URE and/or the CSE.

#### 4.4.2 Production of infectious virus from rSFV4 icDNAs

Infectious SFV4 virus stocks were generated by transfecting rSFV4 icDNA plasmids in to BHK-21 cells as previously described (Chapter 2). The average time for a WT SFV4 icDNA plasmid to produce viable virus following transfection in to BHK-21 cells is 24-48 hours (Rausalu *et al.*, 2009). Interestingly, a deletion of the CSE from the SFV4 3'UTR delayed the time required to produce infectious virus from transfected icDNAs to day 5 post-transfection. The deletion of the URE in addition to part or all of the CSE further delayed infectious virus production (to 7-8 days post transfection) as compared to deletion of the CSE alone. Deletion or additions of the URE with an intact CSE did not affect the number of days required for the propagation of virus (Figure 4.2). The production of virus was determined by



visualisation of cytopathic effect (CPE), a significant luciferase signal compared to controls (from the SFV4-2SG-*Gluc* icDNAs) or visualisation of eGFP (from the SFV4(3F)eGFP icDNAs).

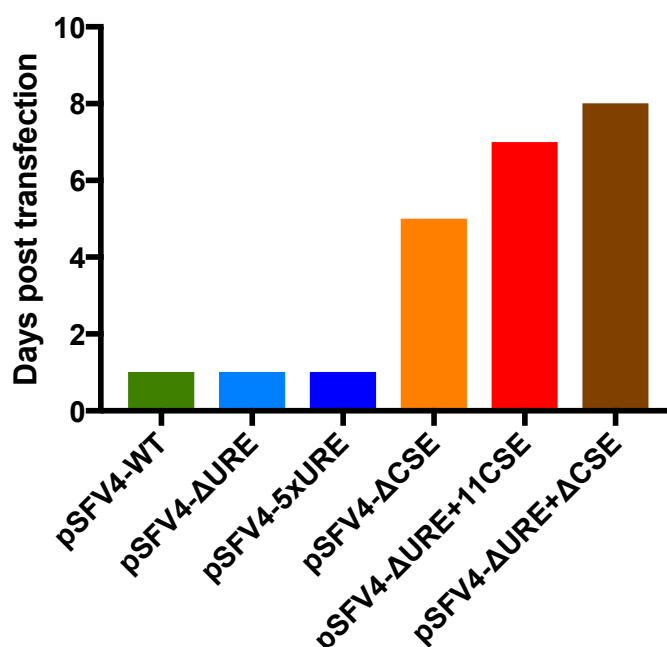


**Figure 4.2** Time taken in days for evidence of virion production and CPE following transfection in to BHK-21 cells of rSFV4 icDNAs containing alterations to the SFV4 3'UTR. The data is representative of 3 replicate experiments.

#### 4.43 Viral reversion and mutagenic pressures

The delayed production of virus from the SFV4 icDNAs containing CSE deletions suggests that the CSE plays a crucial role in virus replication. This is in line with previously published data, which showed that deletion of CSEs from other alphaviruses has a deleterious effect on virus growth and virus production (Hardy and Rice, 2005; George and Raju, 2000; Raju *et al.*, 1999). Interestingly, despite an initial delay in propagation, virus progeny produced from the SFV4 icDNAs with a deleted CSE did not show a significant decrease in virus replication rate nor virus titre following infection of NIH/3T3 cells (Figure 4.12 and 4.14). This suggested that compensatory genetic modifications (reversions) may have occurred in those viral genomes since the virus was now able to replicate its genome to a level comparable to the wild-type virus. To identify if compensatory mutations or full reversion had occurred, BHK-21 cells were infected with each of the rSFV4s for 12 hours, viral RNA was extracted

and reverse transcribed. The 3' end of the SFV 3'UTR was subject to PCR and the PCR product ligated in to a vector and sequenced (Figure 4.3).

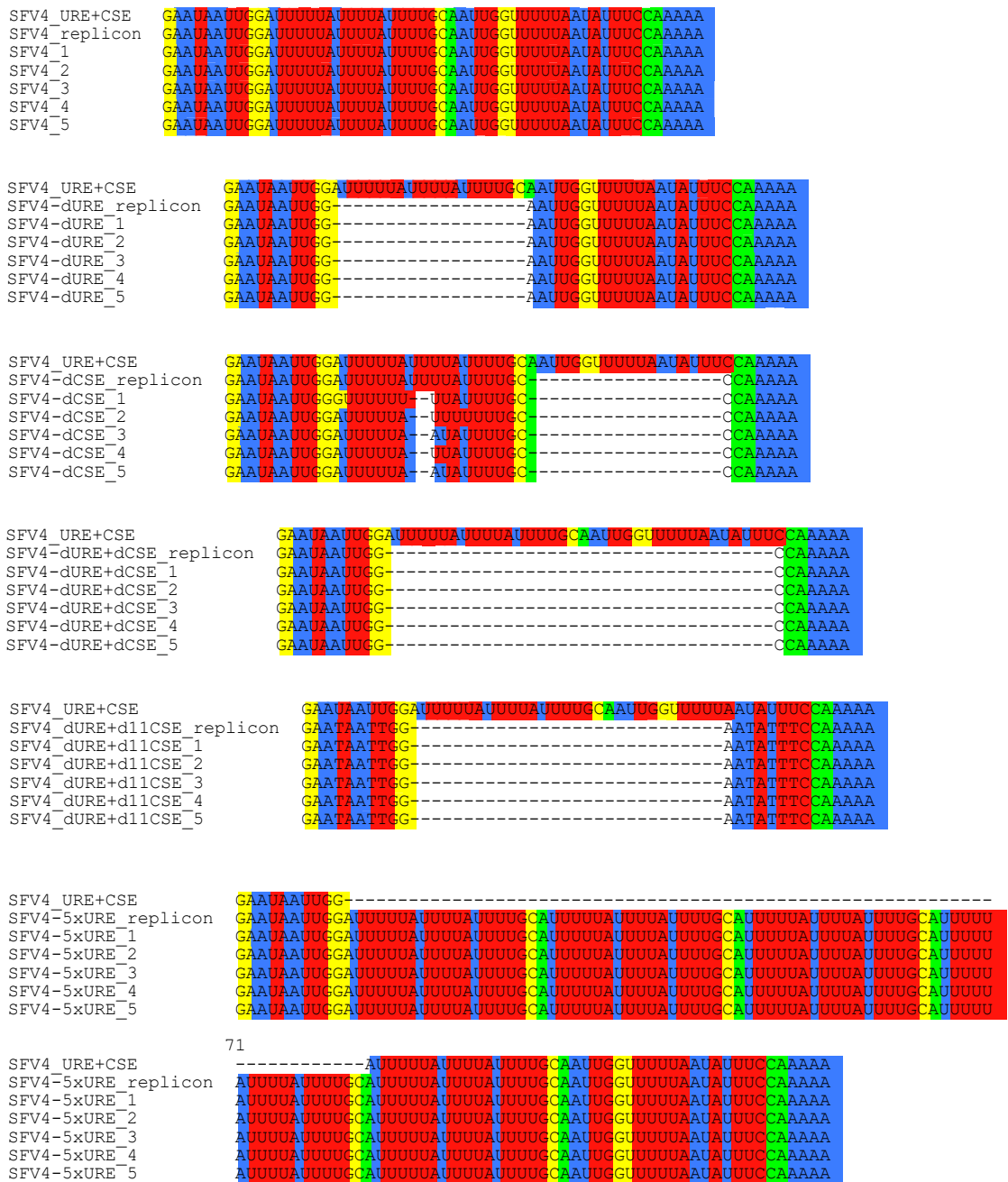


**Figure 4.3. Sequencing of the 3'UTR of the rSFV4.** The expected sequence is shown first, followed by the sequence of the transfected icDNA and then 5 individual sequences obtained from the given viral stock. No reversion was seen in this part of the viral genome for any of the rSFV4 viruses apart from viruses from the SFV4-2SG-*Gluc*-ΔCSE stock.

Of the five separate amplified sequences for each virus the 3'UTR matched the corresponding sequence of the transfected (parental) icDNA in all instances apart from virus propagated from the SFV4-2SG-*Gluc*- $\Delta$ CSE icDNA. Each sequence reverse-transcribed from virions from the SFV4-2SG-*Gluc*- $\Delta$ CSE viral stock had an additional deletion of 2 nucleotides. Furthermore, one sequence contained an A to G substitution. The nucleotides deleted from two samples from the SFV4-2SG-*Gluc*- $\Delta$ CSE viral stock reverted part of the wild-type SFV4-2SG-*Gluc* CSE sequence "UUUUUAAUAUUU" but this is not the case for all samples in which the two base deletions show no obvious reconstruction of the CSE sequence. Interestingly, SFV4-2SG-*Gluc*- $\Delta$ URE+ $\Delta$ CSE and SFV4-2SG-*Gluc*- $\Delta$ URE+ $\Delta$ 11CSE did not show any nucleotide sequence changes (reversion or novel) in the amplified section of the 3'UTR.

Despite no reversion or novel sequence changes seen in the viral stocks of all the rSFV4 viruses apart from SFV4-2SG-*Gluc*- $\Delta$ CSE, there may have been other compensatory sequence changes that have occurred in the viral genome to enable efficient viral replication. The consistency of the plaques produced from a viral stock can suggest how heterogeneous the virion population of the stock is. The plaque morphology can also suggest the ability of the virus to spread from cell to cell and induce cell death.

The morphology of plaques produced by the rSFV4-2SG-*Gluc* viruses in BHK-21 cells was assessed. The plaques produced from SFV4-2SG-*Gluc*-5xURE are similar in appearance to those produced by SFV4-2SG-*Gluc*-WT. When the URE is removed, as for SFV4-2SG-*Gluc*- $\Delta$ URE, the plaques are slightly larger but turbid. The turbid nature of the plaques suggests a reduction in virus mediated lysis or virus replication rate since all the cells in the plaque have not lysed before a new layer of cells have taken their place.

The viruses containing CSE deletions, SFV4-2SG-*Gluc*- $\Delta$ CSE, SFV4-2SG-*Gluc*- $\Delta$ URE+ $\Delta$ CSE and SFV4-2SG-*Gluc*- $\Delta$ URE+ $\Delta$ 11CSE, produced a heterogeneous population of plaque sizes. This suggests the presence of viral quasispecies in each of these virus stocks (Liu and Wu, 2004).

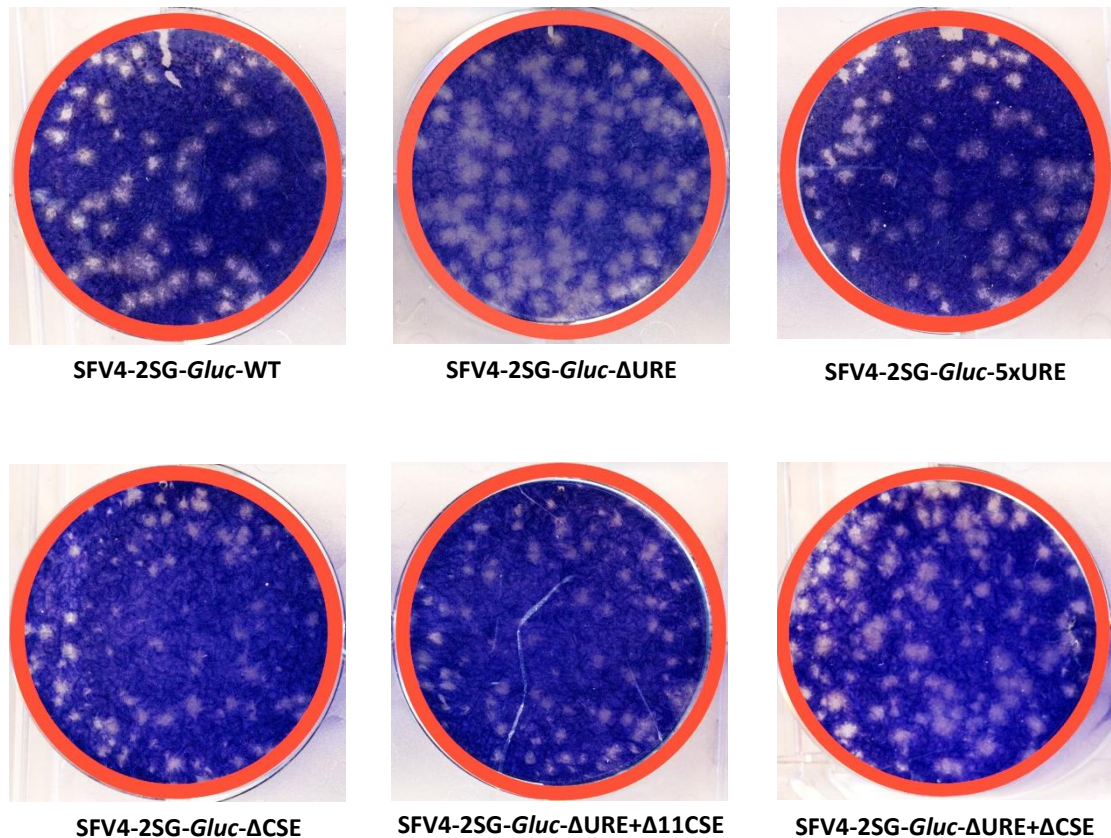


**Figure 4.4 Plaque morphology from rSFV4.** Serial dilutions from rSFV4 stocks were used to infect BHK-21 cells in standard plaque assay. SFV4-2SG-*Gluc*-ΔURE exhibited turbid plaques, SFV4-2SG-*Gluc*-5xURE plaques are comparable to SFV4-2SG-*Gluc*-WT. Plaques produced from infection with virus stocks that contained deletions from the CSE exhibit a heterogeneous population of small and large plaques suggesting genetic variations between virions within the same virus stocks.

#### 4.4.4 SFV4 infection causes HuR subcellular relocalisation

As part of this study, the potential roles mediated by URE and CSE of the 3'UTR of SFV4 to bind host protein HuR were investigated. To assess the subcellular location of HuR following infection with the rSFV4 viruses, murine NIH/3T3 cells were immunostained against HuR protein. Previous groups have shown that HuR relocates to the cytoplasm where it binds to the alphavirus 3'UTR during infection (Sokoloski *et al.*, 2010). However key parameters such as the proportion of HuR that relocates to the cytoplasm compared to the proportion remaining in the nucleus during SFV4 infection, the rate at which this occurs and whether this is maintained throughout infection had not been addressed fully. A second cellular RNA-binding cellular protein, PABPC, was also investigated because PABPC also binds viral RNA (due to the presence of a poly(A) tail) and can affect RNA stability and translation.

In murine NIH/3T3 cells HuR is located predominantly (~80%) in the nucleus (*Figure 4.5 and 4.10*). Infection of NIH/3T3 cells with SFV4 viruses retaining the WT 3'UTR results in HuR relocating predominantly (79.8%) to the cytoplasm by 6 h.p.i., reaching 91.2% by 9 h.p.i. and being retained in the cytoplasm during the remaining course of infection (*Figure 4.5 and 4.10*). HuR was dispersed throughout the cytoplasm and appeared to colocalise with PABPC, and sometimes in discrete cytoplasmic foci. The cytoplasmic HuR and PABPC had left large areas in the cytoplasm by 15 h.p.i. and concentrated around the cytoplasmic face of the nuclear and cytoplasmic membranes (*Figure 4.5 and 4.10*). The SFV4(3F)-eGFP virus encodes eGFP fused to nsP3.; therefore, the location of nsP3 can be used as a marker for SFV4 induced CPV-I spherules where SFV genome replication is actively taking place. The re-localised HuR to the cytoplasm following infection with SFV4(3F)-eGFP did not co-localise with nsP3-eGFP suggesting that the HuR was removed from the SFV4 CPV-I (*Figure 4.5*). Taken together, imaging data illustrates a cumulative migration of HuR into the cytoplasm from 3 h.p.i. onwards in NIH/3T3 cells following infection with SFV4(3F)-eGFP. The relocalised HuR is retained in the cytoplasm but not in SFV4 CPV-Is and appears to co-localise with PABPC.



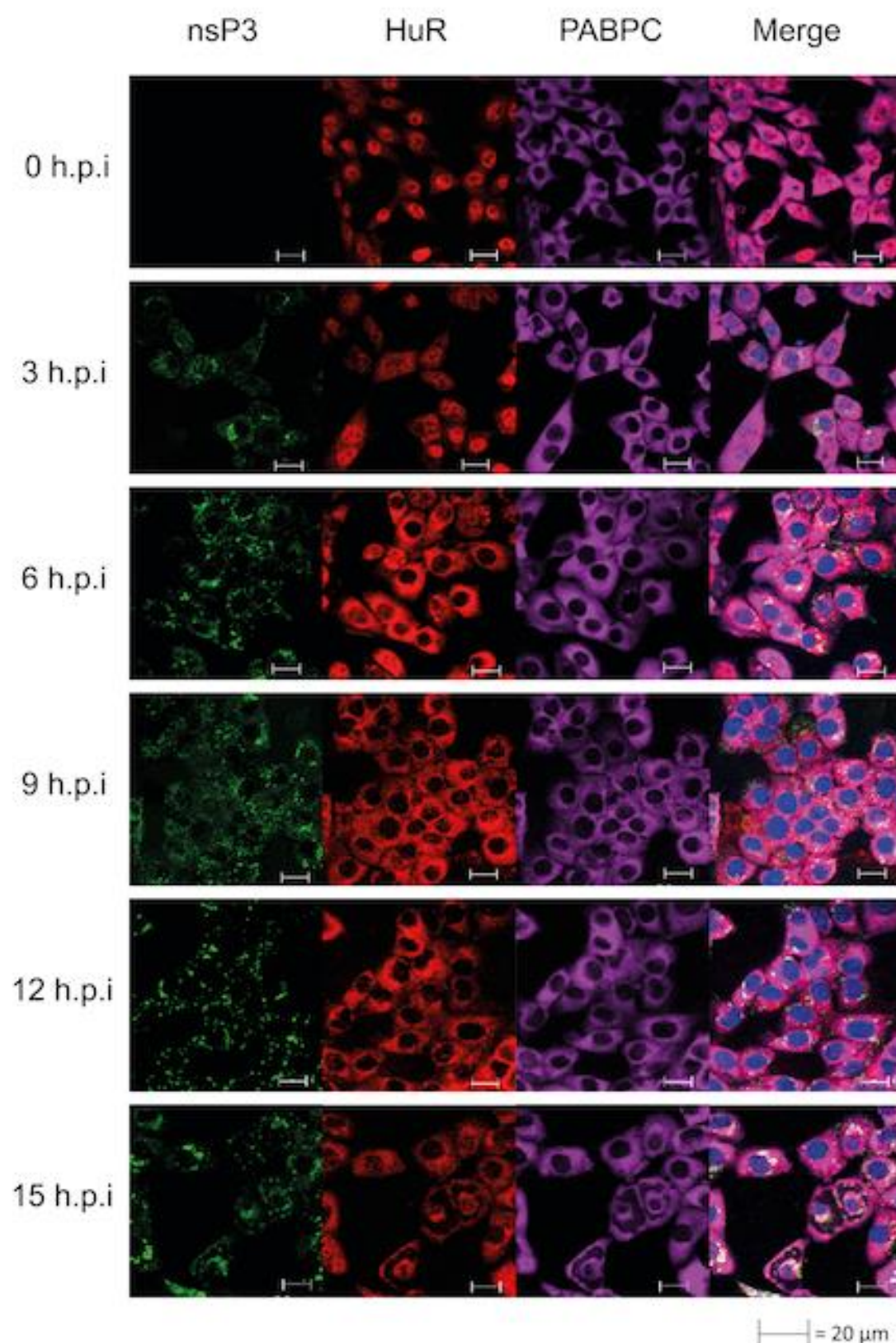
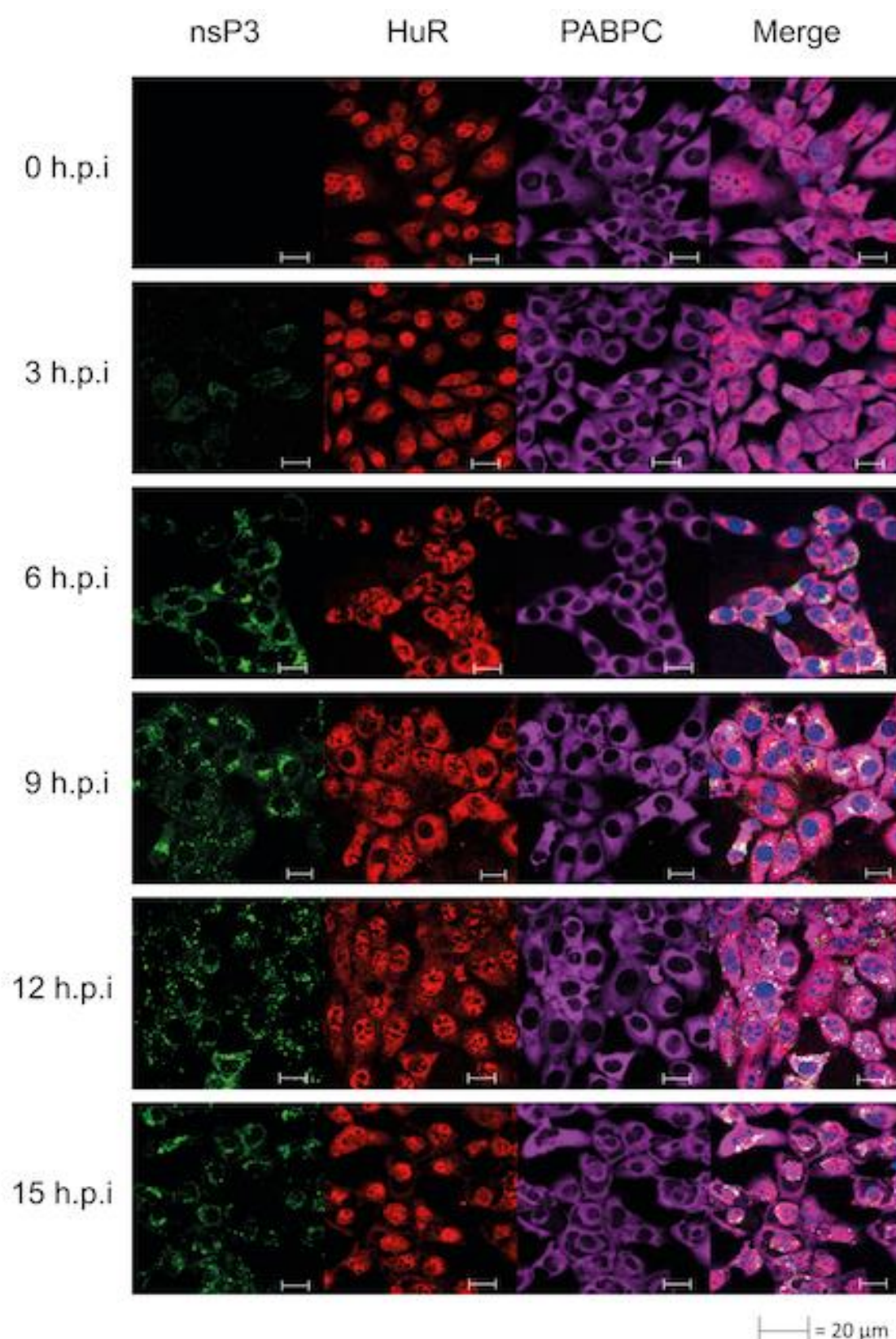


**Figure 4.5.** During infection with SFV4(3F)-eGFP-WT, HuR relocalises predominantly to the cytoplasm by 9 h.p.i. NIH/3T3 cells were infected at an MOI of 10 with SFV4(3F)-eGFP-WT and fixed at various time points post infection. Cells were stained with antibodies against HuR (red) and PABPC (pink) with DAPI stain (blue) and had endogenous nsP3-eGFP fluorescence (green).

Previous studies have shown that HuR binds the URE of alphaviral 3'UTRs including SFV4. This interaction may be responsible for the re-localisation of HuR to the cytoplasm following infection with SFV4(3F)-eGFP. The deletion of URE from the SFV4 3'UTR resulted in a lower proportion of HuR relocating to the cytoplasm following infection with SFV4(3F)-eGFP- $\Delta$ URE compared to SFV4(3F)-eGFP during the entire course of infection (*Figure 4.6*). The proportion of HuR in the cytoplasm following infection with SFV4(3F)-eGFP- $\Delta$ URE increased from 20.2% at 0 h.p.i. to 27.5% by 3 h.p.i. (*Figure 4.6 and 4.10*). This proportion peaked at a mean of 57% at 9 h.p.i. and dropped to 43% by 12 h.p.i. and 34% by 15 h.p.i. (*Figure 4.6 and 4.10*). Although a significant amount of HuR was relocated to the cytoplasm by 9 h.p.i. (57%) compared to NIC (20%), there was a following drop in the proportion of cytoplasmic HuR by 12 h.p.i. This 14% drop in quantity of cytoplasmic HuR in three hours was in contrast to the 11.4% increase from 9 to 12 h.p.i. observed following infection with SFV4(3F)-eGFP. Taken together these data show that HuR re-localisation to the cytoplasm following SFV4 infection still occurs when the URE of the SFV4 3'UTR is deleted but is significantly reduced. Furthermore, less HuR is retained in the cytoplasm following the initial re-localisation from the nucleus.





Addition of 4 extra URE elements to SFV4 3'UTR resulted in HuR relocating at a faster rate to the cytoplasm, 46.3% by 3 h.p.i and 98% by 6 h.p.i. Furthermore, this ratio of cytoplasmic HuR to nuclear HuR was maintained during the course of infection, still 98% at 12 h.p.i. and 94.5% by 15 h.p.i. (*Figure 4.7 and Figure 4.10*). The differences in the ratio of re-localised HuR between infection with SFV4(3F)-eGFP-5xURE compared to SFV4(3F)-eGFP was statistically significant at all time points post-infection. As with the other rSFV4 viruses the re-localised cytoplasmic HuR following SFV4(3F)-eGFP-5xURE infection co-localised with PABPC but not with nsP3-eGFP.

Taken together these data suggest that the relocalisation of HuR during SFV4 infection is significantly decreased by the deletion of the URE from the SFV4 3'UTR and significantly increased by the addition of multiple URE to the SFV4 3'UTR.

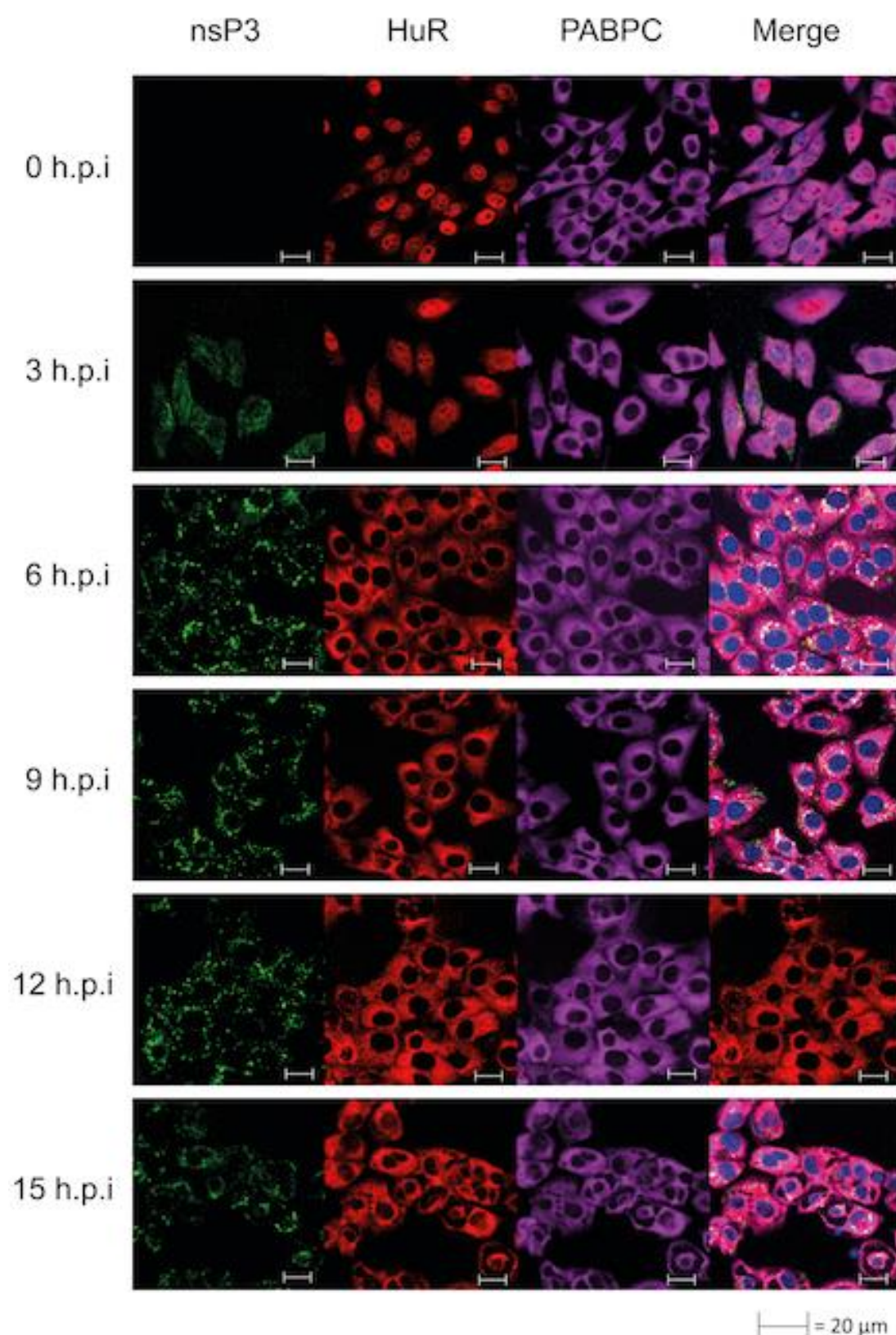


**Figure 4.7** HuR relocates predominantly to the cytoplasm by 6 h.p.i. following infection with an SFV4 mutant containing four additional URE's in the 3'NTR. NIH/3T3 cells were infected at an MOI of 10 with SFV4(3F)-eGFP-5xURE and fixed at various time points post infection. Cells were stained with antibodies against HuR (red) and PABPC (pink) with DAPI stain (blue) and had endogenous nsP3-eGFP fluorescence (green).

Infection of NIH/3T3 cells with SFV4(3F)-eGFP- $\Delta$ CSE resulted in cellular HuR re-localising to the cytoplasm to 31.9% by 3 h.p.i., 65.8% by 6 h.p.i. and peaking at 79.1% by 9 h.p.i. (*Figure 4.8 and Figure 4.10*). The proportion of HuR which was cytoplasmic then dropped between 9 and 12 h.p.i. similar to infection with SFV4(3F)-eGFP- $\Delta$ URE but only by 3% to 75.9%. The re-localised HuR co-localised with PABPC, including in distinct foci in some cells as with the other rSFV4 viruses. The difference in the ratio of cytoplasmic HuR between infection with SFV4(3F)-eGFP- $\Delta$ CSE and SFV4(3F)-eGFP was not statistically significant ( $p=0.07$ ) at 3 h.p.i, but was significant at all later time points measured ( $p<0.05$ ).

Taken together these results indicate that the initial re-localisation and subsequent retention of HuR in the cytoplasm following SFV4 infection is partially increased by the retention of the CSE in the SFV4 3'NTR but to a lesser extent than retention of the URE.

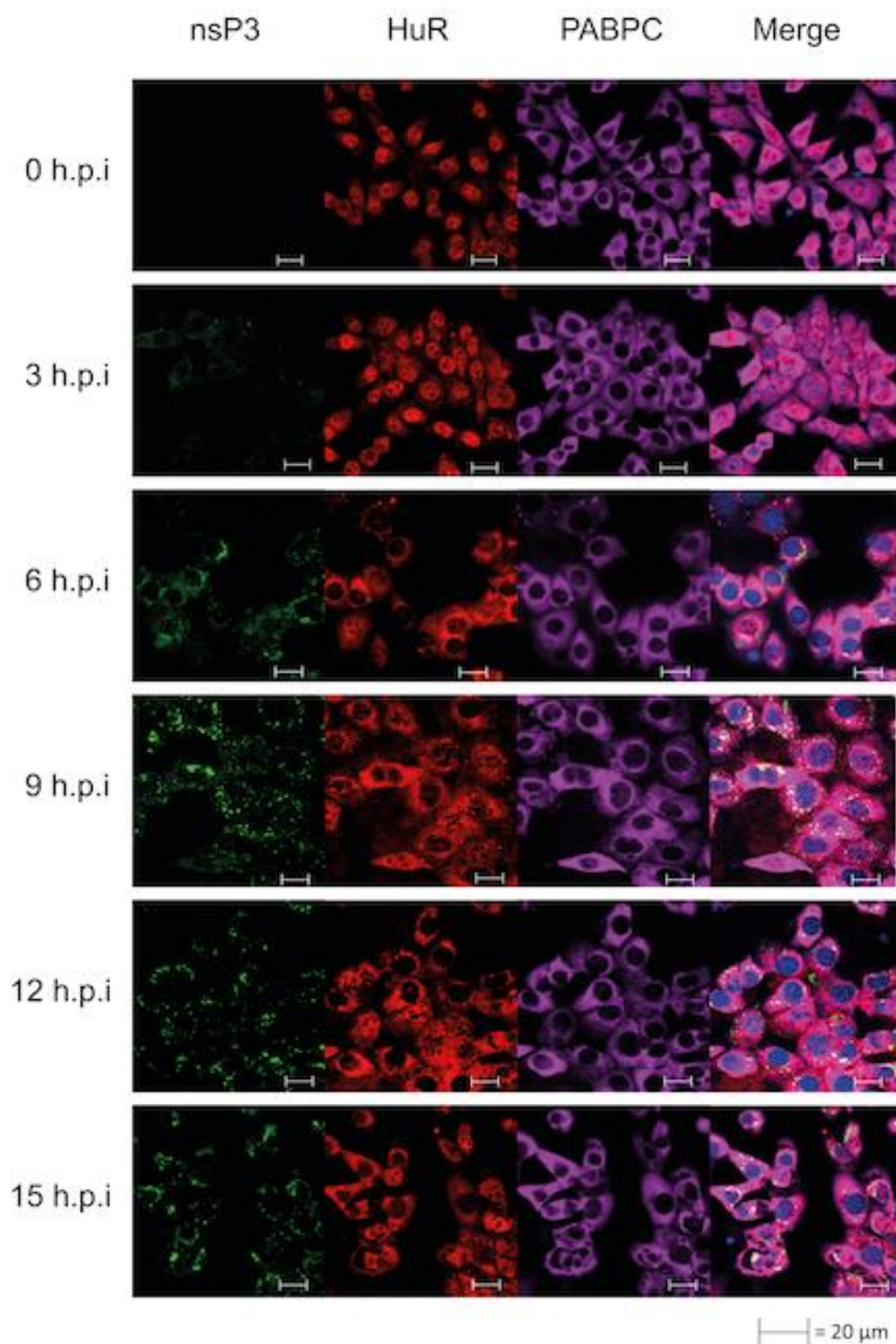


**Figure 4.8. HuR relocalises predominantly to the cytoplasm by 6 h.p.i. with SFV4(3F)-eGFP- $\Delta$ CSE but remains partially nuclear during infection.** NIH/3T3 cells were infected at an MOI of 10 with SFV4(3F)-eGFP- $\Delta$ CSE and fixed at various time points post infection. Cells were stained with antibodies against HuR (red) and PABPC (pink) with DAPI stain (blue) and had endogenous nsP3-eGFP fluorescence (green).

Infection with SFV4(3F)-eGFP- $\Delta$ URE+ $\Delta$ CSE caused an initial rate of HuR relocalisation comparable to the control, i.e. 71% at 6 h.p.i., but dropped sharply to 64% at 9 h.p.i. and 51% at 12 h.p.i, respectively (*Figure 4.9 and Figure 4.10*). The difference in percentage of cytoplasmic HuR during infection between SFV4(3F)eGFP- $\Delta$ URE+ $\Delta$ CSE and SFV4(3F)eGFP was not significant at 3 or 6 h.p.i. ( $p=0.47$  and  $p=0.18$  respectively), but was significant at all later time points measured.

There are large standard deviations when analysing the ratios of cytoplasmic HuR to nuclear HuR between individual cells following infection with SFV4(3F)eGFP- $\Delta$ URE, SFV4(3F)eGFP- $\Delta$ CSE and SFV4(3F)eGFP- $\Delta$ URE+ $\Delta$ CSE. In contrast, there is a relatively small standard deviation seen during infection with SFV4-2SG-*Gluc*-5xURE. This may suggest that the overall phenotype is dominated by a single molecular event rather than many varied events but further study is required.



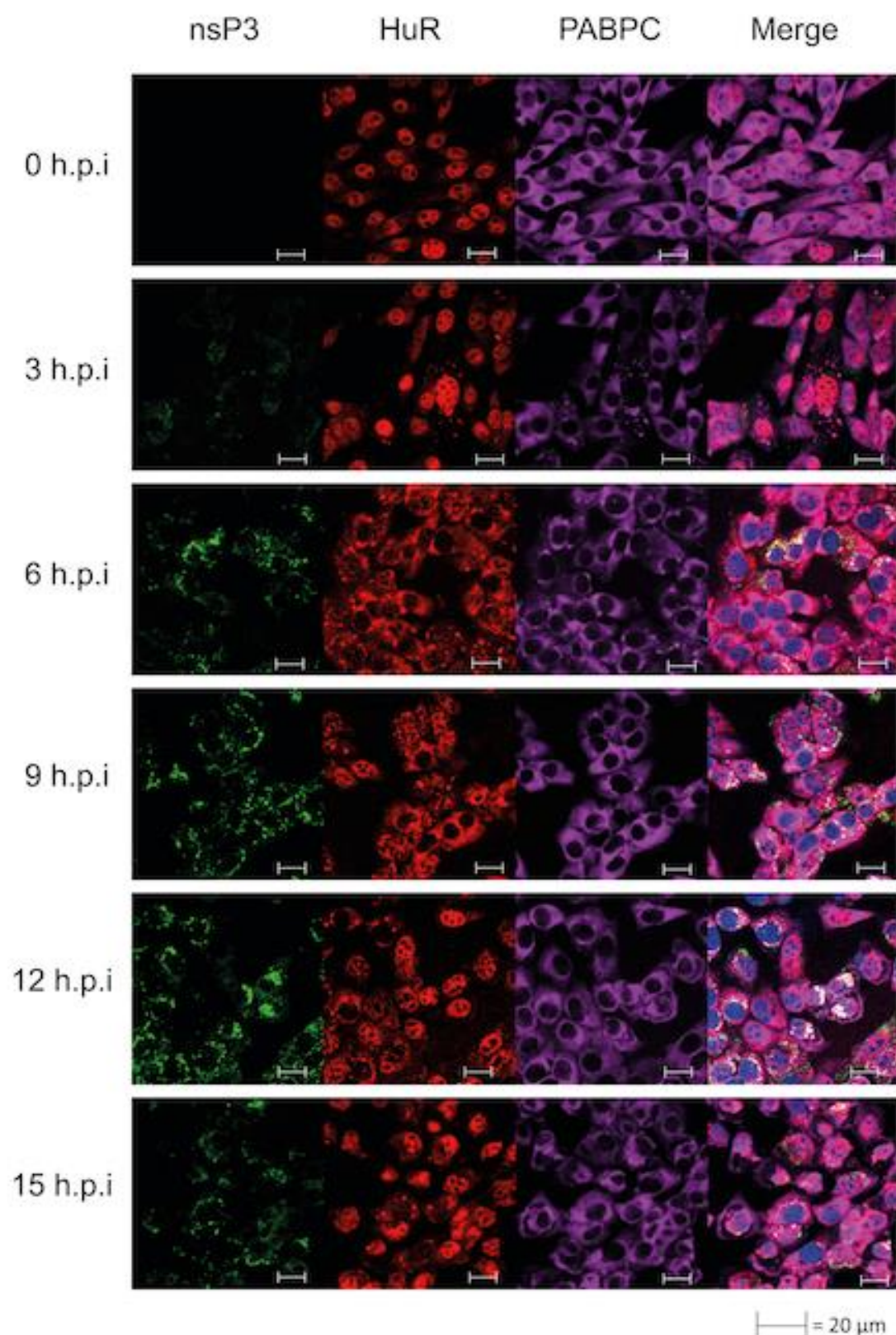


**Figure 4.9. HuR relocalises partially to the cytoplasm by 6 h.p.i. following infection with SFV4(3F)-eGFP- $\Delta$ URE/CSE and then is predominantly nuclear once again by 12 h.p.i.** NIH/3T3 cells were infected at an MOI of 10 with SFV4(3F)-eGFP- $\Delta$ URE/CSE and fixed at various time points post infection. Cells were stained with antibodies against HuR (red) and PABPC (pink) with DAPI stain (blue) and had endogenous nsP3-eGFP fluorescence (green).

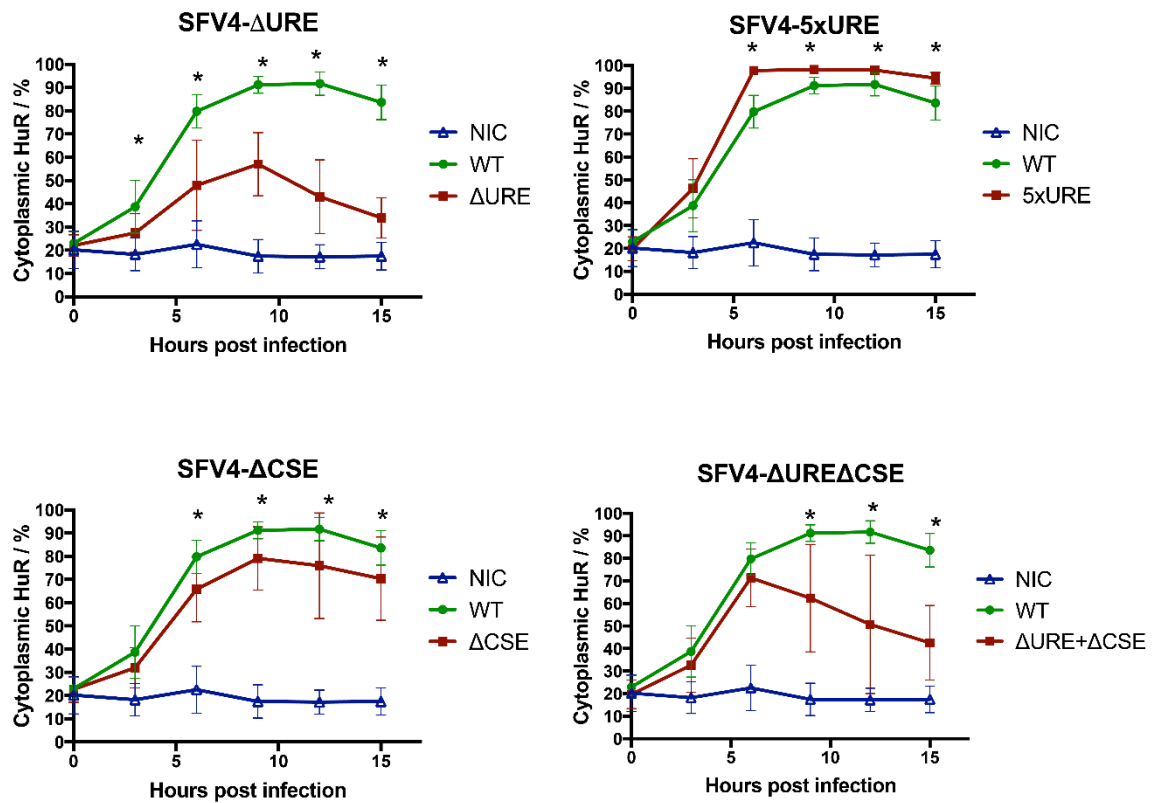


**Figure 4.10. The percentage of total HuR immunostaining present in the cytoplasm in relation to the whole cell during infection with rSFV4 mutants containing URE and/or CSE deletions and/or additions to the viral 3'NTR.** NIH/3T3 cells were infected with rSFV4 at an MOI of 10 and fixed and immunostained at various time points post-infection. The percentage of cytoplasmic HuR was calculated from a total of 20 individual cells for each time point for each virus. Error bars are standard deviation which indicate a large variation between individual cells for some viral mutants. All data sets were statistically significant ( $p < 0.05$ ) by ANOVA analysis. Asterisks mark time points where the difference between the WT and the mutant is statistically significant by multiple-t test ( $p < 0.05$ ).

#### 4.4.5 Viral replication of rSFV4 URE+CSE mutants

The replication of the rSFV4 mutants in single and multi-step growth curves were assessed by plaque assay. The deletion of the URE from the SFV4 3'UTR not only resulted in the least proportion of HuR being retained in the cytoplasm during infection but also caused a significant reduction in infectious virion production (*Figure 4.11*).

At a high MOI (MOI=10), infection of murine NIH/3T3 cells with SFV4-2SG-*Gluc*- $\Delta$ URE caused a significant reduction in virus production in the initial hours of infection (6 h.p.i.,  $p < 0.001$ ) compared to infection with SFV4-2SG-*Gluc*-WT (*Figure 4.11*). SFV4-2SG-*Gluc*- $\Delta$ URE produced similar levels of virus compared to wild type infection by 12 h.p.i. During a multi-step growth curve (infection at MOI = 0.01) SFV4-2SG-*Gluc*- $\Delta$ URE produced infectious virus at consistently lower titres compared to SFV4-2SG-*Gluc*-WT throughout the course of infection (*Figure 4.11*).

The deletion of the URE resulted in the reduction of infectious virus released following infection of NIH/3T3 cell. In contrast, the addition of 4 extra URE elements in the SFV4-2SG-*Gluc*-5xURE virus resulted in an increase in production of infectious virus compared to SFV4-2SG-*Gluc*-WT (*Figure 4.11*). During a one-step growth curve (MOI=10) in NIH/3T3 cells following infection with SFV4-2SG-*Gluc*-5xURE, there was a significantly higher production of infectious virus produced compared to SFV4-2SG-*Gluc*-WT infection at 6 and 9 h.p.i. ( $p = < 0.01$  at both time points) (*Figure 4.11*). The higher quantities of infectious virus produced during SFV4-2SG-*Gluc*-5xURE infection compared to SFV4-2SG-*Gluc*-WT showed a reduced trend by 12 h.p.i. and thereafter; reaching levels which were no longer statistically significant ( $p = 0.98$  at 12 h.p.i.) (*Figure 4.11*). Following infection at a lower MOI (0.01) SFV4-2SG-*Gluc*-5xURE infection of NIH/3T3 cells produced higher quantities of infectious virus from 6 to 18 h.p.i. ( $p < 0.01$  at all time points), and was comparable to infection with SFV4-2SG-*Gluc*-WT at 24 h.p.i.

Taken together these results indicate the frequency of the URE in the SFV4 3'UTR affects the initial concentration of infectious virus propagated in murine NIH/3T3 cells. A deletion of the URE results in an initial significant decrease in production of infectious virus and the addition of 4 extra URE results in an initial significant increase of propagated infectious virus following infection.



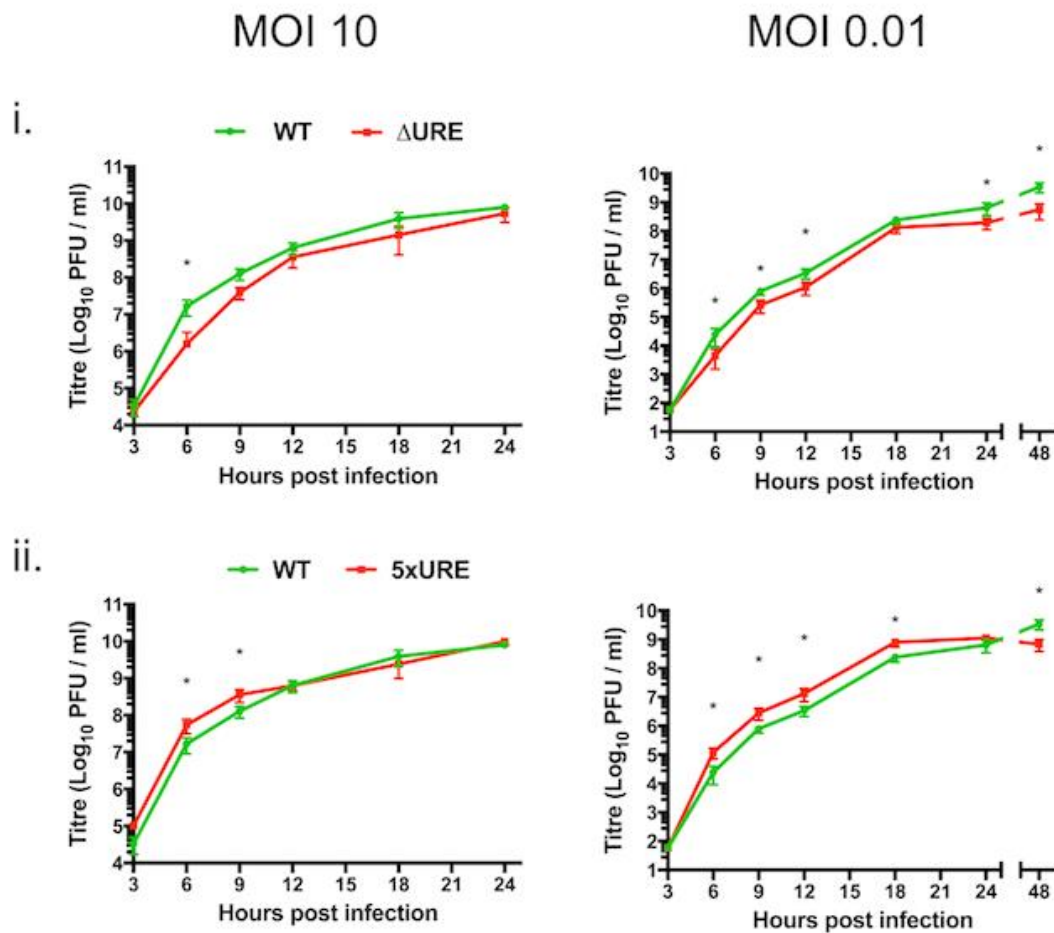


**Figure 4.11. Growth kinetics of rSFV4-2SG-*Gluc* viruses in NIH/3T3 cells containing URE deletion or additions in the 3'NTR of the SFV4 genome as measured by plaque assay.** Single-step (MOI 10) and multi-step (MOI 0.01) viral growth were measured by infecting NIH/3T3 cells at the given MOI. Samples taken from infected medium the virion titre measured by plaque assay in BHK-21 cells. Values represent an average of 3 biological replicates and error bars represent standard deviation. The results are representative of 3 replicate experiments. Asterisks represent a statistically significant difference ( $p < 0.05$ ) for the given time point. (i) URE deletion (ii) 4 x URE additions

Despite the delayed propagation of virus from the counterpart icDNAs, the three rSFV4 viruses that contained CSE deletions in their 3'UTR, SFV-2SG-*Gluc*- $\Delta$ CSE, SFV4-2SG-*Gluc*- $\Delta$ URE+ $\Delta$ 11CSE and SFV4-2SG-*Gluc*- $\Delta$ URE+ $\Delta$ CSE replicated in NIH/3T3 cells at a rate comparable to the SFV4-2SG-*Gluc*-WT virus (*Figure 4.12*).

The SFV-2SG-*Gluc*- $\Delta$ CSE replicated at levels comparable to SFV4-2SG-*Gluc*-WT for both one-step and multi-step growth curves. In the one step-growth curve the SFV-2SG-*Gluc*- $\Delta$ CSE virus produced infectious virus at levels (PFU) that were not significantly different to infection with SFV4-2SG-*Gluc*-WT at all points throughout the course of infection (*Figure 4.12*). During the multi-step growth, the SFV4-2SG-*Gluc*- $\Delta$ CSE virus produced less infectious virus at 6 h.p.i. but then later surpassed the levels of infectious virus from cells infected with SFV4-2SG-*Gluc*-WT at later time points post infection. However, this increase was not statistically significant (*Figure 4.12*).

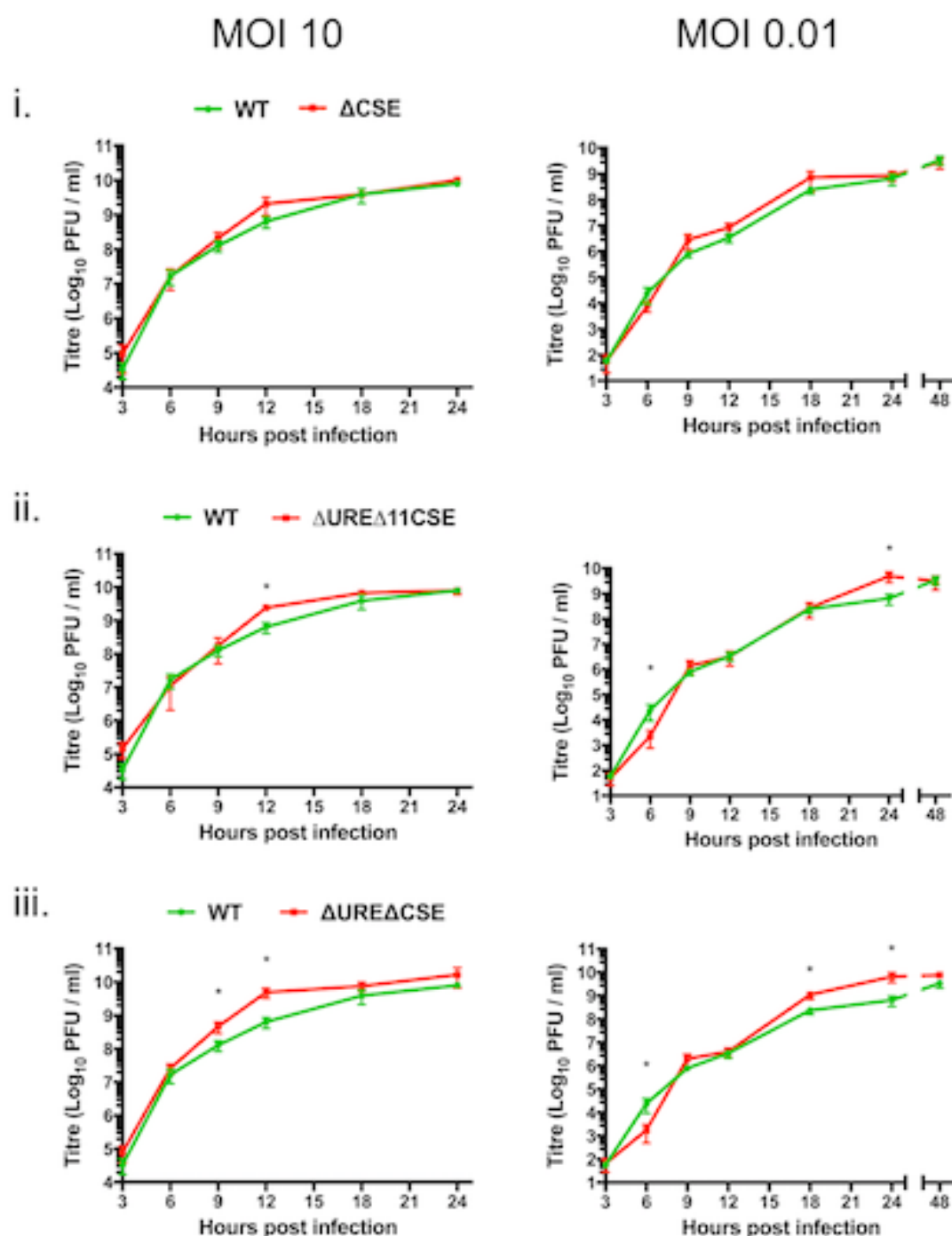


**Figure 4.12. Growth kinetics of rSFV4-2SG-*Gluc* viruses in NIH/3T3 cells containing deletions of the CSE and URE as measured by plaque assay.** Single-step (MOI 10) and multi-step (MOI 0.01) viral growth were measured by infecting NIH/3T3 cells at the given MOI. Samples taken from infected medium were used to determine titre by plaque assay in BHK-21 cells. Values represent an average of 3 biological replicates and error bars represent standard deviation. The results are representative of 3 replicate experiments. Asterisks represent a statistically significant difference for the given time point ( $p < 0.05$ ). (i) CSE deletion (ii) URE and 11CSE deletion (iii) URE and CSE deletion.

At a MOI of 0.01, the two rSFV4 viruses which contained both deletion of the URE and either partial or almost full deletion of the CSE, initially grew significantly slower up to 6 h.p.i. when compared to the wild type virus SFV4-2SG-*Gluc*-WT (Figure 4.12,  $p < 0.01$  for both viruses). Thereafter, both mutant viruses (SFV4-2SG-*Gluc*- $\Delta$ URE+ $\Delta$ 11CSE and SFV4-2SG-*Gluc*- $\Delta$ URE+ $\Delta$ CSE) propagated at comparable levels to SFV4-2SG-*Gluc*-WT (Figure 4.12). Infection of NIH/3T3 cells with SFV4-2SG-*Gluc*- $\Delta$ URE+ $\Delta$ 11CSE produced significantly more infectious virus comparable to WT virus at 24 h.p.i (Figure 4.12,  $p < 0.01$ ), and infection with SFV4-2SG-*Gluc*- $\Delta$ URE+ $\Delta$ CSE produced significantly more infectious virus comparable to WT virus at both 18 and 24 h.p.i. (Figure 4.12,  $p < 0.01$  for both time points).

During a one-step growth curve SFV4-2SG-*Gluc*- $\Delta$ URE+ $\Delta$ 11CSE and SFV4-2SG-*Gluc*- $\Delta$ URE+ $\Delta$ CSE viruses initially replicated at comparable levels to the wild type virus SFV4-2SG-*Gluc*-WT. SFV4-2SG-*Gluc*- $\Delta$ URE+ $\Delta$ 11CSE then produced significantly higher amount of infectious virus compared to the SFV4-2SG-*Gluc*-WT at 12 h.p.i (Figure 4.12,  $p < 0.01$ ). Moreover, SFV4-2SG-*Gluc*- $\Delta$ URE+ $\Delta$ CSE propagated at a significantly higher levels compared to the wild type virus SFV4-2SG-*Gluc*-WT at both 9 and 12 h.p.i. (Figure 4.12,  $p < 0.01$  for both time points).

The SFV4 genome replication was also monitored by measurement of luciferase activity which is proportional to the concentration of luciferase produced during infection with the rSFV4 viruses expressing *Guassia* luciferase under a duplicated subgenomic promoter. The luciferase mRNA is replicated with the same 3' UTR as the viral genome and thus the changes to the URE/CSE should affect the luciferase mRNA and expression in an analogous manner to the viral genome. The luciferase expression therefore reflects the viral RNA abundance, stability and translation rather than the production of viable virus.

The analysis of viral replication through luciferase production complements the plaque assay data for SFV4-2SG-*Gluc*- $\Delta$ URE and SFV4-2SG-*Gluc*-5xURE infection at both MOI of 10 and MOI of 0.01. Luciferase production was significantly lower at all time points post infection (apart from 48 h.p.i.) following infection of NIH/3T3 cells with SFV4-2SG-*Gluc*- $\Delta$ URE at a MOI of 0.01 compared to the wild type virus SFV4-2SG-*Gluc*-WT (Figure 4.13,  $p < 0.01$ ). Furthermore, luciferase production was significantly lower at 3 h.p.i. following infection with SFV4-2SG-*Gluc*- $\Delta$ URE at MOI 10 compared to SFV4-2SG-*Gluc*-WT (Figure 4.13,  $p < 0.01$ ) but then reached a comparable level to the wild type virus at later time points post infection.

In direct contrast to SFV4-2SG-*Gluc*- $\Delta$ URE, infection with SFV4-2SG-*Gluc*-5xURE produced significantly higher levels of luciferase at all time points post infection (apart from 48 h.p.i.) in NIH/3T3 cells at a MOI of 0.01 compared to SFV4-2SG-*Gluc*-WT (Figure 4.13,  $p < 0.01$ ). In addition, luciferase activity was significantly higher at 3 h.p.i. following infection with SFV4-2SG-*Gluc*-5xURE at MOI 10 compared to

the wild type virus SFV4-2SG-*G/luc*-WT but comparable levels were reached thereafter (*Figure 4.13*,  $p<0.01$ ).

Taken together the results from luciferase assays suggest that the URE sequence promotes viral protein production either through stability and/or translation of viral RNA. This compliments the data from plaque assay which indicated the URE increases the propagation of infectious virus during initial replication in NIH/3T3 cells.

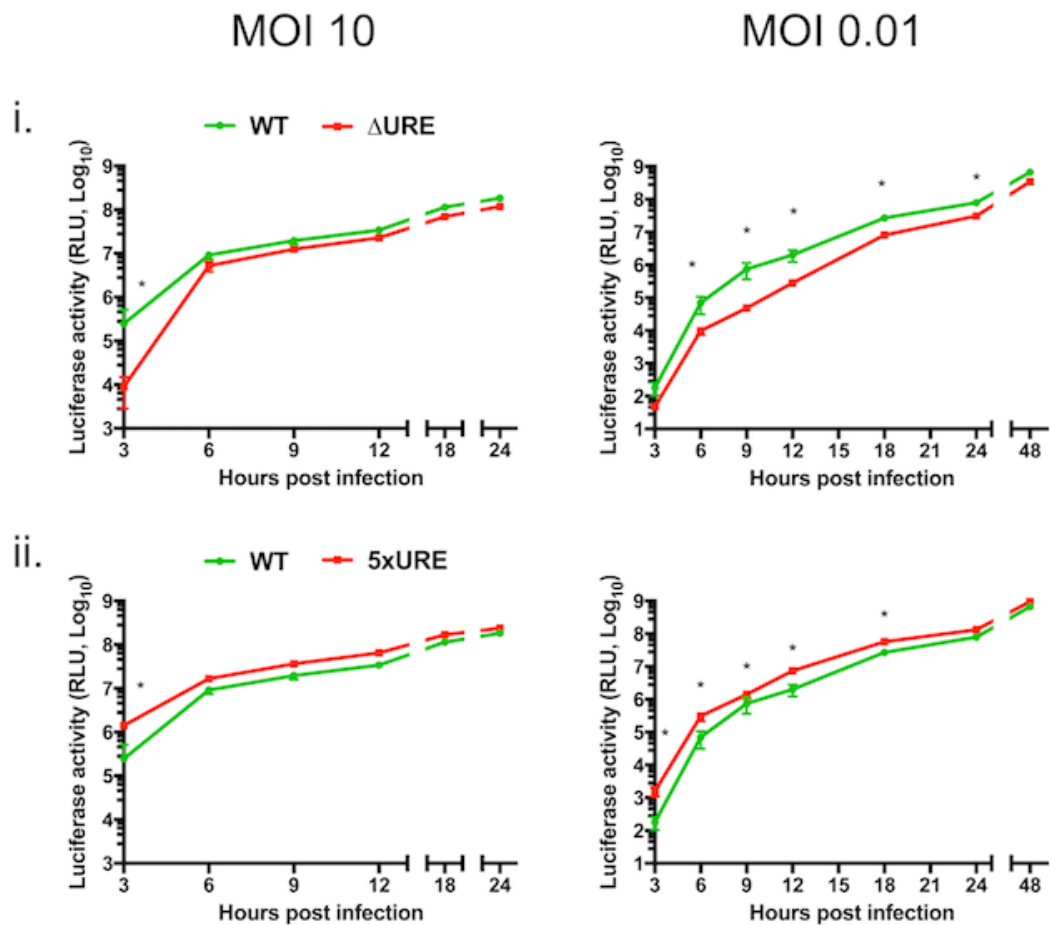


**Figure 4.13. Growth kinetics of rSFV4-2SG-*Gluc* viruses in NIH/3T3 cells containing URE deletion or additions in the 3'NTR of the SFV4 genome as measured by *Gaussia* luciferase activity.** Single-step (MOI 10) and multi-step (MOI 0.01) viral growth were measured by infecting NIH/3T3 cells at the given MOI. Samples taken from infected medium were used to measure secreted *Gaussia* luciferase which is expressed from the given virus genome under a secondary sub-genomic promoter. Values represent an average of 3 biological replicates and error bars represent standard deviation. The results are representative of 3 replicate experiments. Asterisks represent a statistically significant difference for the given time point ( $p < 0.05$ ). (i) URE deletion (ii) 4 x URE additions

Deletion of the CSE appears to have minimal effect on luciferase signal. There were no significant changes in luciferase activity produced following infection of NIH/3T3 cells with SFV4-2SG-*Gluc*- $\Delta$ CSE compared to the wild type virus SFV4-2SG-*Gluc*-WT at any time point post infection either at low or high MOI (*Figure 4.14*). A plausible suggestion is that deletion of the CSE has minimal effect on viral RNA replication rate through either RNA stability or translation. An alternative possibility is that virions that are eventually propagated from a transfected SFV4 icDNA with a deleted CSE, replicate at a comparable rate to the wild-type SFV4 despite a delay in initial propagation from icDNA.

An engineered virus with a deletion of the entire URE element and 18 bases of the CSE element (SFV4-2SG-*Gluc*- $\Delta$ URE+ $\Delta$ CSE), produced less luciferase at all time points post infection when compared to the wild type virus SFV-2SG-*Gluc*-WT (*Figure 4.14*). The differences in luciferase production following NIH/3T3 infection with SFV4-2SG-*Gluc*- $\Delta$ URE+ $\Delta$ CSE compared to SFV-2SG-*Gluc*-WT was substantial and statistically significant at all time points measured and at both high (10) and low (0.01) MOI (*Figure 4.14*,  $p < 0.01$  for all time points).

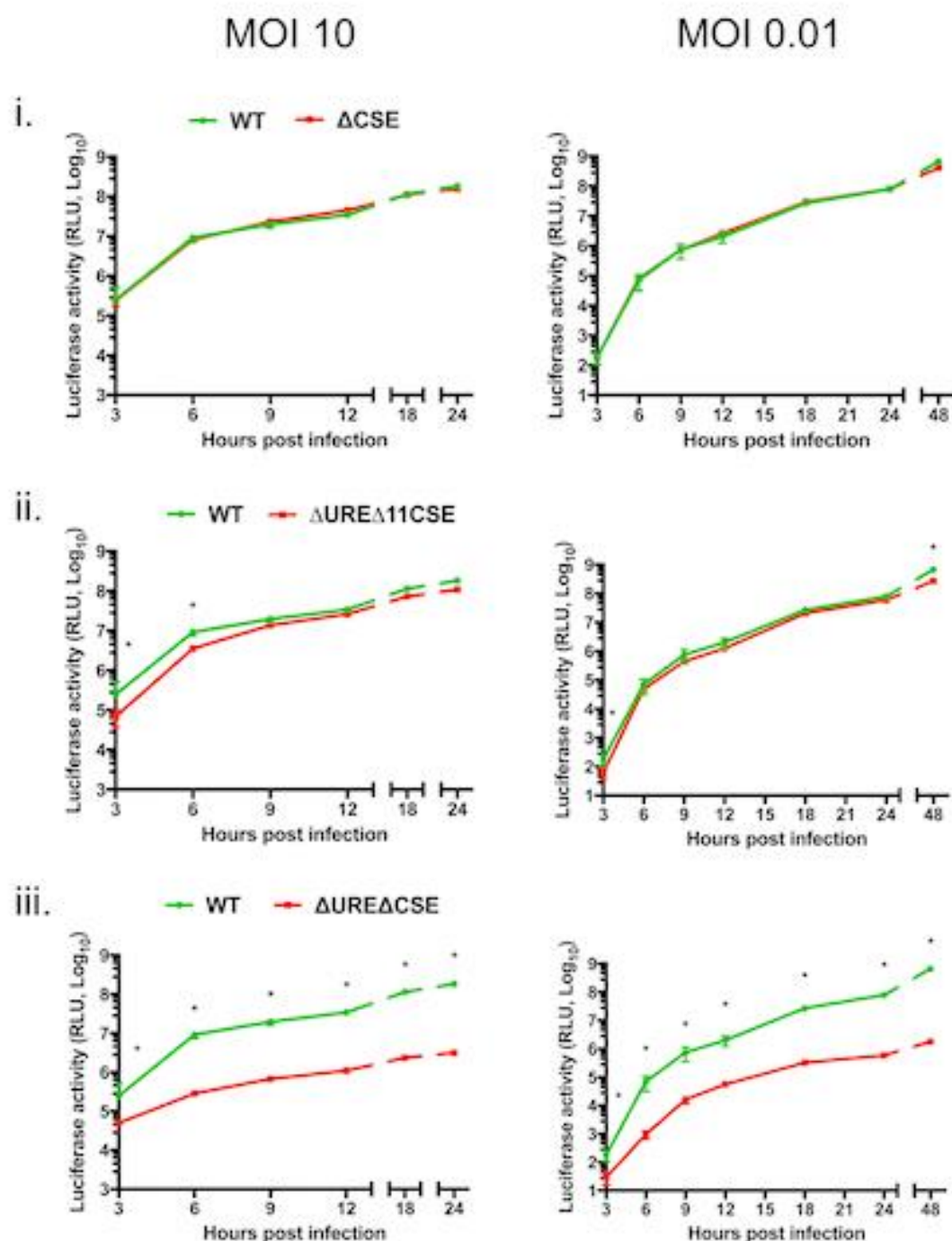


**Figure 4.14 Growth kinetics of rSFV4-2SG-Gluc viruses in NIH/3T3 cells containing partial deletion of the CSE as measured by *Gaussia* luciferase activity.** Single-step (MOI 10) and multi-step (MOI 0.01) viral growth were measured by infecting NIH/3T3 cells at the given MOI. Samples taken from infected medium were used to measure secreted *Gaussia* luciferase which is expressed from the given virus genome under a secondary sub-genomic promoter. Values represent an average of 3 biological replicates and error bars represent standard deviation. The results are representative of 3 replicate experiments. Asterisks represent a statistically significant difference for the given time point ( $p < 0.05$ ). (i) CSE deletion (ii) URE and 11CSE deletion (iii) URE and CSE deletion.



#### 4.4.6 Analysis of caspase-mediated apoptosis following infection of rSFV4 URE+CSE mutants

The HuR protein has been implicated in both cell survival as well as caspase-mediated apoptosis. Therefore, caspase activity and cell viability assays were utilised to assess if deletions or additions of the viral URE and CSE could result in enhanced or reduced caspase-mediated apoptosis.

At low MOI, deletion of the viral URE element resulted in a reduction in rate and quantities of caspase 3/7 activities and a slower rate of cell viability decline (*Figure 4.14*). Moreover, following infection of NIH/3T3 cells with SFV4-2SG-*Gluc*- $\Delta$ URE at an MOI of 10, the caspase 3/7 activity was significantly lower at 30 h.p.i compared to infection with the wild type virus SFV-2SG-*Gluc*-WT (*Figure 4.14*,  $p < 0.01$ ), and then increased and was significantly higher at 42 h.p.i. (*Figure 4.14*,  $p < 0.01$ ). At MOI of 0.01, cell viability also declined more rapidly from 30 to 42 h.p.i. following infection of NIH/3T3 cells when compared with SFV-2SG-*Gluc*-WT compared to SFV4-2SG-*Gluc*- $\Delta$ URE (*Figure 4.14*,  $p < 0.01$ ). At a higher MOI of 10 there was no significant change in caspase 3/7 activity between infection of SFV-2SG-*Gluc*-WT and SFV4-2SG-*Gluc*- $\Delta$ URE and only a significantly higher decline in cell viability was observed at 24 h.p.i. These data suggest that deletion of the URE from the SFV4 3'UTR results in delayed caspase 3/7 activity and a corresponding reduction in loss of cell viability at low MOI but not at high MOI. Given the reduction in virus replication and production of infectious virus as indicated by viral replication luciferase assay and the plaque assay, respectively, the reduction in caspase 3/7 activity and loss of cell viability may correspond to concentration of virus and not be directly related to the deletion of the URE.

Infection of NIH/3T3 cells with SFV4-2SG-*Gluc*-5xURE resulted in an earlier peak of caspase 3/7 activity at 30 h.p.i. at a high MOI (while caspase 3/7 activity peaks at 42 h.p.i. during infection with SFV-2SG-*Gluc*-WT) but the differences were not statistically significant (*Figure 4.15*). Furthermore, there were no significant differences in loss of cell viability at high MOI nor significant differences in either caspase 3/7 activity or cell viability between at MOI of 0.01 (*Figure 4.15*). Taken together these results suggest that the deletion or addition of URE to the SFV4 3'UTR has minimal effect on caspase 3/7 activity or loss of cell viability following infection of NIH/3T3 cells.

Following infection of NIH/3T3 cells with SFV4-2SG-*Gluc*- $\Delta$ CSE or SFV4-2SG-*Gluc*- $\Delta$ URE+ $\Delta$ 11CSE there was a significant increase in caspase 3/7 activity from 12 to 18 h.p.i. at 10 MOI compared to infection with the wild type virus SFV-2SG-*Gluc*-WT (*Figure 4.16*,  $p < 0.01$ ). Infection of NIH/3T3 cells with SFV4-2SG-*Gluc*- $\Delta$ URE $\Delta$ CSE resulted in increased caspase 3/7 activity compared to infection with the wild type virus but this increased trend was only statistically significant at 30 h.p.i and thereafter (*Figure 4.16*,

$p < 0.01$ ). The increase in caspase 3/7 activity was matched by a corresponding decrease in cell viability compared to WT that was not significant following SFV4-2SG-*Gluc*- $\Delta$ CSE infection but significant at 30 h.p.i. following SFV4-2SG-*Gluc*- $\Delta$ URE+ $\Delta$ 11CSE infection and 30 and 36 h.p.i. infection following SFV4-2SG-*Gluc*- $\Delta$ URE $\Delta$ CSE infection (Figure 4.16,  $p < 0.01$ ). Following infection at a low MOI (0.01) there was a significant increase in caspase 3/7 activity at 60 h.p.i., 48 and 60 h.p.i. and 42, 48 and 60 h.p.i. from infection of NIH/3T3 cells with SFV4-2SG-*Gluc*- $\Delta$ CSE, SFV4-2SG-*Gluc*- $\Delta$ URE+ $\Delta$ 11CSE and SFV4-2SG-*Gluc*- $\Delta$ URE $\Delta$ CSE respectively compared to SFV-2SG-*Gluc*-WT (Figure 4.16,  $p < 0.01$ ). This is correlated with a significant higher reduction in cell viability at 48 and 60 h.p.i. following infection with SFV4-2SG-*Gluc*- $\Delta$ CSE, SFV4-2SG-*Gluc*- $\Delta$ URE+ $\Delta$ 11CSE and SFV4-2SG-*Gluc*- $\Delta$ URE $\Delta$ CSE compared WT at all time points but these were not statistically significant (Figure 4.16). Infections in NIH/3T3 cells at low MOIs with SFV4-2SG-*Gluc*- $\Delta$ CSE resulted in caspase 3/7 activity levels comparable to the wild type SFV-2SG-*Gluc*-WT infection (from 0 to 42 h.p.i.); caspase activity was significantly higher levels at 60 h.p.i. (Figure 4.16,  $p < 0.01$ ). There was a corresponding increased drop in cell viability of NIH/3T3 cells infected at low MOIs with SFV4-2SG-*Gluc*- $\Delta$ CSE, SFV4-2SG-*Gluc*- $\Delta$ URE+ $\Delta$ 11CSE, and SFV4-2SG-*Gluc*- $\Delta$ URE $\Delta$ CSE compared to with the wild type SFV-2SG-*Gluc*-WT; these reductions in cell viabilities were statistically significant at both 48 and 68 h.p.i. (Figure 4.16,  $p < 0.01$ ).

Taken together these results indicate that the deletion of the CSE with either no deletion of the URE (SFV4-2SG-*Gluc*- $\Delta$ CSE), partial deletion of the URE (SFV4-2SG-*Gluc*- $\Delta$ URE+ $\Delta$ 11CSE) or full deletion of the URE (SFV4-2SG-*Gluc*- $\Delta$ URE+ $\Delta$ CSE) results in higher levels of caspase 3/7 activity and a larger reduction in cell viability following infection of NIH/3T3 cells when compared to SFV-2SG-*Gluc*-WT. These three viruses also produced higher levels of infectious virus at the corresponding time points at high and low MOIs respectively in NIH/3T3 cells.

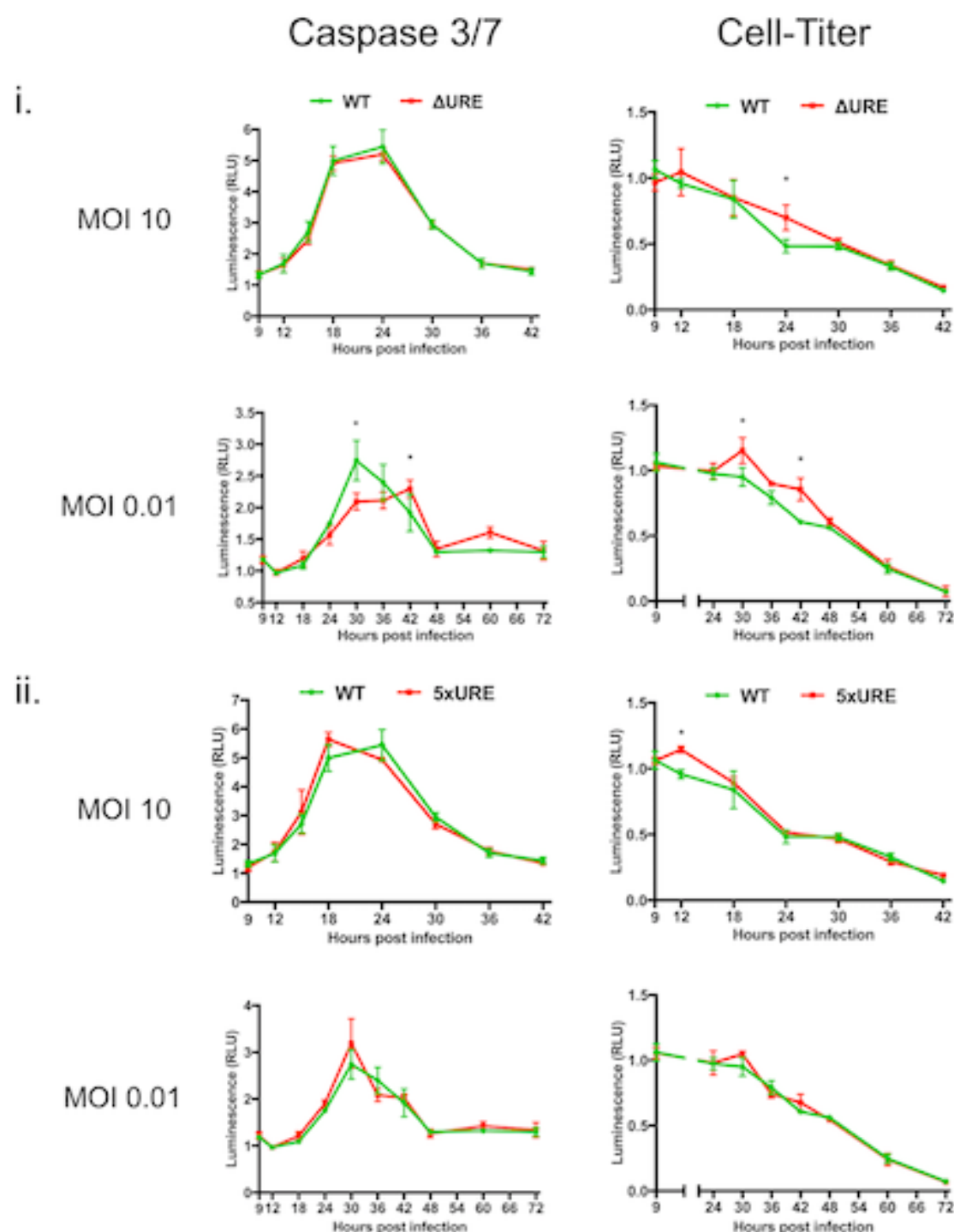


**Figure 4.15** Caspase 3/7 induction and drop in cell viability following infection of NIH/3T3 cells with SFV4-2SG-*Glu*c viruses containing deletion or additions of the URE from/to the 3'NTR of the SFV4 genome. Caspase 3/7 induction and cell death was measured by infecting NIH/3T3 cells at the given MOI and utilising the Promega CellTiter-Glo® 2.0 and Caspase-Glo® 3/7 Assays. Values represent an average of 3 biological replicates and error bars represent standard deviation. The results are representative of 3 replicate experiments. Asterisks represent a statistically significant difference for the given time point ( $p < 0.05$ ). (i) URE deletion (ii) 4 x URE additions

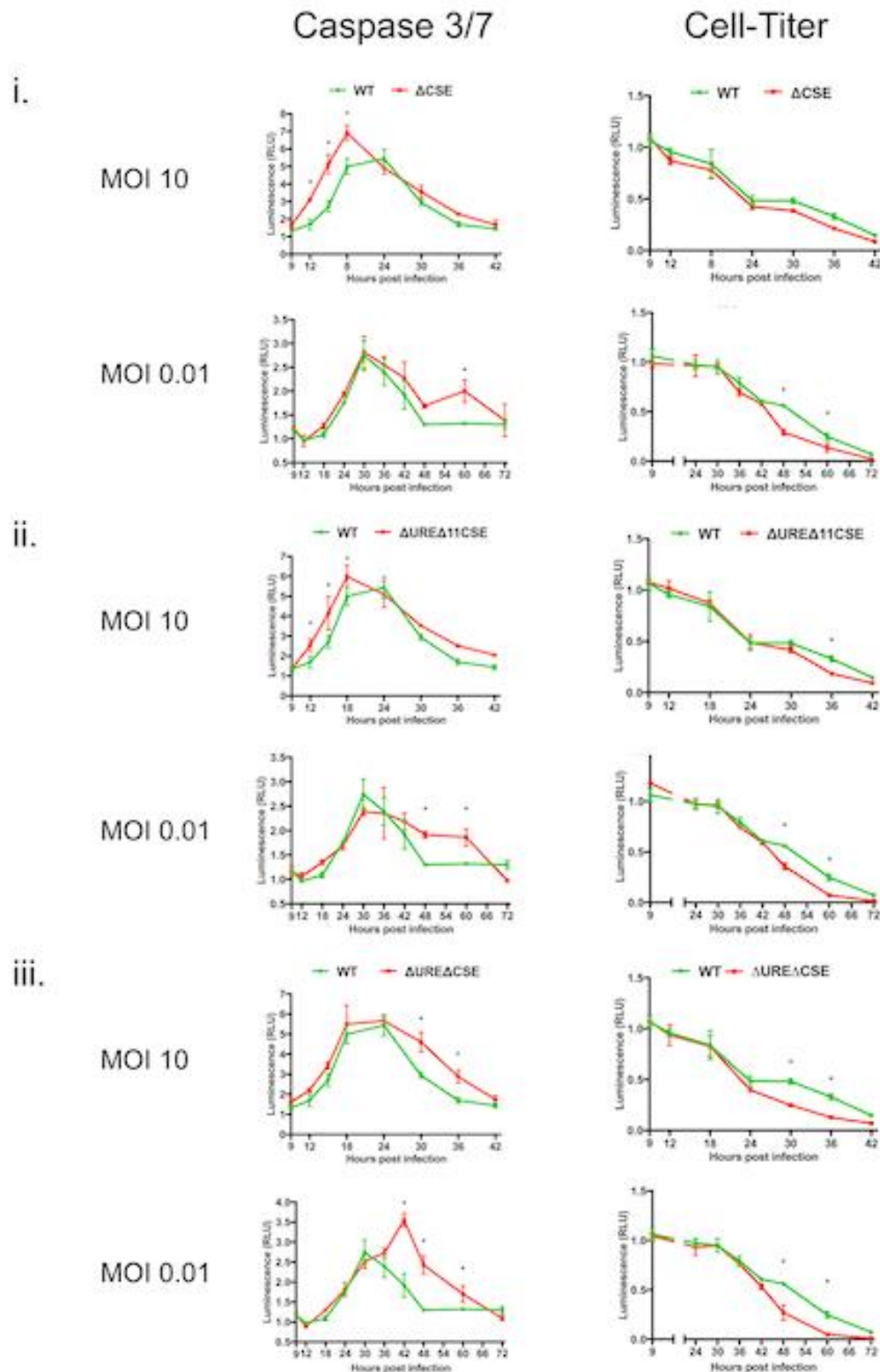


**Figure 4.16** Caspase 3/7 induction and drop in cell viability following infection of NIH/3T3 cells with SFV4-2SG-Gluc viruses containing varying CSE deletions. Caspase 3/7 induction and cell death was measured by infecting NIH/3T3 cells at the given MOI and utilising the Promega CellTiter-Glo® 2.0 and Caspase-Glo® 3/7 Assays. Values represent an average of 3 biological replicates and error bars represent standard deviation. The results are representative of 3 replicate experiments. Asterisks represent a statistically significant difference for the given time point ( $p < 0.05$ ). (i) CSE deletion (ii) URE and 11CSE deletion (iii) URE and CSE deletion

#### 4.4.7 Effect on host-cell mRNA transcripts following sequestration of HuR

The sequestration of HuR on the viral genome can deplete the nuclear pool of HuR. To decipher if this HuR re-localisation and sequestration on the viral genome resulted in changes in gene expression of host mRNA transcripts containing HuR binding sites, the abundance of several host transcripts containing HuR binding sites was assessed during virus infection. In SINV infection where cellular mRNAs containing HuR binding sites encoding TUT1, RSPRY1, LEPROTL1 and DDX58 were assessed, it was shown that these cellular transcripts degraded at a faster rate following actinomycin D treatment and when compared to mock infected cells (Barnhart *et al.*, 2013). Interestingly, host mRNAs encoding RNase-L and KAT5 (both contain putative HuR binding sites), were not shown to degrade faster than mock infected controls.

The  $\beta$ -actin mRNA contains multiple HuR binding sites. Following infection of NIH/3T3 cells with SFV-2SG-*Gluc*-WT there was a significant decrease in  $\beta$ -actin mRNA abundance in both the nucleus and the cytoplasm compartments at both 6 and 12 h.p.i when compared to NIC (Figure 4.17,  $p = <0.01$ ). Furthermore, a smaller reduction in  $\beta$ -actin mRNA abundance occurs following infection with SFV-2SG-*Gluc*- $\Delta$ URE compared to infection with SFV-2SG-*Gluc*-WT at both 6 and 12 h.p.i. in both the nuclear and the cytoplasmic fractions. In comparison, a significantly higher loss of  $\beta$ -actin mRNA abundance occurs following infection with SFV-2SG-*Gluc*-5xURE compared to infection with SFV-2SG-*Gluc*-WT at both 6 and 12 h.p.i. in both the nuclear and the cytoplasmic fractions. This suggests that the frequency of URE in the SFV4 3'UTR is correlated to the loss of  $\beta$ -actin mRNA during infection.

i. ***Mus musculus* 3'UTR of  $\beta$ -actin mRNA**

```

GCGGACUGUUACUGAGCUGCGUUUUACACCCUUUCUUUGACAAAACCUAACUUGCGCAGAAAAAAA
AAAAUAAGAGACAACAUUGGCAUGGCUUUGUUUUUUUAUUUUUUUUUAAGUUUUUUUUUUUUUU
UUUUUUUUUUUUUUUUUAAGUUUUUUUUUUUUUUUUUUUUUUUUUUUUUUUUUUUUUUUUUUUUUU
AACGGUGAAGGCGACAGCAGUUGGUUGGAGCAAACAUCUUUUUUUUUUUUUUUUUUUUUUUUUUUU
ACUUUGUACAUAUGUUUUUUUUUUUUUUUUUUUUUUUUUUUUUUUUUUUUUUUUUUUUUUUUUUUU
UCCAUGAAAUAAGUGGUUACAGGAAGUCCCUACCCUCCCAAAGCCACCCCCACUCCUAAGAGGA
GGAUGGUCGCGUCCAUGCCUGAGUCCACCCCGGGGAAGGUGACAGCAUUGCUUCUGUGUAAAUA
UGUACUGCAAAAUUUUUUUUUAUAUCUCCGCCUAAUACUUCUUUUUUUUUUUUUUUUUUUUUUUU
GCCCAGGUCUGAGGCCUCCUUUUUUUUUUUUUUUUUUUUUUUUUUUUUUUUUUUUUUUUUUUUUU
GGGAGGGGGUUGAGGUGUUGAGGCAGCCAGGGCUGGCCUGUACACUGACUUGAGACCAAUAAAAGU
GCACACCUUACCUUACACAAACAAAAA

```

ii.

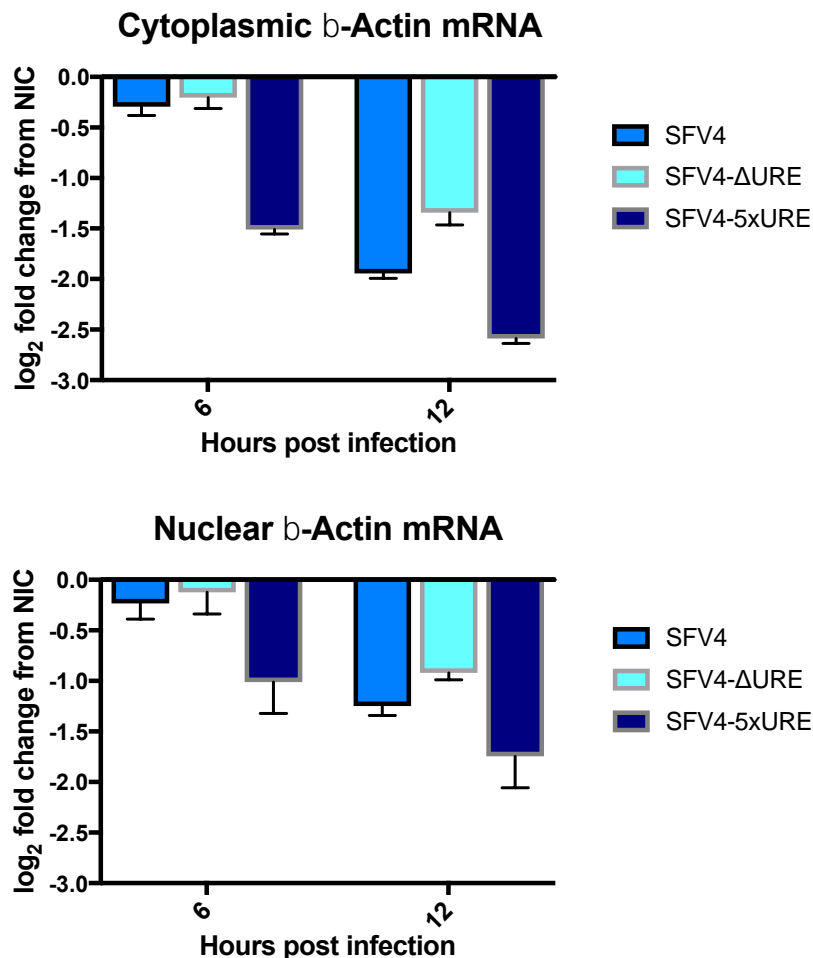


**Figure 4.17  $\beta$ -actin mRNA reduction during SFV infection is relative to abundance of uracil rich elements (to which HuR binds) in the viral 3'NTR.** i) Putative HuR binding sites in the murine  $\beta$ -actin mRNA 3'UTR. ii)  $\beta$ -actin mRNA levels in the cytoplasm and nucleus following infection with SFV4 containing URE deletions or additions. NIH/3T3 cells were infected with rSFV4 virus at an MOI of 10 and subject to nuclear and cytoplasmic fractionation, RNA extraction and qPCR at 6 or 12 hpi. Values represent an average of 3 biological replicates and error bars represent standard deviation. Differences in  $\beta$ -actin mRNA abundance between the rSFV4 viruses are significant in both the cytoplasmic and nuclear fractions ( $p = <0.0001$ ). The results are representative of 2 replicate experiments.

Another cellular transcript that contains putative HuR binding sites is IFN- $\beta$ . IFN- $\beta$  as discussed in *Chapter 1* is pivotal in the initiation of the antiviral responses and the subsequent production of a large number of anti-viral IFN-stimulated genes (ISGs). Infection of NIH/3T3 cells with SFV-2SG-*Gluc*-WT, SFV-2SG-*Gluc*- $\Delta$ URE or SFV-2SG-*Gluc*-5xURE resulted in significantly higher IFN- $\beta$  mRNA abundance in the nuclear and cytoplasmic fractions of NIH/3T3 cells compared to NIC. Interestingly, infection with SFV-2SG-*Gluc*-5xURE results in significantly higher level of IFN- $\beta$  mRNA in the nucleus and the cytoplasm at 6 hp.i. compared to infection with SFV-2SG-*Gluc*-WT. Furthermore, infection with SFV-2SG-*Gluc*- $\Delta$ URE results in a significantly lower level of IFN- $\beta$  mRNA in the nucleus and cytoplasm at 6 hp.i. when compared to infection with the SFV-2SG-*Gluc*-WT. Differences in IFN- $\beta$  mRNA abundance between the three viruses at 12 h.p.i. were not statistically significant (Figure 4.18,  $p=0.04$ ).

i. ***Mus musculus* 3'UTR of IFN- $\beta$  mRNA**

AGACCUGUCAGUUGAUGCCUCAGAAUGAGUGGUGGUUGCAGGCA  
 ACCUUUUAAGCAUCAGAGGCGGACUCUGGGACUGGUAGUGAAUCU  
 ACUGCAUUUUGAAAGGUCAAAGGAAAACAGAGUUUUUAUUAUUUUA  
 UAUUUUAAUUUUUUUCUACUUUUUAUUUAAACUUUUUAACCUCA  
 GAAAAUAAAAUUAUUUAUAAUACA%

ii.

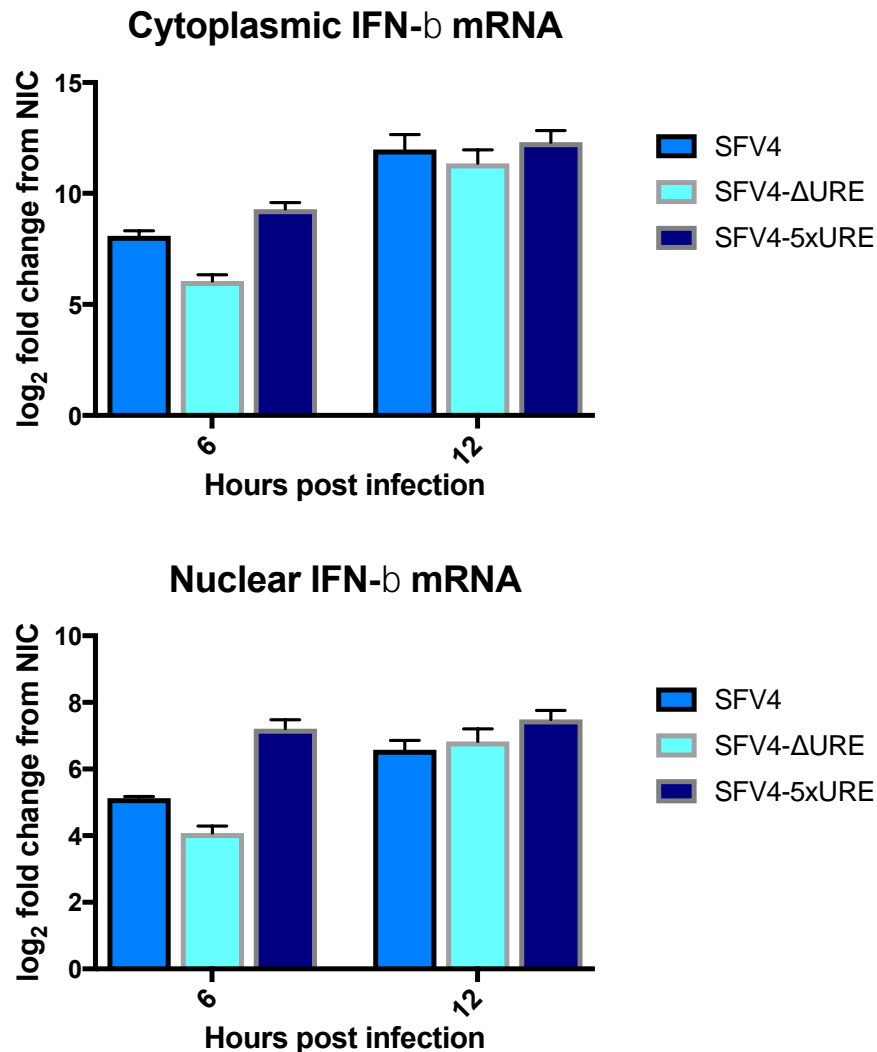


**Figure 4.18 IFN- $\beta$  mRNA abundance during SFV infection following infection with rSFV4 with URE deletions or additions.** i) Putative HuR binding sites in the murine IFN- $\beta$  mRNA 3'UTR. ii) IFN- $\beta$  mRNA levels in the cytoplasm and nucleus following infection with SFV4 containing URE deletions or additions. NIH/3T3 cells were infected with rSFV4 virus at an MOI of 10 and subject to nuclear and cytoplasmic fractionation, RNA extraction and qPCR at 6 or 12 hpi. Values represent an average of 3 biological replicates and error bars represent standard deviation. Differences in IFN- $\beta$  mRNA abundance between the rSFV4 viruses are significant in both the cytoplasmic and nuclear fractions ( $p = <0.0001$ ) at 6 hpi but not at 12 hpi. The results are representative of 2 replicate experiments.



The control of cellular apoptosis is mediated through a number of host proteins and cellular signaling pathways involving caspase enzymes as discussed in *Chapter 1*. Caspase 9 mRNA contains putative HuR binding sites. Caspase 9 mRNA abundance was lower in the cytoplasm at 12 h.p.i. following SFV-2SG-*Gluc*-5xURE infection compared to the SFV-2SG-*Gluc*-WT, yet higher following SFV-2SG-*Gluc*- $\Delta$ URE compared to SFV-2SG-*Gluc*-WT. These differences between caspase 9 mRNA levels in the cytoplasm between the three viruses were significant at 6 and 12 h.p.i. (*Figure 4.19*,  $p < 0.01$ ). Caspase-9 mRNA abundance was significantly decreased in the cytoplasm and the nucleus of cells at 12 h.p.i. following infection with SFV-2SG-*Gluc*-WT, SFV-2SG-*Gluc*-5xURE or SFV-2SG-*Gluc*- $\Delta$ URE compared to NICs (*Figure 14.19*,  $p < 0.01$ ). Differences in caspase 9 mRNA abundance were not significant between SFV-2SG-*Gluc*-WT, SFV-2SG-*Gluc*- $\Delta$ URE or SFV-2SG-*Gluc*-5xURE in the nuclear fractions at both 6 or 12 h.p.i (*Figure 4.19*,  $p < 0.01$ ).

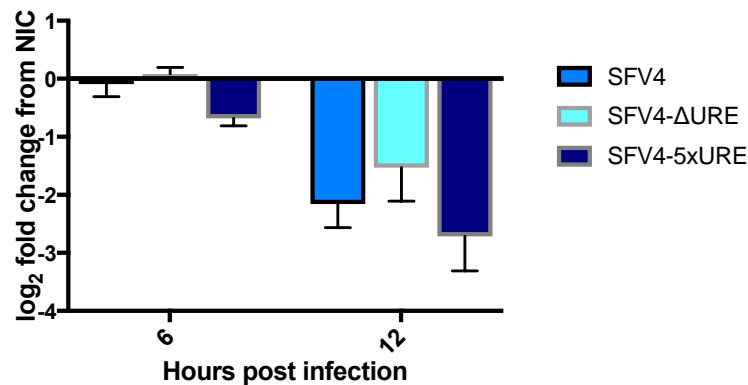
## Mus musculus 3'UTR of Caspase-9 mRNA

i.

GGCUCGGGGCUCUCUCUGCCUACUUAUUCUCUCCGAGCUCUACUGGCUUGGAGCUGGCCAAGGCCAUACUGUCUCCUUAAGAUA  
 GGUUUUUGAACUGGGGAGGCGUCUCUUCUUCUUGGCGAUGCAAAACUGCUCUAGCAGCUUUCAGGUUGUAGGGCAAUGUGGAGC  
 AGUGGUCGGAAGAAGACCGGAGUGCAUUGGAUGCUCUGGCCUUAUCUUGGUUAGGGAUUGGCCUGGAGCUCUCCAGGCCU  
 CUCAGAAGACAGGGCUUCUCUGCCACUGUACUACUGACAUUGCGGUUGUAUAAUCCUGUACUGGGAGCUGCCUCUGUAUUGUAGAGG  
 GUUUUUAGCUGUCUCUCUACUCCUGCCAGCUGCCAGGAGCAGCCUCCUGAGAUUCGCCAACCAAAAUUGUCUUCAGACAUUGU  
 CACAUUGGCCUGGGGACAUUAUAGCACUCCUUCUCUGCUCUCCACCCCGGGGGGGGUAUCAACCCACAGGGGUCUAGCAUCUCU  
 CCUUCACAGACUCAAAGUCCAGCUGGGCCAGUGUGCAUACUUGGAUCUGGGCUGCAUCUCUCCAGUUAACCAAGAGGGCUAAU UC  
 UCCUUGAGAACAUUAUUAUUCUUAACAAUAAUUCUUGCGCAUAGGACUGUAUUAUAGCCUGUAUUGCCUACCCCAACUCUGUC  
 CUUCUUAACAAAGGAGACAUGUUUUUUCCUGGCUUUUUCUCUGUGUCUUAAGGUCCUGCCGAGCCAGCAGGUGACCCAGAUAG  
 GAGUCAGGAGUCCCAAGAUCAAGUCUCCUGUCUGAAGGAUUCUUGGUUACCCUAGUGGGGACACAGGACAGAGCUCU GCUGUUUG  
 GGGUCUCCAAUUCUCCAUUGUCUUCUUGCUAAGUGAGCUGGCCAGGUGGACUGACAGGCAGUACUGAAGUGCUGGGACU  
 UCCUUGAAAAGUGGCCUCCUCCUGUCUUUUUAAGCGAUUCUGCCUUCACUUUUUUUUCUUUCUUCUGGUUCCUCUACUCUUCU  
 UUGUGAAAAGUCCAUUGAGUUUAGAUUGGUAUGUGCCAAGCCUUGUUUGUUUUUUUUUGAGCUAGGGUCUUAUUCUUGAGCCAGG  
 CUGACCACAAAUCUCCAUACCAUGCCUCCUGGGUACCAAGGAUUAUAGCUUGUCCACUGCCCAUUCUCCUCCUGAAAGAGCAU  
 GCUUUCAGGGCCCGAGGUUAGGGUACUGGGGUAAGAAGACAGACUUAUUAAGGAUGUGAUUCUUAUUUACUUUUUUUAUUAUUC  
UUUUUCUAUGGCAUUAUCCAGGGGACAGUGGAGUAUUGUCUAGUUAUUCUUGCCAUACCCUGCAG GACACACAGGAGAGAGAG  
 GAGGUUAGCUGGAACACUGGGCAUUGAGUUCAGUGACUCUCAGGGCCAAAGAGGGGUAAGAAGGGCUUAAGCCCGGAUCCUGCUCU  
 GGUUACAGGCCAGGAAGCCCGGAUACCAUUAUUAUACUAGCCAAUUGCAGCCGAGUGGUUAGUUUUUGUUUUUUUUUUUUCAUGUU  
 GUCUGUUUCUUGUUGUUGUUGUUGUUGUUUUUCCUGAGACUGGGGUCUCUGUGUAGCCUUGGCUUGCCAGAACUCACCAUG  
 AAGACAAGACUGGCCUUAACUCAGAGAUCCGCCUGCCUUGCCUUGAGUAGUGGUUUAUAAAGUGGAGCAGUGCACAGGCCCC  
 UCACAGUUCAGAAUGGCAGGUGCCAGCUGAGUUAUUAACAAAGGAAAUUGUCUUGAGGCUUAUUGGUGAGCAGACCAUUCACAU  
 GCAGUUGUGGGCGUUUCUUGUUGUUGUUUUUGAGGCUUGGACUCACUUAUGUAGCCUAGGCGGCCUUAUUAACCAUUAUUGGCU  
 UCAUUGGUUGGUUGGUUUUUUUUUUGAGACACUGUCUUAUGUAGCCAGGCGCCUUAUUAACCAUUAUUGCCUUCUUAUUCUCCAG  
 UUCUGGCCAUUAUGCAUCUUUACCAUCCUGCCAAUACAGGAUCCUUUGUUUUUUUUUUUUUUUUUUUUUUUUUGCAGUUUUUGC  
 GUCUAGCACACAAGGCCAGGUGAGCAGAGCAUACAAUUGACAGCGAUUGC CUCUGUGGAUUGGGCGCAAGGUUAAGCCAGG  
 GGAAUCUUCUUUUUCUUACGUGAUACACUCUUGUUGCUUUUUAAGCAAUUUUUUAAUAAAGCAUUGAUUCCUUCUGAACCAA  
 AAUAAAGCUGUGAUUGUAGGCU

ii.

### Caspase 9 Cytoplasmic



### Caspase 9 Nuclear

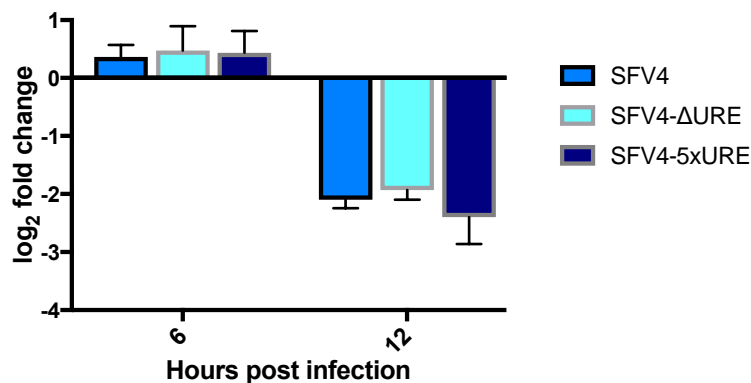


**Figure 14.19 Caspase-9 mRNA abundance during SFV4 infection following infection with rSFV4 with URE deletions or additions** i) Putative HuR binding sites in the murine caspase-9 mRNA 3'UTR. ii) Caspase-9 mRNA levels in the cytoplasm and nucleus following infection with SFV4 containing URE deletions or additions. NIH/3T3 cells were infected with rSFV4 virus at an MOI of 10 and subject to nuclear and cytoplasmic fractionation, RNA extraction and qPCR at 6 or 12 hpi. Values represent an average of 3 biological replicates and error bars represent standard deviation. Differences in caspase-9 mRNA abundance between the rSFV4 viruses are significant in cytoplasmic fractions at 6 and 12 hpi but not in the nuclear fractions. The results are representative of 2 replicate experiments.

RNAse-L is a key anti-viral effector and it is activated in the host cell as a response to viral infections and subsequently degrades global RNA in the cytoplasm. RNAse-L mRNA abundance was comparable in the cytoplasm of NIH/3T3 cells following infection with SFV-2SG-*Gluc*-WT, SFV-2SG-*Gluc*- $\Delta$ URE or SFV-2SG-*Gluc*-5xURE when compared to NIC. When the NIC sample is included in the statistical analysis the differences in RNAse-L mRNA in the nucleus following infection with SFV-2SG-*Gluc*-WT, SFV-2SG-*Gluc*- $\Delta$ URE or SFV-2SG-*Gluc*-5xURE were statistically significant (*Figure 4.20*,  $p = <0.01$ ) but not when NIC is excluded from the analysis (*Figure 4.20*,  $p = 0.2565$ ). Taken together these data suggest that SFV4 infection results in a higher level of RNAse-L mRNA in the nucleus but not in the cytoplasm and the differences in the frequency of URE in the SFV4 3'UTR produces no corresponding significant differences in RNAse-L mRNA abundance (*Figure 4.20*).

## i.

GUCUUGCAAGCUCUAUGGGACC AUUUUU CCAAUACAGCAGAGUUCUUGGGAAGUUGUAC AUUUU CUGGUC UUUUU AGC  
AGCCUGGUUACUUGUGAGCAUAGAGUAGACUAGCAGUUGUAGUUUCUGAUACAGAUUGUUCUACACUAAUUGC  
UAUGAUCAAAAGCAGUAUGCUACAAUACUACUGUCCAUUUUUGAGUAGGAUCGAGGAGAGCCUUGUUUA  
AGACUUCGUUAAAGAAAAAACAUUAUGUGUGUGUGUGUGUGUGUGUGUGUGUUAUUGUCAGAUUAGCCUCACA  
ACAUAAGUUAUUAUUCUGGAGACCCAUUAAAGGUGUGUAGGAGAAAACCAUCUCCACAAUUGUGGCCUUCUCC  
CCUUCUCAAACACACACUCAAACACACACUAACUCCUUCACACACACACUCAAACACACACACACACACAC  
ACACACACACACACACACACACAGAGCAUCUUCUUGUAUAGAAUUCAGAAUUGCCUUAUUAUGCCAAA  
GGGCUCCAGAAAGCUACAG AUUUU CGUGGGACUGUAUAAAGCCUAGGUACUGUAUAAAGUUAUCCUUAUUUC  
UGGAGGCAUCUGUACCGGUGUCUACUGACUUAAGUUAUAGCUCUCACUUGAAGUC AUUUU UCAGUGUCACGGG  
UGGGGGGGGAGGGGUGGUCUACUGGCCUUGAGACAGGAGGAACACGGUGGCCACAACAUUCCGGGGAUG  
CAGAAAGCAGCUACCCCAUUGCCCAUACGAGCAGAUACAUAGUUGGUGUGUGAGGAAGAACUGUCU  
GAAGAGAUUGGAACACUUCUUGGCCGGCCUGGACAGAGGCUGGUGAGUGCAUUGAACACCCCAAGAAGAC  
GUGGUGGUGUGUUCUUGCUGGUAUCGAGUUAAGUAGCCAGUCC AUUUU GGUGUCCACUUGAGAGCCCU AUU  
CCCCCAUUCUCCAUUGCUGCCGUGGUGCAUAGUC DAUUU GGGGUGCUCUCUAGCUCUCCUGACACAGUCAC  
CUCAGCGGCGUCCUUAUCCACUUIUGCC UUUU GUACUCCAGCCUCCACAAUCAAAGCCUUCUUAAGGCCUUU  
GUAC UUUUU GCUUAGUUAUUUUU DUUU GUUCUGGUGAUGUUGACAUUUU CACUGAAUUAUUAAGGAC  
CC UUUUU GAUGGUGAUGAUGAUGAUGAUGAUGAUGGUAC UUUU GAUUUUU CACAUUUGUAUCUUAU AUUUUU A  
AUUUUUUUU UUUU GAAAUUAGCAGCUUAAGCUAAGCACUGUGAUU UUUUUU GACAAUGAAGAAUGAAGGCU  
AGAAUUAUUUUU AUUUU CUCUAGGCAUUAUGGCAUAGAGUUGCUCUGUUG AUUUU GACAGAC DUUUU GGUGU  
GACAUUGAUGUUC UUUU CACCUAUCACACAGCGUGGUCUAGGUGGAGC UUUU GGAAUGGGAUUUUUAGGCUAUCU  
UAGAUUUUUUAUUGAAGGAGGACUUGGACUUGGAGCAGUAGUGGUGCUCUAGUAGGAAUUAAGCACACUGGAG  
AAACAAGAUUGGCUUAAAGAUUGGC UUUU AACUGGGCAGUGGCGGCACAGCC UUUU AUCCGACGACUUGGGA  
GCGAGAGGACAGUGAUUUCUGAGUCGAGGCGCAGGUCUAGGAGUGAUUCAGGACAGCGACGGCUACA  
CAGAGAAAACCCUGUCUCAAACAAAAACAAAAACAAAAAAUAAAAACAAAAAUAAGUACUUAUUAAUU  
AAAAAAGAUUGC DUUU AAACUUAU AUUUU AAAAGG UUUU AAAUUGAG UUUU GUUGUCUGACUGGUAUCGCUAA  
UCAAAAGUUCUACUAGUGAAGAAUACUCUAAUAAAAUU GAUUGUUCUUAUUAU%

## ii.

A bar chart showing the log<sub>2</sub> fold change from NIC for three conditions: SFV4 (blue), SFV4-ΔURE (cyan), and SFV4-5xURE (dark blue) at 6 and 12 hours post-infection. The y-axis ranges from -1.0 to 1.0. Error bars represent standard deviation.

Hours post infection	SFV4	SFV4-ΔURE	SFV4-5xURE
6	~0.1	~0.1	~-0.1
12	~0.1	~0.0	~-0.1

A bar chart showing the log<sub>2</sub> fold change from NIC for three conditions: SFV4 (blue), SFV4-ΔURE (cyan), and SFV4-5xURE (dark blue) at 6 and 12 hours post-infection. The y-axis ranges from 0 to 3. Error bars represent standard deviation.

Hours post infection	SFV4	SFV4-ΔURE	SFV4-5xURE
6	~1.35	~1.95	~2.35
12	~1.70	~1.00	~1.05

132

i.

ii.

A bar chart showing the log<sub>2</sub> fold change from NIC for three viral constructs: SFV4 (blue), SFV4-ΔURE (cyan), and SFV4-5xURE (dark blue) at 6 and 12 hours post-infection. The y-axis represents the log<sub>2</sub> fold change from NIC, ranging from 0 to 5. The x-axis shows the time points 6 and 12 hours post-infection. Error bars represent standard deviation.

Hours post infection	SFV4	SFV4-ΔURE	SFV4-5xURE
6	~2.9	~2.5	~3.2
12	~3.9	~3.5	~3.6

Bar chart showing the log<sub>2</sub> fold change from NIC for three viral constructs: SFV4 (blue), SFV4-ΔURE (cyan), and SFV4-5xURE (dark blue) at 6 and 12 hours post-infection. The y-axis represents the log<sub>2</sub> fold change from NIC, ranging from 0 to 8. The x-axis shows the time points in hours post-infection. Error bars represent standard deviation.

Hours post infection	SFV4	SFV4-ΔURE	SFV4-5xURE
6	~4.6	~4.2	~5.8
12	~5.7	~6.3	~6.5

133

In contrast to RNase-L, RNA degradation can be orchestrated indirectly through the binding of TTP-BPs such as tristetraprolin. TTP binds uracil rich sequences that are similar or identical to those which HuR binds. Following infection of NIH/3T3 cells with SFV-2SG-*Gluc*-WT, SFV-2SG-*Gluc*-ΔURE or SFV-2SG-*Gluc*-5xURE the abundance of TTP was significantly higher than in the NIC sample in both the nucleus and the cytoplasmic fractions at both 6 and 12 h.p.i. (*Figure 4.21*,  $p < 0.001$ ). The differences in TTP mRNA abundance between cells infected with SFV-2SG-*Gluc*-WT, SFV-2SG-*Gluc*-ΔURE or SFV-2SG-*Gluc*-5xURE not including NIC sample were only significant when the time points are analysed separately whereby differences are significant at 6 h.p.i. (*Figure 4.21*,  $p < 0.001$  for nucleus and cytoplasmic fractions) but not 12 h.p.i. (*Figure 4.21*,  $p = 0.7531$  and  $p = 0.4714$  for cytoplasmic and nuclear fractions, respectively). At the earlier time points post infection the higher frequency of URE in the SFV4-3'UTR the higher the abundance of TTP mRNA in both the nucleus and the cytoplasm (*Figure 4.21*). Taken together these results suggest that TTP is upregulated during SFV4 infection compared to NIC regardless of the frequency of URE in the SFV4 3'UTR and is upregulated significantly earlier in infection with a higher frequency of URE in the SFV4-3'UTR.

The host cellular HuR binds the SFV4-3'UTR and relocates HuR to the cytoplasm where the viral RNA is replicated and HuR binding generally promotes RNA stability. This suggests that the greater the extent of HuR binding to the SFV4-3'UTR the greater the stability to the SFV4 RNA. Infection of NIH/3T3 with SFV-2SG-*Gluc*-5xURE resulted in higher abundance of SFV4 nsP3 RNA (and by extension the full RNA genome) at 6, 9 and 12 h.p.i. compared to infection with SFV-2SG-*Gluc*-WT or SFV-2SG-*Gluc*-ΔURE. Infection of NIH/3T3 with SFV-2SG-*Gluc*-ΔURE resulted in lower abundance of SFV4 nsP3 RNA at 6 and 9 h.p.i. when compared to infection with SFV-2SG-*Gluc*-WT or SFV-2SG-*Gluc*-5xURE. The difference in SFV4 nsP3 RNA following infection with the three viruses were larger at the earlier time points post infection and were statistically significant (*Figure 4.22*,  $p = < 0.001$ ). These data suggest additional URE in the SFV4 3'UTR result in a greater abundance of viral RNA in murine cells during SFV4 infection, particularly early during infection.

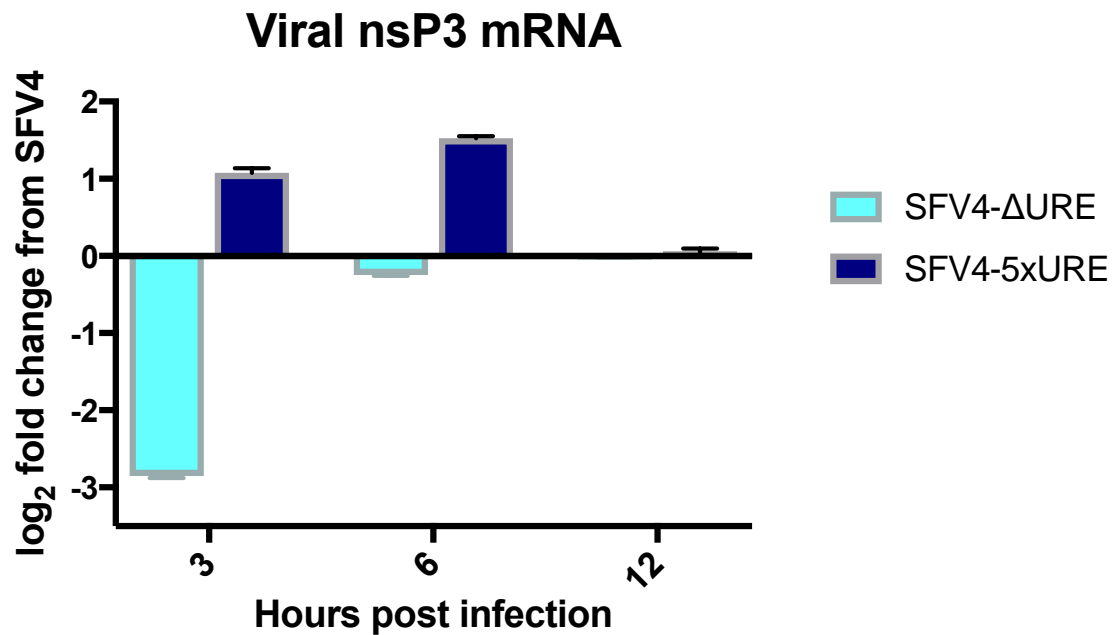


**Figure 4.22 Viral nsP3 RNA abundance during SFV infection following infection with rSFV4 with URE deletions or additions.** mRNA bundance is shown as fold change from SFV4-WT. NIH/3T3 cells were infected with rSFV4 virus at an MOI of 10 and subject to RNA extraction and qPCR at 3, 6 and 12 hpi. Values represent an average of 3 biological replicates and error bars represent standard deviation. Differences in viral nsP3 RNA levels are highly significant between rSFV4 viruses ( $p = <0.001$ ). The results are representative of 2 replicate experiments

The SFV4-3'UTR binds HuR and TTP is upregulated during SFV4 infection (*Figure 4.21*). TTP binds uracil rich sequences similar to those which HuR binds. On a number of host mRNA transcripts, HuR and TTP competitively bind the same uracil rich sequences and promote transcript stability or turnover, respectively. Therefore, HuR and TTP may both bind the SFV4-3'UTR and co-localise in the cytoplasm. TTP localizes in both the nucleus and the cytoplasm in NIH/3T3 cells (*Figure 4.23*). Following infection with SFV4, TTP remains localised in the nucleus and the cytoplasm. Furthermore, the vast majority of cytoplasmic TTP does not co-localise with cytoplasmic HuR. It is known that both HuR and TTP co-localise in stress-granules and there are a small number of foci in which TTP and HuR co-localise. Most of the cytoplasmic TTP did not co-localise with HuR following infection with any of the rSFV4 tested irrespective to sequence changes to the SFV4-3'UTR. Taken together, these results suggest that HuR and TTP do not co-localise in the cytoplasm, the implications of which are discussed later.



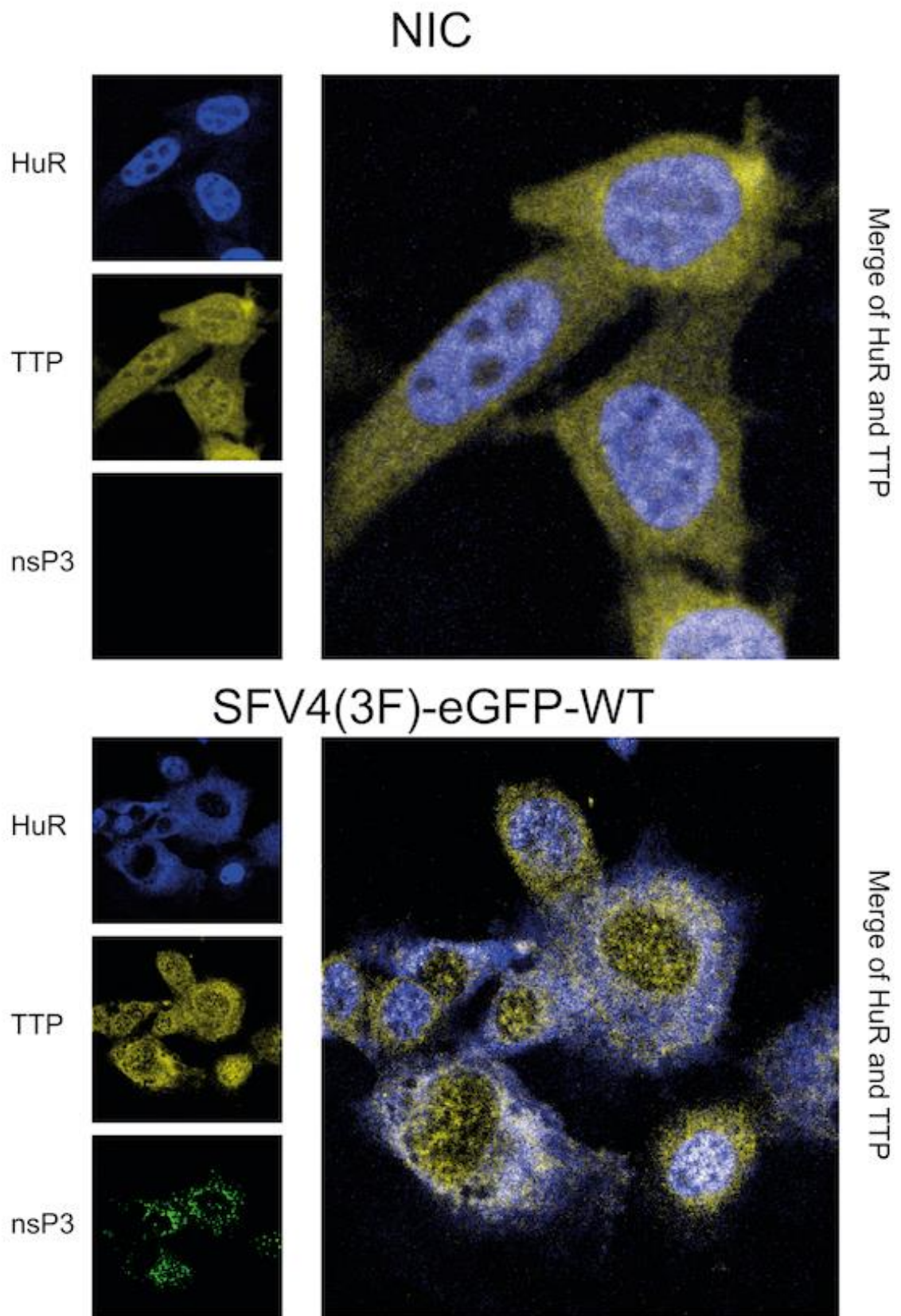


**Figure 4.23.** During infection with SFV4 HuR relocates to the cytoplasm, the majority of which does not colocalise with TTP. NIH/3T3 cells were infected at MOI 10 with SFV4-(3F)-eGFP-WT and fixed at various time points post infection. Cells were stained against HuR (blue), TTP (yellow) and had endogenous nsP3-eGFP fluorescence (green).

## 4.5 Discussion

HuR binding sites have been stringently conserved in alphaviral genomes indicating the significance of the role they play during infection. Alphaviruses which do not encode the conserved URE, such as CHIKV and RRV, have evolved other HuR binding sites in their 3'UTR (Dickson *et al.*, 2012). Furthermore, the CSE, which also binds HuR, is conserved among all known alphaviruses (George and Raju, 2000). This study has demonstrated the significance of the URE during SFV4 infection. The SFV4 URE is likely responsible for the sequestration of HuR in the cytoplasm during infection of mammalian cells (shown by immunostaining against HuR), since HuR has previously been shown to bind directly to the SFV4 URE (Dickson *et al.*, 2012). The study also found that retention of the URE and additional URE present in the SFV4 3'UTR, result in increased viral RNA replication, viral RNA stability, viral RNA translation and increased infectious virion production. This was shown by luciferase assay following infection of mammalian cells with rSFV4 encoding *gaussia* luciferase, SFV4 nsP3 viral RNA levels during infection as determined by RT-qPCR, and infectious virus concentrations shown by plaque assay. A possible destabilising effect on a number of host mRNA transcripts (containing putative HuR binding sites) may also be evident during rSFV4 infection. The sequestration of HuR on the viral SFV4 genome may be responsible for this reduction in host mRNA transcript abundance. This work also indicates that TTP mRNA abundance is increased during SFV4 infection and the majority of the re-localised cytoplasmic HuR following SFV4 infection does not co-localise with TTP.

The utilisation of a host RNA-binding proteins to enhance viral infection is not specific to Alphaviruses. Until recently, however, the utilisation of specifically HuR having a significant role during a viral infection was only demonstrated in alphaviral infections (Sokoloski *et al.*, 2010; Dickson *et al.*, 2012; Barnhart *et al.*, 2013; Hyde *et al.*, 2015). There are now emerging roles for HuR during infections of other virus families that bare striking resemblance to those of alphavirus; HuR has been shown to bind the 3'UTR of Hepatitis C virus (HCV) RNA, resulting in HuR relocalisation to the cytoplasm and stabilisation of HCV RNA (Shwetha *et al.*, 2015). Furthermore, HuR is used to facilitate the formation of the cellular and viral ribonucleoprotein complexes used to circularise the HCV RNA and facilitate HCV replication. In contrast, during SFV4 replication, HuR appears to not localise to replication complexes as indicated through the absence of its co-localisation with nsP3, meaning that unlike HCV infection, the binding of HuR to the SFV4 3'NTR is not likely to play a direct role in viral RNA replication despite increasing SFV4 RNA stability and translation. It is worth noting, however, that the URE is situated adjacent to the CSE at the very end of the SFV4 3'UTR (Hardy and Rice, 2005). The CSE is the start site of the negative strand SFV genome replication; CSE also binds HuR itself. Therefore, a direct role for HuR in the assembly of proteins for negative strand replication cannot be ruled out.

The CSE sequence element found in the 3'NTR of all known alphaviruses has been proposed to act as an RNA promoter for negative strand synthesis (Hill *et al.*, 1997; Lemm *et al.*, 1998) but also contains AU-rich regions which can bind host cell RNA binding proteins including HuR. The 19 nt CSE of SINV has been proposed to be indispensable for viral replication and negative strand synthesis (Hardy and Rice, 2005). Other groups have shown that SINV lacking part (Kuhn, Hong and Strauss, 1990) or all (Raju *et al.*, 1999) of the 19nt CSE in its 3'NTR is still able to produce viable virus and propagate an infection of BHK-21 cells. Following a number of virus passages many of the SINV CSE deletion mutants gained AU-rich additions to their 3'NTR (Raju *et al.*, 1999, George and Raju, 2000). These data suggest that although not absolutely required for viral replication in BHK-21 cells the CSE is important for viral replication and the AU-richness of the CSE plays an important role in its function.

The rSFV4 viruses which contained deletions of the CSE, SFV4-2SG-*Gluc*- $\Delta$ CSE, SFV4-2SG-*Gluc*- $\Delta$ URE $\Delta$ 11CSE and SFV4-2SG-*Gluc*- $\Delta$ URE $\Delta$ CSE, showed delayed growth kinetics to propagate virus following transfection into BHK-21 cells compared to SFV4-2SG-*Gluc*-WT, SFV4-2SG-*Gluc*- $\Delta$ URE or SFV4-2SG-*Gluc*-5xURE. Some virions propagated from pSFV4-2SG-*Gluc*- $\Delta$ CSE contained two additional nucleotide deletions in its 3'UTR near the site of the CSE deletion compared to the transfected replicon. The two additional nucleotide deletions were not identical between virions. It is possible that the two deleted nucleotides allowed for an RNA secondary structure to re-form that is lost following deletion of the CSE, or reformed part of the CSE sequence to facilitate replication. Virus propagated from pSFV4-2SG-*Gluc*- $\Delta$ URE $\Delta$ 11CSE and pSFV4-2SG-*Gluc*- $\Delta$ URE $\Delta$ CSE did not, however, contain nucleotide changes adjacent to the intended deletions. Since CSE is involved in the initiation of negative strand replication of alphaviruses (Hardy and Rice, 2005; Raju *et al.*, 1999), the delayed propagation from transfected icDNAs encoding viruses which contain a CSE deletion was not unexpected.

The amount of infectious virus produced over time (as shown by plaque assay) at high MOIs by SFV4-2SG-*Gluc*- $\Delta$ CSE, SFV4-2SG-*Gluc*- $\Delta$ URE $\Delta$ 11CSE and SFV4-2SG-*Gluc*- $\Delta$ URE $\Delta$ CSE was comparable or higher than the levels produced following infection with the wild type virus SFV4-2SG-*Gluc*-WT. The contrast between the delayed time taken for production of virus from transfected icDNAs containing a CSE deletion and the number of virions produced over time following infection of NIH/3T3's is intriguing. It is possible that virions in the generated viral stocks from icDNA containing CSE deletions have acquired compensatory mutations to allow efficient replication in murine cells despite not containing a CSE in their 3'UTR. For instance, a compensatory mutation may have occurred in the RNA-dependent polymerase so that it can still bind the 3'UTR of the SFV4 genome without the CSE. This theory is supported by the heterogeneous population of plaque sizes in BHK-21 cells following

infection with SFV4-2SG-*Gluc*- $\Delta$ CSE, SFV4-2SG-*Gluc*- $\Delta$ URE $\Delta$ 11CSE and SFV4-2SG-*Gluc*- $\Delta$ URE $\Delta$ CSE which suggest variations between virions (Liu and Wu, 2004) in contrast to the homogenous plaque sizes formed following infection with SFV4-2SG-*Gluc*-WT, SFV4-2SG-*Gluc*- $\Delta$ URE and SFV4-2SG-*Gluc*-5xURE. Further study to sequence the full genomes of these viruses is required before drawing any strong conclusions as to whether compensatory mutations may have occurred in their genomes.

The luciferase assay indicated that SFV4-2SG-*Gluc*- $\Delta$ URE $\Delta$ CSE replicates/translated its RNA at significantly slower rate than SFV4-2SG-*Gluc*-WT in contrast to the plaque assay data. One reason for this could be that the double deletion (URE+CSE) removed all the proposed HuR binding sites from this part of the viral genome. The complete loss of HuR binding sites from the 3' end of the 3'UTR may cause the significant loss of luciferase activity seen during replication with SFV4-2SG-*Gluc*- $\Delta$ URE+ $\Delta$ CSE compared to control. An alternative explanation is a range of mutations that have acquired in the viral genome from the URE/CSE mutants which took significantly longer to produce viable virus from the icDNAs. A number of mutations that were acquired during virus stock production from the SFV4-2SG-*Gluc*- $\Delta$ URE+ $\Delta$ CSE may have occurred in the non-essential luciferase gene which may impede the luciferase activity of the luciferase encoded by this virus. Full sequencing of the SFV4-2SG-*Gluc*- $\Delta$ URE+ $\Delta$ CSE including the luciferase gene would be needed to determine if mutations have occurred in this gene that may have affected the luciferase assay.

HuR relocalisation to the cytoplasm occurs in the early hours of infection following infection with SFV4-2SG-*Gluc*- $\Delta$ URE and SFV4-2SG-*Gluc*- $\Delta$ URE $\Delta$ CSE but is not retained in the cytoplasm to the same proportions when compared to infection with SFV4-2SG-*Gluc*-WT or SFV4-2SG-*Gluc*-5xURE. This suggests that initial HuR relocalisation may be less dependent on the presence of the URE but caused by a separate event. This may be caused by stress to cells by the virus infection (Peng *et al.*, 1998) and/or the phosphorylation state of HuR (Pullmann *et al.*, 2007). It has been previously demonstrated that HuR is dephosphorylated at a residue on the protein's hinge region during SINV infection (Dickson *et al.*, 2012) and that this may result in re-localisation to the cytoplasm. The amount of HuR that is retained in the cytoplasm following an initial relocalisation to the cytoplasm is shown to be correlated to the number of URE in the SFV4 genome. It has been previously shown the URE of a number of alphaviruses including SINV and SFV directly binds cellular HuR (Dickson *et al.*, 2012). This suggests that the high levels of retention of HuR in the cytoplasm following infection with SFV4-2SG-*Gluc*-5xURE is because the virus contains more HuR binding sites on the viral RNA which sequester HuR on the viral RNA in the cytoplasm. In support of this, the nuclear localization of HuR during the later hours of infection with SFV4-2SG-*Gluc*- $\Delta$ URE after an initial partial movement of HuR to the cytoplasm is likely due to a limited number of HuR binding sites on the SFV4-2SG-*Gluc*- $\Delta$ URE viral RNA (SFV4 CSE

loosely binds HuR so retains a smaller percentage of HuR in the cytoplasm (Dickson *et al.*, 2012)). Unbound HuR in the cytoplasm is likely to shuttle back to the nucleus or bind host mRNAs.

There are large standard deviations when analyzing the ratio of cytoplasmic HuR to nuclear HuR between individual cells following infection with SFV4(3F)eGFP-ΔCSE and SFV4(3F)eGFP-ΔURE+ΔCSE. This may be a result of varying virion populations in the virus preparations or the number of virions that initially infect each individual cell. The contrasting relatively small standard deviation seen during infection with SFV4-2SG-*Gluc*-5xURE is likely due to the increased HuR binding sites in the 3'UTR which bind all relocated HuR irrespective of small differences in viral RNA concentration between cells.

Infection with an rSFV4, in particular with SFV4(3F)-eGFP-ΔURE+ΔCSE, caused foci of HuR and PABPC co-localisation in the cytoplasm. These foci may be stress-granules which are known to form during environmental stress including viral infections and contain both HuR and PABPC. SFV4 disrupts the formation of stress-granules on viral RNA through the action of nsP3. SFV4 nsP3 binds Ras-GAP SH3-domain-binding protein (G3BP) and sequesters it into CPV-I replication complexes inhibiting G3BP from forming stress-granules (Panas *et al.*, 2012). The increased number of putative stress-granules seen during SFV4(3F)-eGFP-ΔURE+ΔCSE may be relating to an increase in stress induced on the cell by this virus or a loss of the nsP3-mediated G3BP inhibition.

The relocated HuR colocalises with PABPC in the cytoplasm even when not in discrete foci. This is not surprising since both host proteins bind viral RNA and are both likely omitted from similar subcellular compartments. Interestingly, it has been reported that HuR can increase stability of an mRNA when bound to the 3'UTR through interaction with PABPC. The 3' end of β-casein structurally interacts with the poly(A) tail through the formation of a protein complex of HuR (binding to the 3'UTR) and PABPC (binding to the poly(A) tail) (Nagaoka *et al.*, 2006). Given the proximity of the URE and CSE (known to bind HuR) to the poly(A) tail (known to bind PABPC) in the SFV4 genome it is reasonable to suggest that the SFV4 RNA may form such an interaction possibly via a stem-loop structure to inhibit deadenylation in host cells.

The mechanisms by which HuR protects viral transcripts in host mammalian cells have not been fully elucidated. The rate limiting step of basal decay of host mRNA transcripts typically starts with deadenylation. Deadenylation is mediated in two pathways involving a super complex of PAN2-PAN3 and CCR4-NOT which binds poly(A) tails and shortens them however most commonly poly(A) specific ribonuclease (PARN) mediates host cell mRNA deadenylation (Wu *et al.*, 2005; Moraes, Wilusz and Wilusz, 2007; Bartlam and Yamamoto, 2010). Once the tail is removed deadenylation-dependent decapping can occur utilising the decapping complex (Wu *et al.*, 2005) of decapping enzymes 1 and 2

which remove the m<sup>7</sup>G cap (Coller and Parker, 2004). The remaining transcript is then degraded at the 5' or 3' by XRN1 or the exosome respectively (Parker and Song, 2004). The interaction of HuR and PABPC while bound to mRNA (Nagaoka *et al.*, 2006) suggests this interaction may inhibit the recruitment of deadenylation enzymes and its subsequent degradation.

The deletion of the URE from the SFV4 3'UTR not only decreased retention of HuR in the cytoplasm but it also reduced the levels of infectious virus (as shown by plaque assay) produced in the early hours of infection and initial rate of viral RNA replication and/or translation (as shown by luciferase assay). This observation concurs with studies which show HuR increases the translation rate of mRNA to which HuR binds (Mazan-Mamczarz *et al.*, 2003; Galban *et al.*, 2008). This effect was augmented during a multi-step growth curve. Adding validity to the URE's role in initial viral replication/translation and effect on production of infectious virions, an SFV4 virus containing four additional UREs had the opposite effect to deleting the URE. Infection with SFV4-2SG-*Gluc*-5xURE increased the initial amount of infectious virus and initial rate of viral RNA replication/translation and again the effect was augmented when infecting murine cells at a low MOI. Interestingly, the increased initial rate at which the SFV4-2SG-*Gluc*-5xURE virus replicated during the 1-step growth curve sharply reduced at 12 hpi and this slower rate was maintained during the course of infection. This could be a result of the cell's anti-viral IFN responses, which is supported by the higher IFN-beta mRNA levels produced during infection with SFV-2SG-*Gluc*-5xURE compared to SFV-2SG-*Gluc* infection.

The advantage that multiple URE in the SFV4 3'UTR has on initial viral replication following infection with SFV4(3F)-eGFP-5xURE may appear contradictory to predicted course of virus evolution since SFV4 has not duplicated these URE sequences over time. There are multiple logical deductions as to why this has not occurred. Firstly, the replication of alphaviruses is complex; alphaviruses not only replicate in vertebrate hosts but also in arthropod vectors such as mosquitoes, which spread these viruses. This means that any change on the viral genome which optimises replication in the vertebrate hosts may in turn eliminate their ability to establish a consistent (and not fatal) infection in their arthropod hosts. Secondly, the additional URE in the SFV4 increased initial viral replication but did not result in a higher number of virions at later time points post infection at a high MOI. This is not surprising when identifying the higher IFN- $\beta$  mRNA levels produced during infection with SFV4(3F)-eGFP-5xURE. IFN- $\beta$  as discussed is a primary and broad initiator of the anti-viral response during alphaviral infections (Ryman and Klimstra, 2008; Akhrymuk, Frolov and Frolova, 2016; Chawla-Sarkar *et al.*, 2003). The initial higher levels of SFV4 RNA produced during infection with SFV4(3F)-eGFP-5xURE as compared to the wild type virus may infer a stronger anti-viral response since double stranded RNA acts as a pathogen associated molecular pattern (PAMP). This stimulates an antiviral IFN response through

recognition by PRR (pathogen recognition receptors) as discussed in Chapter 1 (Akhrymuk, Frolov and Frolova, 2016). Thirdly, since the recruitment of HuR to viral genomes infers a disadvantage to host cells, mammalian cells may have evolved a secondary pathway to promote the transcription of IFN- $\beta$  when available HuR levels are depleted.

The deletion or addition of URE to the SFV4 3'UTR did not appear to have a significant effect on caspase 3/7 activity and cell death although small and when statistically significant differences did occur, these correlated with differences in production of infectious virus and virus RNA abundance which are known to affect apoptosis pathway.

The presence and frequency of URE in the viral genome affects the rate of HuR relocalisation to, and predominantly its retention in the cytoplasm. HuR binds to a number of host transcripts in basal and/or stress conditions and increases their stability and half-lives. This suggests that during SFV4 infection, the SFV4 3'UTR acts as a molecular sponge to quench the infected cell with HuR binding sites so less HuR is available to bind to host-cell transcripts. A destabilising effect on host mRNA (containing HuR binding sites) occurs during SINV infection following HuR sequestration on SINV RNA (Barnhart *et al.*, 2013). It, therefore, seems likely that the sequestration of HuR on the SFV4 URE during SFV4 infection would have a similar effect. The significant decrease seen in  $\beta$ -actin mRNA during SFV4 infection supports this assumption. Furthermore, this decrease is inhibited or enhanced with the removal or addition of URE to the SFV4 3'UTR, respectively. This is further supported by studies which have shown the down regulation of  $\beta$ -actin expression observed following silencing of HuR at the mRNA and protein levels. Silencing of HuR using siRNA in HeLa cells results in a 70% decrease in beta-actin mRNA (Dormoy-Raclet *et al.*, 2007) and similar effects are seen in corneal fibroblasts (Joseph, Srivastava and Pfister, 2014). This supports the theory that the more HuR binding sites in the viral genome (URE's), the higher the subsequent destabilising effect during infection on host cell transcripts which bind HuR.

Herdy *et al.* (2015) used affinity purification, mass spectrometry and immunoprecipitation against HuR followed by RNA isolation and qPCR to show specific binding of HuR to IFN- $\beta$  mRNA. Overexpression of HuR in HeLaS3 cells showed no effect on IFN-beta mRNA levels, however, lowering HuR expression or chemically inhibiting its dimerisation significantly inhibited the IFN- $\beta$  response in HeLaS3 cells and in rheumatoid arthritis fibroblast like synoviocytes (FLSs) (Herdy *et al.*, 2015). Unexpectedly more HuR binding sites in the SFV4 3'UTR resulted in higher levels of IFN- $\beta$  mRNA in host cells at 6hpi. Although unexpected, there is a number of logical explanations for this. Firstly, infection with SFV4-2SG-*Gluc*-5xURE in NIH/3T3 cells results in higher levels of viral RNA during the early hours of infection. Double-stranded RNA present during viral genome replication of an RNA virus infection is known to be

detected by pattern recognition receptors (PRRs) such as RIG-I and MDA5 as well as the toll-like receptors which then stimulate IFN transcription. The differences in cytoplasmic IFN- $\beta$  mRNA abundance between the rSFV4 viruses is less pronounced at 12 hpi than at 6hpi which would coincide with differences in SFV4 RNA abundance, lending support to the theory that the increased viral RNA abundance seen during infection with SFV4-2SG-*Gluc*-5xURE is responsible for the increased IFN- $\beta$  levels. Alternatively, mammalian cells may have evolved a redundant pathway to stimulate IFN- $\beta$  mRNA transcription during a viral infection which sequesters HuR. Finally, the increased IFN- $\beta$  abundance may be a result of decreased IFN protein levels if IFN-beta mRNA is being inefficiently translated following the sequestration of HuR on the viral genome. HuR has been shown in many instances to increase the translation of mRNA to which it binds (Mazan-Mamczarz *et al.*, 2003; Galban *et al.*, 2008) thus the absence of HuR to bind to IFN- $\beta$  mRNA may result in a decrease translation of that mRNA. Reduced IFN- $\beta$  protein levels may stimulate the cell to increase IFN- $\beta$  mRNA transcription. Further analysis to measure IFN- $\beta$  protein levels by western blot or other protein analysis would help elucidate if a lack of IFN- $\beta$  protein was evident during infection with SFV4-2SG-*Gluc*-5xURE despite higher levels of IFN- $\beta$  mRNA, this would suggest an inhibition of IFN- $\beta$  mRNA translation.

Apoptosis is orchestrated through a number of caspase enzymes. Caspase 9 contains HuR binding sites which are thought to stabilize the caspase-9 mRNA. Furthermore, during initial apoptosis signaling, a proportion of HuR is cleaved in a caspase-dependent manner and the HuR cleavage products have been demonstrated to amplify the apoptotic response (Mazroui *et al.*, 2008). HuR that translocates to the cytoplasm during SINV infection has been demonstrated not to be the cleaved form of HuR (Sokoloski *et al.*, 2010). The sequestration of HuR on the viral genome in SFV4 infection may therefore reduce the available HuR that is able to bind and stabilize caspase-9 mRNA and also reduce the amount of HuR available to be cleaved and promote apoptosis which would lead to decreased caspase-9 mRNA levels. This is reflected in caspase-9 cytoplasmic mRNA abundance during infection with SFV4 whereby the caspase-9 mRNA levels were significantly decreased to when compared to NIC. When more URE elements are present in the 3'UTR of the SFV4 genome, caspase-9 mRNA levels are decreased most significantly and when the URE is removed from the viral genome caspase-9 mRNA levels are decreased least significantly. This supports the notion that the more URE present in the viral genome, the larger proportion of cellular HuR is sequestered on the viral genome and thus the less HuR is able to bind caspase-9 mRNA and stabilize it resulting in reduced levels of caspase-9 mRNA in the cytoplasm.



RNase-L mRNA 3'UTR contains cis-acting elements which bind TTR-RBPs that either promote or inhibit its degradation. HuR binds the RNase-L mRNA in the 3'UTR region and has been shown to increase its stability and protein expression. Furthermore, this interaction has been demonstrated to enhance antiviral activity presumably by creating higher levels of RNase-L (Li *et al.*, 2007). Interestingly, RNase-L has been shown to downregulate HuR expression which is dependent on the 3'UTR of the HuR mRNA. In one study the half-life of HuR mRNA increased from 1.5 to 6 hours from wild-type to RNase-L KO cell lines, respectively (Al-Ahmadi *et al.*, 2009b). The significance of the RNase-L inhibitory effect on HuR expression in wild-type cells was shown to have variations depending on the cell-cycle state, the confluency of the cells, and the subcellular location of HuR (Al-Ahmadi *et al.*, 2009b). The abundance of RNase-L mRNA during infection with the rSFV4 tested shows no direct correlation to frequency of URE elements in the SFV4 3'UTR. There could be a more complicated explanation for this such as the wild type virus produces a better infection than SFV4-2SG-*Gluc*- $\Delta$ URE so stimulates the production of more RNase-L but sequesters more HuR in the cell to its genome so RNase-L is destabilised or unable to be exported out of the nucleus. However, when comparing to NIC, it appears there is a higher ratio of RNase-L mRNA in the nucleus compared to the cytoplasm at both 6 and 12 hpi for all rSFV4 viruses. This suggests SFV4 infection may be inhibiting RNase-L mRNA's nuclear export. An alternative explanation could be the abundance of RNase-L mRNA in the nucleus is increased during SFV4 infection compared to NIC because of an increase in transcription but this difference is quenched when looking at the cytoplasmic fraction due to the increased mRNA density in this fraction.

TTP mRNA was significantly increased at both 6 and 12 hpi for all 3 rSFV4 viruses compared to NIC. Since the frequency of URE in the SFV4 3'UTR appears to affect TTP mRNA abundance significantly at the beginning of infection (6hpi) but not later, this may be an indirect effect on viral replication and viral RNA abundance rather than sequestration of HuR on the viral genome. TTP is known to bind sequences analogous to HuR, i.e. AU-rich elements in particular AUUUA, AUUUUA, AUUUUUA and there is evidence that HuR and TTP competitively bind the same mRNA to regulate its stability or degradation, respectively (Young *et al.*, 2009; Dean *et al.*, 2004). The increased TTP mRNA abundance may be stimulated by SFV4 to facilitate TTP binding to host cell transcripts, which have lost HuR after HuR has been sequestered by the virus RNA. TTP almost exclusively promotes mRNA degradation so this would promote degradation of those host-cell transcripts to which TTP and HuR competitively bind.

It is unclear which effect of the URE and HuR is more significant for enhancing infection. The URE appears to promote translation of virus RNA and increase stability of the RNA but it also destabilises host cell transcripts through the sequestration of HuR away from host transcripts. During SINV infection the sequestration of HuR on the viral genome was shown to inhibit a range of mRNA including RIG-1 (DDX58) which is involved in initiating the anti-viral response (Barnhart *et al.*, 2013). It is possible the increased translation and stability of viral RNA is most significant in initiating infection of the host cell and the destabilisation of host transcripts inhibits the anti-viral response, possibly apoptosis and therefore promotes the late stages of infection.

The increase in TTP mRNA during SFV4 infection is also interesting since it is a TTR-RBP which promotes degradation of RNA. This suggests that the host cell may have upregulated TTP to increase the degradation of viral RNA. However, the majority of TTP does not colocalise with HuR during SFV4 infection which suggests that TTP is not binding the viral RNA (since HuR has been previously shown to bind SFV4 3'UTR) so it may be binding host mRNAs instead. Despite TTP and HuR binding different transcripts in some instances and competitively binding other, the binding of HuR to viral RNA may sterically inhibit TTP binding thus protect it from degradation. Other RNA binding proteins which bind the 3'UTR of transcripts and promote their degradation are the TTP paralog Bfr1 and the different isoforms of Auf1. In contrast to HuR, these RNA-binding proteins act in synergy to recruit mRNA decay machinery and promote mRNA decay (Gratacos and Brewer, 2010; Raineri *et al.*, 2004). For instance Auf1 can act as a co-activator of TTP by facilitating its recruitment to the 3'UTR (Kedar *et al.*, 2012). HuR has been shown to bind to TTP mRNA and increase its stability (Pullmann *et al.*, 2007), so given that HuR is sequestered during SFV4 infection and thus not able to stabilize TTP mRNA an increase in TTP abundance is surprising. The SFV4 virus infection may have stimulated the transcription of TTP. This may be beneficial to SFV infection since it may assist in the degradation of host mRNA which bind TTP in the absence of HuR.

The ability of the URE to increase protein levels either through increasing the stability of RNA and/or its translation lends itself to be utilised as a stability element perhaps to be located immediately 5' of a polyadenylation signal sequence for transfected RNA or RNA transcribed from plasmids or vector inserted transgenes (Powell, Rivera-Soto and Gray, 2015). This will likely increase the protein production from the transfected or inserted transgene.

# Chapter 5

## Host mRNA nuclear export and MHV-68 infection

---

## 5.1 Overview

In *Chapter 3*, translocation dynamics of key RNA-binding protein were investigated during lytic infections with SFV (an RNA virus) and MHV-68 (a DNA virus). The ability to compare two viruses which cause comparable lytic infections in murine cells provided the opportunity to investigate whether changes in translocation dynamics of key RNA-binding proteins were primarily driven by viruses or were the results of stress response from cells and therefore virus-independent. The observations that MHV-68 infection resulted in the translocation of PABPC, suggested obstructions in bulk mRNA export which warranted further investigation.

The alkaline DNase gene, found in all herpesviruses studied so far, has evolved a distinct function in gamma-herpesviruses to enable viral mediated host shut-off. The homologs discussed in *Chapter 1*, kSOX, muSOX and BGLF5 induce a significant increase in the rate of host mRNA turnover during KSHV, MHV-68 and EBV lytic infection, respectively (Covarrubias *et al.*, 2009; Rowe *et al.*, 2007; Glaunsinger, Chavez and Ganem, 2005). The expression of these homologs in host cells also results in the build-up of PABPC in the nucleus (Kumar and Glaunsinger, 2010).

The current established mechanism by which PABPC builds up in the nucleus during MHV-68 infection is due to the loss of poly(A) mRNA in the cytoplasm following viral muSOX expression (Kumar, Shum and Glaunsinger, 2011). In basal conditions, PABPC is retained in the cytoplasm while bound to the poly(A) tail on mRNA. When poly(A)+ mRNA in the cytoplasm is degraded post-muSOX expression the cytoplasmic PABPC binds to Importin-alpha and is translocated back to the nucleus (Kumar, Shum and Glaunsinger, 2011).

An alternative mechanism by which PABPC accumulates in the nucleus occurs when bulk poly(A) mRNA nuclear export is blocked (Burgess *et al.*, 2011). Results from PABPC immunostaining following MHV-68 infection in NIH/3T3 cells indicated that the translocation of PABPC to the nucleus occurs gradually from 8 to 24 h.p.i. This supports a model whereby the PABPC relocation is gradual over the course of infection. PABPC is a known nucleo-cytoplasmic shuttling protein and it has been demonstrated to be exported from the nucleus into the cytoplasm while bound to poly(A) mRNA. Furthermore, when bulk poly(A) mRNA nuclear export is blocked via knock-down of NXF1 a build-up of PABPC in the nucleus occurs (Burgess *et al.*, 2011). It is therefore possible that a build-up of PABPC in the nucleus occurs as a consequence of a block in bulk poly(A) mRNA nuclear export rather than as a pre-requisite (Kumar and Glaunsinger, 2010).

The mRNA nuclear export of host mRNA transcripts is a dynamic process involving ribonucleoprotein complexes which facilitate the transport of mRNA through the nuclear pore; mRNA is then released in the cytoplasm. As discussed in *Chapter 1*, the bulk of mRNA is exported out the nucleus as part of a ribonucleoprotein complex containing NXF1-NXT1 (Carmody and Wente, 2009). The NXF1 ribonucleocomplex is bound by RAE1 which directs it to the nuclear pore, binds Nup98 of the nuclear pore and translocates through it (Blevins *et al.*, 2003). RAE1 does not dissociate from the ribonucleoprotein complex until in the cytoplasm at which point it shuttles back in to the nucleus.

## 5.2 Objectives

In *Chapter 3* it was concluded that in stark contrast to infection with SFV, PABPC enters the nucleus gradually over 24 hours following muSOX expression during MHV-68 infection. It was hypothesised that the gradual nuclear build-up of PABPC in MHV-68 lytic infection occurs because of a gradual block in mRNA nuclear export.

1. The study aimed to determine if muSOX results in a block in mRNA nuclear export during MHV-68 infection by specifically assessing:
  - The subcellular localisation of RAE1 in NIH/3T3 cells after infection with MHV-68 or MHV-68 ORF37stop viruses.
  - A possible build-up of host mRNA transcripts in the nucleus following infection with MHV-68 or MHV-68 ORF37stop viruses.
2. The study also assessed if host mRNA degradation is inhibited during MHV-68 ORF37stop infection as compared to MHV-68 infection and if this occurs predominantly in the cytoplasm or nucleus.

## 5.3 Results

As discussed in *Chapter 1* many RNA-binding proteins are utilised in mRNA nuclear export that shuttle between the nucleus and cytoplasm as part of a ribonucleoprotein complex with mRNA. To decipher if muSOX created a block in the mRNA nuclear export protein machinery the sub-cellular location of RAE1 during infection with MHV-68 or MHV-68 ORF37stop was assessed.

RAE1 is distributed between the nucleus and cytoplasm in basal conditions in NIH/3T3 cells with a higher proportion in the nucleus and no distinct build-up at the nuclear envelope (Figure 5.1). This is akin to the subcellular location of RAE1 in the same cell type following infection with MHV-68 ORF37stop virus at both 12 and 24 h.p.i (Figure 5.1). Interestingly, during infection of NIH/3T3 cells with MHV-68 with a functional muSOX gene, RAE1 builds up at the nuclear envelope by 12 h.p.i and this build-up is retained and prominent at 24 h.p.i. (Figure 5.1).

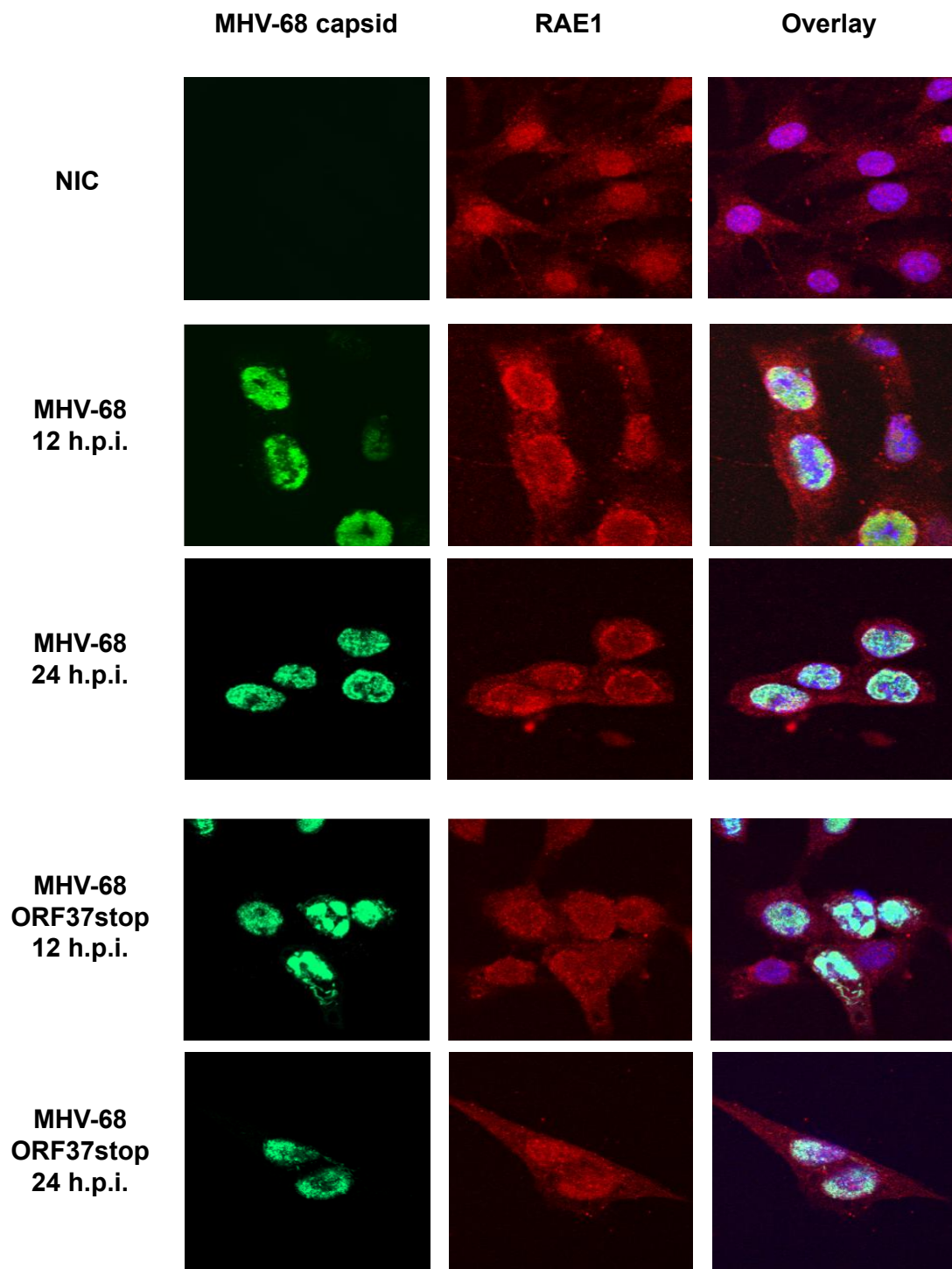


**Figure 5.1. RAE1 builds-up around nuclear envelope following MHV-68 infection but not MHV-68 ORF37stop infection or NIC.** NIH/3T3 cells were infected at an MOI of 5 with MHV-68 or MHV-68 ORF37stop viruses and fixed at 12 or 24 hours post infection. Cells were stained against MHV-68 capsid (green), RAE1 (red) and DAPI staining (blue). Experiment was repeated 3 times with similar results.

The build-up of RAE1 at the nuclear envelope following infection with MHV-68 suggests there may be a break-down of bulk mRNA nuclear export since RAE1 is exported out of the nucleus as part of a ribonucleoprotein complex that exports mRNA out of the nucleus (Blevins *et al.*, 2003; Cheng *et al.*, 2006). To assess this at the mRNA level NIH/3T3 cells were infected with MHV-68 and MHV-68 ORF37stop viruses and the nuclear and cytoplasmic fractions were separated. Following separation of subcellular fractions, RNA was extracted for analysis by qPCR for viral and cellular transcripts.

Following infection of mammalian cells with MHV-68, muSOX is expressed from 6-8 h.p.i. onwards and muSOX mediated host shut-off is evident from 8-12 h.p.i. and continues throughout the course of infection (Covarrubias *et al.*, 2009). The build-up of PABPC in the nucleus was measured as 53% nuclear at 16 h.p.i. infection in murine NIH/3T3 cells (*Chapter 3*). Therefore, if a block in mRNA nuclear export was responsible for the nuclear build-up of PABPC following muSOX expression then 16 h.p.i. was deemed an adequate time point to quantify the level of specific mRNA transcripts in the nucleus and cytoplasm.

The relative abundance of MHV-68 gB mRNA was assessed as an indication of the level of viral mRNA expression and by extension, viral lytic infection. Infection of NIH/3T3 cells with MHV-68 resulted in an abundance of MHV-68 gB mRNA in the cytoplasm that was moderately yet significantly higher than the level of MHV-68 gB mRNA in the cytoplasm in cells infected with MHV-68 ORF37stop virus (Figure 5.2,  $p = 0.011$ ). The levels of MHV-68 gB in the nucleus following infection from the two viruses were not-significantly different (Figure 5.2,  $p = 0.273$ ). This suggests that both viruses were able to produce a comparable and active lytic infection cycle in the NIH/3T3 cells in this assay.



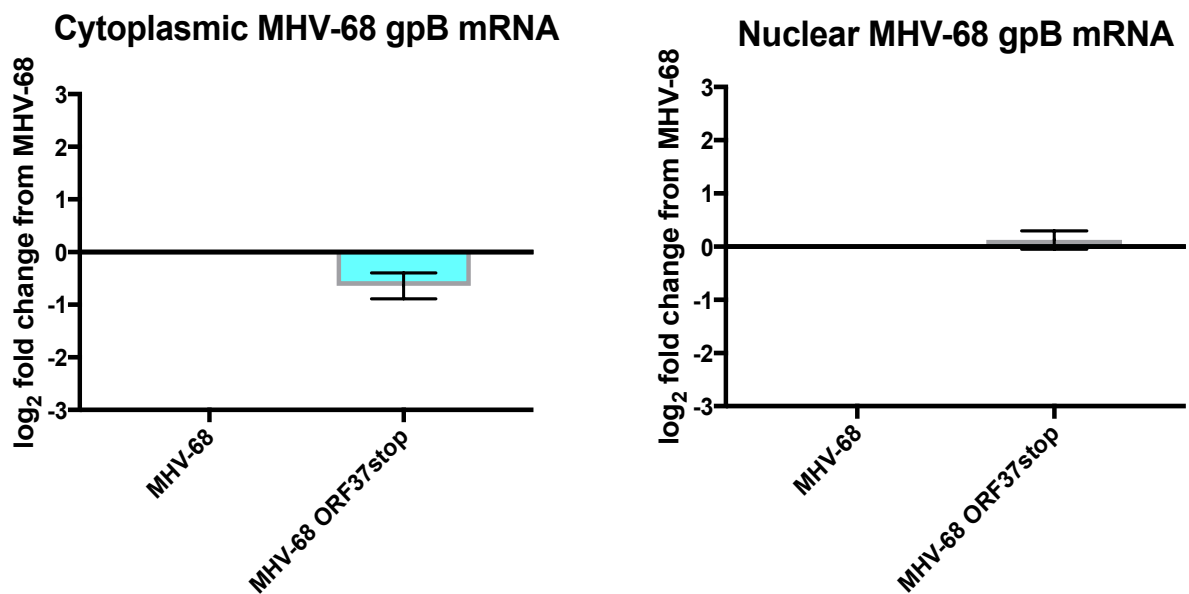


**Figure 5.2 MHV-68 and MHV-68 ORF37stop viruses produce comparable levels of MHV-68 gpB mRNA in the cytoplasmic and nuclear fraction following infection of NIH/3T3 cells.** NIH/3T3 cells were infected an MOI of 10 with MHV-68 or MHV-68 ORF37stop. Samples were collected at 16 h.p.i. The results are representative of n=2 experiments.

As discussed in Chapter 1, it has been indicated that host mRNA nuclear export machinery begins to assemble on pre-mRNA simultaneously to on-going transcription and splicing, illustrating that mRNA maturation and its nuclear export are physically linked processes (Masuda *et al.*, 2005). Subtle differences in mRNA nuclear export machinery and dynamics can also occur depending on the existence or absence of introns within the gene (Masuda *et al.*, 2005; Chi *et al.*, 2013). Therefore, a block in mRNA nuclear export may occur at any one of multiple steps during mRNA transcription, maturation and nuclear export. Although the NXF-1-dependent pathway for mRNA nuclear export is responsible for host bulk mRNA nuclear export it has been demonstrated that viruses can adapt the pathway or utilise NXF1-independent pathways (such as via CRM1 and an adapter protein) (Carmody and Wentz, 2009)) for viral mRNA nuclear export. Alterations to the host ribonucleoprotein complexes involved in mRNA nuclear export pathways have been identified during herpes simplex virus (Soliman and Silverstein, 2000) and KSHV (Jackson *et al.*, 2011).

For this reason, a range of representative transcripts, which either were intronless or contained a varied number of introns, were chosen. These transcripts may follow subtly different sets of processes before nuclear export and may be exported by messenger ribonucleoprotein (mRNP) complexes of varying compositions of nuclear export proteins.

For detection of host cyclophilin A mRNA, primers that amplify an amplicon containing a splice junction were designed. With the designed primers, the cyclophilin A spliced mRNA should amplify an amplicon of 100 bases. Any larger amplicon (from a build-up of unspliced cyclophilin A mRNA) would be detected during the melt-curve assay in the qPCR as a double peak.

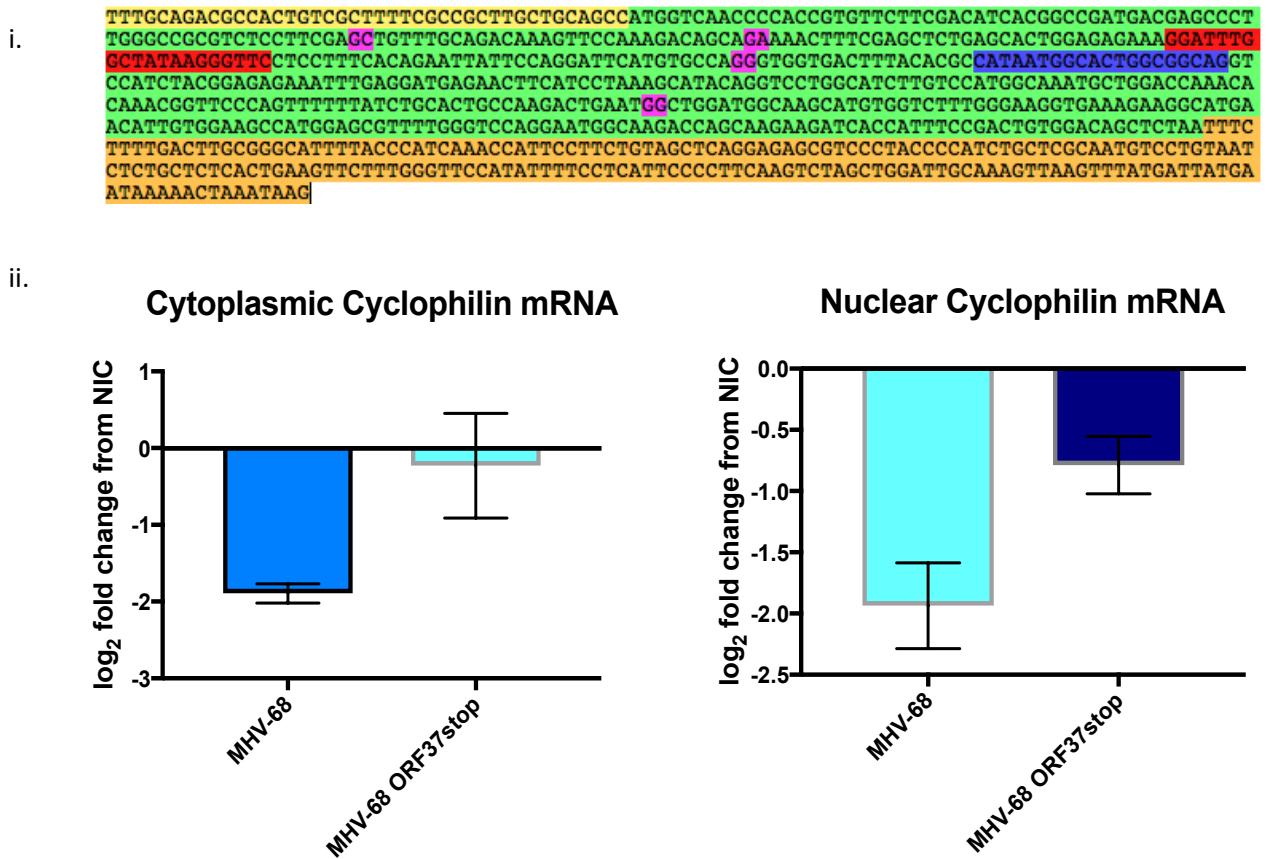


**Figure 5.3 Cyclophilin A mRNA abundance is decreased in the cytoplasmic and nuclear fraction during MHV-68 infection compared to NIC or MHV-68 ORF37stop infection. (i) Cyclophilin A mRNA sequence** with indicated splice junctions (pink) and primers used (red and blue) in qPCR **(ii) Cyclophilin A mRNA abundance in cytoplasm and nucleus** following infection with MHV-68 or MHV68 lacking functional muSOX gene. NIH/3T3 cells were infected an MOI of 10 with MHV-68 or MHV-68 ORF37stop. Samples were collected at 16 h.p.i. The results are representative of n=2 experiments.

The abundance of cyclophilin A mRNA in the cytoplasm of NIH/3T3 cells infected with MHV-68 is significantly less compared to its levels in the NIC (Figure 5.4,  $p < 0.01$ ) and cells infected with MHV-68 ORF37stop virus ( $p = 0.01$ ). This decrease in cyclophilin A mRNA is also seen in the nucleus and is significant compared to NIC ( $p < 0.01$ ) and following MHV-68 ORF37stop infection ( $p < 0.01$ ). There

is also a decline in cyclophilin A mRNA in the nucleus of cells infected with MHV-68 ORF37stop virus compared to NIC ( $p = <0.01$ ).

Taken together these results suggest that a significant decrease in cyclophilin A mRNA in the cytoplasm occurs following infection with MHV-68 but not MHV-68 lacking a functional muSOX gene. A similar significant decrease of cyclophilin A mRNA is seen in the nucleus following MHV-68 infection and to a lesser extent following MHV-68 ORF37stop infection. This may relate to a decrease in cyclophilin A transcription or an increase in cyclophilin A mRNA turnover. No apparent build-up of cyclophilin A mRNA occurred in the nucleus following infection of MHV-68 as compared to NIC or MHV-68 ORF37stop infection. The meltcurve from the qPCR showed one clean peak suggesting that minimal or no unspliced pre-mRNA was duplicated in the qPCR reaction. This suggests that a build-up of non-spliced cyclophilin A mRNA also did not occur in the nucleus. Taken together, these data suggest that a block in cyclophilin A mRNA nuclear export does not occur during MHV-68 infection.

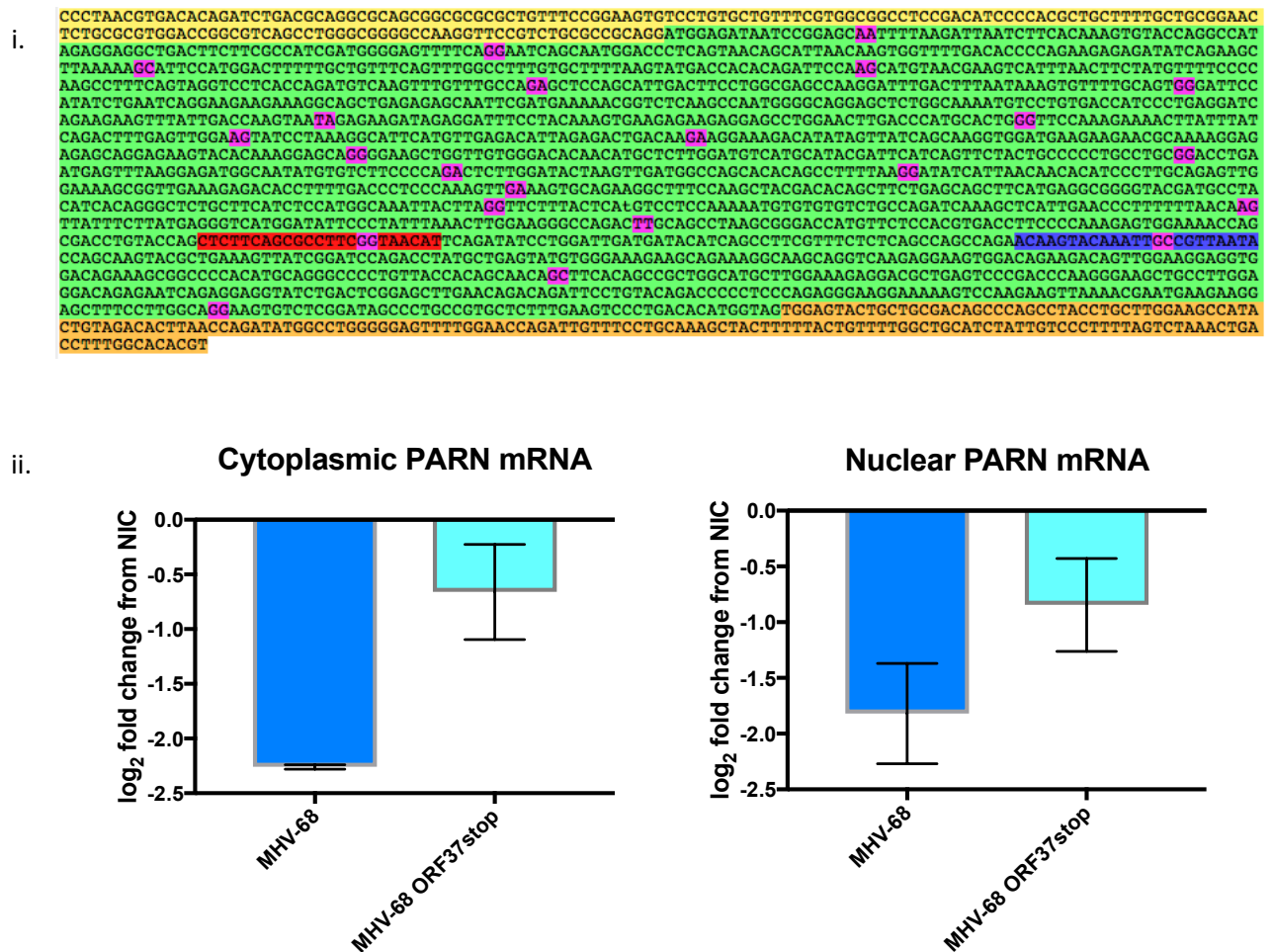


**Figure 5.4 Cytoplasmic PARN mRNA abundance is decreased in the cytoplasm and nucleus during MHV-68 infection compared to NIC or MHV-68 ORF37stop infection. (i) PARN mRNA sequence with indicated splice junctions (pink) and primers (red and blue) used in qPCR (ii) PARN mRNA abundance in cytoplasm and nucleus following infection with MHV-68 or MHV68 lacking functional muSOX gene. NIH/3T3 cells were infected at an MOI of 10 with MHV-68 or MHV-68 ORF37stop. Samples were collected at 16 h.p.i. The results are representative of n=2 experiments.**

PARN mRNA decreases in abundance in NIH/3T3 cells following infection with MHV-68 in both the cytoplasm (Figure 5.5,  $p < 0.01$ ) and nucleus compared to NIC ( $p < 0.01$ ). There is a decrease in PARN mRNA levels following MHV-68 ORF37stop virus infection in both the cytoplasm ( $p = 0.06$ ) and nucleus ( $p = 0.02$ ) compared to NIC but this decrease is only significant in the nucleus. The difference between PARN abundance between MHV-68 infection and MHV-68 ORF37stop infection is also significant both in the cytoplasm ( $p = 0.01$ ) and nucleus ( $p = 0.04$ ). This suggests that muSOX results in a significant decrease in PARN mRNA at 16 h.p.i. in both the cytoplasm and nucleus following infection with MHV-68. There is no apparent build-up of PARN mRNA in the nucleus following infection of MHV-68 as

compared to NIC or MHV-68 ORF37stop infection suggesting muSOX does not cause a nuclear build-up of PARN mRNA.

Primers against host XRN1 mRNA amplified an amplicon containing no introns despite containing many in the full pre-mRNA transcript. This enabled inclusion of the relative quantification of XRN1 unspliced pre-mRNA as well as spliced XRN1 mRNA in to the total relative XRN1 mRNA abundance compared to NIC. This would allow detection of a block in XRN1 mRNA nuclear export if it was occurring before splicing took place or alongside aberrant splicing.

[illegible]

ii.

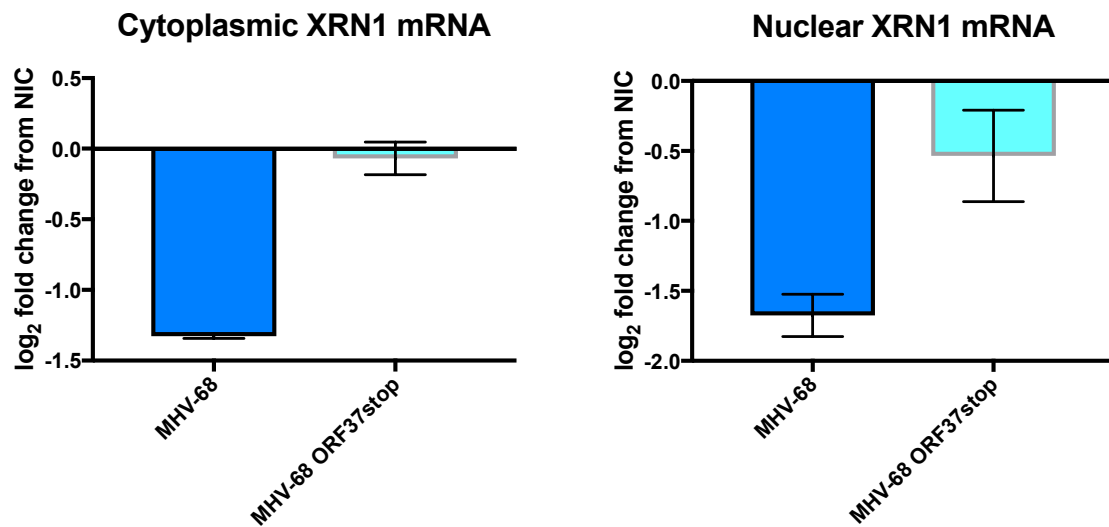


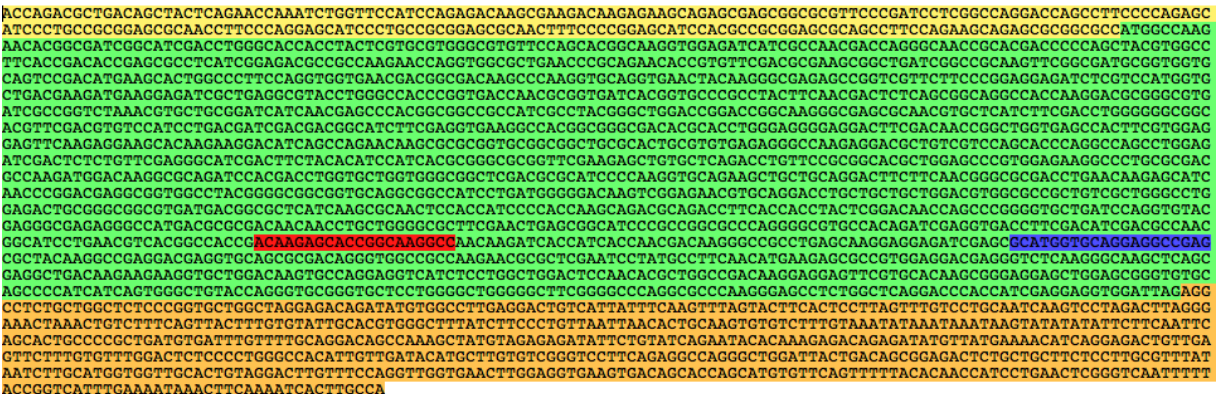
**Figure 5.5 Cytoplasmic XRN1 mRNA abundance is decreased in the cytoplasm and nucleus during MHV-68 infection compared to NIC or MHV-68 ORF37stop infection. (i) XRN1 mRNA sequence with indicated splice junctions (pink) and primers (red and blue) used in qPCR (ii) XRN1 mRNA abundance in cytoplasm and nucleus** following infection with MHV-68 or MHV68 lacking functional muSOX gene. NIH/3T3 cells were infected at an MOI of 10 with MHV-68 or MHV-68 ORF37stop. Samples were collected at 16 h.p.i. The results are representative of n=2 experiments.

Cytoplasmic XRN1 decreases in mRNA abundance following MHV-68 infection compared to NIC (Figure 5.6,  $p < 0.01$ ) or MHV-68 ORF37stop infection ( $p < 0.01$ ). XRN1 mRNA abundance also decreases in the nucleus following MHV-68 infection compared to NIC ( $p < 0.01$ ) or MHV-68 ORF37stop infection ( $p < 0.01$ ). Infection of NIH/3T3 cells with MHV-68 ORF37stop infection causes no significant changes in XRN1 abundance compared to NIC in the cytoplasm ( $p = 0.36$ ) and a marginally



significant reduction in the nucleus ( $p=0.047$ ). There is no significant increase in XRN1 mRNA abundance in the nucleus following infection with MHV-68 suggesting that MHV-68 infection with or without a functional muSOX gene has not caused a build-up of XRN1 mRNA in the nucleus.

Finally, host HSP70 mRNA abundance was measured because HSP70 transcript is intronless so its mRNA maturation and nuclear export pathway may involve mRNP complexes and processes that differ slightly from transcripts with introns that undergo splicing. This allowed for assessment of a wider range of mRNA export pathways.

i. 

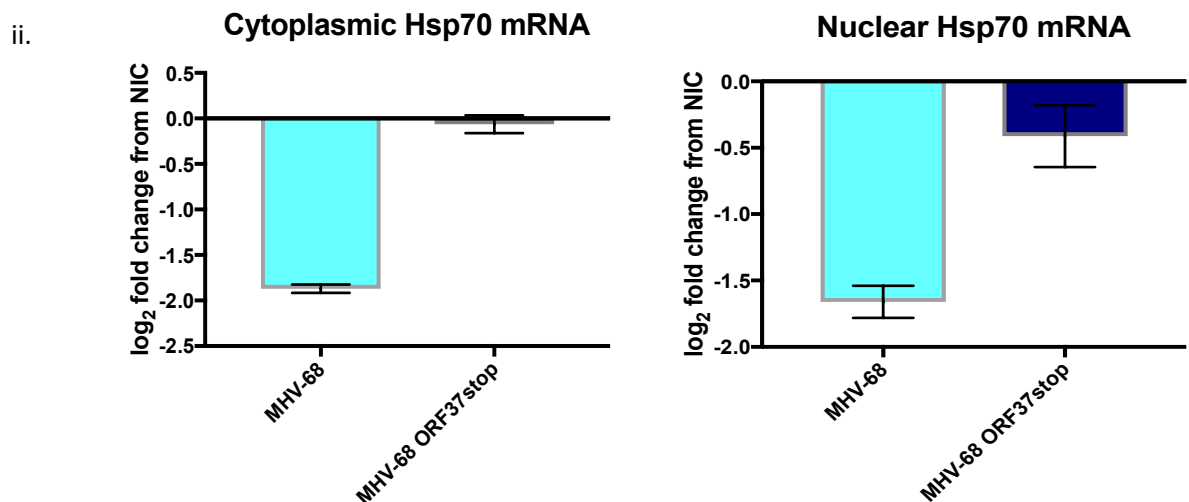


**Figure 5.6 Cytoplasmic HSP70 mRNA abundance is decreased in the cytoplasm and nucleus during MHV-68 infection compared to NIC or MHV-68 ORF37stop infection. (i) HSP70 mRNA sequence containing no splice junctions, primers (red and blue) used in qPCR (ii) HSP70 mRNA abundance in cytoplasm and nucleus following infection with MHV-68 or MHV68 lacking functional muSOX gene.** NIH/3T3 cells were infected at an MOI of 10 with MHV-68 or MHV-68 ORF37stop. Samples were collected at 16 h.p.i. The results are representative of  $n=2$  experiments.

The abundance of HSP70 mRNA in the cytoplasm of NIH/3T3 cells significantly decreased by 16 h.p.i. with MHV-68 compared to NIC (Figure 5.7,  $p < 0.01$ ) and MHV-68 ORF37stop infection ( $p < 0.01$ ). Following MHV-68 infection in the nucleus this reduction is also seen compared to NIC ( $p < 0.01$ ) and MHV-68 ORF37stop infection ( $p < 0.01$ ). There are no significant differences between HSP70 mRNA abundance in the cytoplasm at 16 h.p.i with MHV-68 ORF37stop compared to NIC ( $p = 0.32$ ) and a small but significant decrease in the nucleus ( $p = 0.04$ ). Taken together this data suggests that despite not undergoing splicing HSP70 mRNA does also not build-up in the nucleus following MHV-68 infection.

## 5.4 Discussion

The inhibition of host mRNA nuclear export is targeted by a wide range of virus families. Since inhibition of mRNA nuclear export inhibits host-cell protein production this targeted action results in suppression of the host-cell anti-viral response. It also increases the availability of host translation machinery for translation of viral proteins.

The bulk of host mRNA nuclear export occurs through a NXF1/NXT1 pathway (as discussed in Chapter 1) whereby the host mRNA-NXF1/NXT1 mRNP translocates to the nuclear pore through binding to RAE1 (Blevins *et al.*, 2003). RAE1 is targeted during vesicular stomatitis virus (VSV) infection of mammalian cells. Vesicular stomatitis virus (VSV) inhibits host cell protein production through inhibition of transcription and host mRNA nuclear export (von Kobbe *et al.*, 2000; Petersen *et al.*, 2000). The inhibition affects poly(A) mRNA nuclear export without affecting nucleocytoplasmic traffic of host proteins. VSV M protein interacts with Nup98 via Nup98 amino acids 173-213 (Faria *et al.*, 2005) containing the GLEBS motif (Pritchard *et al.*, 1999) which binds RAE1. VSV M protein interaction with RAE1 is independent of Nup98 whereas VSV M protein interaction with Nup98 is RAE1 dependent. This promotes a model whereby RAE1 is the primary interaction target of VSV M protein which forms incompetent export complexes with RAE1 and Nup98 (Faria *et al.*, 2005). The block in host mRNA export is alleviated/prevented by transfection with RAE1 or Nup98 on an expression plasmid (Faria *et al.*, 2005). The increased Nup98 expression may outcompete VSV M protein for binding to RAE1 and thus alleviate an inhibition of mRNA nuclear export. The reversion of host mRNA export block by RAE1 over expression was shown to be RAE1 dose dependent in cells transfected with M protein or VSV infected cells (Faria *et al.*, 2005). This suggests quenching the cell with RAE1 provides enough to alleviate a block in mRNA export despite the presence of VSV M protein.



The build-up of RAE1 around the nuclear envelope during MHV-68 infection may indicate a breakdown or adjustment to the host bulk mRNA nuclear export pathway. This change in RAE1 subcellular location may be occurring directly due to changes to the RAE1 protein itself, or other indirect changes including changes to the mRNA nuclear export machinery. Despite the build-up of RAE1 around the nuclear envelope however, no nuclear build-up of the host mRNA transcripts analysed in this chapter was observed. Recently a similar study has found that MHV-68 and KSHV ORF10 protein bind RAE1 and form a complex with Nup98. This results in a block in nuclear export of a subset of host mRNA transcripts (Gong *et al.*, 2016).

It was demonstrated using a sequential Immunoprecipitation assay (IP) that KSHV and MHV-68 ORF10 form a complex with Nup98 through an interaction with RAE1 (Gong *et al.*, 2016). Furthermore, using oligod(T) *in-situ* hybridisation it was shown that expression of ORF10 from either KSHV and MHV-68 results in poly(A) nuclear accumulation. The increased signal from oligod(T) staining was attributed to a block in mRNA nuclear export to a subset of host mRNA transcripts and it was also demonstrated that the mRNA transcripts blocked from nuclear export become hyper-adenylated (Gong *et al.*, 2016).

RAE1 is thought to be a key RNA nuclear export protein in the bulk mammalian mRNA nuclear export pathway. However, knock-down of RAE1 did not duplicate the same phenotype as ORF10 protein expression (Gong *et al.*, 2016). Therefore it was concluded that it is the complex of ORF10, RAE1 and Nup98 which selectively inhibits a sub-set of host mRNA transcripts and not just the removal of available RAE1 through sequestration by ORF10 (Gong *et al.*, 2016). Through RNA sequencing analysis of host nuclear and cytoplasmic fractions, the block in mRNA nuclear export following ORF10 expression was evident in only a subset of genes analysed (Gong *et al.*, 2016). Of the 12,181 host genes analysed, 686 genes had more than a 50% increase in their nuclear to cytoplasmic mRNA transcript location ratios. Importantly, despite some of the genes analysed in this study being included in the original 12,181 genes analysed in the ORF10 study, CYPA, PARN, XRN1 or HSP70 did not show an increase in their nuclear to cytoplasmic mRNA transcript location ratios following ORF10 expression (Gong *et al.*, 2016). This agrees with the data in this study which found no nuclear build-up of mRNA from these four genes following MHV-68 infection (during which ORF10 is expressed). Since all four genes tested, including HSP70, did not build-up in the nucleus following MHV-68 infection then any muSOX or ORF10 mediated block in mRNA export is likely not defined to all transcripts with introns or all transcripts without introns. This is important because the bulk NXF1-NXT1 mRNA nuclear export pathway (which includes RAE1) has been previously demonstrated to be functionally linked to mRNA splicing (Masuda *et al.*, 2005; Cheng *et al.*, 2006) so any nuclear mRNA export block involving RAE1 may have been specific to spliced transcripts.

Interestingly, poly(A) transcript nuclear accumulation including host transcript hyper-adenylation following MHV-68 or KSHV infection has already been previously attributed to expression of viral muSOX (MHV-68) or SOX (KSHV) and the subsequent nuclear build-up of poly(A) binding protein (Kumar and Glaunsinger, 2010; Covarrubias *et al.*, 2009). This suggests that there are two gamma-herpesviral proteins, muSOX/SOX and ORF10, resulting in a nuclear accumulation of host mRNA transcripts and host mRNA hyperadenylation. This study suggests however that CYP4A, PARN, XRN1 and HSP70 are genes that are not susceptible to this nuclear accumulation resulting either through expression of muSOX or ORF10. Interestingly in this study, a build-up of RAE1 around the nuclear envelope during infection of MHV-68 only occurred during infection with MHV-68 encoding a functional muSOX gene. This suggests that either muSOX also directly effects RAE1 function or alternatively that the functions of muSOX, including host mRNA degradation, have an indirect effect on RAE1 subcellular location. It has been demonstrated that muSOX and SOX target similar subsets of host mRNAs but both proteins elicit a more potent host shut-off when expressed during viral infection rather than on an expression plasmid (Clyde and Glaunsinger, 2011). This supports the idea that multiple gamma-herpesviral proteins contribute to the host shut-off phenotype evident during gammaherpesviral infection. Finally, the expression of RAE1 and NUP98/96 is up-regulated by IFN- $\gamma$  (Faria *et al.*, 2005) suggested that cells have evolved to attempt to compensate for viral infections targeting RAE1 and/or NUP98.

Degradation of the host mRNA transcripts analysed occurred significantly in both the cytoplasm and nucleus of NIH/3T3 cells infected with MHV-68 compared to NIC or cells infected with MHV-68 ORF37stop virus. This coincides with current data that identifies muSOX (and its homologs in other gamma-herpesviruses) as the principal viral protein responsible for the bulk of host mRNA degradation that is evident during gammaherpesvirus infection (Glaunsinger and Ganem, 2004; Ebrahimi *et al.*, 2003). However, in contrast to previous works muSOX expression during MHV-68 infection in this study elicited a decrease in mRNA abundance in both the cytoplasm and the nuclear fractions.

KSHV SOX contains a nuclear localization signal 315PRKKRK320, and is predominantly located in the nucleus during infection (Glaunsinger, Chavez and Ganem, 2005). Its nuclear localization is important for its alkaline exonuclease and resolvase activity, conserved among homologs seen in other herpesviruses, used to process and package the herpesviral DNA genome. The exonuclease and resolvase functions of KSHV SOX and the ability to induce global mRNA turnover have been shown to be genetically separable by mutagenesis of SOX genes (Glaunsinger *et al.*, 2005). This supports the contention that KSHV SOX has evolved the ability to promote mRNA turnover separately from the

protein's DNase functions. Interestingly, following transfection of SOX and GFP expression plasmids in to 293T cells and subsequent sub-cellular fractionation, the SOX mediated mRNA turnover was found to occur predominantly in the cytoplasm. This finding was strengthened by the ability of a mutant SOX protein with a deleted nuclear localization signal (SOX-ΔNLS) and thus predominant (but not total) localization in the cytoplasm that retained the ability to cause host shutoff (Glaunsinger et al., 2005). These findings were not conclusive since SOX-ΔNLS still partially resided in the nucleus. Furthermore, the GFP plasmid may have been transcribed at such a rate as to overcome a loss of GFP mRNA levels seen in the nuclear fraction. Additionally, a block in a subset of mRNA nuclear export may have compensated for the RNA loss induced by SOX in the nuclear fraction. For instance GFP mRNA was found to be blocked from nuclear export following ORF10 interaction with RAE1 during KSHV and MHV-68 infection (Gong *et al.*, 2016) and this study suggests that both muSOX and ORF10 affect RAE1 function.

During MHV-68 infection, muSOX also locates predominantly to the nucleus but akin to KSHV SOX and EBV BGLF5 it also partially resides in the cytoplasm (Covarrubias *et al.*, 2009). A mutant muSOX fused to a nuclear retention peptide, muSOX-NRS, can restrict muSOX subcellular location to the nucleus. muSOX-NRS is unable retain host shutoff activity following transfection suggesting the requirement for at least partial cytoplasmic location of muSOX to induce host shutoff (Covarrubias *et al.*, 2009). However, despite muSOX-NRS retaining in vitro DNase activity, the same NRS fused to KSHV SOX caused a complete inhibition of DNase activity. This suggests the NRS tag could interfere with host shut-off activity in muSOX-NRS since even though the NRS doesn't interfere with DNase activity in muSOX-NRS the DNase and host shut-off functions are genetically separable. Furthermore, the notion that muSOX location in the cytoplasm is required for host shut-off activity does not confirm that mRNA loss is also not seen in the nucleus since muSOX may be degrading mRNA through indirect and/or multiple mechanisms. Finally, the retention of muSOX-NRS in the nucleus may appear to prevent host shut-off in the cell as a whole rather than just the cytoplasm because the cytoplasm contains a much higher abundance of mRNA.

Due to the vastly higher concentration of mRNA in the cytoplasm of mammalian cells compared to the nucleus it should be noted that minor amounts of cytoplasmic mRNA contaminating the nuclear mRNA fractions prepared in this study may also confound results. Therefore, further study should be able to confirm or refute the findings of this study that muSOX can elicit mRNA loss in both the nucleus and cytoplasm and whether this also occurs with KSHV SOX. Most transcripts studied also showed loss of mRNA in the nucleus following infection of MHV-68 ORF37stop compared to NIC. This relatively smaller loss of mRNA compared to that seen during infection with MHV-68 infection was significant

when comparing to NIC. This loss is likely attributed to the viral genome hijacking the host transcription machinery for transcription of its genes thereby causing some level of inhibition to host cell gene transcription.

# Chapter 6

## **General Discussion**

## 6.1 Successful manufacture of recombinant viruses used in this study

For this study recombinant SFV4-based viruses were successfully engineered to encode SFV4 with sequence additions or deletions in the SFV4 URE and/or CSE region(s). Recombinant viruses containing deletions of the CSE took  $\geq 3$  days longer (than WT viruses or viruses containing only URE deletions or additions) to produce cytopathic effect (CPE) following transfection of BHK-21 cells. The rSFV4 viruses with CSE deletions generated some virions with mutations in virion DNA sequence that differed from their parental sequence at the 3'UTR however there was poor recovery of the WT CSE sequence. These rSFV4s ( $\Delta$ CSE) replicated at comparable rates to WT SFV4 and produced heterogenous plaque populations of varying sizes (compared to uniform plaque size produced by the other rSFV4 viruses used in these studies). This suggested asymmetry between virions derived from  $\Delta$ CSE viruses possibly arising from compensatory mutations occurring elsewhere in the viral genome, however full sequencing of these viral genomes would be required to confirm this. This makes drawing conclusions and comparisons from results using viruses derived from  $\Delta$ CSE viruses subject to possible confounding variables. Future work could investigate which, if any, mutations occurred elsewhere in the genome of rSFV4s with deletions in their CSE ( $\Delta$ CSE). This may highlight/identify which viral proteins or RNA sequences interact with the CSE and/or sequences which promote viral efficacy in murine cells. More reliable conclusions can be drawn from the comparison between SFV4-dURE, SFV4-5xURE and WT SFV4 which, when electroporated/transfected in susceptible cells produced CPE at similar time points post-transfection, produced plaques with a uniform plaque size, **and** sequence analysis of their genomes showed that their 3'UTR sequences were identical to the transfected icDNA's.

The MHV-68 ORF37stop mutant has been engineered and tested for reversion during previous work (Sheridan *et al.*, 2014) and in this study (data not shown). This study contradicted previous findings by Sheridan *et al.* which showed that MHV-68 ORF37stop could not replicate in IFN- $\alpha/\beta$  receptor-positive cells (NIH/3T3).

## 6.2 Sub-cellular localisation of TTR-RBPs during SFV4 infection

Viral infection induces changes in the sub-cellular localisation of a broad set of host proteins, many of which are TTR-RBPs and their exact topology in the cell is often linked to their activity (Pullmann *et al.*, 2007; Kishore, Lubner and Zavolan, 2010). The findings of this study suggest that the nuclear localisation of nsP2 is unlikely to be involved in the nuclear efflux of HuR seen during SFV4 infection. However, it is not possible to extract concrete conclusions since SFV4-RDR, which has a mutation in the nuclear localisation signal (NLS) of nsP2, allows some nsP2 to enter the nucleus. Further studies could utilise a virus strain capable to better exclude nsP2 from the nuclear compartment such as SFV4-RDD (Tamm, Merits and Sarand, 2008).

SFV4-WT infection was shown to result in HuR subcellular re-localisation to the cytoplasm, starting at approximately 3 hpi. An initial influx of HuR in to the cytoplasm following infection with SFV4-ΔURE is comparable to WT however less HuR is subsequently retained in the cytoplasm during the late stages of infection. This suggests that a biochemical event may initiate the HuR nuclear efflux following SFV4 infection and how much HuR is retained in the cytoplasm is dependent on the frequency of HuR binding sites in the 3'UTR of the SFV4 RNA. Previous work has suggested that this initial event relates to the phosphorylation state of HuR (Dickson *et al.*, 2012) but the exact mechanism is yet to be determined. The addition of 4 additional URE copies to the 3'UTR of SFV4 increased the retention of HuR in the cytoplasm suggesting that the addition of UREs to other viruses or transfected nucleic acids may produce a similar phenotype. Further work could investigate the use of the URE sequence in producing this phenotype and/or acting as an element with the ability to stabilise viral RNA and/or enhance its translation efficiency.

Immunostaining against HuR during infection with the rSFV4 viruses in this study also suggested that HuR does not predominantly co-localise with nsP3. This proposes that HuR is omitted from CPV1 replication complexes where SFV4 negative strand synthesis takes place (Kallio *et al.*, 2016; Kujala *et al.*, 2001). This is intriguing since it suggests that HuR may not be directly required for SFV4 genome negative strand synthesis despite binding to the N'terminus of the SFV4 3'UTR. Further study could attempt to isolate such replication complexes and determine if HuR is associated with CPV1.

TTP and HuR have been previously shown to bind overlapping/identical uracil rich RNA sequences on host mRNA transcripts (Khalaj *et al.*, 2017; Wang *et al.*, 2016). TTP and re-localised cytoplasmic HuR do not co-localise during infection of NIH/3T3 cells with any of the rSFV4 used in this study, suggesting that TTP may not be binding to the 3'UTR of SFV4. Interestingly, TTP mRNA abundance increased during infection with all rSFV4 in this study, indicating that increased host TTP mRNA transcription and/or stability may be a general feature of SFV4 infection. TTP can facilitate host cell shut-off during infection by recruiting deadenylases (Fabian *et al.*, 2013), RNase-L (Brennan-Laun *et al.*, 2014) or viral enzymes to host cell transcripts. This is observed during HSV infection when TTP recruits the viral host shut off RNase (VHS) to cellular mRNAs leading to their degradation (Shu, Taddeo and Roizman, 2015). The possibility of TTP facilitating host cell mRNA degradation during alphavirus infection has not yet been investigated. In addition, the recruitment of muSOX to host cell transcripts by TTP during MHV-68 infection could also be the focus of an intriguing future study.

### 6.3 Sub-cellular localisation of TTR-RBPs during MHV-68 infection

PABPC co-localised with HuR in the cytoplasm during infection with the rSFV4 viruses. During MHV-68 infection host HuR also localised in the same subcellular compartment as PABPC but in the nucleus rather than the cytoplasm. The colocalisation of HuR and PABPC during SFV4 infection is likely attributed to both host proteins binding to the 3' end of viral RNA (Dickson *et al.*, 2012). During MHV-68 infection both HuR and PABPC in the nucleus may be bound to newly transcribed viral mRNA and likely bound to host mRNA. There is suspected interaction of PABPC with HuR when bound to mRNA that provides the bound transcript with protection from deadenylation (Nagaoka *et al.*, 2006). AU-rich sequences similar to those which HuR bind to, are present in both IL-6 and AEN mRNA, both of which show resistance to muSOX mediated turnover (Clyde and Glaunsinger, 2011).

A role for HuR in protecting host transcripts during MHV-68 infection is unlikely however since the addition of these specific AU-rich 3'UTR's to reporter RNA's fail to confer protection from muSOX mediated degradation (Clyde and Glaunsinger, 2011). Further study could examine the protection of host transcripts during MHV-68 infection in TTR-RBP KO cell lines. This would not only elucidate if the transcripts that are resistant to muSOX utilise host TTR-RBPs but also if host RNA-destabilising RBPs are involved in the muSOX mediated host RNA turnover.

PABPC begins to build-up in the nucleus of MHV-68 infected cells by 8 h.p.i. In contrast to the HuR build-up in the cytoplasm seen during SFV4 infection, the PABPC is not retained in the nucleus by binding viral RNA since the PABPC nuclear build-up is observed in mammalian cells transfected with a muSOX expression plasmid (Covarrubias *et al.*, 2009). The PABPC nuclear influx, which is not seen in this study during infection with MHV-68 ORF37stop virus, is thought to be initiated by muSOX expression. There are a number of mechanisms by which this could occur directly or indirectly as a consequence of mRNA degradation (Kumar, Shum and Glaunsinger, 2011) or a block in host mRNA nuclear export (Burgess *et al.*, 2011).

### 6.4 Interplay of HuR, TTP and RNase-L in SFV4 infection

Regardless of HuR being sequestered on viral RNA, an increased TTP abundance alone may facilitate SFV4 infection though increased instability of host mRNAs involved in the innate and acquired immune responses. For instance, TTP has been shown to bind to and decrease the half-life of IFN-gamma mRNA thereby reducing the anti-viral response (Ogilvie *et al.*, 2009). Since HuR and TTP co-regulate a number of host mRNA transcripts, the increased TTP mRNA abundance and the sequestration of HuR on viral RNAs may simultaneously promote host mRNA transcript



degradation. TTP has also been shown to recruit deadenylases specifically the CCR4-NOT complex (Lai *et al.*, 1999; Fabian *et al.*, 2013) and/or RNase-L (Brennan-Laun *et al.*, 2014) to mRNA to assist in the degradation of the transcript. This study found that RNase-L mRNA transcript abundance in the cytoplasm during infection with any rSFV4 in this study was comparable to a NIC yet the abundance in the nuclear fraction was raised compared to NIC suggesting active transcription or a block in nuclear export of RNase-L mRNA. RNase-L activity degrades both host HuR (Al-Ahmadi *et al.*, 2009b) and TTP mRNA in mammalian cells (Al-Haj, Blackshear and Khabar, 2012) whereas HuR stabilises host RNase-L mRNA.

The interplay of these TTR-RBPs is likely to facilitate SFV4 infection. HuR binds to the viral transcripts while TTP may bind specific host transcripts during infection. HuR likely provides SFV4 RNA with protection from degradation (deadenylation) and possibly RNase-L activity, which along with host deadenylases, can be recruited to host transcripts via TTP (Brennan-Laun *et al.*, 2014).

## **6.5 Interplay of muSOX generated RNA loss and PABPC during MHV-68 infection**

This study found that NIH/3T3 cells infected with MHV-68 ORF37stop virus showed comparable abundance of the host mRNA transcripts tested in this study to the abundance in NIC. There was a significantly larger reduction in host mRNA transcript abundance seen during MHV-68 infection compared to NIC and MHV-68 37stop infection. Only MHV-68 infection resulted in the nuclear build-up of host PABPC. This suggests a link between muSOX, RNA loss and PABPC nuclear retention. Previous work has shown that muSOX causes host RNA loss and this leaves PABPC unbound to mRNA in the cytoplasm so its RNA recognition motif (RRM) is available to bind importin-alpha which imports PABPC in to the nucleus (Kumar, Shum and Glaunsinger, 2011). This study showed that over 85% of host PABPC resided in the nucleus of NIH/3T3 cells during late infection with MHV-68 suggesting that a partial loss in RNA is not solely responsible to the nuclear build-up of PABPC since host and viral RNA (both of which bind PABPC) are still present in the cytoplasm. PABPC is a nuclear shuttling protein and is exported out of the nucleus bound to mRNA (Burgess *et al.*, 2011). Not surprisingly an additional cause for PABPC nuclear build-up is a block in host mRNA nuclear export (Burgess *et al.*, 2011) which is thought to occur partially during MHV-68 infection (Kumar and Glaunsinger, 2010). This study did not find nuclear build-up of the specific host mRNA transcripts tested following MHV-68 infection suggesting that these transcripts are not blocked from mRNA nuclear export. Alternatively, there may be no net gain of mRNA abundance in the nucleus of the specific host transcripts because a build-up of mRNA in the nucleus is prevented by an increase in host transcript turnover and/or reduction in

host transcription as the transcription machinery is utilised for viral transcription. There may also be technical limitations in the absolute fractionation of the nucleus and cytoplasm as explained later.

## 6.6 The effect of the manipulation of SFV4 URE on host and viral transcripts

This study showed that following infection of NIH/3T3 cells with SFV4, the presence of URE in the 3'UTR of the viral genome appears to increase the abundance of viral RNA, the translation of viral RNA, the amount of infectious virus particles produced and a decrease in the abundance of host transcripts that usually bind HuR (albeit an increase in IFN- $\beta$  mRNA). These differences are not only illustrated following the deletion of the URE from the 3'UTR of SFV4 but are also shown to significantly increase when additional UREs are added to the 3'UTR of SFV4. The effects are likely resulting from the ability of the URE to bind host HuR (Sokoloski *et al.*, 2010). This is due to the known functions of HuR resulting in increased RNA stability and translation (Mazan-Mamczarz *et al.*, 2003; Brennan and Steitz, 2001). Similar results have been shown during SINV infection (Sokoloski *et al.*, 2010; Dickson *et al.*, 2012; Barnhart *et al.*, 2013).

This study found that the higher the frequency of URE in the SFV4 3'UTR the more HuR protein is retained in the cytoplasm, most likely bound to viral RNA. In addition, the higher the frequency of URE in the 3'UTR of SFV4 the more HuR was likely sequestered on viral RNA, suggesting less HuR was available to bind host transcripts. This would predict that those host transcripts which usually bind HuR would have decreased stability and abundance. Both  $\beta$ -actin and caspase-9 mRNA (containing HuR binding sites) had decreased abundance the higher the frequency of URE in the 3'UTR of SFV4 however the opposite was true for IFN- $\beta$ .  $\beta$ -actin represents host transcripts that usually bind HuR in their 3'UTR for increased stability but are not universally and significantly affected by viral infections. IFN- $\beta$  mRNA levels may have been increased more following infections with SFV4 containing higher numbers of UREs as these rSFV4s result in higher levels of viral RNA and virions which induce antiviral responses and production of IFN- $\beta$  (Akhrymuk, Frolov and Frolova, 2016; Ryman and Klimstra, 2008; Randall and Goodbourn, 2008).

The higher the frequency of URE in the 3'UTR of SFV4 the greater the abundance of viral RNA (nsP3) in murine cells that there was present early in infection (at 3 and 6 h.p.i.), also the higher the luciferase activity observed during infection with rSFV4s expressing *Gaussia* luciferase (SFV4-2SG-*Gluc*). This was also reflected in the initial number of infectious virus particles produced. These findings suggest that omitting the URE from the SFV4 genome inhibits viral replication by reducing the stability and translation of viral RNA. Furthermore, by including 4 additional copies of the URE in the SFV4 3'UTR

viral infection is enhanced by increasing viral RNA stability and translation. As discussed earlier, following infection of murine cells, RNase-L and tristetraprolin mRNA abundance were not affected at both 6 and 9 h.p.i. or just 9 h.p.i. respectively, by the frequency of UREs in the 3'UTR of the rSFV4.

## **6.7 The effect of the manipulation of MHV-68 muSOX on host and viral transcripts**

Multiple studies have demonstrated that muSOX of MHV68 causes both RNA loss and nuclear retention of PABPC in mammalian cells (Covarrubias *et al.*, 2009). This is also evident through the activity of SOX during KSHV infection (Glaunsinger, Chavez and Ganem, 2005) and BGLF5 (Rowe *et al.*, 2007) and ZEBRA (Park *et al.*, 2014) during EBV infection. Evidence for at least two theories as to how the PABPC nuclear retention and host RNA loss are correlated, exist. Firstly, a loss in RNA via the action of muSOX causes PABPC to expose its RRM that is able to bind importin- $\alpha$  and thus is imported in to the nucleus (Kumar, Shum and Glaunsinger, 2011). Secondly, PABPC nuclear build-up leads to hyperadenylation of host transcripts and subsequent degradation (Kumar and Glaunsinger, 2010).

This study highlighted that the nuclear build-up of PABPC observed in NIH/3T3 cells is a gradual process spread over the course of lytic infection and is relying on a functional muSOX protein. This provides evidence that unlike BGLF5 and ZEBRA (Park *et al.*, 2014) during EBV infection there are not multiple viral proteins in muSOX infection that elicit PABPC nuclear retention. Since PABPC is a nucleo-shuttling protein and is exported bound to mRNA (Burgess *et al.*, 2011) this suggests that PABPC nuclear retention could also be caused by a block in mRNA nuclear export. The mRNA nuclear export pathway that is used for a given transcript can be different depending on the specific transcript (Cheng *et al.*, 2006; Chi *et al.*, 2013; Carmody and Wente, 2009). The mRNA maturation and splicing requirements can also affect which export pathway is utilised (Chi *et al.*, 2013). Four different host transcripts containing either no or multiple splice junctions were tested for nuclear build-up during infection and no build-up was observed. This may be a result of the nuclear and cytoplasm fractionation process since the cytoplasmic fraction is likely to have RNA in excess compared to the nuclear fraction. It also may mean that retained host transcripts are reserved for a sub-set of host mRNAs or the retained mRNAs are quickly degraded. This study confirmed that host transcripts containing either no or many splice junctions are destabilised in the cytoplasm during lytic infection with MHV-68 only when muSOX protein is functional. The lack of RNA loss seen during MHV-68 ORF37stop infection was not the result of a poor infection since both MHV-68 and MHV-68 ORF37stop produced comparable levels of MHV-68 gpB mRNA in the nucleus and cytoplasm following infection of NIH/3T3 cells.

The build-up of RAE1 around the nuclear envelope is evident during MHV-68 infection with a functional muSOX gene but not without. Interestingly MHV-68 ORF10 is known to interact with RAE1 and Nup98 leading to a block in the nuclear export of a subset of mRNAs and their hyperadenylation (Gong *et al.*, 2016). MHV-68 muSOX has been previously shown to lead to a block in mRNA nuclear export and hyperadenylation (Kumar and Glaunsinger, 2010) so the possibility of muSOX interacting directly or indirectly with RAE1 is plausible. Further work could note the 686 different mRNA transcripts (genes) blocked from nuclear export by ORF10 expression (Gong *et al.*, 2016) (none of which were analysed for the purposes of the present study) and investigate their nuclear and cytoplasmic abundance following transfection of a muSOX expression plasmid. This will decipher if a similar subset of mRNA transcripts are inhibited from nuclear export following muSOX expression as those which are inhibited from nuclear export following ORF10 expression.

## **6.8 Evaluation of qRT-PCR data and subcellular fractionation method**

The fractionation process despite being performed by a commercial kit (QIAGEN, PARIS kit) and confirmed by western blot, is not believed to be absolute in terms of mRNA contamination between the cytoplasmic and nuclear fractions. Since there is usually a much higher concentration of mRNA in the cytoplasm of NIH/3T3 cells compared to the nucleus then any small contamination of the nuclear fraction with the cytoplasm fraction could confound results derived from the nuclear mRNA. Since spliced mRNA occurs in both the nucleus and cytoplasm it is difficult to test for contamination of the nuclear fraction with cytoplasmic mRNA. Results from the cytoplasmic mRNA are likely to be unaffected by the fractionation process. Results from the nuclear mRNA could be more reliable if new and more stringent fractionation processes are developed in the future.

## **6.9 Medical intervention for alphaviruses and gammaherpesviruses**

Alphaviruses have been utilised as vectors in the development of vaccines against a wide range of viruses including alphaviruses themselves (Lundstrom, 2014). The targeting of TTR-RBPs through antivirals could be an avenue for future research considering that many of the TTR-RBPs activities are controlled through phosphorylation or other post-translational events (Pullmann *et al.*, 2007; Abdelmohsen *et al.*, 2007). TTR-RBPs are however required for normal physiological functions of mammalian cells and are involved in developmental processes in mammals (Colombrita, Silani and Ratti, 2013), immune responses (Ogilvie *et al.*, 2009) and normal organ function (Pullmann and Rabb, 2014). TTR-RBPs KO cell lines (Al-Haj, Blackshear and Khabar, 2012) and conditional KO mice (Gubin *et al.*, 2014; Qiu, Stumpo and Blackshear, 2012) have been successfully manufactured suggesting that temporary inhibition of TTR-RBP function may be a feasible target for the development of novel antiviral drugs. The mechanisms through which viruses manipulate TTR-RBPs can also significantly

improve our knowledge on the functions of TTR-RBPs and how these are regulated. Given the role of TTR-RBPs in human cancers (Wang *et al.*, 2016; Young *et al.*, 2009), manipulation of their activities may prove useful in the development of cancer treatments.

## References

- Abdelmohsen, K., Pullmann, R., Lai, A., Kim, H. H., Galban, S., Yang, X. L., Blethrow, J. D., Walker, M., Shubert, J., Gillespie, D. A., Furneaux, H. and Gorospe, M. (2007) 'Phosphorylation of HuR by Chk2 regulates SIRT1 expression', *Molecular Cell*, 25(4), pp. 543-557.
- Ackermann, M. (2005) 'Virus in sheep's skin', *Schweizer Archiv Fur Tierheilkunde*, 147(4), pp. 155-164.
- Ackermann, M. (2006) 'Pathogenesis of gammaherpesvirus infections', *Veterinary Microbiology*, 113(3), pp. 211-222.
- Ahola, T., Lampio, A., Auvinen, P. and Kaariainen, L. (1999) 'Semliki Forest virus mRNA capping enzyme requires association with anionic membrane phospholipids for activity', *Embo Journal*, 18(11), pp. 3164-3172.
- Akhrymuk, I., Frolov, I. and Frolova, E. I. (2016) 'Both RIG-I and MDA5 detect alphavirus replication in concentration-dependent mode', *Virology*, 487, pp. 230-241.
- Akhrymuk, I., Kulemzin, S. V. and Frolova, E. I. (2012) 'Evasion of the Innate Immune Response: the Old World Alphavirus nsP2 Protein Induces Rapid Degradation of Rpb1, a Catalytic Subunit of RNA Polymerase II', *Journal of Virology*, 86(13), pp. 7180-7191.
- Akira, S. and Hemmi, H. (2003) 'Recognition of pathogen-associated molecular patterns by TLR family', *Immunology Letters*, 85(2), pp. 85-95.
- Al-Ahmadi, W., Al-Ghamdi, M., Al-Haj, L., Al-Saif, M. and Khabar, K. S. A. (2009a) 'Alternative polyadenylation variants of the RNA binding protein, HuR: abundance, role of AU-rich elements and auto-Regulation', *Nucleic Acids Research*, 37(11), pp. 3612-3624.
- Al-Ahmadi, W., Al-Haj, L., Al-Mohanna, F. A., Silverman, R. H. and Khabar, K. S. A. (2009b) 'RNase L downmodulation of the RNA-binding protein, HuR, and cellular growth', *Oncogene*, 28(15), pp. 1782-1791.
- Al-Haj, L., Blackshear, P. J. and Khabar, K. S. A. (2012) 'Regulation of p21/CIP1/WAF-1 mediated cell-cycle arrest by RNase L and tristetraprolin, and involvement of AU-rich elements', *Nucleic Acids Research*, 40(16), pp. 7739-7752.
- Ali, M. and Rayes-Danan, R. (2016) 'Multicentric Castleman Disease and Kaposi sarcoma: Two HHV8 diseases with different prognosis and treatment A case report and review of literature', *Hiv & Aids Review*, 15(3), pp. 127-130.
- Alvarez, E., Castello, A., Menendez-Arias, L. and Carrasco, L. (2006) 'HIV protease cleaves poly(A)-binding protein', *Biochemical Journal*, 396, pp. 219-226.
- Amaral, P. P., Dinger, M. E., Mercer, T. R. and Mattick, J. S. (2008) 'The eukaryotic genome as an RNA machine', *Science*, 319(5871), pp. 1787-1789.
- Arias, C., Weisburd, B., Stern-Ginossar, N., Mercier, A., Madrid, A. S., Bellare, P., Holdorf, M., Weissman, J. S. and Ganem, D. (2014) 'KSHV 2.0: A Comprehensive Annotation of the Kaposi's Sarcoma-Associated Herpesvirus Genome Using NextGeneration Sequencing Reveals Novel Genomic and Functional Features', *Plos Pathogens*, 10(1).
- Armstrong, P. M. and Andreadis, T. G. (2010) 'Eastern Equine Encephalitis Virus in Mosquitoes and Their Role as Bridge Vectors', *Emerging Infectious Diseases*, 16(12), pp. 1869-1874.
- Askjaer, P., Jensen, T. H., Nilsson, J., Englmeier, L. and Kjems, J. (1998) 'The specificity of the CRM1-Rev nuclear export signal interaction is mediated by RanGTP', *Journal of Biological Chemistry*, 273(50), pp. 33414-33422.
- Barnhart, M. D., Moon, S. L., Emch, A. W., Wilusz, C. J. and Wilusz, J. (2013) 'Changes in Cellular mRNA Stability, Splicing, and Polyadenylation through HuR Protein Sequestration by a Cytoplasmic RNA Virus', *Cell Reports*, 5(4), pp. 909-917.
- Barrett, L. W., Fletcher, S. and Wilton, S. D. (2012) 'Regulation of eukaryotic gene expression by the untranslated gene regions and other non-coding elements', *Cellular and Molecular Life Sciences*, 69(21), pp. 3613-3634.

Barry, G., Breakwell, L., Frangkoudis, R., Attarzadeh-Yazdi, G., Rodriguez-Andres, J., Kohl, A. and Fazakerley, J. K. (2009) 'PKR acts early in infection to suppress Semliki Forest virus production and strongly enhances the type I interferon response', *Journal of General Virology*, 90, pp. 1382-1391.

Bartlam, M. and Yamamoto, T. (2010) 'The structural basis for deadenylation by the CCR4-NOT complex', *Protein & Cell*, 1(5), pp. 443-452.

Beckham, J. D. and Tyler, K. L. (2015) 'Arbovirus infections', *Continuum (Minneapolis, Minn.)*, 21(6 Neuroinfectious Disease), pp. 1599.

Bhattacharyya, S. N., Habermacher, R., Martine, U., Closs, E. I. and Filipowicz, W. (2006) 'Stress-induced reversal of microRNA repression and mRNA P-body localization in human cells', *Cold Spring Harbor Symposia on Quantitative Biology*, 71, pp. 513-521.

Bildfell, R. J., Li, H., Alcantar, B. E., Cunha, C. W., Bradway, D. S. and Thomas, K. S. (2017) 'Alcelaphine gammaherpesvirus 1-induced malignant catarrhal fever in a Watusi (*Bos taurus africanus*) steer in a North American game park', *Journal of Veterinary Diagnostic Investigation*, 29(4), pp. 579-582.

Blakqori, G., van Knippenberg, I. and Elliott, R. M. (2009) 'Bunyamwera Orthobunyavirus S-Segment Untranslated Regions Mediate Poly(A) Tail-Independent Translation', *Journal of Virology*, 83(8), pp. 3637-3646.

Blaskovic, D., Stanceková, M., Svobodová, J. and Mistríková, J. (1981) *Isolation of five strains of herpesviruses from two species of free living small rodents.*

Blevins, M. B., Smith, A. M., Phillips, E. M. and Powers, M. A. (2003) 'Complex formation among the RNA export proteins Nup98, Rae1/Gle2, and TAP', *Journal of Biological Chemistry*, 278(23), pp. 20979-20988.

Bradish, C. J., Allner, K. and Maber, H. B. (1971) 'The Virulence of Original and Derived Strains of Semliki Forest Virus for Mice, Guinea-pigs and Rabbits', *Journal of General Virology*, 12(2), pp. 141-160.

Breakwell, L., Dosenovic, P., Hedestam, G. B. K., D'Amato, M., Liljestrom, P., Fazakerley, J. and McInerney, G. M. (2007) 'Semliki forest virus nonstructural protein 2 is involved in suppression of the type I interferon response', *Journal of Virology*, 81(16), pp. 8677-8684.

Brennan, C. M., Gallouzi, I. E. and Steitz, J. A. (2000) 'Protein ligands to HuR modulate its interaction with target mRNAs in vivo', *Journal of Cell Biology*, 151(1), pp. 1-13.

Brennan, C. M. and Steitz, J. A. (2001) 'HuR and mRNA stability', *Cellular and Molecular Life Sciences*, 58(2), pp. 266-277.

Brennan-Laun, S. E., Li, X.-L., Ezelle, H. J., Venkataraman, T., Blackshear, P. J., Wilson, G. M. and Hassel, B. A. (2014) 'RNase L Attenuates Mitogen-stimulated Gene Expression via Transcriptional and Post-transcriptional Mechanisms to Limit the Proliferative Response', *Journal of Biological Chemistry*, 289(48), pp. 33629-33643.

Buchan, J. R. and Parker, R. (2009) 'Eukaryotic Stress Granules: The Ins and Outs of Translation', *Molecular Cell*, 36(6), pp. 932-941.

Burgess, H. M., Richardson, W. A., Anderson, R. C., Salaun, C., Graham, S. V. and Gray, N. K. (2011) 'Nuclear relocalisation of cytoplasmic poly(A)-binding proteins PABP1 and PABP4 in response to UV irradiation reveals mRNA-dependent export of metazoan PABPs', *Journal of Cell Science*, 124(19), pp. 3344-3355.

Cannon, M. (2007) 'The KSHV and other human herpesviral G protein-coupled receptors', *Kaposi Sarcoma Herpesvirus: New Perspectives*, 312, pp. 137-156.

Carel, J. C., Myones, B. L., Frazier, B. and Holers, V. M. (1990) 'Structural requirements for epstein-barr-virus receptor (cr-2 cd21) ligand-binding, internalization, and viral-infection', *Journal of Biological Chemistry*, 265(21), pp. 12293-12299.

Carey, B. D., Bakovic, A., Callahan, V., Narayanan, A. and Kehn-Hall, K. (2019) 'New World alphavirus protein interactomes from a therapeutic perspective', *Antiviral Research*, 163, pp. 125-139.

Carmody, S. R. and Wenthe, S. R. (2009) 'mRNA nuclear export at a glance', *Journal of Cell Science*, 122(12), pp. 1933-1937.

- Casamassimi, A. and Napoli, C. (2007) 'Mediator complexes and eukaryotic transcription regulation: An overview', *Biochimie*, 89(12), pp. 1439-1446.
- Chang, Y. F., Imam, J. S. and Wilkinson, M. E. (2007) 'The nonsense-mediated decay RNA surveillance pathway', *Annual Review of Biochemistry Annual Review of Biochemistry*. Palo Alto: Annual Reviews, pp. 51-74.
- Chawla-Sarkar, M., Lindner, D. J., Liu, Y. F., Williams, B., Sen, G. C., Silverman, R. H. and Borden, E. C. (2003) 'Apoptosis and interferons: Role of interferon-stimulated genes as mediators of apoptosis', *Apoptosis*, 8(3), pp. 237-249.
- Chen, C. Y. A. and Shyu, A. B. (2011) 'Mechanisms of deadenylation-dependent decay', *Wiley Interdisciplinary Reviews-Rna*, 2(2), pp. 167-183.
- Chen, L. H., Wang, M., Zhu, D. J., Sun, Z. Z., Ma, J., Wang, J. L., Kong, L. F., Wang, S. D., Liu, Z. A., Wei, L. L., He, Y. W., Wang, J. F. and Zhang, X. Z. (2018) 'Implication for alphavirus host-cell entry and assembly indicated by a 3.5 angstrom resolution cryo-EM structure', *Nature Communications*, 9, pp. 8.
- Cheng, H., Dufu, K., Lee, C. S., Hsu, J. L., Dias, A. and Reed, R. (2006) 'Human mRNA export machinery recruited to the 5' end of mRNA', *Cell*, 127(7), pp. 1389-1400.
- Chi, B. K., Wang, Q. L., Wu, G. F., Tan, M., Wang, L. T., Shi, M., Chang, X. Y. and Cheng, H. (2013) 'Aly and THO are required for assembly of the human TREX complex and association of TREX components with the spliced mRNA', *Nucleic Acids Research*, 41(2), pp. 1294-1306.
- Chirico, N., Vianelli, A. and Belshaw, R. (2010) 'Why genes overlap in viruses', *Proceedings of the Royal Society B-Biological Sciences*, 277(1701), pp. 3809-3817.
- Chitimia-Dobler, L., Lemhofer, G., Krol, N., Bestehorn, M., Dobler, G. and Pfeffer, M. (2019) 'Repeated isolation of tick-borne encephalitis virus from adult Dermacentor reticulatus ticks in an endemic area in Germany', *Parasites & Vectors*, 12.
- Clement, M. and Humphreys, I. R. (2019) 'Cytokine-Mediated Induction and Regulation of Tissue Damage During Cytomegalovirus Infection', *Frontiers in Immunology*, 10.
- Clyde, K. and Glaunsinger, B. A. (2011) 'Deep Sequencing Reveals Direct Targets of Gammaherpesvirus-Induced mRNA Decay and Suggests That Multiple Mechanisms Govern Cellular Transcript Escape', *Plos One*, 6(5).
- Coller, J. and Parker, R. (2004) 'Eukaryotic mRNA decapping', *Annual Review of Biochemistry*, 73, pp. 861-890.
- Colombrita, C., Silani, V. and Ratti, A. (2013) 'ELAV proteins along evolution: Back to the nucleus?', *Molecular and Cellular Neuroscience*, 56, pp. 447-455.
- Conrad, N. K., Shu, M. D., Uyhazi, K. E. and Steitz, J. A. (2007) 'Mutational analysis of a viral RNA element that counteracts rapid RNA decay by interaction with the polyadenylate tail', *Proceedings of the National Academy of Sciences of the United States of America*, 104(25), pp. 10412-10417.
- Covarrubias, S., Richner, J. M., Clyde, K., Lee, Y. J. and Glaunsinger, B. A. (2009) 'Host Shutoff Is a Conserved Phenotype of Gammaherpesvirus Infection and Is Orchestrated Exclusively from the Cytoplasm', *Journal of Virology*, 83(18), pp. 9554-9566.
- Cross, R. K. (1983) 'Identification of a unique guanine-7-methyltransferase in Semliki Forest virus (SFV) infected cell-extracts', *Virology*, 130(2), pp. 452-463.
- de Cedron, M. G., Ehsani, N., Mikkola, M. L., Garcia, J. A. and Kaariainen, L. (1999) 'RNA helicase activity of Semliki Forest virus replicase protein NSP2', *Febs Letters*, 448(1), pp. 19-22.
- de Mello, C. P. P., Bloom, D. C. and Paixao, I. (2016) 'Herpes simplex virus type-1: replication, latency, reactivation and its antiviral targets', *Antiviral Therapy*, 21(4), pp. 277-286.
- De Tulleo, L. and Kirchhausen, T. (1998) 'The clathrin endocytic pathway in viral infection', *Embo Journal*, 17(16), pp. 4585-4593.
- Dean, J. L. E., Sully, G., Clark, A. R. and Saklatvala, J. (2004) 'The involvement of AU-rich element-binding proteins in p38 mitogen-activated protein kinase pathway-mediated mRNA stabilisation', *Cellular Signalling*, 16(10), pp. 1113-1121.



- Delaleau, M. and Borden, K. L. (2015) 'Multiple export mechanisms for mRNAs', *Cells*, 4(3), pp. 452-473.
- Deuber, S. A. and Pavlovic, J. (2007) 'Virulence of a mouse-adapted Semliki Forest virus strain is associated with reduced susceptibility to interferon', *Journal of General Virology*, 88, pp. 1952-1959.
- Dickson, A. M., Anderson, J. R., Barnhart, M. D., Sokoloski, K. J., Oko, L., Opyrchal, M., Galanis, E., Wilusz, C. J., Morrison, T. E. and Wilusz, J. (2012) 'Dephosphorylation of HuR Protein during Alphavirus Infection Is Associated with HuR Relocalization to the Cytoplasm', *Journal of Biological Chemistry*, 287(43), pp. 36229-36238.
- Dobrikova, E., Shveygert, M., Walters, R. and Gromeier, M. (2010) 'Herpes Simplex Virus Proteins ICP27 and UL47 Associate with Polyadenylate-Binding Protein and Control Its Subcellular Distribution', *Journal of Virology*, 84(1), pp. 270-279.
- Dormoy-Raclet, V., Menard, I., Clair, E., Kurban, G., Mazroui, R., Di Marco, S., von Roretz, C., Pause, A. and Gallouzi, I. E. (2007) 'The RNA-binding protein HuR promotes cell migration and cell invasion by stabilizing the beta-actin mRNA in a U-rich-element-dependent manner', *Molecular and Cellular Biology*, 27(15), pp. 5365-5380.
- Ebrahimi, B., Dutia, B. M., Roberts, K. L., Garcia-Ramirez, J. J., Dickinson, P., Stewart, J. P., Ghazal, P., Roy, D. J. and Nash, A. A. (2003) 'Transcriptome profile of murine gammaherpesvirus-68 lytic infection', *Journal of General Virology*, 84, pp. 99-109.
- Eckmann, C. R., Rammelt, C. and Wahle, E. (2011) 'Control of poly(A) tail length', *Wiley Interdisciplinary Reviews-Rna*, 2(3), pp. 348-361.
- Enquist, L. W., Husak, P. J., Banfield, B. W. and Smith, G. A. (1999) 'Infection and spread of alphaherpesviruses in the nervous system', *Advances in Virus Research*, Vol 51, 51, pp. 237-347.
- Fabian, M. R., Cieplak, M. K., Frank, F., Morita, M., Green, J., Srikumar, T., Nagar, B., Yamamoto, T., Raught, B., Duchaine, T. F. and Sonenberg, N. (2012) 'miRNA-mediated deadenylation is orchestrated by GW182 through two conserved motifs that interact with CCR4-NOT (vol 18, pg 1211, 2011)', *Nature Structural & Molecular Biology*, 19(3), pp. 365-365.
- Fabian, M. R., Frank, F., Rouya, C., Siddiqui, N., Lai, W. S., Karetnikov, A., Blackshear, P. J., Nagar, B. and Sonenberg, N. (2013) 'Structural basis for the recruitment of the human CCR4-NOT deadenylase complex by tristetraprolin', *Nature Structural & Molecular Biology*, 20(6), pp. 735-+.
- Fan, X. H. C. and Steitz, J. A. (1998) 'Overexpression of HuR, a nuclear-cytoplasmic shuttling protein, increases the *in vivo* stability of ARE-containing mRNAs', *Embo Journal*, 17(12), pp. 3448-3460.
- Faria, P. A., Chakraborty, P., Levay, A., Barber, G. N., Ezelle, H. J., Enninga, J., Arana, C., van Deursen, J. and Fontoura, B. M. A. (2005) 'VSV disrupts the Rae1/mrnp41 mRNA nuclear export pathway', *Molecular Cell*, 17(1), pp. 93-102.
- Fayzuln, R. and Frolov, I. (2004) 'Changes of the secondary structure of the 5' end of the Sindbis virus genome inhibit virus growth in mosquito cells and lead to accumulation of adaptive mutations', *Journal of Virology*, 78(10), pp. 4953-4964.
- Fazakerley, J. K., Cotterill, C. L., Lee, G. and Graham, A. (2006) 'Virus tropism, distribution, persistence and pathology in the corpus callosum of the Semliki Forest virus-infected mouse brain: a novel system to study virus-oligodendrocyte interactions', *Neuropathology and Applied Neurobiology*, 32(4), pp. 397-409.
- Fazakerley, J. K., Pathak, S., Scallan, M., Amor, S. and Dyson, H. (1993) 'Replication of the A7(74) strain of Semliki Forest virus is restricted in neurons', *Virology*, 195(2), pp. 627-637.
- Feng, X. M., Huo, X., Tang, B., Tang, S. Y., Wang, K. and Wu, J. H. (2019) 'Modelling and Analyzing Virus Mutation Dynamics of Chikungunya Outbreaks', *Scientific Reports*, 9, pp. 15.
- Ferreira-de-Lima, V. H. and Lima-Camara, T. N. (2018) 'Natural vertical transmission of dengue virus in *Aedes aegypti* and *Aedes albopictus*: a systematic review', *Parasites & Vectors*, 11, pp. 8.
- Firth, A. E., Chung, B. Y. W., Fleeton, M. N. and Atkins, J. F. (2008) 'Discovery of frameshifting in Alphavirus 6K resolves a 20-year enigma', *Virology Journal*, 5.
- Flemington, E. K. (2001) 'Herpesvirus lytic replication and the cell cycle: Arresting new developments', *Journal of Virology*, 75(10), pp. 4475-4481.

Fortuna, C., Toma, L., Remoli, M. E., Amendola, A., Severini, F., Boccolini, D., Romi, R., Venturi, G., Rezza, G. and Di Luca, M. (2018) 'Vector competence of *Aedes albopictus* for the Indian Ocean lineage (IOL) chikungunya viruses of the 2007 and 2017 outbreaks in Italy: a comparison between strains with and without the E1:A226V mutation', *Eurosurveillance*, 23(22), pp. 6-10.

Fragkoudis, R., Breakwell, L., McKimmie, C., Boyd, A., Barry, G., Kohl, A., Merits, A. and Fazakerley, J. K. (2007) 'The type I interferon system protects mice from Semliki Forest virus by preventing widespread virus dissemination in extraneural tissues, but does not mediate the restricted replication of avirulent virus in central nervous system neurons', *Journal of General Virology*, 88(12), pp. 3373-3384.

Fragkoudis, R., Chi, Y., Siu, R. W. C., Barry, G., Attarzadeh-Yazdi, G., Merits, A., Nash, A. A., Fazakerley, J. K. and Kohl, A. (2008) 'Semliki Forest virus strongly reduces mosquito host defence signaling', *Insect Molecular Biology*, 17(6), pp. 647-656.

Frolov, I., Hardy, R. and Rice, C. M. (2001) 'Cis-acting RNA elements at the 5' end of Sindbis virus genome RNA regulate minus- and plus-strand RNA synthesis', *Rna-a Publication of the Rna Society*, 7(11), pp. 1638-1651.

Frolova, E. I., Gorchakov, R., Pereboeva, L., Atasheva, S. and Frolov, I. (2010) 'Functional Sindbis Virus Replicative Complexes Are Formed at the Plasma Membrane', *Journal of Virology*, 84(22), pp. 11679-11695.

Fros, J. J., Domeradzka, N. E., Baggen, J., Geertsema, C., Flipse, J., Vlak, J. M. and Pijlman, G. P. (2012) 'Chikungunya Virus nsP3 Blocks Stress Granule Assembly by Recruitment of G3BP into Cytoplasmic Foci', *Journal of Virology*, 86(19), pp. 10873-10879.

Fuentes-Panana, E. M., Peng, R. S., Brewer, G., Tan, J. and Ling, P. D. (2000) 'Regulation of the Epstein-Barr virus C promoter by AUF1 and the cyclic AMP/protein kinase A signaling pathway', *Journal of Virology*, 74(17), pp. 8166-8175.

Galban, S., Kuwano, Y., Pullmann, R., Martindale, J. L., Kim, H. H., Lal, A., Abdelmohsen, K., Yang, X. L., Dang, Y. J., Liu, J. O., Lewis, S. M., Holcik, M. and Gorospe, M. (2008) 'RNA-Binding proteins HuR and PTB promote the translation of hypoxia-inducible factor 1 alpha', *Molecular and Cellular Biology*, 28(1), pp. 93-107.

George, J. and Raju, R. (2000) 'Alphavirus RNA genome repair and evolution: Molecular characterization of infectious sindbis virus isolates lacking a known conserved motif at the 3' end of the genome', *Journal of Virology*, 74(20), pp. 9776-9785.

Gibbons, D. L., Vaney, M. C., Roussel, A., Vigouroux, A., Reilly, B., Lepault, J., Kielian, M. and Rey, F. A. (2004) 'Conformational change and protein protein interactions of the fusion protein of Semliki Forest virus', *Nature*, 427(6972), pp. 320-325.

Glasgow, G. M., Sheahan, B. J., Atkins, G. J., Wahlberg, J. M., Salminen, A. and Lilieström, P. (1991) 'Two mutations in the envelope glycoprotein E2 of semliki forest virus affecting the maturation and entry patterns of the virus alter pathogenicity for mice', *Virology*, 185(2), pp. 741-748.

Glaunsinger, B., Chavez, L. and Ganem, D. (2005) 'The exonuclease and host shutoff functions of the SOX protein of Kaposi's sarcoma-associated herpesvirus are genetically separable', *Journal of Virology*, 79(12), pp. 7396-7401.

Glaunsinger, B. and Ganem, D. (2004) 'Lytic KSHV infection inhibits host gene expression by accelerating global mRNA turnover', *Molecular Cell*, 13(5), pp. 713-723.

Gong, D. Y., Kim, Y. H., Xiao, Y. C., Du, Y. S., Xie, Y. F., Lee, K. K., Feng, J., Farhat, N., Zhao, D. W., Shu, S., Dai, X. H., Chanda, S. K., Rana, T. M., Krogan, N. J., Sun, R. and Wu, T. T. (2016) 'A Herpesvirus Protein Selectively Inhibits Cellular mRNA Nuclear Export', *Cell Host & Microbe*, 20(5), pp. 642-653.

Gonzalez-Navajas, J. M., Lee, J., David, M. and Raz, E. (2012) 'Immunomodulatory functions of type I interferons', *Nature Reviews Immunology*, 12(2), pp. 125-135.

Gorchakov, R., Frolova, E., Sawicki, S., Atasheva, S., Sawicki, D. and Frolov, I. (2008) 'A new role for ns polyprotein cleavage in Sindbis virus replication', *Journal of Virology*, 82(13), pp. 6218-6231.

Goss, D. J. and Kleiman, F. E. (2013) 'Poly(A) binding proteins: are they all created equal?', *Wiley Interdisciplinary Reviews-Rna*, 4(2), pp. 167-179.

- Gotte, B., Liu, L. and McInerney, G. M. (2018) 'The Enigmatic Alphavirus Non-Structural Protein 3 (nsP3) Revealing Its Secrets at Last', *Viruses-Basel*, 10(3).
- Gratacos, F. M. and Brewer, G. (2010) 'The role of AUF1 in regulated mRNA decay', *Wiley Interdisciplinary Reviews-Rna*, 1(3), pp. 457-473.
- Gubin, M. M., Techasintana, P., Magee, J. D., Dahm, G. M., Calaluze, R., Martindale, J. L., Whitney, M. S., Franklin, C. L., Besch-Williford, C., Hollingsworth, J. W., Abdelmohsen, K., Gorospe, M. and Atasoy, U. (2014) 'Conditional Knockout of the RNA-Binding Protein HuR in CD4(+) T Cells Reveals a Gene Dosage Effect on Cytokine Production', *Molecular Medicine*, 20, pp. 93-108.
- Gui, H. X., Lu, C. W., Adams, S., Stollar, V. and Li, M. L. (2010) 'hnRNP A1 interacts with the genomic and subgenomic RNA promoters of Sindbis virus and is required for the synthesis of G and SG RNA', *Journal of Biomedical Science*, 17.
- Hahn, Y. S., Strauss, E. G. and Strauss, J. H. (1989) 'Mapping of RNA- temperature-sensitive mutants of Sindbis virus - assignment of complementation group-A, group-B, and group-G to nonstructural proteins', *Journal of Virology*, 63(7), pp. 3142-3150.
- Harb, M., Becker, M. M., Vitour, D., Baron, C. H., Vende, P., Brown, S. C., Bolte, S., Arold, S. T. and Poncet, D. (2008) 'Nuclear Localization of Cytoplasmic Poly(A)-Binding Protein upon Rotavirus Infection Involves the Interaction of NSP3 with eIF4G and RoXaN', *Journal of Virology*, 82(22), pp. 11283-11293.
- Hardy, R. W. and Rice, C. M. (2005) 'Requirements at the 3' end of the Sindbis virus genome for efficient synthesis of minus-strand RNA', *Journal of Virology*, 79(8), pp. 4630-4639.
- Herdy, B., Karonitsch, T., Vladimer, G. I., Tan, C. S. H., Stukalov, A., Trefzer, C., Bigenzahn, J. W., Theil, T., Holinka, J., Kiener, H. P., Colinge, J., Bennett, K. L. and Superti-Furga, G. (2015) 'The RNA-binding protein HuR/ELAVL1 regulates IFN-beta mRNA abundance and the type I IFN response', *European Journal of Immunology*, 45(5), pp. 1500-1511.
- Hernandez, R., Luo, T. C. and Brown, D. T. (2001) 'Exposure to low pH is not required for penetration of mosquito cells by Sindbis virus', *Journal of Virology*, 75(4), pp. 2010-2013.
- Herrero, L. J., Taylor, A., Foo, S. S., Roberts, L., Ketheesan, N. and Mahalingam, S. (2016) 'Clinical Manifestations of Arthritogenic Alphaviruses', in Mahalingam, S., Herrero, L.J. and Herring, B.L. (eds.) *Alphaviruses: Current Biology*. Wymondham: Caister Academic Press, pp. 125-137.
- Higuera, A. and Ramirez, J. D. (2019) 'Molecular epidemiology of dengue, yellow fever, Zika and Chikungunya arboviruses: An update', *Acta Tropica*, 190, pp. 99-111.
- Hill, K. R., Hajjou, M., Hu, J. Y. and Raju, R. (1997) 'RNA-RNA recombination in Sindbis virus: Roles of the 3' conserved motif, poly(A) tail, and nonviral sequences of template RNAs in polymerase recognition and template switching', *Journal of Virology*, 71(4), pp. 2693-2704.
- Houseley, J., LaCava, J. and Tollervey, D. (2006) 'RNA-quality control by the exosome', *Nature Reviews Molecular Cell Biology*, 7(7), pp. 529-539.
- Houseley, J. and Tollervey, D. (2009) 'The Many Pathways of RNA Degradation', *Cell*, 136(4), pp. 763-776.
- Hughes, D. J., Kipar, A., Sample, J. T. and Stewart, J. P. (2010) 'Pathogenesis of a Model Gammaherpesvirus in a Natural Host', *Journal of Virology*, 84(8), pp. 3949-3961.
- Hutin, S., Lee, Y. and Glaunsinger, B. A. (2013) 'An RNA Element in Human Interleukin 6 Confers Escape from Degradation by the Gammaherpesvirus SOX Protein', *Journal of Virology*, 87(8), pp. 4672-4682.
- Hyde, J. L., Chen, R. B., Trobaugh, D. W., Diamond, M. S., Weaver, S. C., Klimstra, W. B. and Wilusz, J. (2015) 'The 5' and 3' ends of alphavirus RNAs - Non-coding is not non-functional', *Virus Research*, 206, pp. 99-107.
- Ilkow, C. S., Mancinelli, V., Beatch, M. D. and Hobman, T. C. (2008) 'Rubella virus capsid protein interacts with poly(A)-binding protein and inhibits translation', *Journal of Virology*, 82(9), pp. 4284-4294.

Ingelfinger, D., Arndt-Jovin, D. J., Luhrmann, R. and Achsel, T. (2002) 'The human LSm1-7 proteins colocalize with the mRNA-degrading enzymes Dcp1/2 and Xrn1 in distinct cytoplasmic foci', *Rna-a Publication of the Rna Society*, 8(12), pp. 1489-1501.

Izquierdo, J. M. (2008) 'Hu antigen R (HuR) functions as an alternative pre-mRNA splicing regulator of Fas apoptosis-promoting receptor on exon definition', *Journal of Biological Chemistry*, 283(27), pp. 19077-19084.

Jackson, B. R., Boyne, J. R., Noerenberg, M., Taylor, A., Hautbergue, G. M., Walsh, M. J., Wheat, R., Blackbourn, D. J., Wilson, S. A. and Whitehouse, A. (2011) 'An Interaction between KSHV ORF57 and UIF Provides mRNA-Adaptor Redundancy in Herpesvirus Intronless mRNA Export', *Plos Pathogens*, 7(7).

Jehung, J. P., Kitamura, T., Yanagawa-Matsuda, A., Kuroshima, T., Towfik, A., Yasuda, M., Sano, H., Kitagawa, Y., Minowa, K., Shindoh, M. and Higashino, F. (2018) 'Adenovirus infection induces HuR relocalization to facilitate virus replication', *Biochemical and Biophysical Research Communications*, 495(2), pp. 1795-1800.

Jones, J. E., Long, K. M., Whitmore, A. C., Sanders, W., Thurlow, L. R., Brown, J. A., Morrison, C. R., Vincent, H., Peck, K. M., Browning, C., Moorman, N., Lim, J. K. and Heise, M. T. (2017) 'Disruption of the Opal Stop Codon Attenuates Chikungunya Virus-Induced Arthritis and Pathology', *Mbio*, 8(6).

Jose, J., Snyder, J. E. and Kuhn, R. J. (2009) 'A structural and functional perspective of alphavirus replication and assembly', *Future Microbiology*, 4(7), pp. 837-856.

Joseph, R., Srivastava, O. P. and Pfister, R. R. (2014) 'Downregulation of beta-actin and its regulatory gene HuR affect cell migration of human corneal fibroblasts', *Molecular Vision*, 20, pp. 593-605.

Joshi, S., Kaur, S., Kroczyńska, B. and Plataniás, L. C. (2010) 'Mechanisms of mRNA translation of interferon stimulated genes', *Cytokine*, 52(1-2), pp. 123-127.

Kallio, K., Hellstrom, K., Jokitalo, E. and Ahola, T. (2016) 'RNA Replication and Membrane Modification Require the Same Functions of Alphavirus Nonstructural Proteins', *Journal of Virology*, 90(3), pp. 1687-1692.

Karlsson, G. B. and Liljeström, P. (2004) 'Delivery and expression of heterologous genes in mammalian cells using self-replicating alphavirus vectors', *Gene Delivery to Mammalian Cells: Volume 2: Viral Gene Transfer Techniques*, pp. 543-557.

Kedar, V. P., Zucconi, B. E., Wilson, G. M. and Blackshear, P. J. (2012) 'Direct Binding of Specific AUF1 Isoforms to Tandem Zinc Finger Domains of Tristetraprolin (TTP) Family Proteins', *Journal of Biological Chemistry*, 287(8), pp. 5459-5471.

Kemenesi, G. and Banyai, K. (2019) 'Tick-Borne Flaviviruses, with a Focus on Powassan Virus', *Clinical Microbiology Reviews*, 32(1), pp. 29.

Kempf, B. J. and Barton, D. J. (2008) 'Poly(rC) binding proteins and the 5' cloverleaf of uncapped poliovirus mRNA function during de novo assembly of polysomes', *Journal of Virology*, 82(12), pp. 5835-5846.

Kenney, J. L., Adams, A. P. and Weaver, S. C. (2010) 'Transmission Potential of Two Chimeric Western Equine Encephalitis Vaccine Candidates in *Culex tarsalis*', *American Journal of Tropical Medicine and Hygiene*, 82(2), pp. 354-359.

Khalaj, K., Ahn, S. H., Bidarimath, M., Nasirzadeh, Y., Singh, S. S., Fazleabas, A. T., Young, S. L., Lessey, B. A., Koti, M. and Tayade, C. (2017) 'A balancing act: RNA binding protein HuR/TTP axis in endometriosis patients', *Scientific Reports*, 7.

Kielian, M. and Rey, F. A. (2006) 'Virus membrane-fusion proteins: more than one way to make a hairpin', *Nature Reviews Microbiology*, 4(1), pp. 67-76.

Kiiver, K., Tagen, I., Zusinaite, E., Tamberg, N., Fazakerley, J. K. and Merits, A. (2008) 'Properties of non-structural protein 1 of Semliki Forest virus and its interference with virus replication', *Journal of General Virology*, 89, pp. 1457-1466.

Kim, H. H. and Gorospe, M. (2008) 'Phosphorylated HuR shuttles in cycles', *Cell Cycle*, 7(20), pp. 3124-3126.

- Kim, H. H., Kuwano, Y., Srikantan, S., Lee, E. K., Martindale, J. L. and Gorospe, M. (2009) 'HuR recruits let-7/RISC to repress c-Myc expression', *Genes & Development*, 23(15), pp. 1743-1748.
- Kim, K. H., Rumenapf, T., Strauss, E. G. and Strauss, J. H. (2004) 'Regulation of Semliki Forest virus RNA replication: a model for the control of alphavirus pathogenesis in invertebrate hosts', *Virology*, 323(1), pp. 153-163.
- Kimura, T., Hashimoto, I., Nagase, T. and Fujisawa, J. I. (2004) 'CRM1-dependent, but not ARE-mediated, nuclear export of IFN- $\alpha$  I mRNA', *Journal of Cell Science*, 117(11), pp. 2259-2270.
- Kishore, S., Lubner, S. and Zavolan, M. (2010) 'Deciphering the role of RNA-binding proteins in the post-transcriptional control of gene expression', *Briefings in Functional Genomics*, 9(5-6), pp. 391-404.
- Koonin E.V., Dolja V.V., Krupovic M. (2015) 'Origins and evolution of viruses of eukaryotes: The ultimate modularity', *Virology*, 25(2), pp. 479-480.
- Kuhn, R. J., Hong, Z. and Strauss, J. H. (1990) 'Mutagenesis of the 3' nontranslated region of Sindbis virus-RNA', *Journal of Virology*, 64(4), pp. 1465-1476.
- Kujala, P., Ikaheimonen, A., Ehsani, N., Vihinen, H., Auvinen, P. and Kaariainen, L. (2001) 'Biogenesis of the Semliki Forest virus RNA replication complex', *Journal of Virology*, 75(8), pp. 3873-3884.
- Kumar, B. and Chandran, B. (2016) 'KSHV Entry and Trafficking in Target Cells Hijacking of Cell Signal Pathways, Actin and Membrane Dynamics', *Viruses-Basel*, 8(11).
- Kumar, G. R. and Glaunsinger, B. A. (2010) 'Nuclear Import of Cytoplasmic Poly(A) Binding Protein Restricts Gene Expression via Hyperadenylation and Nuclear Retention of mRNA', *Molecular and Cellular Biology*, 30(21), pp. 4996-5008.
- Kumar, G. R., Shum, L. and Glaunsinger, B. A. (2011) 'Importin  $\alpha$ -Mediated Nuclear Import of Cytoplasmic Poly(A) Binding Protein Occurs as a Direct Consequence of Cytoplasmic mRNA Depletion', *Molecular and Cellular Biology*, 31(15), pp. 3113-3125.
- Kuno, G. (2001) 'Transmission of arboviruses without involvement of arthropod vectors', *Acta Virologica*, 45(3), pp. 139-150.
- Kuno, G. and Chang, G. J. J. (2005) 'Biological transmission of arboviruses: Reexamination of and new insights into components, mechanisms, and unique traits as well as their evolutionary trends', *Clinical Microbiology Reviews*, 18(4), pp. 608-+.
- Kuyumcu-Martinez, M., Belliot, G., Sosnovtsev, S. V., Chang, K. O., Green, K. Y. and Lloyd, R. E. (2004) 'Calicivirus 3C-like proteinase inhibits cellular translation by cleavage of poly(A)-binding protein', *Journal of Virology*, 78(15), pp. 8172-8182.
- Lai, W. S., Carballo, E., Strum, J. R., Kennington, E. A., Phillips, R. S. and Blackshear, P. J. (1999) 'Evidence that tristetraprolin binds to AU-rich elements and promotes the deadenylation and destabilization of tumor necrosis factor  $\alpha$  mRNA', *Molecular and Cellular Biology*, 19(6), pp. 4311-4323.
- Lal, A., Mazan-Mamczarz, K., Kawai, T., Yang, X. L., Martindale, J. L. and Gorospe, M. (2004) 'Concurrent versus individual binding of HuR and AUF1 to common labile target mRNAs', *Embo Journal*, 23(15), pp. 3092-3102.
- Lastarza, M. W., Grakoui, A. and Rice, C. M. (1994) 'Deletion and duplication mutations in the c-terminal nonconserved region of Sindbis virus nsP3 - effects on phosphorylation and on virus-replication in vertebrate and invertebrate cells', *Virology*, 202(1), pp. 224-232.
- Lee, T. I. and Young, R. A. (2000) 'Transcription of eukaryotic protein-coding genes', *Annual Review of Genetics*, 34, pp. 77-137.
- Lee, Y. J. and Glaunsinger, B. A. (2009) 'Aberrant Herpesvirus-Induced Polyadenylation Correlates With Cellular Messenger RNA Destruction', *Plos Biology*, 7(5), pp. 16.
- Lemm, J. A., Bergqvist, A., Read, C. M. and Rice, C. M. (1998) 'Template-dependent initiation of Sindbis virus RNA replication in vitro', *Journal of Virology*, 72(8), pp. 6546-6553.
- Levis, R., Schlesinger, S. and Huang, H. V. (1990) 'Promoter for Sindbis virus RNA-dependent subgenomic RNA-transcription', *Journal of Virology*, 64(4), pp. 1726-1733.

- Li, L., Jose, J., Xiang, Y., Kuhn, R. J. and Rossmann, M. G. (2010) 'Structural changes of envelope proteins during alphavirus fusion', *Nature*, 468(7324), pp. 705-U131.
- Li, X. L., Andersen, J. B., Ezelle, H. J., Wilson, G. M. and Hassel, B. A. (2007) 'Post-transcriptional regulation of RNase-L expression is mediated by the 3'-untranslated region of its mRNA', *Journal of Biological Chemistry*, 282(11), pp. 7950-7960.
- Liljestrom, P. and Garoff, H. (1991) 'A new generation of animal-cell expression vectors based on the Semliki Forest virus replicon', *Bio-Technology*, 9(12), pp. 1356-1361.
- Lim, E. X. Y., Lee, W. S., Madzokere, E. T. and Herrero, L. J. (2018) 'Mosquitoes as Suitable Vectors for Alphaviruses', *Viruses-Basel*, 10(2).
- Lin, J. Y., Shih, S. R., Pan, M. J., Li, C., Lue, C. F., Stollar, V. and Li, M. L. (2009) 'hnRNP A1 Interacts with the 5' Untranslated Regions of Enterovirus 71 and Sindbis Virus RNA and Is Required for Viral Replication', *Journal of Virology*, 83(12), pp. 6106-6114.
- Lindsey, N. P., Staples, J. E. and Fischer, M. (2018) 'Eastern Equine Encephalitis Virus in the United States, 2003-2016', *American Journal of Tropical Medicine and Hygiene*, 98(5), pp. 1472-1477.
- Linger, B. R., Kunovska, L., Kuhn, R. J. and Golden, B. L. (2004) 'Sindbis virus nucleocapsid assembly: RNA folding promotes capsid protein dimerization', *Rna-a Publication of the Rna Society*, 10(1), pp. 128-138.
- Liu, C. C. and Wu, S. C. (2004) 'Mosquito and mammalian cells grown on microcarriers for four-serotype dengue virus production: Variations in virus titer, plaque morphology, and replication rate', *Biotechnology and Bioengineering*, 85(5), pp. 482-488.
- Liu, F. Y. and Zhou, Z. H. (2007) 'Comparative virion structures of human herpesviruses', *Human Herpesviruses: Biology, Therapy, and Immunoprophylaxis*, pp. 27-43.
- Loewy, A., Smyth, J., Vonbonsdorff, C. H., Liljestrom, P. and Schlesinger, M. J. (1995) 'The 6-kilodalton membrane-protein of Semliki Forest virus is involved in the budding process', *Journal of Virology*, 69(1), pp. 469-475.
- Luna, R. E., Zhou, F. C., Baghian, A., Chouljenko, V., Forghani, B., Gao, S. J. and Kousoulas, K. G. (2004) 'Kaposi's sarcoma-associated herpesvirus glycoprotein K8.1 is dispensable for virus entry', *Journal of Virology*, 78(12), pp. 6389-6398.
- Lundstrom, K. (2014) 'Alphavirus-Based Vaccines', *Viruses-Basel*, 6(6), pp. 2392-2415.
- Lusa, S., Garoff, H. and Liljestrom, P. (1991) 'Fate of the 6k membrane-protein of Semliki Forest virus during virus assembly', *Virology*, 185(2), pp. 843-846.
- Ma, W. J., Cheng, S., Campbell, C., Wright, A. and Furneaux, H. (1996) 'Cloning and characterization of HuR, a ubiquitously expressed Elav-like protein', *Journal of Biological Chemistry*, 271(14), pp. 8144-8151.
- Magalhaes, T., Foy, B. D., Marques, E. T. A., Ebel, G. D. and Weger-Lucarelli, J. (2018) 'Mosquito-borne and sexual transmission of Zika virus: Recent developments and future directions', *Virus Research*, 254, pp. 1-9.
- Majerciak, V. and Zheng, Z. M. (2016) 'Alternative RNA splicing of KSHV ORF57 produces two different RNA isoforms', *Virology*, 488, pp. 81-87.
- Mangus, D. A., Evans, M. C. and Jacobson, A. (2003) 'Poly(A)-binding proteins: multifunctional scaffolds for the post-transcriptional control of gene expression', *Genome Biology*, 4(7), pp. 14.
- Martinez, E. (2002) 'Multi-protein complexes in eukaryotic gene transcription', *Plant Molecular Biology*, 50(6), pp. 925-947.
- Masuda, S., Das, R., Cheng, H., Hurt, E., Dorman, N. and Reed, R. (2005) 'Recruitment of the human TREX complex to mRNA during splicing', *Genes & Development*, 19(13), pp. 1512-1517.
- Mathur, K., Anand, A., Dubey, S. K., Sanan-Mishra, N., Bhatnagar, R. K. and Sunil, S. (2016) 'Analysis of chikungunya virus proteins reveals that non-structural proteins nsP2 and nsP3 exhibit RNA interference (RNAi) suppressor activity', *Scientific Reports*, 6, pp. 12.
- Mazan-Mamczarz, K., Galban, S., de Silanes, I. L., Martindale, J. L., Atasoy, U., Keene, J. D. and Gorospe, M. (2003) 'RNA-binding protein HuR enhances p53 translation in response to ultraviolet

light irradiation', *Proceedings of the National Academy of Sciences of the United States of America*, 100(14), pp. 8354-8359.

Mazroui, R., Di Marco, S., Clair, E., von Roretz, C., Tenenbaum, S. A., Keene, J. D., Saleh, M. and Gallouzi, I. E. (2008) 'Caspase-mediated cleavage of HuR in the cytoplasm contributes to pp32/PHAP-I regulation of apoptosis', *Journal of Cell Biology*, 180(1), pp. 113-127.

McInerney, G. M., Kedersha, N. L., Kaufman, R. J., Anderson, P. and Liljestrom, P. (2005) 'Importance of eIF2 alpha phosphorylation assembly in alphavirus translation and stress granule regulation', *Molecular Biology of the Cell*, 16(8), pp. 3753-3763.

McInerney, G. M., Smit, J. M., Liljestrom, P. and Wilschut, J. (2004) 'Semliki Forest virus produced in the absence of the 6K protein has an altered spike structure as revealed by decreased membrane fusion capacity', *Virology*, 325(2), pp. 200-206.

McIntosh, B. M., Brooke Worth, C. and Kokernot, R. H. (1961) 'Isolation of semliki forest virus from Aedes (Aedimorphus) argenteopunctatus (theobald) collected in Portuguese East Africa', *Transactions of the Royal Society of Tropical Medicine and Hygiene*, 55(2), pp. 192-198.

Melton, J. V., Ewart, G. D., Weir, R. C., Board, P. G., Lee, E. and Gage, P. W. (2002) 'Alphavirus 6K proteins form ion channels', *Journal of Biological Chemistry*, 277(49), pp. 46923-46931.

Michel, G., Petrakova, O., Atasheva, S. and Frolov, I. (2007) 'Adaptation of Venezuelan equine encephalitis virus lacking 51-nt conserved sequence element to replication in mammalian and mosquito cells', *Virology*, 362(2), pp. 475-487.

Moraes, K. C. M., Wilusz, C. J. and Wilusz, J. (2007) 'CUG-BP and 3'UTR sequences influence PARN-mediated deadenylation in mammalian cell extracts', *Genetics and Molecular Biology*, 30(3), pp. 646-655.

Mukhopadhyay, S., Zhang, W., Gabler, S., Chipman, P. R., Strauss, E. G., Strauss, J. H., Baker, T. S., Kuhn, R. J. and Rossmann, M. G. (2006) 'Mapping the structure and function of the E1 and E2 glycoproteins in alphaviruses', *Structure*, 14(1), pp. 63-73.

Muller, U., Steinhoff, U., Reis, L. F. L., Hemmi, S., Pavlovic, J., Zinkernagel, R. M. and Aguet, M. (1994) 'Functional-role of type-I and type-II interferons in antiviral defense', *Science*, 264(5167), pp. 1918-1921.

Mulvey, M. and Brown, D. T. (1996) 'Assembly of the Sindbis virus spike protein complex', *Virology*, 219(1), pp. 125-132.

Mushi, E. Z. and Rurangirwa, F. R. (1981) 'Epidemiology of bovine malignant catarrhal fevers - a review', *Veterinary Research Communications*, 5(2), pp. 127-142.

Myles, K. M., Pierro, D. J. and Olson, K. E. (2003) 'Deletions in the putative cell receptor-binding domain of Sindbis virus strain MRE16 E2 glycoprotein reduce midgut infectivity in Aedes aegypti', *Journal of Virology*, 77(16), pp. 8872-8881.

Nagaoka, K., Suzuki, T., Kawano, T., Imakawa, K. and Sakai, S. (2006) 'Stability of casein mRNA is ensured by structural interactions between the 3'-untranslated region and poly(A) protein tail via the HuR and poly(A)-binding complex', *Biochimica Et Biophysica Acta-Gene Structure and Expression*, 1759(3-4), pp. 132-140.

Ogilvie, R. L., SternJohn, J. R., Rattenbacher, B., Vlasova, I. A., Williams, D. A., Hau, H. H., Blackshear, P. J. and Bohjanen, P. R. (2009) 'Tristetraprolin Mediates Interferon-gamma mRNA Decay', *Journal of Biological Chemistry*, 284(17), pp. 11216-11223.

Ostfeld, R. S. and Brunner, J. L. (2015) 'Climate change and Ixodes tick-borne diseases of humans', *Philosophical Transactions of the Royal Society B-Biological Sciences*, 370(1665), pp. 11.

Ou, J. H., Strauss, E. G. and Strauss, J. H. (1983) 'The 5'-terminal sequences of the genomic RNAs of several alphaviruses', *Journal of Molecular Biology*, 168(1), pp. 1-15.

Ou, J. H., Trent, D. W. and Strauss, J. H. (1982) 'The 3'-non-coding regions of alphavirus RNAs contain repeating sequences', *Journal of Molecular Biology*, 156(4), pp. 719-730.

Pabis, M., Neufeld, N., Steiner, M. C., Bojic, T., Shav-Tal, Y. and Neugebauer, K. M. (2013) 'The nuclear cap-binding complex interacts with the U4/U6.U5 tri-snRNP and promotes spliceosome assembly in mammalian cells', *Rna-a Publication of the Rna Society*, 19(8), pp. 1054-1063.

Panas, M. D., Varjak, M., Lulla, A., Eng, K. E., Merits, A., Hedestam, G. B. K. and McInerney, G. M. (2012) 'Sequestration of G3BP coupled with efficient translation inhibits stress granules in Semliki Forest virus infection', *Molecular Biology of the Cell*, 23(24), pp. 4701-4712.

Papa, A., Tsergouli, K., Tsioka, K. and Mirazimi, A. (2017) 'Crimean-Congo Hemorrhagic Fever: Tick-Host-Virus Interactions', *Frontiers in Cellular and Infection Microbiology*, 7, pp. 7.

Park, R., El-Guindy, A., Heston, L., Lin, S.-F., Yu, K.-P., Nagy, M., Borah, S., Delecluse, H.-J., Steitz, J. and Miller, G. (2014) 'Nuclear Translocation and Regulation of Intranuclear Distribution of Cytoplasmic Poly(A)-Binding Protein Are Distinct Processes Mediated by Two Epstein Barr Virus Proteins', *Plos One*, 9(4).

Parker, R. and Song, H. W. (2004) 'The enzymes and control of eukaryotic mRNA turnover', *Nature Structural & Molecular Biology*, 11(2), pp. 121-127.

Peng, L., Ryazantsev, S., Sun, R. and Zhou, Z. H. (2010) 'Three-Dimensional Visualization of Gammaherpesvirus Life Cycle in Host Cells by Electron Tomography', *Structure*, 18(1), pp. 47-58.

Peng, S. S. Y., Chen, C. Y. A., Xu, N. H. and Shyu, A. B. (1998) 'RNA stabilization by the AU-rich element binding protein, HuR, an ELAV protein', *Embo Journal*, 17(12), pp. 3461-3470.

Peranen, J., Rikonen, M., Liljestrom, P. and Kaariainen, L. (1990) 'Nuclear-localization of Semliki Forest virus-specific nonstructural protein-nsP2', *Journal of Virology*, 64(5), pp. 1888-1896.

Petersen, J. M., Her, L. S., Varvel, V., Lund, E. and Dahlberg, J. E. (2000) 'The matrix protein of vesicular stomatitis virus inhibits nucleocytoplasmic transport when it is in the nucleus and associated with nuclear pore complexes', *Molecular and Cellular Biology*, 20(22), pp. 8590-8601.

Piao, X. H., Zhang, X., Wu, L. G. and Belasco, J. G. (2010) 'CCR4-NOT Deadensylates mRNA Associated with RNA-Induced Silencing Complexes in Human Cells', *Molecular and Cellular Biology*, 30(6), pp. 1486-1494.

Pietla, M. K., Hellstrom, K. and Ahola, T. (2017) 'Alphavirus polymerase and RNA replication', *Virus Research*, 234, pp. 44-57.

Piron, M., Vende, P., Cohen, J. and Poncet, D. (1998) 'Rotavirus RNA-binding protein NSP3 interacts with eIF4G1 and evicts the poly(A) binding protein from eIF4F', *Embo Journal*, 17(19), pp. 5811-5821.

Ponnusamy, R., Petoukhov, M. V., Correia, B., Custodio, T. F., Juillard, F., Tan, M., de Miranda, M. P., Carrondo, M. A., Simas, J. P., Kaye, K. M., Svergun, D. I. and McVey, C. E. (2015) 'KSHV but not MHV-68 LANA induces a strong bend upon binding to terminal repeat viral DNA', *Nucleic Acids Research*, 43(20), pp. 10039-10054.

Powell, S. K., Rivera-Soto, R. and Gray, S. J. (2015) 'Viral Expression Cassette Elements to Enhance Transgene Target Specificity and Expression in Gene Therapy', *Discovery Medicine*, 19(102), pp. 49-57.

Powers, A. M., Brault, A. C., Shirako, Y., Strauss, E. G., Kang, W. L., Strauss, J. H. and Weaver, S. C. (2001) 'Evolutionary relationships and systematics of the alphaviruses', *Journal of Virology*, 75(21), pp. 10118-10131.

Pritchard, C. E. J., Fornerod, M., Kasper, L. H. and van Deursen, J. M. A. (1999) 'RAE1 is a shuttling mRNA export factor that binds to a GLEBS-like NUP98 motif at the nuclear pore complex through multiple domains', *Journal of Cell Biology*, 145(2), pp. 237-253.

Pullmann, R., Jr., Kim, H. H., Abdelmohsen, K., Lal, A., Martindale, J. L., Yang, X. and Gorospe, M. (2007) 'Analysis of turnover and translation regulatory RNA-Binding protein expression through binding to cognate mRNAs', *Molecular and Cellular Biology*, 27(18), pp. 6265-6278.

Pullmann, R. and Rabb, H. (2014) 'HuR and other turnover- and translation-regulatory RNA-binding proteins: implications for the kidney', *American Journal of Physiology-Renal Physiology*, 306(6), pp. F569-F576.

Qiu, L. Q., Stumpo, D. J. and Blackshear, P. J. (2012) 'Myeloid-Specific Tristetraprolin Deficiency in Mice Results in Extreme Lipopolysaccharide Sensitivity in an Otherwise Minimal Phenotype', *Journal of Immunology*, 188(10), pp. 5150-5159.



Raineri, I., Wegmueller, D., Gross, B., Certa, U. and Moroni, C. (2004) 'Roles of AUF1 isoforms, HuR and BRF1 in ARE-dependent mRNA turnover studied by RNA interference', *Nucleic Acids Research*, 32(4), pp. 1279-1288.

Raju, R., Hajjou, M., Hill, K. R., Botta, V. and Botta, S. (1999) 'In vivo addition of poly(A) tail and AU-rich sequences to the 3' terminus of the Sindbis virus RNA genome: A novel 3'-end repair pathway', *Journal of Virology*, 73(3), pp. 2410-2419.

Raju, R. and Huang, H. V. (1991) 'Analysis of Sindbis virus promoter recognition in vivo, using novel vectors with 2 subgenomic messenger-RNA promoters', *Journal of Virology*, 65(5), pp. 2501-2510.

Randall, R. E. and Goodbourn, S. (2008) 'Interferons and viruses: an interplay between induction, signalling, antiviral responses and virus countermeasures', *Journal of General Virology*, 89, pp. 1-47.

Rausalu, K., Iofik, A., Ulper, L., Karo-Astover, L., Lulla, V. and Merits, A. (2009) 'Properties and use of novel replication-competent vectors based on Semliki Forest virus', *Virology Journal*, 6.

Reigel, F. and Koblet, H. (1979) 'Isolation of subviral particles with different methods from Semliki Forest virus (sfv) infected chick-embryo fibroblasts (CEF) and Vero cells', *Experientia*, 35(7), pp. 975-975.

Rikonen, M. (1996) 'Functional significance of the nuclear-targeting and NTP-Binding motifs of semliki forest virus nonstructural protein nsP2', *Virology*, 218(2), pp. 352-361.

Rivera, C. I. and Lloyd, R. E. (2008) 'Modulation of enteroviral proteinase cleavage of poly(A)-binding protein (PABP) by conformation and PABP-associated factors', *Virology*, 375(1), pp. 59-72.

Rowe, M., Glaunsinger, B., van Leeuwen, D., Zuo, J. M., Sweetman, D., Ganem, D., Middeldorp, J., Wiertz, E. and Rensing, M. E. (2007) 'Host shutoff during productive Epstein-Barr virus infection is mediated by BGLF5 and may contribute to immune evasion', *Proceedings of the National Academy of Sciences of the United States of America*, 104(9), pp. 3366-3371.

Rozanov, M. N., Koonin, E. V. and Gorbalenya, A. E. (1992) 'Conservation of the putative methyltransferase domain - a hallmark of the Sindbis-like supergroup of positive-strand RNA viruses', *Journal of General Virology*, 73, pp. 2129-2134.

Rubach, J. K., Wasik, B. R., Rupp, J. C., Kuhn, R. J., Hardy, R. W. and Smith, J. L. (2009) 'Characterization of purified Sindbis virus nsP4 RNA-dependent RNA polymerase activity in vitro', *Virology*, 384(1), pp. 201-208.

Rupp, J. C., Sokoloski, K. J., Gebhart, N. N. and Hardy, R. W. (2015) 'Alphavirus RNA synthesis and non-structural protein functions', *Journal of General Virology*, 96, pp. 2483-2500.

Russo, A. T., White, M. A. and Watowich, S. J. (2006) 'The crystal structure of the Venezuelan equine encephalitis alphavirus nsP2 protease', *Structure*, 14(9), pp. 1449-1458.

Ryman, K. D. and Klimstra, W. B. (2008) 'Host responses to alphavirus infection', *Immunological Reviews*, 225, pp. 27-45.

Ryman, K. D., White, L. J., Johnston, R. E. and Klimstra, W. B. (2002) 'Effects of PKR/RNase L-dependent and alternative antiviral pathways on alphavirus replication and pathogenesis', *Viral Immunology*, 15(1), pp. 53-76.

Sahu, A., Das, B., Das, M., Patra, A., Biswal, S., Kar, S. K. and Hazra, R. K. (2013) 'Genetic characterization of E2 region of Chikungunya virus circulating in Odisha, Eastern India from 2010 to 2011', *Infection Genetics and Evolution*, 18, pp. 113-124.

Saisawang, C., Sillapee, P., Sinsirimongkol, K., Ubol, S., Smith, D. R. and Ketterman, A. J. (2015) 'Full length and protease domain activity of chikungunya virus nsP2 differ from other alphavirus nsP2 proteases in recognition of small peptide substrates', *Bioscience Reports*, 35, pp. 9.

Salaun, C., MacDonald, A. I., Larralde, O., Howard, L., Lochtie, K., Burgess, H. M., Brook, M., Malik, P., Gray, N. K. and Graham, S. V. (2010) 'Poly(A)-Binding Protein 1 Partially Relocalizes to the Nucleus during Herpes Simplex Virus Type 1 Infection in an ICP27-Independent Manner and Does Not Inhibit Virus Replication', *Journal of Virology*, 84(17), pp. 8539-8548.

Salonen, A., Vasiljeva, L., Merits, A., Magden, J., Jokitalo, E. and Kaariainen, L. (2003) 'Properly folded nonstructural polyprotein directs the Semliki Forest virus replication complex to the endosomal compartment', *Journal of Virology*, 77(3), pp. 1691-1702.

Santagati, M. G., Itaranta, P. V., Koskimies, P. R., Maatta, J. A., Salmi, A. A. and Hinkkanen, A. E. (1994) 'Multiple repeating motifs are found in the 3'-terminal non-translated region of Semliki Forest virus-A7 variant genome', *Journal of General Virology*, 75, pp. 1499-1504.

Santos, C. A. Q. (2016) 'Cytomegalovirus and Other beta-Herpesviruses', *Seminars in Nephrology*, 36(5), pp. 351-361.

Saul, S., Ferguson, M., Cordonin, C., Fragkoudis, R., Ool, M., Tamberg, N., Sherwood, K., Fazakerley, J. K. and Merits, A. (2015) 'Differences in Processing Determinants of Nonstructural Polyprotein and in the Sequence of Nonstructural Protein 3 Affect Neurovirulence of Semliki Forest Virus', *Journal of Virology*, 89(21), pp. 11030-11045.

Sawicki, D. L., Silverman, R. H., Williams, B. R. and Sawicki, S. G. (2003) 'Alphavirus minus-strand synthesis and persistence in mouse embryo fibroblasts derived from mice lacking RNase L and protein kinase R', *Journal of Virology*, 77(3), pp. 1801-1811.

Scheller, N., Mina, L. B., Galao, R. P., Chari, A., Gimenez-Barcons, M., Noueiry, A., Fischer, U., Meyerhans, A. and Diez, J. (2009) 'Translation and replication of hepatitis C virus genomic RNA depends on ancient cellular proteins that control mRNA fates', *Proceedings of the National Academy of Sciences of the United States of America*, 106(32), pp. 13517-13522.

Schmidt, M. F. G., Bracha, M. and Schlesinger, M. J. (1979) 'Evidence for covalent attachment of fatty-acids to Sindbis virus glycoproteins', *Proceedings of the National Academy of Sciences of the United States of America*, 76(4), pp. 1687-1691.

Schoffel, N., Braun, M., Volante, G., Bendels, M. H. K. and Groneberg, D. A. (2018) 'Rift Valley fever. A review of the literature', *Zentralblatt Fur Arbeitsmedizin Arbeitsschutz Und Ergonomie*, 68(3), pp. 164-166.

Scholte, F. E. M., Tas, A., Albulescu, I. C., Zusinaite, E., Merits, A., Snijder, E. J. and van Hemert, M. J. (2015) 'Stress Granule Components G3BP1 and G3BP2 Play a Proviral Role Early in Chikungunya Virus Replication', *Journal of Virology*, 89(8), pp. 4457-4469.

Sheridan, V., Polychronopoulos, L., Dutia, B. M. and Ebrahimi, B. (2014) 'A shutoff and exonuclease mutant of murine gammaherpesvirus-68 yields infectious virus and causes RNA loss in type I interferon receptor knockout cells', *Journal of General Virology*, 95, pp. 1135-1143.

Shirako, Y. and Strauss, J. H. (1994) 'Regulation of Sindbis virus-RNA replication - uncleaved p123 and nsP4 function in minus-strand RNA-synthesis, whereas cleaved products from p123 are required for efficient plus-strand RNA-synthesis', *Journal of Virology*, 68(3), pp. 1874-1885.

Shu, M., Taddeo, B. and Roizman, B. (2015) 'Tristetraprolin Recruits the Herpes Simplex Virion Host Shutoff RNase to AU-Rich Elements in Stress Response mRNAs To Enable Their Cleavage', *Journal of Virology*, 89(10), pp. 5643-5650.

Shwetha, S., Kumar, A., Mullick, R., Vasudevan, D., Mukherjee, N. and Das, S. (2015) 'HuR Displaces Polypyrimidine Tract Binding Protein To Facilitate La Binding to the 3' Untranslated Region and Enhances Hepatitis C Virus Replication', *Journal of Virology*, 89(22), pp. 11356-11371.

Sidwell, R. W. and Smee, D. F. (2003) 'Viruses of the Bunya- and Togaviridae families: potential as bioterrorism agents and means of control', *Antiviral Research*, 57(1-2), pp. 101-111.

Sjoberg, M., Lindqvist, B. and Garoff, H. (2011) 'Activation of the Alphavirus Spike Protein Is Suppressed by Bound E3', *Journal of Virology*, 85(11), pp. 5644-5650.

Slideplayer (2015) Eukaryotic Viruses Taxonomy characters: nucleic acid type; enveloped or naked; capsid shape; assembly site in host (nucleus or cytoplasm). Available at: <https://slideplayer.com/slide/4652613/>. [Accessed 14 September 2019].

Smithburn, K. C. and Haddow, A. J. (1944) 'Semliki Forest virus I. Isolation and pathogenic properties', *Journal of Immunology*, 49(3), pp. 141-157.

Snyder, J. E., Kulcsar, K. A., Schultz, K. L. W., Riley, C. P., Neary, J. T., Marr, S., Jose, J., Griffin, D. E. and Kuhn, R. J. (2013) 'Functional Characterization of the Alphavirus TF Protein', *Journal of Virology*, 87(15), pp. 8511-8523.

- Soiluhanninen, M., Eralinna, J. P., Hukkanen, V., Roytta, M., Salmi, A. A. and Salonen, R. (1994) 'Semliki-Forest virus infects mouse-brain endothelial-cells and causes blood-brain-barrier damage', *Journal of Virology*, 68(10), pp. 6291-6298.
- Sokoloski, K. J., Dickson, A. M., Chaskey, E. L., Garneau, N. L., Wilusz, C. J. and Wilusz, J. (2010) 'Sindbis Virus Usurps the Cellular HuR Protein to Stabilize Its Transcripts and Promote Productive Infections in Mammalian and Mosquito Cells', *Cell Host & Microbe*, 8(2), pp. 196-207.
- Soliman, T. M. and Silverstein, S. J. (2000) 'Herpesvirus mRNAs are sorted for export via Crm1-dependent and -independent pathways', *Journal of Virology*, 74(6), pp. 2814-2825.
- Spuul, P., Salonen, A., Merits, A., Jokitalo, E., Kaariainen, L. and Ahola, T. (2007) 'Role of the amphipathic peptide of semliki forest virus replicase protein nsP1 in membrane association and virus replication', *Journal of Virology*, 81(2), pp. 872-883.
- Steele, K. E. and Twenhafel, N. A. (2010) 'Pathology of Animal Models of Alphavirus Encephalitis', *Veterinary Pathology*, 47(5), pp. 790-805.
- Stewart, J. P., Silvia, O. J., Atkin, I. M. D., Hughes, D. J., Ebrahimi, B. and Adler, H. (2004) 'In vivo function of a gammaherpesvirus virion glycoprotein: Influence on B-cell infection and mononucleosis', *Journal of Virology*, 78(19), pp. 10449-10459.
- Suopanki, J., Sawicki, D. L., Sawicki, S. G. and Kaariainen, L. (1998) 'Regulation of alphavirus 26S mRNA transcription by replicase component nsP2', *Journal of General Virology*, 79, pp. 309-319.
- Svobodova, J., Blaskovic, D. and Mistrikova, J. (1982) 'Growth-characteristics of herpesviruses isolated from free living small rodents', *Acta Virologica*, 26(4), pp. 256-&.
- Svobodova, J., Stancekova, M., Blaskovic, D., Mistrikova, J., Lesso, J., Russ, G. and Masarova, P. (1982) 'Antigenic relatedness of alpha-herpesviruses isolated from free-living rodents', *Acta Virologica*, 26(6), pp. 438-&.
- Takeuchi, O. and Akira, S. (2008) 'MDA5/RIG-I and virus recognition', *Current Opinion in Immunology*, 20(1), pp. 17-22.
- Tamberg, N., Lulla, V., Fragkoudis, R., Lulla, A., Fazakerley, J. K. and Merits, A. (2007) 'Insertion of EGFP into the replicase gene of Semliki Forest virus results in a novel, genetically stable marker virus', *Journal of General Virology*, 88, pp. 1225-1230.
- Tamm, K., Merits, A. and Sarand, I. (2008) 'Mutations in the nuclear localization signal of nsF2 influencing RNA synthesis, protein expression and cytotoxicity of Semliki Forest virus', *Journal of General Virology*, 89, pp. 676-686.
- Tang, J. H., Jose, J., Chipman, P., Zhang, W., Kuhn, R. J. and Baker, T. S. (2011) 'Molecular Links between the E2 Envelope Glycoprotein and Nucleocapsid Core in Sindbis Virus', *Journal of Molecular Biology*, 414(3), pp. 442-459.
- Tarbatt, C. J., Glasgow, G. M., Mooney, D. A., Sheahan, B. J. and Atkins, G. J. (1997) 'Sequence analysis of the avirulent, demyelinating A7 strain of Semliki Forest virus', *Journal of General Virology*, 78, pp. 1551-1557.
- Tavana, A. M. (2015) 'Sandfly fever in the world', *Annals of Tropical Medicine and Public Health*, 8(4), pp. 83-87.
- Taylor, G. S. and Blackbourn, D. J. (2011) 'Infectious agents in human cancers: Lessons in immunity and immunomodulation from gammaherpesviruses EBV and KSHV', *Cancer Letters*, 305(2), pp. 263-278.
- Terry, L. A., Stewart, J. P., Nash, A. A. and Fazakerley, J. K. (2000) 'Murine gammaherpesvirus-68 infection of and persistence in the central nervous system', *Journal of General Virology*, 81, pp. 2635-2643.
- Tomar, S., Hardy, R. W., Smith, J. L. and Kuhn, R. J. (2006) 'Catalytic core of alphavirus nonstructural protein nsP4 possesses terminal adenylyltransferase activity', *Journal of Virology*, 80(20), pp. 9962-9969.
- Torres, R., Samudio, R., Carrera, J. P., Young, J., Marquez, R., Hurtado, L., Weaver, S., Chaves, L. F., Tesh, R. and Caceres, L. (2017) 'Enzootic mosquito vector species at equine encephalitis transmission foci in the Republica de Panama', *Plos One*, 12(9).

Tsetsarkin, K. A., Vanlandingham, D. L., McGee, C. E. and Higgs, S. (2007) 'A single mutation in chikungunya virus affects vector specificity and epidemic potential', *Plos Pathogens*, 3(12), pp. 1895-1906.

Tsetsarkin, K. A. and Weaver, S. C. (2011) 'Sequential Adaptive Mutations Enhance Efficient Vector Switching by Chikungunya Virus and Its Epidemic Emergence', *Plos Pathogens*, 7(12).

Tuittila, M. and Hinkkanen, A. E. (2003) 'Amino acid mutations in the replicase protein nsP3 of Semliki Forest virus cumulatively affect neurovirulence', *Journal of General Virology*, 84, pp. 1525-1533.

Tuittila, M. T., Santagati, M. G., Roytta, M., Maatta, J. A. and Hinkkanen, A. E. (2000) 'Replicase complex genes of Semliki Forest virus confer lethal neurovirulence', *Journal of Virology*, 74(10), pp. 4579-4589.

Ueda, K. (2018) 'KSHV Genome Replication and Maintenance in Latency', *Human Herpesviruses*, 1045, pp. 299-320.

Vaney, M. C., Duquerroy, S. and Rey, F. A. (2013) 'Alphavirus structure: activation for entry at the target cell surface', *Current Opinion in Virology*, 3(2), pp. 151-158.

Varjak, M., Saul, S., Arike, L., Lulla, A., Peil, L. and Merits, A. (2013) 'Magnetic Fractionation and Proteomic Dissection of Cellular Organelles Occupied by the Late Replication Complexes of Semliki Forest Virus', *Journal of Virology*, 87(18), pp. 10295-10312.

Varjak, M., Zusinaite, E. and Merits, A. (2010) 'Novel Functions of the Alphavirus Nonstructural Protein nsP3 C-Terminal Region', *Journal of Virology*, 84(5), pp. 2352-2364.

Vasiljeva, L., Merits, A., Auvinen, P. and Kaariainen, L. (2000) 'Identification of a novel function of the Alphavirus capping apparatus - RNA 5'-triphosphatase activity of Nsp2', *Journal of Biological Chemistry*, 275(23), pp. 17281-17287.

Vasiljeva, L., Merits, A., Golubtsov, A., Sizemskaja, V., Kaariainen, L. and Ahola, T. (2003) 'Regulation of the sequential processing of Semliki Forest virus replicase polyprotein', *Journal of Biological Chemistry*, 278(43), pp. 41636-41645.

Venigalla, R. K. C. and Turner, M. (2012) 'RNA-binding proteins as a point of convergence of the PI3K and p38 MARK pathways', *Frontiers in Immunology*, 3.

Villoing, S., Bearzotti, M., Chilmonczyk, S., Castric, J. and Bremont, M. (2000) 'Rainbow trout sleeping disease virus is an atypical alphavirus', *Journal of Virology*, 74(1), pp. 173-183.

Virgin, H. W., Latreille, P., Wamsley, P., Hallsworth, K., Weck, K. E., DalCanto, A. J. and Speck, S. H. (1997) 'Complete sequence and genomic analysis of murine gammaherpesvirus 68', *Journal of Virology*, 71(8), pp. 5894-5904.

Vogels, C. B. F., Goertz, G. P., Pijlman, G. P. and Koenraadt, C. J. M. (2017) 'Vector competence of European mosquitoes for West Nile virus', *Emerging Microbes & Infections*, 6, pp. 13.

von Kobbe, C., van Deursen, J. M. A., Rodrigues, J. P., Sitterlin, D., Bachi, A., Wu, X. S., Wilm, M., Carmo-Fonseca, M. and Izaurralde, E. (2000) 'Vesicular stomatitis virus matrix protein inhibits host cell gene expression by targeting the nucleoporin Nup98', *Molecular Cell*, 6(5), pp. 1243-1252.

Voss, J. E., Vaney, M. C., Duquerroy, S., Vornrhein, C., Girard-Blanc, C., Crublet, E., Thompson, A., Bricogne, G. and Rey, F. A. (2010) 'Glycoprotein organization of Chikungunya virus particles revealed by X-ray crystallography', *Nature*, 468(7324), pp. 709-U137.

Wang, H., Ding, N. N., Guo, J., Xia, J. Z. and Ruan, Y. L. (2016) 'Dysregulation of TTP and HuR plays an important role in cancers', *Tumor Biology*, 37(11), pp. 14451-14461.

Wang, M. S. and Pestov, D. G. (2011) '5'-end surveillance by Xrn2 acts as a shared mechanism for mammalian pre-rRNA maturation and decay', *Nucleic Acids Research*, 39(5), pp. 1811-1822.

Wang, W. G., Caldwell, M. C., Lin, S. K., Furneaux, H. and Gorospe, M. (2000) 'HuR regulates cyclin A and cyclin B1 mRNA stability during cell proliferation', *Embo Journal*, 19(10), pp. 2340-2350.

Watanabe, M., Fukuda, M., Yoshida, M., Yanagida, M. and Nishida, E. (1999) 'Involvement of CRM1, a nuclear export receptor, in mRNA export in mammalian cells and fission yeast', *Genes to Cells*, 4(5), pp. 291-297.

- Weaver, S. C. and Forrester, N. L. (2015) 'Chikungunya: Evolutionary history and recent epidemic spread', *Antiviral Research*, 120, pp. 32-39.
- Wei, F., Gan, J., Wang, C., Zhu, C. X. and Cai, Q. L. (2016) 'Cell Cycle Regulatory Functions of the KSHV Oncoprotein LANA', *Frontiers in Microbiology*, 7.
- Weiss, B., Nitschko, H., Ghattas, I., Wright, R. and Schlesinger, S. (1989) 'Evidence for specificity in the encapsidation of Sindbis virus RNAs', *Journal of Virology*, 63(12), pp. 5310-5318.
- Wengler, G. and Gros, C. (1996) 'Analyses of the role of structural changes in the regulation of uncoating and assembly of alphavirus cores', *Virology*, 222(1), pp. 123-132.
- Wengler, G., Koschinski, A. and Dreyer, F. (2003) 'Entry of alphaviruses at the plasma membrane converts the viral surface proteins into an ion-permeable pore that can be detected by electrophysiological analyses of whole-cell membrane currents', *Journal of General Virology*, 84, pp. 173-181.
- Wengler, G. and Wurfner, D. (1992) 'Identification of a sequence element in the alphavirus core protein which mediates interaction of cores with ribosomes and the disassembly of cores', *Virology*, 191(2), pp. 880-888.
- Weston, J. H., Welsh, M. D., McLoughlin, M. F. and Todd, D. (1999) 'Salmon pancreas disease virus, an alphavirus infecting farmed Atlantic salmon, *Salmo salar* L', *Virology*, 256(2), pp. 188-195.
- Wesula Olivia, L., Obanda, V., Bucht, G., Mosomtai, G., Otieno, V., Ahlm, C. and Evander, M. (2015) 'Global emergence of Alphaviruses that cause arthritis in humans', *Infection Ecology & Epidemiology*, 5(1), pp. 29853.
- White, R. E., Calderwood, M. A. and Whitehouse, A. (2003) 'Generation and precise modification of a herpesvirus saimiri bacterial artificial chromosome demonstrates that the terminal repeats are required for both virus production and episomal persistence', *Journal of General Virology*, 84, pp. 3393-3403.
- Wielgosz, M. M., Raju, R. and Huang, H. V. (2001) 'Sequence requirements for Sindbis virus subgenomic mRNA promoter function in cultured cells', *Journal of Virology*, 75(8), pp. 3509-3519.
- Wiggins, K., Eastmond, B. and Alto, B. W. (2018) 'Transmission potential of Mayaro virus in Florida *Aedes aegypti* and *Aedes albopictus* mosquitoes', *Medical and Veterinary Entomology*, 32(4), pp. 436-442.
- Wilkinson, T. A., Tellinghuisen, T. L., Kuhn, R. J. and Post, C. B. (2005) 'Association of Sindbis virus capsid protein with phospholipid membranes and the E2 glycoprotein: Implications for alphavirus assembly', *Biochemistry*, 44(8), pp. 2800-2810.
- Wilusz, C. J., Wormington, M. and Peltz, S. W. (2001) 'The cap-to-tail guide to mRNA turnover', *Nature Reviews Molecular Cell Biology*, 2(4), pp. 237-246.
- Wu, M. S., Reuter, M., Lilie, H., Liu, Y. Y., Wahle, E. and Song, H. W. (2005) 'Structural insight into poly(A) binding and catalytic mechanism of human PARN', *Embo Journal*, 24(23), pp. 4082-4093.
- Wu, T. T., Usherwood, E. J., Stewart, J. P., Nash, A. A. and Sun, R. (2000) 'Rta of murine gammaherpesvirus 68 reactivates the complete lytic cycle from latency', *Journal of Virology*, 74(8), pp. 3659-3667.
- Xu, N. H., Chen, C. Y. A. and Shyu, A. B. (1997) 'Modulation of the fate of cytoplasmic mRNA by AU-rich elements: Key sequence features controlling mRNA deadenylation and decay', *Molecular and Cellular Biology*, 17(8), pp. 4611-4621.
- Yamashita, A., Chang, T. C., Yamashita, Y., Zhu, W. M., Zhong, Z. P., Chen, C. Y. A. and Shyu, A. B. (2005) 'Concerted action of poly(A) nucleases and decapping enzyme in mammalian mRNA turnover', *Nature Structural & Molecular Biology*, 12(12), pp. 1054-1063.
- Young, L. E., Sanduja, S., Bemis-Standoli, K., Pena, E. A., Price, R. L. and Dixon, D. A. (2009) 'The mRNA Binding Proteins HuR and Tristetraprolin Regulate Cyclooxygenase 2 Expression During Colon Carcinogenesis', *Gastroenterology*, 136(5), pp. 1669-1679.
- Zhang, B., Morace, G., Gauss-Muller, V. and Kusov, Y. (2007) 'Poly(A) binding protein, C-terminally truncated by the hepatitis A virus proteinase 3C, inhibits viral translation', *Nucleic Acids Research*, 35(17), pp. 5975-5984.

Zhang, R., Hryc, C. F., Cong, Y., Liu, X. G., Jakana, J., Gorchakov, R., Baker, M. L., Weaver, S. C. and Chiu, W. (2011) '4.4 angstrom cryo-EM structure of an enveloped alphavirus Venezuelan equine encephalitis virus', *Embo Journal*, 30(18), pp. 3854-3863.

Zheng, Z. M. (2004) 'Regulation of alternative RNA splicing by exon definition and exon sequences in viral and mammalian gene expression', *Journal of Biomedical Science*, 11(3), pp. 278-294.

Ziemiecki, A., Garoff, H. and Simons, K. (1980) 'Formation of the Semliki Forest virus membrane glycoprotein complexes in the infected cell', *Journal of General Virology*, 50(SEP), pp. 111-123.